

**Asymmetric Hydroformylation of Disubstituted Alkenes and
Application in the Synthesis of Oligomers**

by

Floriana Andreea Foarta

A dissertation submitted in partial fulfillment
of the requirements for the degree of

Doctor of Philosophy
(Chemistry)

at the

UNIVERSITY OF WISCONSIN-MADISON

2017

Date of final oral examination: 06/01/2017

The dissertation is approved by the following members of the Final Oral Committee:

Clark R, Landis, Professor, Chemistry

Jennifer Schomaker, Associate Professor, Chemistry

Steven D. Burke, Professor, Chemistry

Ive Hermans, Associate Professor, Chemistry

John F. Berry, Professor, Chemistry

**Asymmetric Hydroformylation of Disubstituted Alkenes and
Application in the Synthesis of Oligomers**

Floriana Andreea Foarta

Under the supervision of Prof. Clark Landis

At the University of Wisconsin-Madison

Abstract

Rhodium-catalyzed asymmetric hydroformylation is an atom efficient method to synthesize optically active aldehydes from simple alkenes, carbon monoxide and hydrogen. Such aldehydes serve as precursors to pharmaceuticals and fine chemicals. Efficient hydroformylation was demonstrated previously for many monosubstituted alkenes. Access to chiral aldehydes with more diverse branching substituents remains, however, limited. This work extends effective enantioselective hydroformylation to 1,2-disubstituted alkenes, particularly (Z)-enol esters and (Z)-enamides, and to 1,1'-disubstituted alkenes, predominantly alpha-substituted unsaturated esters. Functionalized aldehydes with tertiary and quaternary stereogenic centers are obtained with high stereo and regiocontrol at mild pressures in the presence of Rh-BisDiazaphos or Ph-BPE catalysts. The iterative application of the sequence Rh-BisDiazaphos catalyzed asymmetric hydroformylation of (Z)-enol esters / aldehyde oxidation / Ru catalyzed alkyne hydroacyloxylation enables catalytic, low-waste synthesis of sequence specific chiral oligoesters. This method demonstrates that short oligomers can be synthesized with sequence specificity and stereocontrol in the absence of coupling reagents and protecting groups.

Acknowledgements

I am very grateful to Clark for teaching me how to think about science. It has been a pleasure interacting with the group, both past and present. I am especially grateful to Dr. Leigh Abrams, I learned a lot from her.

I am also grateful to my committee members for their contribution to my development as a scientist for the past few years.

I am thankful to my family for their endless support, especially to my sister, who showed me that everything is possible through hard work and determination. I am thankful to Brandon for his love and support, as well to my friends here in Madison for all the fun memories.

Table of contents

Abstract	i
Acknowledgements	ii
Chapter 1. Introduction for a lay audience	1
1.1. Chemical Reactions and Catalysis	2
1.2. Hydroformylation	2
Figure 1.1. General reaction scheme for rhodium-catalyzed hydroformylation	3
Chapter 2. Asymmetric Hydroformylation of Z-Enamides and Enol Esters with Rhodium-BisDiazaphos Catalysts	7
2.1. Introduction	8
Figure 2.1.: Bisdiazaphospholane ligand used for hydroformylation.	8
Scheme 2.1. AHF in the synthesis of (+)-Patulolide C	9
Table 2.1. Some representative examples of AHF of 1,1- and 1,2-disubstituted alkenes	10
2.2. Results and Discussion	11
2.2.1. AHF of Enol Esters	11
Table 2.2: Asymmetric hydroformylation of para-substituted Z enol esters	12
Table 2.3: Selectivity of AHF is maintained at higher temperatures	13
Table 2.4. AHF of other enol esters	14

2.2.2. AHF of Enamides	14
Figure 2.2. AHF of enamide N-((Z)-1-hexen-1-yl)benzamide with time	15
Table 2.5. Asymmetric hydroformylation of enamides	16
Figure 2.3. Pressure effects on AHF of styrenyl enamides.	17
2.1.3. Synthesis of a L-DOPA building block	18
Scheme 2.2. AHF of enamides applied to the synthesis of protected analog of L-DOPA aldehyde	19
2.3. Conclusions	19
2.4. Experimental	21
2.4.1. General	21
2.4.2. Synthesis and characterization of (Z)- enol ester and enamide substrates	22
2.4.3. Synthesis and Characterization of Aldehydes	29
2.4.4. Synthesis of L-DOPA Precursor	56
2.5. References	61
Chapter 3. Condensation Oligomers with Sequence Control but without Coupling Reagents and Protecting Groups via Asymmetric Hydroformylation and Hydroacyloxylation	65
3.1. Introduction	66

Figure 3.1. (S,S,S)-Bisdiazaphos ligand used in AHF	67
Scheme 3.1. Synthetic strategy for coupling reagent and protecting group free synthesis of sequence specific oligoesters	68
3.2. Results and Discussion	69
Scheme 3.2. Synthesis of a tetramer via the proposed iterative alkyne hydroacyloxylation / AHF / oxidation sequence	71
Scheme 3.3. Demonstration of coupling between the synthesized tetramer and a carboxamide using a diyne linker	73
3.3 Conclusions	73
3.4. Experimental section	75
3.5 References	87
Chapter 4. Enantioenriched α-Tetrasubstituted Aldehydes via Rhodium-Bisphosphine Catalyzed Asymmetric Hydroformylation	90
4.1. Introduction	91
Figure 4.1 AHF of 1,1'-disubstituted alkenes	91
Figure 4.2 Previous examples of AHF of 1,1'-disubstituted alkenes	92
Figure 4.3 Chiral ligands for AHF	93
4.2. Results and discussion	94
Table 4.1. Ligand screening in the AHF of Methyl 2-fluoroacrylate	95

Table 4.2. CO pressure and temperature effect in the AHF of Methyl 2-fluoroacrylate	96
Table 4.3. AHF of alpha-unsaturated esters	98
Table 4.4. AHF of other 1,1'-disubstituted alkenes	100
Table 4.5. Improved enantioselectivity at lower temperatures	101
Table 4.6. Substrates that do not yield tetrasubstituted aldehydes	103
Scheme 4.1. Linear Selective AHF of N-(1-phenylvinyl) acetamide	103
Table 4.7. Attempts at generating tetrasubstituted aldehydes via AHF of trisubstituted alkenes	104
4.3. Catalyst Speciation via Low Temperature NMR	105
Figure 4.4. Mechanistic model for the observed alkene hydrogenation during the branched hydroformylation pathway	106
Figure 4.5. $^{31}\text{P}\{^1\text{H}\}$ monitoring the reaction between $[\text{Rh}(\text{H})(\text{CO})_2(\text{rac-L7})]$ with 4.1a (10 equiv.) at 0 °C, under 1 atm CO	108
Figure 4.6 $^{31}\text{P}\{^1\text{H}\}$ of alkyl 4.6 (42 and 75 ppm) and acyl 4.7 (59 and 71 ppm); bottom spectrum: at -30 °C; upper spectrum: at -30 °C, after bubbling with CO	109
Figure 4.7 $^{31}\text{P}\{^1\text{H}\}$ monitoring the reaction between $[\text{Rh}(\text{H})(\text{CO})_2(\text{rac-L4.7})]$ (83 ppm, 20 mM) with 4.1a (10 equiv.) while temperature increases from -30°C to room temperature. Spectra every 3.5 min	110
4.4. Deuterioformylation of a linear selective alkene	110

Figure 4.8. Linear selective hydroformylation of 2-(2-methylphenyl)-acrylic acid methyl ester (top scheme) and deuterioformylation (bottom scheme)	111
Figure 4.9. ¹ H NMR (CDCl ₃) of crude deuterioformylation of 2-(2-methylphenyl)-acrylic acid methyl ester at partial substrate conversion	112
4.5. Conclusions	112
4.6. Experimental	114
4.6.1 General	114
4.6.2. Experimental Procedures and Characterization Data	115
4.7. References	125
Appendix	129
Spectra and Supporting Data for Chapters 2-4	129
NMR Spectra for Chapter 2	130
NMR Spectra for Chapter 3	168
NMR Spectra for Chapter 4	184
HPLC and SFC traces for Chapter 2	201
GC traces for Chapter 4	219

Chapter 1

Introduction for a Lay Audience

1.1. Chemical Reactions and Catalysis

Chemical reactions transform one chemical substance to another. Chemical reactions are all around us, from rusting of iron, bleach removing stains in the washing machine or plant photosynthesis. We rely on chemical reactions to synthesize molecules that are important to our daily lives: plastics, drugs, detergents etc. There may be more than one way to synthesize a molecule, however, to be economically viable, the synthesis must be fast, use few and cheap starting materials, and generate little waste. To this end, catalysis has revolutionized how we make molecules. A catalyst reduces the amount of energy needed in a chemical reaction, thus making the reaction faster, but it is not itself consumed in the reaction. Imagine you are headed on foot to a destination located on the other side of a hill. Walking up the hill takes a lot of your time and energy. One day you decide to drive to the same destination, which takes you there faster and requires less of your energy. The car in this case is acting like a catalyst. The chemical reactions used for the synthesis of most industrially important chemicals involve catalysis.

1.2. Hydroformylation

The specific catalytic transformation my research focuses on is called hydroformylation, catalyzed by a rhodium catalyst (Figure 1.1). Hydroformylation transforms relatively simple, widely available reagents, such as olefins, carbon monoxide and hydrogen, into more valuable products called aldehydes.

require fast catalysts and high control of selectivity, while operating at safe pressure conditions. Currently hydroformylation to generate branched aldehydes is relatively underdeveloped compared to hydroformylation to generate linear aldehydes, already used extensively in industry.

One characteristic that makes these branched aldehydes so attractive for pharma applications is a property called chirality. There are actually two branched aldehydes formed in Figure 1.1, not one. The two branched aldehydes are identical, except for the 3D arrangement of the atoms. We call these molecules chiral. Best example of chirality is your hands. If you place your hands both palms face down, you will notice that your thumbs point in the opposite direction, and your hands (just like the two branched aldehydes) are mirror images of each other. Your hands are therefore chiral. The two branched aldehydes may look very similar, but they can behave very differently. Pharma is one industry where chirality information is crucial, since using the wrong form of a chiral drug can have a negative effect in your body. In my research, I aim to not only favor the branched aldehyde over the linear one, but to also control chirality of the branched aldehyde. Achieving both goals in the same time is very challenging. In addition, the structure and size of the variable R group is very important, since different ratios of products can form depending on the identity of the R group. Things become even more complicated when we do not have just one R group, but two R groups.

Chapters 2 and 4 focus on hydroformylation when the olefin has two different R groups. Chapter 2 focuses on alkenes where the two R groups are located on either side of the double bond, whereas chapter 2 focuses on alkenes where the R groups are both located on one side of the double bond. These two categories are generally slower and less

selective. The scope of my research is to maximize the formation of one branched aldehyde and suppress the formation of other products, all while keeping the reaction fast and at mild conditions. The motivation lies in the high synthetic value of the corresponding branched aldehyde products, very hard to obtain using methods other than hydroformylation.

Chapter 3 provides a concrete application of asymmetric hydroformylation to synthesize complex molecules more efficiently. I am not making a specific drug for pharma (although others have done this before), but I am looking to improve how polymers are made. Some polymers are used in pharma for drug delivery for example. But polymers are important beyond pharma, they are all around us, ranging from synthetic polymers, such as plastics, to natural polymers, such as DNA and proteins. Polymers consist of many units bonded together, called monomers. A polymer is like a string of beads, and each bead is one monomer. There are two main types of polymers, one where all monomers are the same, for example polystyrene, and one where monomers are different. In the latter case, the order of monomers matters. For example, in the case of a natural polymer, such as DNA, if one monomer is in the wrong place, a mutation occurs. In the case of synthetic polymers, such as plastics, a drastic change in properties can occur if the monomers are not in the correct order. The safest way to be sure that you have the correct order is to add the beads one at a time, same goes with monomers. The caveat with this stepwise addition is that each time a new monomer is added, we need what is called a “coupling reagent”, which helps link the monomer added last to the rest of the growing chain. This coupling reagent is needed in large amounts and is thrown away once each monomer is added. Given that some polymers have thousands and thousands of monomer units, the

amount of waste generated can be massive. Chapter 3 addresses this issue of coupling reagents by providing a new way of joining monomers together that avoids coupling reagents. How? Using catalysis! I use three consecutive catalytic chemical reactions, one of them hydroformylation, to add each new monomer. This method could substantially reduce the amount of waste generated in the synthesis of polymers.

Chapter 2

Asymmetric Hydroformylation of *Z*-Enamides and Enol Esters

with Rhodium-BisDiazaphos Catalysts

Chapter 2 is published in

Abrams, M. L. Foarta, F. Landis, C. R. *J. Am. Chem. Soc.* **2014**, *136*, 14583 – 14588

This work was accomplished in collaboration with Dr. Leigh Abrams

2.1. Introduction

Chiral aldehydes are versatile building blocks in organic synthesis. Although the conversion of simple, terminal alkenes into aldehydes by hydroformylation with rhodium catalysts constitutes a long-standing commodity process, applications to the synthesis of chiral aldehydes are less common.¹ The emergence of new chiral catalysts that effect rapid, enantioselective, and regioselective hydroformylation of monosubstituted, and to a lesser extent, disubstituted alkenes provide new opportunities for efficient syntheses of chiral aldehydes. In this paper, we demonstrate that disubstituted alkenes comprising Z-enol esters and Z-enamides undergo efficient hydroformylation with excellent selectivity and functional group tolerance using rhodium catalysts in the presence of the (S,S,S)-BisDiazaphos ligand, **L1**.

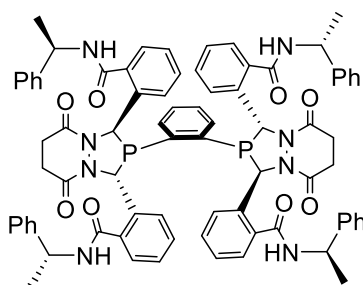
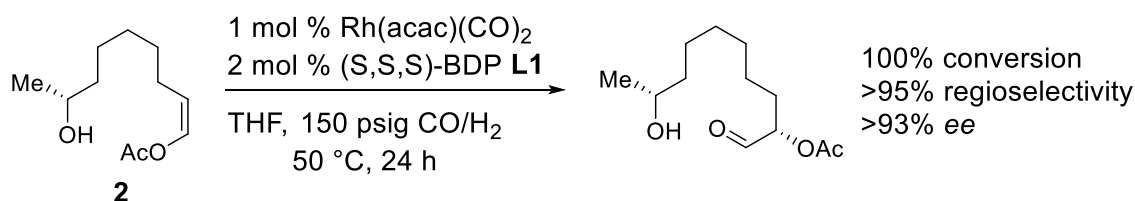


Figure 2.1. Bisdiazaphospholane ligand **L1** used for hydroformylation.

Effective, modern asymmetric hydroformylation (AHF) technology began with the development of the Rh(BINAPHOS) catalyst system.² Applications of this catalyst demonstrated that useful regio- and enantioselectivities could be effected for a variety of alkenes, especially monosubstituted alkenes. Following these initial demonstrations, several notable ligand systems for AHF have been reported. These ligands include diphosphites such as Chiraphite,³ mixed phosphine-phosphoramidites such as Yanphos,⁴

mixed phosphine-phosphite ligands with small bite angles⁵, Duphos-related diphosphines such as Ph-BPE,⁶ and so-called scaffolding mono-phosphine ligands.⁷ Rhodium complexes of the bisdiazaphospholane (BDP) class of ligands exhibit unusual activity and selectivity in AHF reaction for a broad range of alkene substrates. High (> 90% ee) enantioselectivities have been achieved with aryl alkene, 1,3-diene, vinyl acetate and N-vinyl acetamide, dihydrofuran, and other substrates using BDP-derived catalysts.⁸

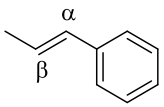
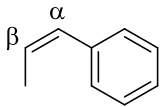
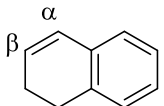
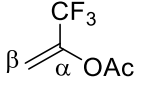
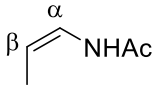
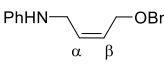
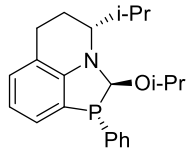
Effective AHF with disubstituted alkene substrates would expand the strategies available for complex molecule synthesis because AHF provides a fundamentally different disconnection than other C-C bond forming reactions. An excellent example is provided by Burke's recent report of a highly efficient synthesis of Patulolide C that features AHF of the Z-enol ester **2**.^{8e} Additional examples include the enantioselective synthesis of Garner's aldehyde⁹ and Leighton's synthesis of Dictyostatin.¹⁰



Scheme 2.1. AHF in the synthesis of (+)-Patulolide C

Many simple, terminal alkenes have been converted into chiral aldehydes with high selectivity by asymmetric hydroformylation. However, selective AHF of more complex substrates requires effective transformation of more highly substituted alkenes. Prior examples of enantioselective AHF of disubstituted alkenes with enantioselectivities that exceed 90% ee are given in Table 2.1.

Table 2.1. Some representative examples of AHF of 1,1- and 1,2-disubstituted alkenes

	Substrate	Ligand	Sub/Ca t Ratio	P _{H₂/CO} (psi)	T (°C)	t (h)	Conv. (%)	α:β	ee (%)
1		Binaphos	250	1470	60	50	10	97:3	92
2		BDP	500	150	40	24	37	92:8	94
3		BDP	500	70	40	24	67	-	93
4		Binaphos	300	1470	60	20	79	96:4	96
5		QuinoxP*	100	145	85	8	46	> 100	91
6		BDP	200	140	70	20	99	97:3	90
7			57 ^a	50	45	14	77	> 100	91

^aRun with 15 mol% ligand (6.7:1 substrate:ligand) and 0.05 mol% pTsOH as an additive.

Application of AHF to 1,2-disubstituted alkenes requires controlling the regioselectivity of CO insertion between two positions that are less sterically differentiated than in monosubstituted or 1,1-disubstituted alkenes. To date, control of regioselectivity has been addressed most effectively for allyl amines and alcohols that are amenable to scaffolding catalysis.⁷ Hydroformylation of disubstituted alkenes commonly requires long reaction times and/or high catalyst loading in order to overcome the substrate bulkiness. With Rh-bisdiazaphospholane catalysts, AHF of alkenes substituted with inductively electron-withdrawing groups, such as acetoxy- or acetamido-substituents, generally yield high regioselectivity and good activity.^{8c} With the exception of particularly electron-deficient alkenes, AHF of 1,1-disubstituted alkenes is sluggish.¹¹ A small set of data indicates that the geometry of the double bond of 1,2-disubstituted alkenes also impacts AHF selectivity, with Z alkenes giving higher regio- and enantioselectivities and faster rates.^{2b,8c} Such observations suggest that AHF can be particularly effective for 1,2-disubstituted alkenes comprising (Z)- enol esters and enamides.

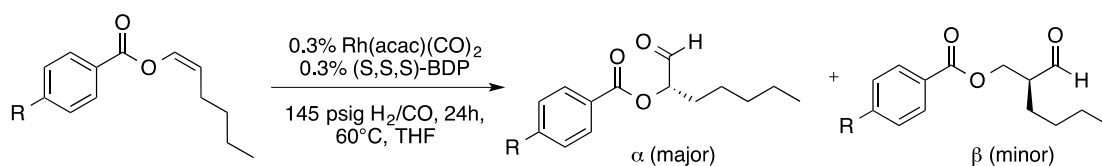
2.2. Results and Discussion

2.2.1. AHF of Enol Esters

Enol ester substrates are attractive candidates for AHF because the two carbons of the alkene are well-differentiated electronically. Benzoyloxy-substituted alkenes are synthetically accessible as the Z isomer via Ru-catalyzed addition of alkynes to carboxylic acids.^{12,13} Hydroformylation of these alkenes in the presence of **L1** and Rh(acac)(CO)₂ produces only the alpha-substituted, 2-benzoyloxy aldehyde with excellent enantioselectivity (90-97% ee) at low catalyst loadings (0.3%) (Table 2.2). Results obtained on the gram scale (Table 2.2, entry 1) are similar to small scale results (Table

2.2, entries 2-7). Hydroformylation is tolerant of a wide variety of functional groups, including potential catalyst poisoning groups such as thioether, benzylic chloride, and free phenol (Table 2.2, entries 3, 6 and 7). The substituent in the para position has little effect on the hydroformylation activity and all substrates tested give high regio- and enantioselectivity under the screening conditions.

Table 2.2: Asymmetric hydroformylation of para-substituted Z enol esters.



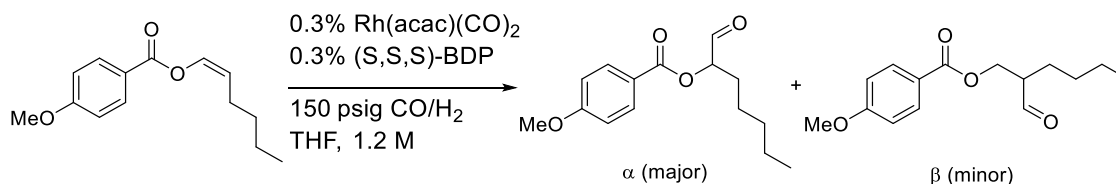
Entry	R=	Conc. alkene	Conv. ^a	α:β ^a	Isolated yield	% ee ^c
1 ^{b,f}	H	1.5 M	>99%	>50:1	92%	97
2 ^f	OMe	1.3M	>99%	>50:1	84%	96
3	SMe	1.8M	>99%	>50:1	85%	90
4	Cl	1.3M	>99%	>50:1	88%	96
5	Br	1.3M	>99%	>50:1	82%	92
6 ^d	CH ₂ Cl	1.5M	94%	>50:1	78%	92
7	OH	1.3M	93%	>50:1	82%	99 ^e

Run with 100 mg alkene. ^aDetermined by ¹H NMR of crude reaction mixture. ^bRun with 1 g alkene. ^cee determined by SFC or HPLC after NaBH₄ reduction. ^d0.5% catalyst loading. ^eTo date we have not been able to resolved these products or their derivatives. ^f

^d The configuration is S as determined by LAH reduction to the diol and comparison of the optical rotation with the previously assigned diol.

While the results in Table 2.2 incorporate 24 hour reaction times, many substrates go to complete conversion at 60 °C in under 16 hours. Significantly, at higher temperatures the reaction time is reduced with no effect on the enantio- or regioselectivity. For (Z)-hex-1-en-1-yl 4'-methoxybenzoate, AHF is complete within 1.5 hours at 100 °C, and the resultant aldehyde is produced in 96 % ee (Table 2.3, entry 3). The enantioselectivity only drops modestly when the temperature is further increased to 120 °C.

Table 2.3: Selectivity of AHF is maintained at higher temperatures.



Entry	Temp (°C)	Time (h)	Conv. ^a	$\alpha:\beta^a$	% ee ^b
1	60	24	>99%	>50:1	96
2	80	5	>99%	>50:1	96
3	100	1.5	>99%	>50:1	95
4	120	0.5	>99%	>50:1	89

Run with 100 mg alkene. ^aDetermined by ¹H NMR of crude reaction mixture. ^b ee determined by HPLC after NaBH₄ reduction.

AHF of enol esters is effective with both acetates and benzoates (Table 2.4, entry 1). Enol esters derived from enantiopure amino acids of opposite chirality undergo AHF with high diastereoselectivity that is predominately catalyst-controlled, with little match-mismatch effect (Table 2.4, entries 2 and 3). Trifluoroacetyl enol esters also were investigated, but these undergo undesirable elimination of trifluoroacetic acid under catalytic conditions and give low conversion (37-60%) to the desired product.

Table 2.4. AHF of other enol esters

Substrate	Product	Conc. alkene	Temp (°C)	Time (h)	Conv. ^a	□:□ ^a	Isolated Yield	% ee or de
		1.3 M	60	24	>99%	>50:1	88%	93 ^{b,d}
		1.1 M	60	24	>99%	>50:1	83%	92 ^a
		1.1 M	60	24	>99%	>50:1	75%	92 ^c

Run with 150 psig H₂/CO. ^aDetermined by ¹H NMR of crude reaction mixture. ^bee determined by HPLC after NaBH₄ reduction. ^cRun with (R,R,R) BisDiazaphos. ^d The configuration is S as determined by LAH reduction to the diol and comparison of the optical rotation with the previously assigned diol.

2.2.2. AHF of Enamides

Z-Enamides can be synthesized by Ru-catalyzed coupling of primary amides to alkynes.¹⁴ These substrates also undergo AHF with high selectivity for the α -amino aldehyde product. The AHF of enamides is slower than that of the corresponding enol esters

(Figure 2.2) and complete conversion within a day requires higher catalyst loading (1%) at 65°C.

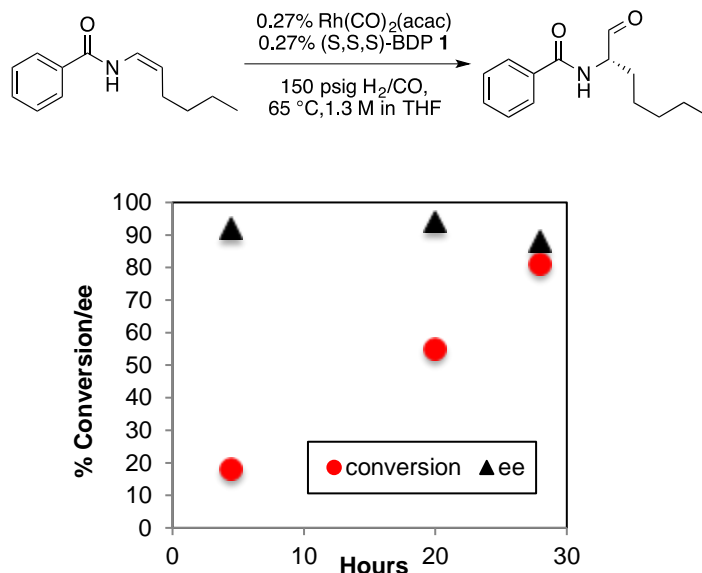


Figure 2.2. AHF of enamide N-((Z)-1-hexen-1-yl)benzamide with time.

Both E- and Z-enamides were tested under standard AHF conditions of 65°C and 150 psig CO/H₂ (Table 2.5, entries 1 and 2). Consistent with prior results for propenamide, the Z-enamide gives both higher enantioselectivity and faster rates. Under standard conditions, the AHF of most enamides proceeds with high selectivity and excellent functional group tolerance, including groups that often react with metal catalysts, such as alkyl chlorides and nitriles (Table 2.5, entries 4 and 5). Important limitations of AHF with BisDiazaphos catalysts are revealed by entries 10 and 11. The α - β unsaturated substrate ethyl-(2-benzamido)ethenoate undergoes hydroformylation but also shows extensive hydrogenation of the double bond and degradation of starting material (entry 10). Second, the tertiary amide N-4-phenyl-1-butenylpyrrolidinone hydroformylates at much

The N-styryl enamides examined undergo hydro-formylation with lower regioselectivity than that seen for enamides with pendant alkyl chains. Presumably this reflects competition between the aryl (which directs formyl insertion in the β position) vs carboxamido (which directs formyl insertion in the α position) directing effects. Because styrene exhibits strongly CO-pressure dependent selectivity, we examined the AHF of N-((Z)-2-phenylvinyl) benzamide as a function of pressure (Figure 2.3).

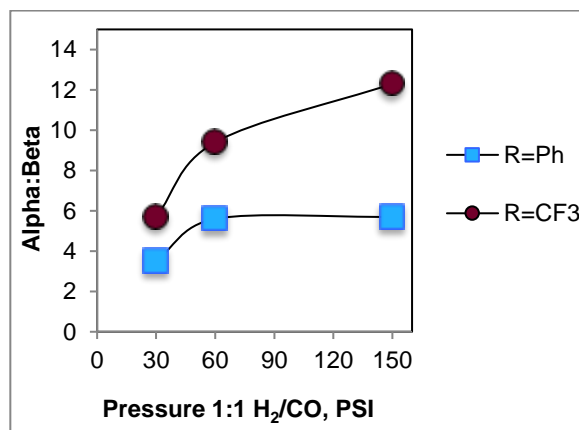
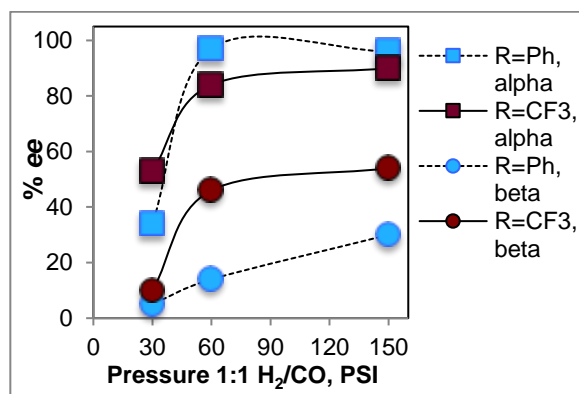
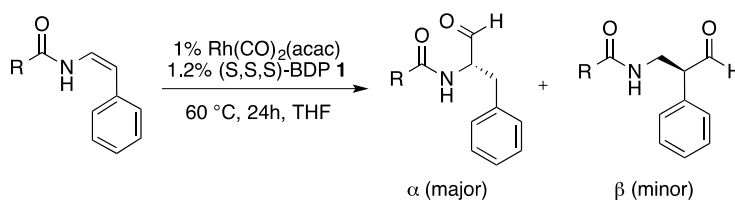


Figure 2.3. Pressure effects on AHF of styrenyl enamides.

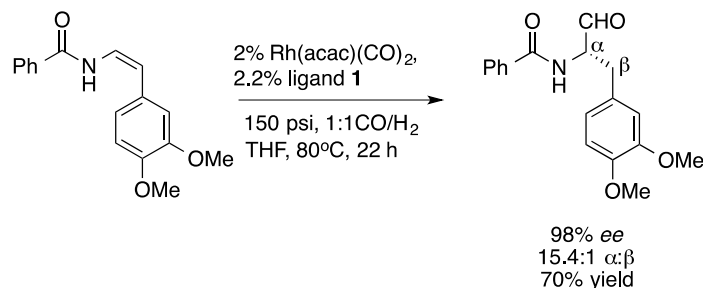
As seen for simple styrenes, the regio- and enantioselectivity of (Z)-styreneamides decrease with decreased syngas pressure. Increasing the electron-withdrawing nature of the carboxamide (trifluoroacetamido vs. benzamido) improves the regioselectivity at a given syngas pressure and the trend of increasing regio- and enantioselectivity with increased syngas pressure persevere. Such results demonstrate the importance of manipulating reaction conditions to control selectivity in the hydroformylation of styrenyl substrates.

2.1.3. Synthesis of a L-DOPA building block

AHF provides more atom efficient and direct access to highly enantioenriched α -amino aldehydes than methods involving multiple-step reactions and multiple changes in oxidation state to reach the desired aldehyde functionality.¹⁵ Although alpha substituted aldehydes potentially are susceptible to racemization via enolization, the intrinsically neutral conditions unique to aldehyde synthesis by hydroformylation obviate racemization even at temperatures in excess of 100 °C.¹⁶ As a demonstration of the practical utility of AHF, the synthesis of a protected L-DOPA aldehyde was performed. While the acid form is accessible through various synthetic methods (the most notable of which is Knowles' asymmetric hydrogenation), the aldehyde form is a valuable intermediate for formation of peptides and analogs.¹⁷

The desired Z-enamide was synthesized by Ru-catalyzed coupling of benzamide to an alkyne de-rived from vanillin.¹⁸ Asymmetric hydroformylation of this substrate proceeds cleanly to produce the aldehyde with 98% ee and 15.4:1 branch selectivity. The improved selectivity relative to the styrenyl enamides in Figure 2.3 is likely due to the electron-

donating methoxy substituents on the aryl ring disfavoring acyl formation at the β position.^{8b}



Scheme 2.2. AHF of enamides applied to the synthesis of protected analog of L-DOPA aldehyde

2.3. Conclusions

AHF provides a direct, catalytic, and atom-efficient route to useful chiral building blocks, including un-natural amino aldehydes. A variety of Z enol esters and enamides undergo asymmetric hydroformylation in the presence of **L1** and Rh(acac)(CO)₂ to produce α -chiral aldehydes with high regio- and enantioselectivity. Five of the products were determined to have the S configuration by comparison of optical rotations of known compounds; all data are consistent with S configurations for all aldehydes reported herein. These studies highlight critical attributes of the BisDiazaphos hydroformylation catalysts: high intrinsic reactivity (with complete conversion and > 90% ee in just 90 minutes at 0.3 mol% catalyst loading in simple pressure bottles), reliably high enantioselectivities (>90% ee) for a variety of Z-enol esters and enamides, and tolerance of functional groups such as phenols, thioethers, aryl bromides, and benzylic chlorides. For 1,2-disubstituted alkenes with competing regiodirecting substituents, such as styrenyl

enamides, increased pressure can effect increased regio- and enantioselectivities for the α -carboxamido aldehyde. Overall, these results significantly expand efficient access to chiral α -functionalized aldehydes.

2.4. Experimental

2.4.1. General

All manipulations were carried out under nitrogen using standard Schlenk, high vacuum, and glovebox techniques. Ethyl acetate, hexane, dichloromethane and anhydrous DMF were obtained from Sigma-Aldrich. Dichloro(*p*-cymene)Ru(II) dimer and Ru(COD)(2-methallyl)₂ were purchased from Alfa Aesar. Dicyclohexylphosphinobutane, tris-(*p*-Cl-C₆H₄) phosphine, DMAP, and all alkynes, carboxylic acids, and primary amides were purchased from Sigma-Aldrich. Unless mentioned below, all chemicals were purchased and used without further purification. Enol esters^{12,13} and enamides¹⁴ were prepared by literature methods and purified by silica column chromatography prior to use (see section II). Bisdiazaphospholane ligands were prepared as reported in literature.^{8g} [Rh(acac)(CO)₂] was used as received from Dow Chemical and stored in a N₂-filled glovebox. 1:1 CO:H₂ was purchased from Airgas. THF and toluene were either distilled from sodium/benzophenone ketyl under N₂ or dried by safety columns prior to use. Alkynes were degassed prior to use by either three freeze-pump-thaw cycles or sparging with N₂. Flash chromatography was performed on Silicycle Siliaflash P60 silica gel (40-63 μ m, 230-400 mesh). Chiral HPLC analysis was performed on a Gilson analytical HPLC with Chiralpak IA, IB, IC, and ID columns. Chiral super critical fluid chromatography (SFC) analysis was performed on a Berger SFC with Chiracel OJ-H or AD-H columns or on a TharSFC investigator instrument equipped with a Waters 2996 photodiode array detector.

Optical rotations were measured at room temperature using a 1 mL cell with a 0.5 dm path length on a Randolph digital polarimeter. Absolute configuration was determined by optical rotation for (-)(2S)-(benzoyloxy)heptanal, (S)-1-oxoheptan-2-yl 4-methoxybenzoate, (S)-1-oxo-5-phenylpentan-2-yl acetate, (-)(S)N-(1-Formyl-2-phenylethyl) benzamide, 2,2,2-Trifluoro-N-[(1S)-1-formyl-2-phenylethyl]acetamide and assigned by analogy for other reported aldehydes. All pressures given are gauge pressures unless otherwise noted.

NMR spectra were recorded at ambient temperature on Varian Mercury-300, Inova-500 or Unity-500 and Bruker AC-300, Avance III 400, or Avance III 500 spectrometers. ¹H and ¹³C NMR chemical shifts were referenced to tetramethylsilane if present or residual solvent. ³¹P and ¹⁹F NMR chemical shifts were referenced to TMS in the proton spectrum using the unified scale. ¹H NMR splitting patterns were designated as singlet (s), doublet (d), triplet (t), quartet (q), doublet of doublets (dd), apparent (ap), broad (br). First-order splitting patterns were assigned on the basis of the multiplet. Splitting patterns that could not be interpreted are designated as multiplet (m) or broad (br). Mass spectra were collected on a Waters (Micromass) LCT® for electrospray ionization experiments with a sample cone voltage of 20.

2.4.2. Synthesis and characterization of (Z)- enol ester and enamide substrates

All enol ester substrates were prepared according to procedures slightly modified from the reported procedures, as reported below.

General procedure for the synthesis of enol esters (Method 1)¹³

An oven-dried Schlenk flask equipped with a magnetic stir bar and carboxylic acid (1 eq, 5 mmol) was brought into a N₂ glove box. A vial was charged with [Ru(p-cumene)Cl₂]₂ (1 mol%, 0.05 mmol), P(p-Cl-C₆H₄)₃ (3 mol%, 0.15 mmol), DMAP (4 mol%, 0.20 mmol), dry toluene (15 mL) and transferred to the Schlenk flask via a Pasteur pipette, followed by 1-hexyne (1.3 eq, 6.5 mmol) via a syringe. In a fume hood, the flask was immersed in a silicone oil bath and stirred for 16 h at 60°C under N₂. When reaction complete, the solution was allowed to cool down at room temperature for 30 min, then passed through a plug of silica gel and washed with dichloromethane. The solvent was removed in vacuo and the product was purified via silica gel flash chromatography with hexane/ethyl acetate as eluents. The enol ester was filtered through a plug of silica prior to hydroformylation.

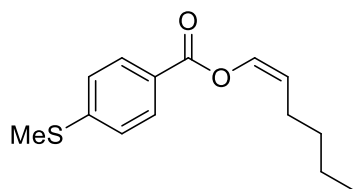
General procedure for the synthesis of enol esters (Method 2)¹²

An oven-dried Schlenk flask equipped with a magnetic stir bar and carboxylic acid (1 eq, 10 mmol) was brought into a N₂ glove box. A vial was charged with Ru(2-methallyl)2-bis(diphenylphosphino)butane (1 mol%, 0.1 mmol) and solvent (5 mL) and transferred to the Schlenk flask via a Pasteur pipette. Degassed 4-Phenyl-1-butyne (1 eq, 10 mmol) was added via a syringe in a fume hood. The flask was immersed in a silicone oil bath and stirred for 24h under N₂. When reaction complete, the solution was allowed to cool down at room temperature for 30 min, then passed through a plug of silica gel and washed with dichloromethane. The solvent was removed in vacuo and the product was purified via silica gel flash chromatography with hexane/ethyl acetate as eluents. The enol ester was filtered through a plug of silica prior to hydroformylation.

General procedure for the synthesis of enamides

All enamide substrates were prepared according to a procedure slightly modified from the reported procedure, as reported below. Their spectroscopic properties match those previously reported,^{14,19} or are reported below.

In an oven-dried Schlenk flask inside a nitrogen-filled glovebox, bis(2-methylallyl)(COD)ruthenium(II) (5%, 0.25 mmol), 1,4-bis(dicyclohexylphosphino)butane (6%, 0.30 mmol), ytterbium triflate (4%, 0.20 mmol), and amide (5.0 mmol) were combined, and anhydrous DMF (15 mL) was added. On a Schlenk line, degassed alkyne (10.0 mmol) was added via syringe, followed by N₂-sparged H₂O (0.540 mL, 30 mmol). The resulting solution was stirred for 6-18h in a 60 °C oil bath, then poured into a saturated aqueous sodium bicarbonate solution (150 mL). This mixture was extracted with ethyl acetate (3x60 mL), the combined organics were washed with water (5x50 mL) and brine (1x50 mL), dried over magnesium sulfate, filtered, and the volatiles were removed by rotary evaporation. The dark brown oil was purified by column chromatography on silica gel with 9:1 Hexane/EtOAc. Two or more columns were frequently necessary for clean product isolation.

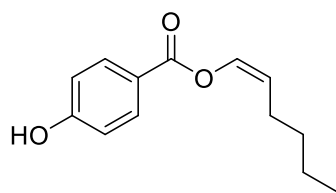


(Z)-hex-1-en-1-yl 4-(methylthio)benzoate

Prepared according to method 1. Product purified by silica gel flash chromatography (10:1 hexane/ethyl acetate) to afford a yellow oil in 72% isolated yield.

^1H NMR (400 MHz, Chloroform- d) δ 7.99 (d, J = 8.5 Hz, 2H), 7.33 – 7.20 (m, 3H), 5.05 – 4.93 (m, 1H), 2.53 (s, 3H), 2.35 – 2.23 (m, 2H), 1.48 – 1.33 (m, 4H), 0.93 (t, J = 7.0 Hz, 3H). ^{13}C NMR (101 MHz, CDCl_3) δ 163.39, 146.26, 134.17, 130.15, 125.46, 124.98, 114.72, 31.38, 24.36, 22.26, 14.80, 13.93.

HRMS (ESI-TOF) m/z : $[\text{M}]^+$ calcd for $\text{C}_{14}\text{H}_{18}\text{O}_2\text{S}$ 250.1023; found 250.1019.

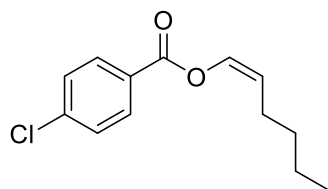


(Z)-hex-1-en-1-yl 4-hydroxybenzoate

Prepared according to method 1. Reaction refluxed in THF. Product purified by silica gel flash chromatography (5:1 hexane/ethyl acetate) to afford a dark yellow oil in 40% isolated yield.

^1H NMR (500 MHz, Chloroform- d) δ 8.08 – 7.96 (m, 2H), 7.24 – 7.21 (m, 1H), 6.97 – 6.83 (m, 2H), 4.98 (tdd, J = 7.5, 6.4, 1.3 Hz, 1H), 2.31 – 2.24 (m, 2H), 1.46 – 1.34 (m, 4H), 0.93 (t, J = 7.1 Hz, 3H). ^{13}C NMR (126 MHz, CDCl_3) δ 164.10, 160.95, 134.09, 132.33, 121.30, 115.56, 114.98, 31.34, 24.34, 22.24, 13.90.

HRMS (ESI-TOF) m/z : $[\text{M}]^+$ calcd for $\text{C}_{13}\text{H}_{16}\text{O}_3$ 220.1094; found 220.1095.



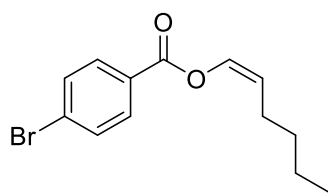
(Z)-hex-1-en-1-yl 4-chlorobenzoate

Prepared according to method 1. Product purified by silica gel flash chromatography (10:1 hexane/ethyl acetate) to afford a yellow oil in 26% isolated yield.

Characterization data agrees with previously reported results.²⁰

¹H NMR (400 MHz, Chloroform-d) δ 8.19 – 7.92 (m, 2H), 7.57 – 7.38 (m, 2H), 7.31 – 7.17 (m, 1H), 5.13 – 4.94 (m, 1H), 2.36 – 2.21 (m, 2H), 1.51 – 1.27 (m, 4H), 0.93 (d, J = 7.0 Hz, 3H). ¹³C NMR (126 MHz, CDCl₃) δ 162.79, 139.93, 134.03, 131.22, 128.92, 127.90, 115.22, 31.30, 24.35, 22.23, 13.90.

HRMS (ESI-TOF) m/z: [M]⁺ calcd for C₁₃H₁₅ClO₂ 238.0756; found 238.0759.

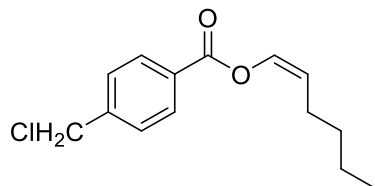


(Z)-hex-1-en-1-yl 4-bromobenzoate

Prepared according to method 1. Product purified by silica gel flash chromatography (10:1 hexane/ethyl acetate) to afford a yellow oil in 22% isolated yield.

¹H NMR (400 MHz, Chloroform-d) δ 8.01 – 7.90 (m, 2H), 7.69 – 7.57 (m, 2H), 7.23 (dt, J = 6.4, 1.6 Hz, 1H), 5.03 (td, J = 7.5, 6.3 Hz, 1H), 2.33 – 2.21 (m, 2H), 1.49 – 1.30 (m, 4H), 0.93 (t, J = 7.0 Hz, 3H). ¹³C NMR (126 MHz, CDCl₃) δ 162.92, 134.02, 131.91, 131.33, 128.62, 128.36, 115.24, 31.29, 24.35, 22.23, 13.89.

HRMS (ESI-TOF) m/z: [M]⁺ calcd for C₁₃H₁₅BrO₂ 282.0250; found 282.0252.

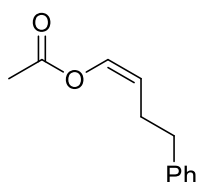


(Z)-hex-1-en-1-yl 4-(chloromethyl)benzoate

Prepared according to method 1. Product purified by silica gel flash chromatography (10:1 hexane/ethyl acetate) to afford a light yellow oil in 15% isolated yield.

^1H NMR (500 MHz, Chloroform- d) δ 8.13 – 8.07 (m, 2H), 7.54 – 7.47 (m, 2H), 7.25 (dt, J = 6.3, 1.6 Hz, 1H), 5.02 (td, J = 7.5, 6.3 Hz, 1H), 4.63 (s, 2H), 2.35 – 2.25 (m, 2H), 1.48 – 1.33 (m, 4H), 0.93 (t, J = 7.1 Hz, 3H). ^{13}C NMR (126 MHz, CDCl_3) δ 162.05, 141.72, 133.07, 129.26, 128.39, 127.59, 114.07, 44.27, 30.28, 23.31, 21.20, 12.86.

HRMS (ESI-TOF) m/z : $[\text{M}]^+$ calcd for $\text{C}_{14}\text{H}_{17}\text{ClO}_2$ 252.0912; found 252.0903.



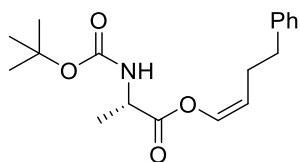
(Z)-4-phenylbut-1-en-1-yl acetate

Prepared according to method 2, using 2 mol% catalyst loading. Reaction run in hexane at 40°C for 24 h. Product purified by silica gel flash chromatography (10:1 hexane/ethyl acetate) to afford a clear oil in 75% isolated yield.

^1H NMR (500 MHz, Chloroform- d) δ 7.31 – 7.27 (m, 2H), 7.20 (d, J = 7.3 Hz, 2H), 7.01 (dt, J = 6.4, 1.4 Hz, 1H), 4.90 (td, J = 7.4, 6.2 Hz, 1H), 2.70 (t, J = 7.7 Hz, 2H), 2.54 – 2.40

(m, 2H), 2.11 (s, 3H). ^{13}C NMR (126 MHz, CDCl_3) δ 168.04, 141.55, 134.39, 128.43, 128.31, 125.95, 112.97, 35.35, 26.21, 20.72.

HRMS (ESI-TOF) m/z : $[\text{M}]^+$ calcd for $\text{C}_{12}\text{H}_{14}\text{O}_2$ 190.0989; found 190.0990.

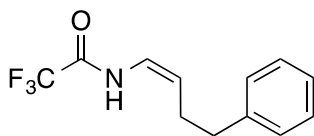


(*S,Z*)-4-phenylbut-1-en-1-yl 2-((tert-butoxycarbonyl)amino)propanoate

Prepared according to method 2. Reaction ran in toluene for 24 h at 75°C. Product purified by silica gel flash chromatography (10:1 hexane/ethyl acetate) to afford a light orange oil in 55% isolated yield.

^1H NMR (500 MHz, Chloroform- d) δ 7.31 – 7.24 (m, 2H), 7.23 – 7.14 (m, 3H), 7.00 (d, J = 6.3 Hz, 1H), 5.03 (d, J = 8.0 Hz, 1H), 4.96 (td, J = 7.4, 6.2 Hz, 1H), 4.37 (h, J = 6.3, 5.2 Hz, 1H), 2.69 (t, J = 7.6 Hz, 2H), 2.54 – 2.42 (m, 2H), 1.44 (s, 9H), 1.39 (d, J = 7.2 Hz, 3H). ^{13}C NMR (126 MHz, CDCl_3) δ 170.47, 155.04, 141.37, 134.29, 128.44, 125.98, 113.96, 80.01, 53.43, 49.04, 35.23, 28.30, 26.22, 18.47.

HRMS (ESI-TOF) m/z : $[\text{M}+\text{NH}_4]^+$ calcd for $\text{C}_{18}\text{H}_{25}\text{NO}_4$ 337.2122; found 337.2119.

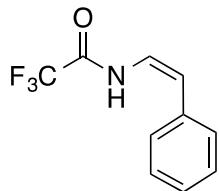


20% yield. Yellow oil.

^1H NMR (400 MHz, Chloroform- d) δ 7.37 – 7.12 (m, 6H), 6.57 (t, J = 9.7 Hz, 1H), 5.12 (ap. q, J = 8.2 Hz, 1H), 2.74 (t, J = 7.1 Hz, 2H), 2.36 (ap. q, J = 7.3 Hz, 2H). ^{19}F NMR

(377 MHz, CDCl₃) δ -75.64 (Z isomer), -75.87 (E isomer). ¹³C NMR (101 MHz, CDCl₃) δ 154.22 (q, J = 37.8 Hz), 140.79, 128.80, 128.43, 126.51, 119.67, 115.63, 115.49 (q, J = 287 Hz), 34.96, 28.23.

HRMS (EI) m/z: [M]⁺ Calcd for C₁₂H₁₂F₃NO 243.0866; found 243.0857.



69% yield (after two flash column chromatography purifications). Yellow oil.

¹H NMR (400 MHz, Chloroform-d) δ 8.31 (br s, 1H), 7.49 – 7.39 (m, 2H), 7.39 – 7.29 (m, 1H), 7.30 – 7.25 (m, 2H), 6.90 (dd, J = 10.9, 9.4 Hz, 1H), 6.10 (d, J = 9.4 Hz, 1H). ¹⁹F NMR (377 MHz, CDCl₃) δ -75.81. ¹³C NMR (101 MHz, CDCl₃) δ 154.57 (q, J = 38 Hz), 134.13, 129.57, 128.16, 127.93, 119.46, 115.78, 115.69 (q, J = 287 Hz), 77.16.

HRMS (EI) m/z: [M]⁺ Calcd for C₁₀H₈F₃NO 215.0553; found 215.0551.

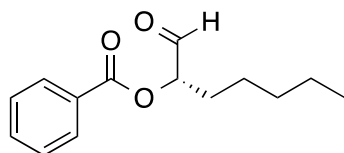
2.4.3. Synthesis and Characterization of Aldehydes

General Method for Hydroformylation

Inside a N₂-purged glovebox, an oven-dried 15mL Ace Glass pressure bottle equipped with a magnetic stir bar was charged with THF stock solutions of Rh(acac)(CO)₂ and bisdiazaphospholane ligand **L1** using 1000μL and 200μL Eppendorf® pipets. The pressure bottle was attached to a pressure reactor and removed from the glovebox, placed in a fume hood, subjected to 5 pressurization (140 psi)/depressurization (15 psi) cycles with syngas to ensure replacement of the dinitrogen atmosphere with syngas, then

filled to the appropriate syngas pressure. The solution was allowed to stir at high speed to ensure gas mixing for 30-60 min in an oil bath at the reaction temperature. The reaction vessel was then removed from the oil bath and allowed to cool for 5 minutes, then the pressure was reduced to <10 psig and the olefin was injected with a gas-tight syringe with a 12 inch needle. Solid olefins were injected as a solution in THF. Reactions were run at 0.8-1.3 M final concentration of olefin. The reaction was then re-pressurized to the reaction pressure after additional pressurization/depressurization cycles and replaced in the oil bath. Upon completion of the reaction, the pressure bottle was removed from the oil bath, allowed to cool to room temperature, and vented in a fume hood. NMR spectra are initially obtained of the crude reaction mixture by adding acetone-d₆, MeOD, or CDCl₃ directly to the reaction mixture. NMR yields were determined by addition of a solution of internal standard (1,3,5-trimethoxybenzene or mesitylene) in NMR solvent and acquiring spectra with a sufficiently long delay. Enantiomeric excess of the branched hydroformylation product was determined by chiral SFC or HPLC.

Data for Enol Ester AHF



(-)(2S)-(Benzoyloxy)heptanal:

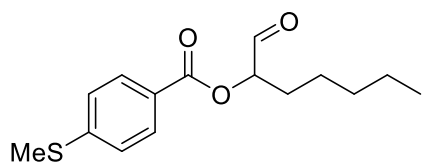
Yield 1.09g (92.0%), 97% ee, colorless oil.

$[\alpha]^{20}_{\text{D}} = -14.7$, $c = 1.24$ in CHCl₃. Lit. $[\alpha]^{20}_{\text{D}} = -31.1$ ($c = 1.41$, CH₂Cl₂).²¹

ABX, ap dd, $J = 12.1, 6.2$ Hz, 1H), 1.81 – 1.66 (m, 2H), 1.66 – 1.27 (m, 6H), 0.93 – 0.83 (m, 3H).

B: (S)-2-hydroxyheptyl benzoate (rearranged)

¹H NMR (400 MHz, Chloroform-*d*) δ 8.08 – 8.01 (m, 2H), 7.56 (tt, $J = 7.5, 1.2$ Hz, 1H), 7.47 – 7.39 (m, 2H), 4.38 (A of ABX, ap dd, $J = 11.4, 3.2$ Hz, 1H), 4.22 (B of ABX, ap dd, $J = 11.4, 7.1$ Hz, 1H), 4.02 – 3.94 (X of ABX, m, 1H), 1.61 – 1.52 (m, 2H), 1.52 – 1.27 (m, 6H), 0.89 (t, $J = 6.9$ Hz, 3H).



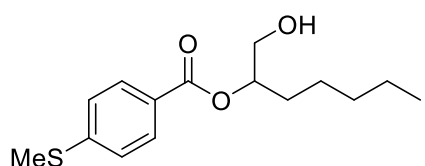
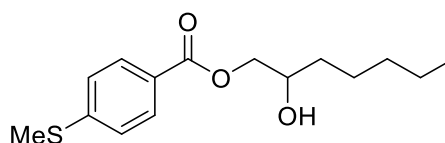
(S)-1-oxoheptan-2-yl 4-(methylthio)benzoate

Crude hydroformylation mixture filtered through a plug of silica and washed with dichloromethane. 84% isolated yield, yellow oil.

¹H NMR (400 MHz, Chloroform-*d*) δ 9.63 (d, $J = 0.9$ Hz, 1H), 7.99 (d, $J = 8.5$ Hz, 2H), 7.28 (d, $J = 8.5$ Hz, 2H), 5.19 (ddd, $J = 8.2, 5.0, 1.0$ Hz, 1H), 2.53 (s, 3H), 2.05 – 1.79 (m, 2H), 1.63 – 1.45 (m, 2H), 1.44 – 1.23 (m, 4H), 0.92 – 0.87 (m, 3H). ¹³C NMR (101 MHz, CDCl₃) δ 198.70, 165.94, 146.44, 130.13, 125.20, 124.98, 78.72, 31.45, 28.90, 24.70, 22.40, 14.82, 13.96.

Enantiomeric excess was determined to be 90% by chiral HPLC analysis, after NaBH₄ reduction in MeOH at room temperature for 16 h, followed by addition of sat. aq. NH₄Cl solution, extraction with dichloromethane and drying over MgSO₄. The reduction conditions afford a mixture of two alcohol isomers, A and B, after partial migration of the

benzoyl protecting group from the secondary alcohol to the primary alcohol, as well as a transesterification by-product in the presence of MeOH. The mixture of alcohols was purified by silica gel flash chromatography (2:1 hexanes/ethyl acetate) prior to HPLC analysis.

**A****B**

Alcohol isomers:

A: (S)-1-hydroxyheptan-2-yl 4-(methylthio)benzoate

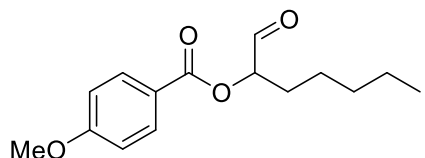
^1H NMR (500 MHz, Chloroform-d) δ 7.92 – 7.82 (m, 2H), 7.22 – 7.14 (m, 2H), 5.10 – 5.03 (m, 1H), 3.74 (dd, $J = 12.1, 3.3$ Hz, 1H), 3.67 (dd, $J = 12.1, 6.2$ Hz, 1H), 2.44 (s, 3H), 2.21 (s, 1H), 1.73 – 1.55 (m, 2H), 1.54 – 1.12 (m, 6H), 0.90 – 0.74 (m, 3H). ^{13}C NMR (126 MHz, CDCl_3) δ 165.83, 144.68, 128.82, 125.19, 123.86, 75.33, 63.96, 30.59, 29.62, 23.99, 21.43, 13.76, 12.93.

B: (S)-2-hydroxyheptyl 4-(methylthio)benzoate (rearranged)

^1H NMR (500 MHz, Chloroform-d) δ 7.92 – 7.82 (m, 2H), 7.22 – 7.14 (m, 2H), 4.29 (A of ABX, ap dd, $J = 11.4, 3.2$ Hz, 1H), 4.18 – 4.10 (m, 1H), 3.93 – 3.86 (m, 1H), 2.44 (s, 3H), 2.21 (br, 1H), 1.54 – 1.12 (m, 8H), 0.90 – 0.74 (m, 3H). ^{13}C NMR (126 MHz, CDCl_3) δ 165.47, 144.79, 128.90, 124.90, 123.86, 69.11, 68.12, 32.41, 30.72, 24.06, 21.53, 13.75, 12.98.

HRMS (ESI-TOF) m/z: [M]⁺ calcd for C₁₅H₂₂O₃S 282.1285; found 282.1290.

Separation by HPLC: CHIRALPAK 1A (AD-H), 3% iPrOH/hexanes, 0.9 ml/min, ambient temperature, 220 nm, tR (A): 31.5 min (major, (S)), 36.7 min (minor, (R)), tR (B): 44.7 min (major, (S)), 51.6 min (minor, (R))



(S)-1-oxoheptan-2-yl 4-methoxybenzoate

Crude hydroformylation mixture filtered through a plug of silica and washed with dichloromethane. 85% isolated yield, yellow oil.

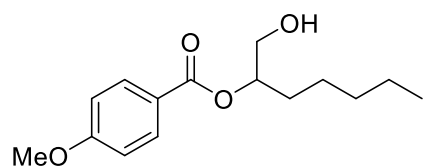
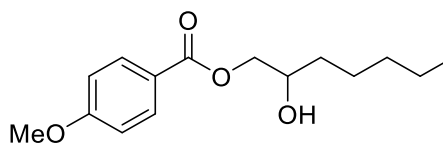
¹H NMR (500 MHz, Chloroform-d) δ 9.63 (d, J = 1.0 Hz, 1H), 8.06 (d, J = 8.9 Hz, 2H), 7.05 – 6.84 (d, J = 8.9 Hz, 2H), 5.17 (ddd, J = 8.2, 4.9, 1.0 Hz, 1H), 3.88 (s, 3H), 2.02 – 1.79 (m, 2H), 1.55 – 1.45 (m, 2H), 1.40 – 1.15 (m, 4H), 1.05 – 0.74 (m, 3H). ¹³C NMR (126 MHz, CDCl₃) δ 198.97, 165.91, 163.83, 131.94, 121.54, 113.80, 78.54, 55.50, 31.44, 28.93, 24.68, 22.38, 13.94.

HRMS (ESI-TOF) m/z: [M+H]⁺ calcd for C₁₅H₂₀O₄ 265.1435; found 265.1438.

[α]²⁰_D = -19.4, c = 1.00 in EtOH. Lit. [α]²⁰_D = -20.6 (c = 1.00, EtOH) for 1,2-Heptanediol.²²

Optical rotation and assignment of absolute configuration were determined by reduction of the aldehyde with LiAlH₄ in dry THF at 0°C warming to room temperature for 24 h total reaction time, followed by slow addition of MeOH, sat aq. NH₄Cl and extraction with ethyl acetate of the resulting 1,2-Heptanediol.

Enantiomeric excess was determined to be 96% by chiral HPLC analysis, after NaBH₄ reduction in MeOH at room temperature for 6 h, followed by addition of sat. aq. NH₄Cl solution, extraction with dichloromethane and drying over MgSO₄. The reduction conditions afford a mixture of two alcohol isomers, A and B, after partial migration of the benzoyl protecting group from the secondary alcohol to the primary alcohol.

**A****B**

Alcohol isomers:

A: (S)-1-hydroxyheptan-2-yl 4-methoxybenzoate

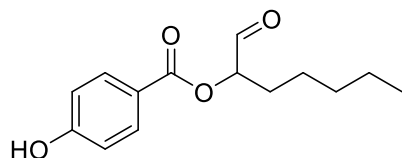
¹H NMR (500 MHz, Chloroform-d) δ 7.96 – 7.89 (m, 2H), 6.87 – 6.81 (m, 2H), 5.10 – 4.99 (m, 1H), 3.77 (s, 1H), 3.75 – 3.64 (m, 2H), 2.39 (br, 1H), 1.72 – 1.55 (m, 2H), 1.52 – 1.16 (m, 6H), 0.87 – 0.75 (m, 3H). ¹³C NMR (126 MHz, CDCl₃) δ 166.77, 163.47, 131.71, 122.57, 113.62, 76.15, 65.03, 55.43, 31.65, 30.72, 25.05, 22.48, 13.98.

B (S)-2-hydroxyheptyl 4-methoxybenzoate (rearranged)

¹H NMR (500 MHz, Chloroform-d) δ 7.96 – 7.89 (m, 2H), 6.87 – 6.81 (m, 2H), 4.27 (A of ABX, ap dd, J = 11.5, 3.2 Hz, 1H), 4.11 (B of ABX, ap dd, J = 11.4, 7.1 Hz, 1H), 3.94 – 3.84 (X of ABX, m, 1H), 3.77 (s, 1H), 2.39 (br, 1H), 1.52 – 1.16 (m, 8H), 0.87 – 0.75 (m, 3H). ¹³C NMR (126 MHz, CDCl₃) δ 166.54, 163.50, 131.71, 122.29, 113.65, 70.17, 69.01, 55.43, 33.46, 31.78, 25.12, 22.58, 14.02.

HRMS (ESI-TOF) m/z : $[M+H]^+$ calcd for $C_{15}H_{22}O_4$ 267.1591; found 267.1599.

Separation by HPLC: CHIRALPAK 1A (AD-H), 5% *i*PrOH/hexanes, 0.8 ml/min, ambient temperature, 254 nm, t_R (A): 20.3 min (major, (S)), 23.6 min (minor, (R)), t_R (B): 26.0 min (major, (S)), 28.7 min (minor, (R)).



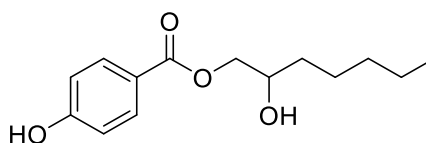
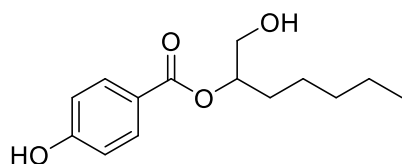
(Z)-hex-1-en-1-yl 4-hydroxybenzoate

Crude hydroformylation mixture filtered through a plug of silica and washed with dichloromethane. 82% isolated yield, dark yellow oil stored under dinitrogen.

1H NMR (500 MHz, Chloroform-*d*) δ 9.64 (s, 1H), 8.00 (d, J = 7.9 Hz, 2H), 7.00 – 6.81 (m, 2H), 6.31 (broad s, 1H), 5.19 (dd, J = 8.3, 4.8 Hz, 1H), 2.04 – 1.79 (m, 2H), 1.57 – 1.45 (m, 2H), 1.40 – 1.29 (m, 4H), 0.96 – 0.87 (m, 3H). ^{13}C NMR (126 MHz, $CDCl_3$) δ 198.12, 165.16, 159.65, 131.24, 120.29, 114.43, 77.64, 30.40, 27.83, 23.66, 21.34, 12.90.

HRMS (ESI-TOF) m/z : $[M+H]^+$ calcd for $C_{14}H_{18}O_4$ 251.1278; found 251.1280.

Enantiomeric excess was determined to be 99% by chiral SFC analysis, after $NaBH_4$ reduction in MeOH at room temperature for 5 h, followed by addition of sat. aq. NH_4Cl solution, extraction with dichloromethane and drying over $MgSO_4$.



A**B**

Alcohol isomers:

A: (S)-1-hydroxyheptan-2-yl 4-hydroxybenzoate

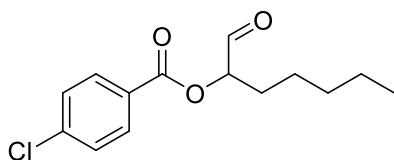
¹H NMR (500 MHz, Chloroform-d) δ 7.98 – 7.92 (m, 2H), 6.88 – 6.83 (m, 2H), 5.19 – 5.09 (m, 1H), 3.84 (A of ABX, ap dd, J = 12.2, 3.0 Hz, 1H), 3.76 (B of ABX, ap dd, J = 12.1, 6.4 Hz, 1H), 2.36 – 2.23 (m, 1H), 1.82 – 1.17 (m, 8H), 0.96 – 0.81 (m, 3H).

¹³C NMR (126 MHz, CDCl₃) δ 166.91, 160.13, 132.05, 122.50, 115.25, 76.24, 65.28, 31.64, 30.69, 25.06, 22.48, 13.99.

B: (S)-2-hydroxyheptyl 4-hydroxybenzoate (rearranged)

¹H NMR (500 MHz, Chloroform-d) δ 7.96 – 7.93 (m, 2H), 6.88 – 6.83 (m, 2H), 4.38 (A of ABX, ap dd, J = 11.5, 3.0 Hz, 1H), 4.20 (B of ABX, ap dd, J = 11.5, 7.2 Hz, 1H), 4.04 – 3.95 (m, 1H), 2.36 – 2.23 (m, 1H), 1.82 – 1.17 (m, 8H), 0.96 – 0.81 (m, 3H). ¹³C NMR (126 MHz, CDCl₃) δ 166.60, 160.17, 132.03, 122.24, 115.28, 70.46, 68.98, 33.42, 31.76, 25.11, 22.57, 14.03.

Separation by SFC: AD-H, 5% modifier, 3 ml/min, methanol, 23.4°C, 101 bar, tR (A): 6.36 min (major, (S)), 8.66 min (minor, (R)).

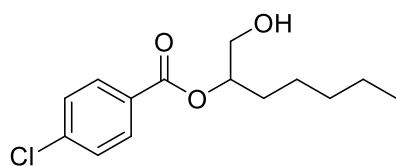
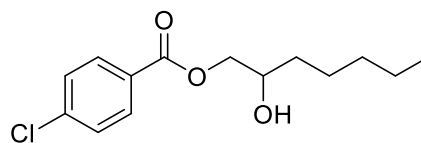
**(S)-1-oxoheptan-2-yl 4-chlorobenzoate**

Crude hydroformylation mixture filtered through a plug of silica and washed with dichloromethane. 88% isolated yield, yellow oil.

^1H NMR (500 MHz, Chloroform- d) δ 9.63 (d, J = 0.8 Hz, 1H), 8.15 – 7.97 (m, 2H), 7.53 – 7.39 (m, 2H), 5.23 (dd, J = 8.3, 4.7 Hz, 1H), 2.04 – 1.81 (m, 2H), 1.63 – 1.43 (m, 2H), 1.34 (dtp, J = 7.4, 5.0, 2.6 Hz, 4H), 1.00 – 0.85 (m, 3H). ^{13}C NMR (101 MHz, CDCl_3) δ 198.07, 165.29, 140.06, 131.24, 128.92, 127.69, 79.00, 31.43, 28.78, 24.70, 22.38, 13.95.

HRMS (ESI-TOF) m/z : $[\text{M}]^+$ calcd for $\text{C}_{14}\text{H}_{17}\text{ClO}_3$ 268.0861; found 268.0851.

Enantiomeric excess was determined to be 96% by chiral HPLC analysis, after NaBH_4 reduction in MeOH at room temperature for 6 h, followed by addition of sat. aq. NH_4Cl solution, extraction with dichloromethane and drying over MgSO_4 . The reduction conditions afford a mixture of two alcohol isomers, A and B, after partial migration of the benzoyl protecting group from the secondary alcohol to the primary alcohol. Another by-product was detected in the region 3.4-3.73 ppm in ^1H NMR, tentatively assigned as a diol formed upon reduction of the ester group. The mixture was purified by silica gel flash chromatography (3:1 hexanes/ethyl acetate) prior to HPLC analysis.

**A****B**

Alcohol isomers:

A: (S)-1-hydroxyheptan-2-yl 4-chlorobenzoate

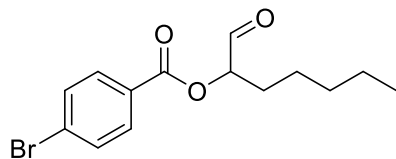
^1H NMR (500 MHz, Chloroform- d) δ 7.99 (d, J = 8.2 Hz, 2H), 7.45 – 7.39 (m, 2H), 5.22 – 5.11 (m, 1H), 3.87 – 3.73 (m, 2H), 1.81 – 1.64 (m, 2H), 1.60 – 1.17 (m, 6H), 0.94 – 0.83 (m, 3H). ^{13}C NMR (126 MHz, CDCl_3) δ 165.07, 138.53, 130.03, 127.71, 127.61, 75.66, 63.80, 30.58, 29.57, 23.99, 21.43, 12.93.

B: (S)-2-hydroxyheptyl 4-chlorobenzoate (rearranged)

^1H NMR (500 MHz, Chloroform- d) δ 7.99 (d, J = 8.2 Hz, 2H), 7.45 – 7.39 (m, 2H), 4.43 – 4.33 (m, 1H), 4.23 (ap dd, J = 11.5, 7.1 Hz, 1H), 4.03 – 3.93 (m, 1H), 1.60 – 1.17 (m, 8H), 0.94 – 0.83 (m, 3H). ^{13}C NMR (126 MHz, CDCl_3) δ 164.90, 138.62, 130.02, 127.76, 127.32, 69.05, 68.36, 32.43, 30.72, 24.06, 21.54, 12.99.

HRMS (ESI-TOF) m/z : $[\text{M}]^+$ calcd for $\text{C}_{14}\text{H}_{19}\text{ClO}_3$ 270.1018; found 270.1026.

Separation by HPLC: CHIRALPAK 1A (AD-H), 2% $i\text{PrOH}$ /hexanes, 0.6 ml/min, ambient temperature, 254 nm, t_R (A): 48.4 min (major, (S)), 55.3 min (minor, (R)).



(S)-1-oxoheptan-2-yl 4-bromobenzoate

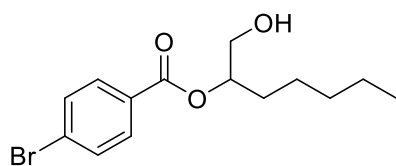
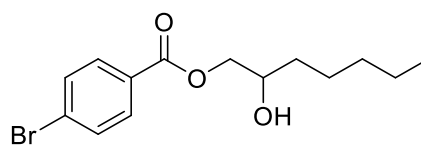
Crude hydroformylation mixture filtered through a plug of silica and washed with dichloromethane. 82% isolated yield, yellow oil.

^1H NMR (500 MHz, Chloroform- d) δ 9.63 (s, 1H), 7.96 (d, J = 8.5 Hz, 2H), 7.62 (d, J = 8.5 Hz, 2H), 5.23 (ddd, J = 8.0, 5.0, 0.8 Hz, 1H), 2.02 – 1.75 (m, 2H), 1.56 – 1.44 (m, 2H),

1.40 – 1.28 (m, 4H), 0.98 – 0.81 (m, 3H). ^{13}C NMR (126 MHz, CDCl_3) δ 196.98, 164.38, 130.87, 130.29, 127.70, 127.09, 77.97, 30.37, 27.72, 23.65, 21.33, 12.89.

HRMS (ESI-TOF) m/z : $[\text{M}]^+$ calcd for $\text{C}_{14}\text{H}_{17}\text{BrO}_3$ 312.0356; found 312.0364.

Enantiomeric excess was determined to be 92% by chiral SFC analysis, after NaBH_4 reduction in MeOH at room temperature for 6 h, followed by addition of sat. aq. NH_4Cl solution, extraction with dichloromethane and drying over MgSO_4 . The reduction conditions afford a mixture of two alcohol isomers, A and B, after partial migration of the benzoyl protecting group from the secondary alcohol to the primary alcohol. Another by-product was detected, tentatively assigned as transesterification product in the presence of MeOH.

**A****B**

Alcohol isomers:

A: (S)-1-hydroxyheptan-2-yl 4-bromobenzoate

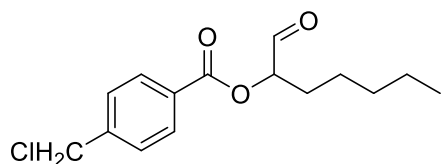
^1H NMR (500 MHz, Chloroform- d) δ 7.97 – 7.85 (m, 2H), 7.62 – 7.55 (m, 2H), 5.23 – 5.11 (X of ABX, m, 1H), 3.83 (A of ABX, ap dd, $J = 12.1, 3.2$ Hz, 1H), 3.76 (B of ABX, ap dd, $J = 12.1, 6.2$ Hz, 1H), 1.85 – 1.63 (m, 2H), 1.62 – 1.16 (m, 6H), 0.97 – 0.80 (m, 3H). ^{13}C NMR (126 MHz, CDCl_3) δ 165.17, 130.71, 130.16, 128.64, 128.07, 75.69, 63.84, 30.58, 29.55, 23.99, 21.43, 12.94.

B: (S)-2-hydroxyheptyl 4-bromobenzoate (rearranged)

^1H NMR (500 MHz, Chloroform- d) δ 7.97 – 7.85 (m, 2H), 7.62 – 7.55 (m, 2H), 4.38 (A of ABX, ap dd, J = 11.4, 3.2 Hz, 1H), 4.28 – 4.18 (B of ABX, m, 1H), 4.02 – 3.94 (m, 1H), 1.62 – 1.16 (m, 8H), 0.97 – 0.80 (m, 3H). ^{13}C NMR (126 MHz, CDCl_3) δ 165.00, 130.76, 130.15, 128.63, 127.79, 69.06, 68.40, 32.43, 30.71, 24.05, 21.54, 12.99.

HRMS (ESI-TOF) m/z : $[\text{M}+\text{H}]^+$ calcd for $\text{C}_{14}\text{H}_{19}\text{BrO}_3$ 315.0591; found 315.0589.

Separation by SFC: Chiralcel OJ-H, 4% modifier, 4 ml/min, methanol, 50°C, 150 bar, tR (A): 5.0 min (major, (S)), 6.5 min (minor, (R)), tR (B): 7.3 min (minor,(R)), 9.8 min (major, (S)).

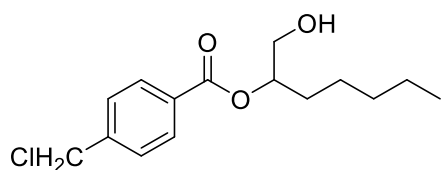
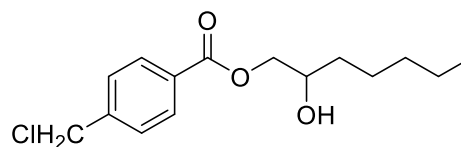
**(S)-1-oxoheptan-2-yl 4-(chloromethyl)benzoate**

Crude hydroformylation mixture filtered through a plug of silica and washed with dichloromethane. 78% isolated yield, yellow oil.

^1H NMR (400 MHz, Chloroform- d) δ 9.63 (d, J = 0.9 Hz, 1H), 8.13 – 8.06 (m, 2H), 7.53 – 7.47 (m, 2H), 5.23 (dd, J = 8.2, 4.9 Hz, 1H), 4.63 (s, 2H), 2.02 – 1.83 (m, 2H), 1.57 – 1.45 (m, 2H), 1.40 – 1.30 (m, 4H), 0.95 – 0.86 (m, 3H). ^{13}C NMR (101 MHz, CDCl_3) δ 198.31, 161.54, 142.94, 130.31, 129.18, 128.66, 78.92, 45.30, 31.43, 28.83, 24.70, 22.39, 13.96.

Enantiomeric excess was determined to be 92% by chiral HPLC analysis, after NaBH_4 reduction in MeOH at room temperature for 6 h, followed by addition of sat. aq. NH_4Cl

solution, extraction with dichloromethane and drying over MgSO₄. The reduction conditions afford a mixture of two alcohol isomers, A and B, after partial migration of the benzoyl protecting group from the secondary alcohol to the primary alcohol. The mixture was purified by silica gel flash chromatography (3:1 hexanes/ethyl acetate) prior to HPLC analysis.

**A****B**

Alcohol isomers:

A: (S)-1-hydroxyheptan-2-yl 4-(chloromethyl)benzoate

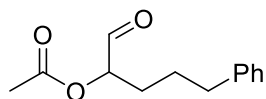
¹H NMR (500 MHz, Chloroform-d) δ 8.05 (d, J = 8.1 Hz, 2H), 7.47 (d, J = 8.1 Hz, 2H), 5.23 – 5.12 (m, 1H), 4.62 (s, 2H), 3.84 (ap dd, J = 12.1, 3.3 Hz, 1H), 3.77 (ap dd, J = 12.1, 6.3 Hz, 1H), 2.09 (s, 1H), 1.83 – 1.64 (m, 2H), 1.62 – 1.22 (m, 6H), 0.95 – 0.83 (m, 3H).
¹³C NMR (126 MHz, CDCl₃) δ 166.40, 142.45, 130.16, 130.12, 128.52, 76.60, 64.98, 45.34, 31.62, 30.62, 25.02, 22.47, 13.97.

B: (S)-2-hydroxyheptyl 4-(chloromethyl)benzoate (rearranged)

¹H NMR (500 MHz, Chloroform-d) δ 8.09 – 8.02 (m, 2H), 7.47 (d, J = 8.1 Hz, 2H), 4.62 (s, 2H), 4.39 (A of ABX, ap dd, J = 11.4, 3.1 Hz, 1H), 4.23 (B of ABX, ap dd, J = 11.4, 7.1 Hz, 1H), 4.04 – 3.94 (m, 1H), 2.09 (br s, 1H), 1.62 – 1.22 (m, 8H), 0.95 – 0.83 (m, 3H).
¹³C NMR (126 MHz, CDCl₃) δ 166.22, 142.51, 130.10, 129.86, 128.54, 70.14, 69.34, 45.32, 33.45, 31.76, 25.09, 22.57, 14.02.

HRMS (ESI-TOF) m/z : $[M+H]^+$ calcd for $C_{15}H_{21}ClO_3$ 285.1252; found 285.1249.

Separation by HPLC: CHIRALPAK 1A (AD-H), 5% iPrOH/hexanes, 0.8 ml/min, ambient temperature, 254 nm, t_R (A): 20.3 min (major, (S)), 23.6 min (minor, (R)), t_R (B): 26.0 min (major, (S)), 28.7 min (minor (R)).



(S)-1-oxo-5-phenylpentan-2-yl acetate

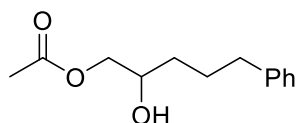
Crude hydroformylation mixture filtered through a plug of silica and washed with dichloromethane. 88% isolated yield, yellow oil.

1H NMR (400 MHz, Chloroform- d) δ 9.50 (d, J = 0.8 Hz, 1H), 7.32 – 7.25 (m, 2H), 7.24 – 7.14 (m, 3H), 5.01 (dd, J = 7.5, 4.3 Hz, 1H), 2.69 – 2.62 (m, 2H), 2.17 (s, 3H), 1.92 – 1.70 (m, 4H). ^{13}C NMR (126 MHz, $CDCl_3$) δ 198.18, 170.59, 141.31, 128.46, 128.37, 126.07, 78.13, 35.38, 28.17, 26.67, 20.62.

HRMS (ESI-TOF) m/z : $[M+H]^+$ calcd for $C_{13}H_{16}O_3$ 221.1173; found 221.1174.

$[\alpha]^{20}_D = -0.8$, $c = 1.00$ in $CHCl_3$. Lit. $[\alpha]^{RT}_D = -0.9$ ($c = 1.00$, $CHCl_3$) for 5-Phenyl-1,2-Pentenediol, $[\alpha]^{20}_D = -13.6$ ($c = 1.00$, $CHCl_3$) for (S)-4-Phenyl-1,2-Butanediol.²³ Optical rotation and assignment of absolute configuration were determined by reduction of the aldehyde with $LiAlH_4$ in dry THF at 0 °C warming to room temperature for 24 h total reaction time, followed by slow addition of MeOH, sat aq. NH_4Cl and extraction with ethyl acetate of the resulting 5-Phenyl-1,2-Pentenediol.

Enantiomeric excess was determined to be 93% by chiral HPLC analysis, after NaBH₄ reduction in MeOH at room temperature for 5 h, followed by addition of sat. aq. NH₄Cl solution, extraction with dichloromethane and drying over MgSO₄. The reduction conditions afford a mixture of two alcohol isomers, A and B, after partial migration of the benzoyl protecting group from the secondary alcohol to the primary alcohol. The mixture was purified and the two isomers separated by silica gel flash chromatography (3:1 hexanes/ethyl acetate) prior to HPLC analysis.



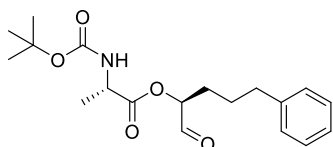
Alcohol isomer:

(S)-2-hydroxy-5-phenylpentyl acetate (rearranged):

¹H NMR (500 MHz, Chloroform-d) δ 7.30 – 7.24 (m, 2H), 7.20 – 7.15 (m, 3H), 4.11 (A of ABX, ap dd, J = 11.4, 3.0 Hz, 1H), 3.93 (B of ABX, ap dd, J = 11.4, 7.4 Hz, 1H), 3.88 – 3.81 (m, 1H), 2.64 (t, J = 7.6 Hz, 2H), 2.22 (d, J = 4.3 Hz, 1H), 2.07 (s, 3H), 1.88 – 1.75 (m, 1H), 1.74 – 1.62 (m, 1H), 1.54 – 1.47 (m, 2H). ¹³C NMR (126 MHz, CDCl₃) δ 171.26, 142.01, 128.42, 128.36, 125.86, 69.75, 68.71, 35.72, 32.83, 27.17, 20.91.

HRMS (ESI-TOF) m/z: [M+H]⁺ calcd for C₁₃H₁₈O₃ 223.1329; found 223.1329.

Separation by HPLC: CHIRALPAK 1D, 6% iPrOH/hexanes/0.1% TFA, 0.6 ml/min, ambient temperature, 220 nm, t_R: 31.3min (major, (S)), 38.8 min (minor, (R)).



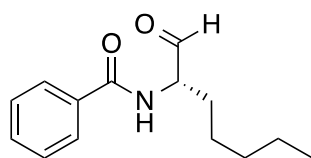
(S)-(S)-1-oxo-5-phenylpentan-2-yl 2-((tert-butoxycarbonyl)amino)propanoate

Reaction mixture filtered through a pad of celite and washed with DCM. 83% isolated yield, orange oil.

^1H NMR (400 MHz, Chloroform- d) δ 9.48 (s, 1H), 7.34 – 7.25 (m, 2H), 7.24 – 7.13 (m, 3H), 5.09 (dd, J = 7.6, 4.5 Hz, 1H), 5.02 (d, J = 7.8 Hz, 1H), 4.47 – 4.35 (m, 1H), 2.66 (dd, J = 8.0, 6.0 Hz, 2H), 1.48 (d, J = 7.2 Hz, 3H), 1.44 (s, 9H). ^{13}C NMR (126 MHz, CDCl_3) δ 197.26, 173.14, 155.14, 141.19, 128.45, 128.38, 126.05, 80.00, 78.54, 49.12, 35.31, 28.29, 27.96, 26.50, 18.55.

HRMS (ESI-TOF) m/z : $[\text{M}+\text{H}]^+$ calcd for $\text{C}_{19}\text{H}_{27}\text{NO}_5$ 350.1962; found 350.1953.

Enantiomeric excess was determined to be 92% by integration of aldehyde signals in crude ^1H NMR.

Data for Enamide AHF

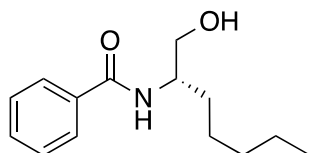
2-benzamido-heptanal.

Started with 100 mg enamide, 100% conversion.

^1H NMR (400 MHz, Chloroform- d) δ 9.67 (s, 1H), 7.91 – 7.76 (m, 2H), 7.58 – 7.49 (m, 1H), 7.49 – 7.37 (m, 2H), 6.86 (d, J = 6.9 Hz, 1H, NH), 4.76 (q, J = 6.6 Hz, 1H), 2.13 – 1.97 (m, 1H), 1.82 – 1.70 (m, 1H), 1.51 – 1.20 (m, 6H), 0.96 – 0.80 (m, 3H). ^{13}C NMR

(101 MHz, CDCl₃) δ 199.46, 167.41, 133.80, 131.88, 128.66 (2C), 127.10 (2C), 59.24, 31.60, 29.09, 24.86, 22.42, 13.96.

HRMS (ESI-TOF) m/z: [M+H]⁺ calcd for C₁₄H₂₀NO₂ 234.1489; found 234.1492.



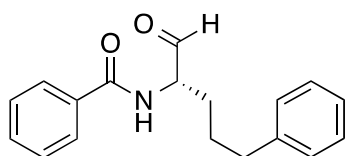
Alcohol: (S)-N-(1-hydroxyheptan-2-yl)benzamide

¹H NMR (400 MHz, Chloroform-d) δ 7.82 – 7.69 (m, 2H), 7.51 – 7.43 (m, 1H), 7.42 – 7.32 (m, 2H), 6.61 (d, J = 8.3 Hz, 1H, NH), 4.12 (m, 1H, X of ABX), 3.78 – 3.70 (m, 1H, A of ABX), 3.70 – 3.60 (m, 1H, B of ABX), 3.50 (br s, 1H, OH), 1.70 – 1.51 (m, 2H), 1.46 – 1.33 (m, 2H), 1.34 – 1.22 (m, 4H), 0.95 – 0.80 (m, 3H). ¹³C NMR (101 MHz, CDCl₃) δ 168.35, 134.50, 131.61, 128.61, 127.09, 65.37, 52.33, 31.80, 31.36, 25.98, 25.95, 22.63, 14.12.

HRMS (ESI-TOF) m/z: [M+H]⁺ calcd for C₁₄H₂₂NO₂ 236.1646; found 236.1638.

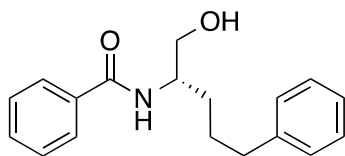
Separation by SFC: 85% ee. Chiralcel OJ-H, 50 °C, 150 bar, MeOH modifier 2% for 1 min, then ramp to 8% over 6 min, hold 20 min, 2 mL/min flow, λ = 210 nm. tr = 14.8 min (S), 16.9 min (R).

Separation by HPLC: 84% ee. Chiralpak IA, 8% 2-propanol / 92% hexane, 1 mL/min flow, ambient temperature, λ =254 or 220 nm. tr = 8.5 min (S), 11.4 min (R).



2-benzamido-5-phenylpentanal.

Started with 104 mg of enamide. 87% conversion, 81.1% yield (aldehyde).

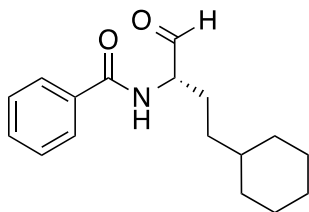


Alcohol: (S)-N-(1-hydroxy-5-phenylpentan-2-yl)benzamide

^1H NMR (500 MHz, Chloroform- d) δ 7.73 (d, J = 7.7 Hz, 2H), 7.46 (t, J = 7.4 Hz, 1H), 7.37 (t, J = 7.6 Hz, 2H), 7.26 (t, J = 7.4 Hz, 2H), 7.21 – 7.11 (m, 3H), 6.46 (d, J = 8.4 Hz, 1H), 4.23 – 4.08 (m, 1H, X of ABX), 3.79 – 3.68 (m, 1H, A of ABX), 3.68 – 3.57 (m, 1H, B of ABX), 3.10 (t, J = 5.0 Hz, 1H, OH), 2.74- 2.54 (m, 2H), 1.78- 1.68 (m, 2H), 1.68 – 1.55 (m, 2H). ^{13}C NMR (126 MHz, CDCl_3) δ 168.28, 142.02, 134.42, 131.69, 128.66, 128.52, 128.48, 127.08, 125.98, 65.41, 52.08, 35.74, 30.94, 28.08.

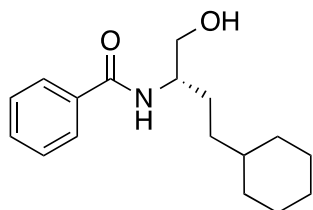
HRMS (ESI-TOF) m/z : $[\text{M}+\text{H}]^+$ calcd for $\text{C}_{18}\text{H}_{22}\text{NO}_2$ 284.1646; found 284.1652.

Separation by HPLC: 90% ee. Chiralpak IA, 8% 2-propanol / 92% hexane, 1 mL/min flow, ambient temperature, $\lambda=254$ or 220 nm. t_r = 10.2 min (major, S), 13.4 min (R).



2-benzamido-4-cyclohexylbutanal.

80% conversion, 78% isolated yield (alcohol). Started with 150 mg enamide, isolated 131.9 mg alcohol.

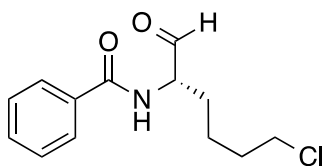


Alcohol: (S)-N-(4-cyclohexyl-1-hydroxybutan-2-yl)benzamide

^1H NMR (400 MHz, Chloroform- d) δ 7.81 – 7.72 (m, 2H), 7.50 (ddt, J = 8.7, 6.3, 1.2 Hz, 1H), 7.42 (tt, J = 6.7, 1.6 Hz, 2H), 6.37 (d, J = 7.9 Hz, 1H, NH), 4.16 – 4.05 (m, 1H, X of ABX), 3.78 (app. dd, J = 11.1, 3.5 Hz, 1H, A of ABX), 3.67 (app. dd, J = 11.0, 5.4 Hz, 1H, B of ABX), 2.96 (br. s, 1H, OH), 1.79 – 1.51 (m, 7H), 1.34 – 1.05 (m, 6H), 0.96 – 0.79 (m, 2H). ^{13}C NMR (101 MHz, CDCl_3) δ 168.26, 134.43, 131.60, 128.60 (2C), 126.99 (2C), 65.72, 52.67, 37.62, 33.84, 33.34, 33.29, 28.69, 26.62, 26.33 (2C).

HRMS (ESI-TOF) m/z : $[\text{M}+\text{H}]^+$ calcd for $\text{C}_{17}\text{H}_{26}\text{NO}_2$ 276.1959; found 276.1956.

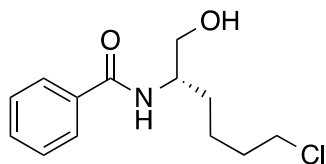
Separation by HPLC: 84% ee. Chiralpak IA, 8% 2-propanol / 92% hexane, 1 mL/min flow, ambient temperature, $\lambda=254$ or 220 nm. t_r = 8.5 min (major, S), 12.6 min (R).



Aldehyde: 2-Benzamido-6-chlorohexanal.

79% conversion, 68% isolated yield. Started with 67 mg of enamide. Isolated alcohol as a yellow oil, 52 mg.

^1H NMR (400 MHz, Chloroform- d) δ 9.69 (s, 1H), 7.88 – 7.77 (m, 2H), 7.57 – 7.50 (m, 1H), 7.50 – 7.41 (m, 2H), 6.85 (d, J = 6.8 Hz, 1H), 4.78 (td, J = 6.9, 5.5 Hz, 1H), 3.54 (td, J = 6.4, 2.1 Hz, 2H), 2.18 – 2.04 (m, 1H), 1.95 – 1.72 (m, 3H), 1.69 – 1.48 (m, 2H).

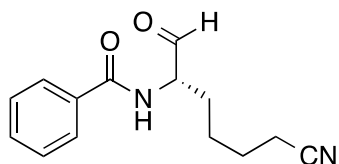


Alcohol: (S)-N-(6-chloro-1-hydroxyhexan-2-yl)benzamide

^1H NMR (500 MHz, Chloroform- d) δ 7.78 – 7.74 (m, 2H), 7.48 (tt, J = 7.5, 1.4 Hz, 1H), 7.40 (t, J = 7.5 Hz, 2H), 6.53 (d, J = 8.3 Hz, 1H), 4.21 – 4.09 (m, 1H, X of ABX), 3.82 – 3.73 (m, 1H, A of ABX), 3.69 (dt, J = 10.7, 4.6 Hz, 1H, B of ABX), 3.54 (t, J = 6.5 Hz, 2H), 3.08 (t, J = 4.9 Hz, 1H, OH), 1.89 – 1.73 (m, 2H), 1.73 – 1.61 (m, 2H), 1.61 – 1.47 (m, 2H). ^{13}C NMR (126 MHz, CDCl_3) δ 168.28, 134.41, 131.76, 128.71 (2C), 127.09 (2C), 65.23, 51.93, 44.90, 32.32, 30.63, 23.54.

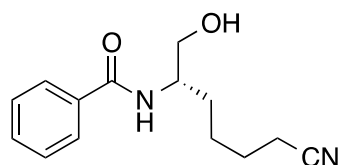
HRMS (ESI-TOF) m/z : $[\text{M}+\text{H}]^+$ calcd for $\text{C}_{13}\text{H}_{19}\text{ClNO}_2$ 256.1099; found 256.1096.

Separation by HPLC: 92% ee. Chiralpak IA, 8% 2-propanol / 92% hexane, 1.2 mL/min flow, ambient temperature, λ =254 or 220 nm. t_r = 9.2 min (major, S), 15.0 min (R).



Aldehyde: 2-Benzamido-6-cyanoheptanal.

100% conversion.

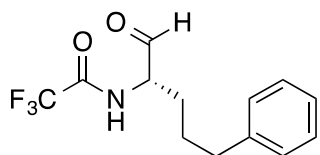


Alcohol: (S)-N-(6-cyano-1-hydroxyhexan-2-yl)benzamide

^1H NMR (400 MHz, Chloroform- d) δ 7.81 – 7.73 (m, 2H), 7.53 – 7.47 (m, 1H), 7.45 – 7.39 (m, 2H), 6.54 (d, J = 8.3 Hz, 1H), 4.22 – 4.07 (m, 1H, X of ABX), 3.82 – 3.66 (m, 2H, AB of ABX), 2.89 (br. s, 1H), 2.35 (t, J = 6.7 Hz, 2H), 1.79 – 1.62 (m, 4H), 1.62 – 1.49 (m, 2H). ^{13}C NMR (126 MHz, CDCl_3) δ 168.13, 134.35, 131.86, 128.78 (2C), 127.10 (2C), 119.72, 77.16, 65.13, 51.53, 30.65, 25.36, 25.21, 17.21.

HRMS (ESI-TOF) m/z : $[\text{M}+\text{H}]^+$ calcd for $\text{C}_{14}\text{H}_{19}\text{N}_2\text{O}_2$ 247.1442; found 247.1438.

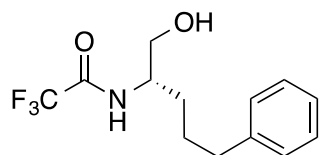
Separation by HPLC: 94% ee. Chiralpak IA, 10% 2-propanol / 90% hexane, 1.2 mL/min flow, ambient temperature, λ =254 or 220 nm. t_r = 13.4 min (major, S), 24.1 min (R).



Aldehyde: (S)-2,2,2-trifluoro-N-(1-oxo-5-phenylpentan-2-yl)acetamide

100% conversion, 91% crude yield. Started from 100 mg enamide, isolated 103.4 mg alcohol.

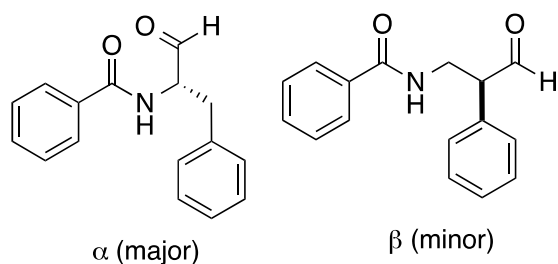
^1H NMR (400 MHz, Chloroform- d) δ 9.49 (s, 1H), 8.30 (d, J = 8.7 Hz, 1H, NH), 7.31 – 7.21 (m, 2H), 7.21 – 7.06 (m, 3H), 4.52 (td, J = 8.4, 4.9 Hz, 1H), 2.77 – 2.54 (m, 2H), 1.77 – 1.56 (m, 4H). ^{19}F NMR (377 MHz, CDCl_3) δ -75.73.



Alcohol: (S)-2,2,2-trifluoro-N-(1-hydroxy-5-phenylpentan-2-yl)acetamide

^1H NMR (400 MHz, Chloroform- d) δ 7.32 – 7.24 (m, 2H), 7.23 – 7.13 (m, 3H), 6.51 (d, J = 8.4 Hz, 1H), 4.12 – 3.98 (m, 1H, X of ABX), 3.73 (app. dd, J = 11.0, 3.6 Hz, 1H, A of ABX), 3.67 (app. dd, J = 11.1, 4.1 Hz, 1H, B of ABX), 2.71 – 2.57 (m, 2H), 1.80 (br s, 1H), 1.75 – 1.54 (m, 4H). ^{13}C NMR (126 MHz, Chloroform- d) δ 157.38 (q, J = 37.0 Hz), 141.66, 128.60 (2C), 128.52 (2C), 126.16, 116.01 (q, J = 288.0 Hz), 63.83, 51.74, 35.57, 30.40, 27.75. ^{19}F NMR (377 MHz, CDCl_3) δ -75.83.

HRMS (ESI-TOF) m/z : $[\text{M}+\text{H}]^+$ calcd for $\text{C}_{13}\text{H}_{17}\text{F}_3\text{NO}_2$ 276.1206; found 276.1198.



Aldehyde, alpha: N-(1-Formyl-2-phenylethyl) benzamide

86.3% conversion, 81.2% isolated yield (aldehyde), 6.3:1 α : β .

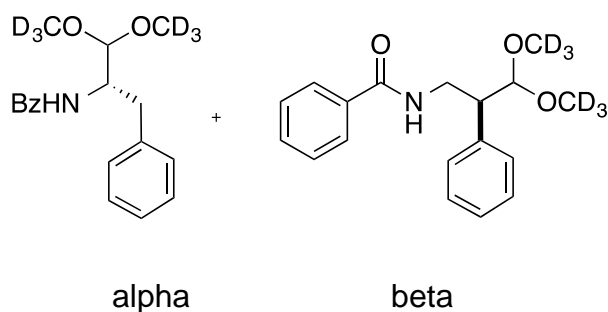
Characterization data are consistent with literature report.²⁴

^1H NMR (400 MHz, Acetone- d_6) δ 9.73 (s, 1H), 8.08 (s, 1H), 7.85 (dd, J = 7.5, 1.7 Hz, 2H), 7.58 – 7.50 (m, 1H), 7.50 – 7.41 (m, 2H), 7.35 – 7.23 (m, 4H), 7.24 – 7.15 (m, 1H), 4.64 (ddd, J = 9.5, 7.3, 4.8 Hz, 1H), 3.36 (dd, J = 14.1, 4.8 Hz, 1H), 3.09 (dd, J = 14.1, 9.6 Hz, 1H).

HRMS (ESI-TOF) m/z : $[M+H]^+$ calcd for $C_{16}H_{16}NO_2$ 254.1176; found 254.1170.

$[\alpha]^{20}_D = -103.1$, $c = 1.29$ in EtOH. Lit. $[\alpha]^{20}_D = -109$ ($c = 3.00$, EtOH) for N-(1-Formyl-2-phenylethyl) benzamide (aldehyde, alpha).²⁵ Pure N-(1-Formyl-2-phenylethyl) benzamide can be separated from the minor regioisomer by addition of $CDCl_3$ to the crude hydroformylation mixture and filtration of the resulting white solid (the alpha regioisomer).

When the NMR is taken in methanol- d_4 (to obtain accurate b:l ratios), the dimethoxyacetal forms spontaneously:

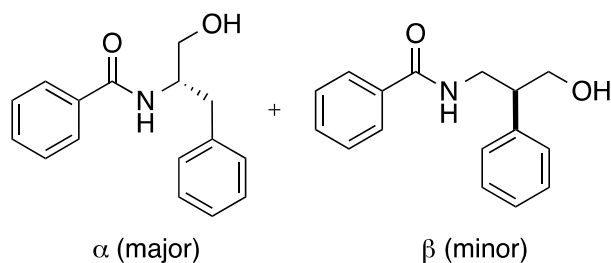


Dimethoxyacetal, alpha: (S)-N-(1,1-dimethoxy-3-phenylpropan-2-yl)benzamide

1H NMR (500 MHz, Methanol- d_4) δ 7.74 – 7.67 (m, 2H), 7.52 – 7.35 (m, 3H), 7.34 – 7.20 (m, 4H), 7.18 – 7.12 (m, 1H), 4.66 (t, $J = 3.4$ Hz, 1H), 4.47 – 4.32 (m, 1H), 3.13 (app. ddd, $J = 13.1, 7.7, 4.7$ Hz, 1H), 2.92 (app. ddd, $J = 14.8, 9.9, 6.1$ Hz, 1H).

Dimethoxyacetal, beta: N-(3,3-dimethoxy-2-phenylpropyl)benzamide

1H NMR (500 MHz, Methanol- d_4) δ 7.76 – 7.10 (m, 10H), 4.81 (d, $J = 4.5$ Hz, 1H, acetal H), 3.94 – 3.82 (m, 1H, A of ABX), 3.79 – 3.70 (m, 1H, B of ABX), 3.29 – 3.21 (m, 1H, X of ABX).



Alcohol, Alpha insertion: (S)-N-(1-hydroxy-3-phenylpropan-2-yl)benzamide

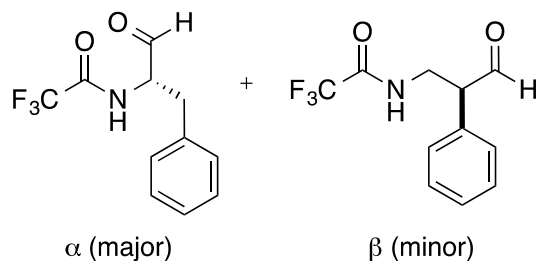
^1H NMR (500 MHz, Methanol- d_4) δ 7.76 – 7.71 (m, 2H), 7.52 (tt, J = 7.4, 1.1 Hz, 1H), 7.47 – 7.40 (m, 2H), 7.33 – 7.25 (m, 4H), 7.19 (tt, J = 6.9, 1.6 Hz, 1H), 4.36 (dq, J = 8.5, 5.7 Hz, 1H), 3.67 (d, J = 5.5 Hz, 2H), 3.04 (dd, J = 13.7, 6.1 Hz, 1H), 2.88 (dd, J = 13.7, 8.5 Hz, 1H). ^{13}C NMR (126 MHz, MeOD) δ 170.35, 139.97, 136.00, 132.49, 130.34 (2C), 129.42 (2C), 129.36 (2C), 128.27 (2C), 127.33, 64.29, 54.96, 49.00, 37.99.

Alcohol, Beta insertion: N-(3-hydroxy-2-phenylpropyl)benzamide

^1H NMR (400 MHz, Methanol- d_4) δ 7.68 (dd, J = 7.2, 1.6 Hz, 2H), 7.53 – 7.45 (m, 2H), 7.44 – 7.36 (m, 2H), 7.33 – 7.21 (m, 4H), 3.82 (d, J = 6.4 Hz, 2H), 3.77 (dd, J = 13.5, 7.2 Hz, 1H), 3.63 (dd, J = 13.7, 7.9 Hz, 1H), 3.23 – 3.11 (m, 1H).

HRMS (ESI-TOF) m/z : $[\text{M}+\text{H}]^+$ calcd for $\text{C}_{16}\text{H}_{18}\text{NO}_2$ 256.1333; found 256.1342.

Separation by HPLC: 98.3% ee α , 31.9% ee β . Chiralpak IA, 8% 2-propanol / 92% hexane, 1 mL/min flow, ambient temperature, $\lambda=220$ nm. t_r (alpha isomer) = 11.5 min (major, S), 13.9 min (minor, R). t_r (beta isomer) = 19.3 min (minor), 21.8 min (major).



Aldehyde, alpha: 2,2,2-Trifluoro-N-[(1S)-1-formyl-2-phenylethyl]acetamide

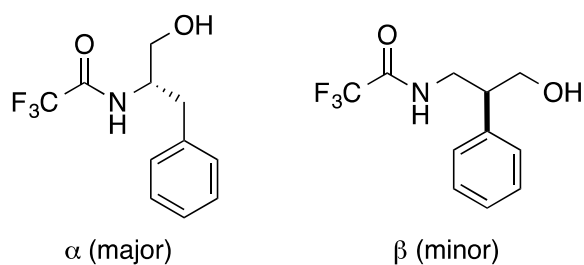
100% conversion, 65.5% isolated yield (alcohol).

Characterization data are consistent with literature report.²⁶

¹H NMR (400 MHz, CDCl₃) δ 9.64 (s, 1H), 7.50 – 7.09 (m, 5H), 7.02 (br. s, 1H), 4.82 (app. q, J = 6.6 Hz, 1H), 3.30 (dd, J = 14.2, 5.5 Hz, 1H), 3.22 (dd, J = 14.2, 7.2 Hz, 1H).

¹⁹F NMR (377 MHz, CDCl₃) δ -75.86 (alpha), -76.05 (beta).

$[\alpha]^{20}_D = -10.0$, $c = 1.7$ in acetone for 12.3:1 α : β mixture of 2,2,2-trifluoro-N-(1-hydroxy-3-phenylpropan-2-yl)acetamide and 2,2,2-trifluoro-N-(3-hydroxy-2-phenylpropyl)acetamide. Lit. $[\alpha]^{RT}_D = -18.1$ ($c = 2.00$, acetone).²⁷



Alcohol, alpha: (S)-2,2,2-trifluoro-N-(1-hydroxy-3-phenylpropan-2-yl)acetamide

Characterization data agrees with literature reports.²⁸

^1H NMR (400 MHz, Methanol- d_4) δ 7.38 – 7.13 (m, 5H), 4.17 (dq, J = 8.7, 5.9 Hz, 1H), 3.60 (qd, J = 11.2, 5.7 Hz, 2H), 2.96 (dd, J = 13.8, 5.9 Hz, 1H), 2.75 (dd, J = 13.8, 8.9 Hz, 1H). ^{19}F NMR (377 MHz, MeOD) δ -77.17.

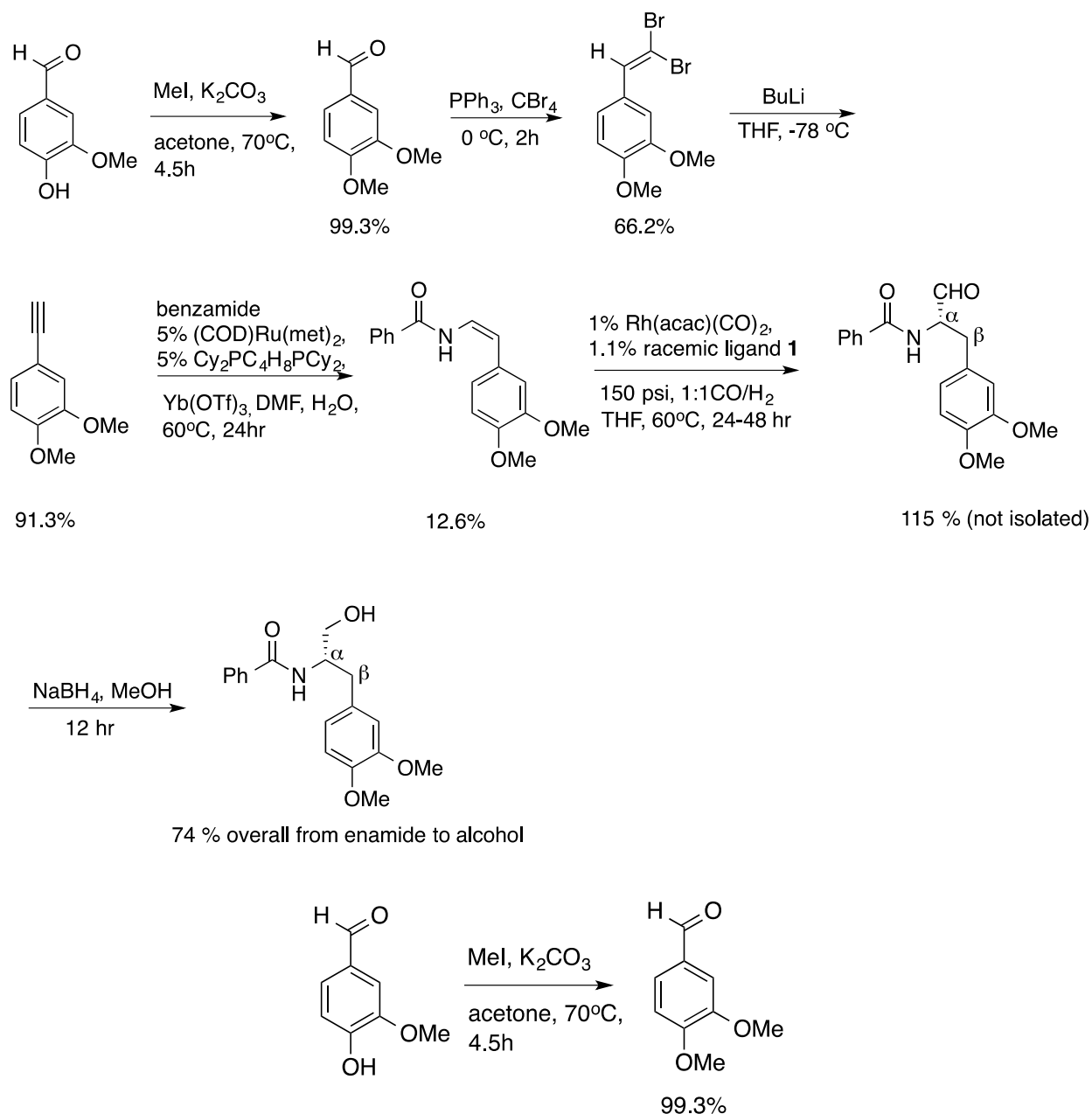
Alcohol, beta: 2,2,2-trifluoro- N -(3-hydroxy-2-phenylpropyl)acetamide

^1H NMR (400 MHz, Methanol- d_4) δ 7.34 – 7.15 (m, 5H), 3.76 (dd, J = 6.5, 2.4 Hz, 2H), 3.67 (dd, J = 13.4, 6.7 Hz, 1H), 3.60 – 3.52 (m, 1H), 3.10 (dq, J = 8.5, 6.7 Hz, 1H). ^{19}F NMR (377 MHz, Methanol- d_4) δ -77.37.

HRMS (ESI-TOF) m/z : $[\text{M}+\text{H}]^+$ calcd for $\text{C}_{11}\text{H}_{13}\text{F}_3\text{NO}_2$ 248.0893; found 248.0897.

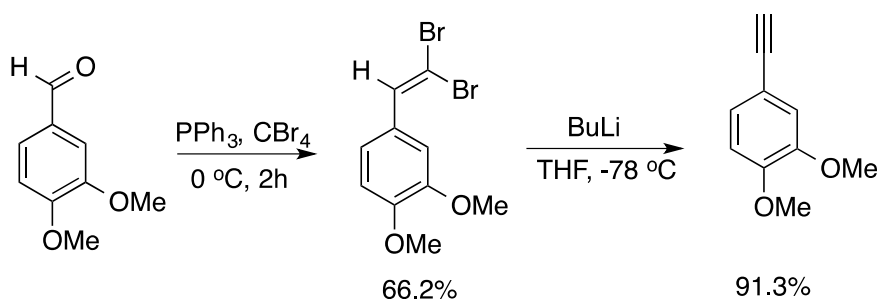
Separation by HPLC: 90% ee α , 54% ee β . Chiralpak IA, 5% 2-propanol / 95% hexane, 1 mL/min flow, ambient temperature, $\lambda=220$ nm. tr (alpha isomer) = 8.2 min (major, S), 9.5 min (minor, R). tr (beta isomer) = 12.9 min (major), 14.1 min (minor).

2.4.4. Synthesis of L-DOPA Precursor



Methylation: 12.172 g (80 mmol) of vanillin was added into 130 mL of acetone, and the mixture was warmed to 60 °C to dissolve the vanillin. Then 11.222 g (80 mmol) of K₂CO₃ and 8 mL (120 mmol) of MeI were added, and the mixture was stirred at 60-70 °C overnight (17 hours) under reflux. The reaction mixture was filtered and the solids washed

with acetone, then the filtrate was concentrated under vacuum to yield the desired product, which was further purified by flash column chromatography, to give 13.2 g (99.3% yield) of pure product. Characterization data are consistent with previously reported results.²⁹

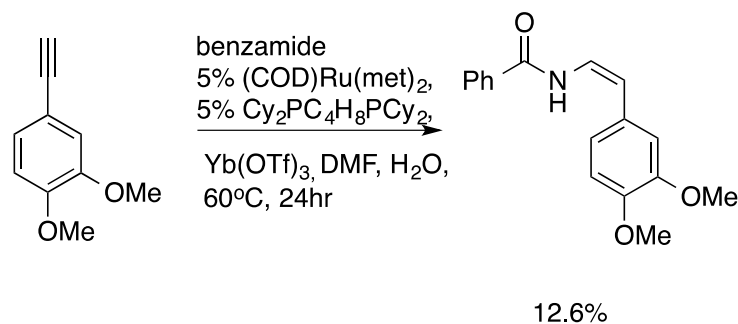


Corey-Fuchs:

1) To a solution of the methylated aldehyde (6.646g, 40 mmol) in dry DCM, triphenylphosphine (20.983g, 80mmol) was added. The mixture was cooled to 0 °C, and a solution of carbon tetrabromide (14.592g, 44 mmol) in dry DCM was added dropwise. The reaction mixture was allowed to gradually warm up to room temperature and stirred for another two hours after reaching room temperature. The reaction mixture was quenched with water, and the organic layer was separated and washed with brine. The crude mixture was dried over magnesium sulfate, filtered, concentrated under vacuum, and purified by flash column chromatography to give the dibromoethene derivative (8.521g, 66.2%). Characterization data are consistent with previously reported results.³⁰

2) nBuLi (26.46 mL of 2.5 M solution in hexane, 66.15 mmol) was added dropwise to a solution of the dibromoethene derivative (8.521g, 26.46 mmol) in dry THF at -78 °C. The resulting solution was stirred at -78 °C for 1h, and then gradually warmed to room temperature. The reaction was quenched using saturated aqueous NH₄Cl, and the

mixture was extracted with EtOAc. The organic layer was washed with water (x1) and brine (x1). After drying over magnesium sulfate and concentration under vacuum, the crude product was purified by column chromatography to yield alkyne (3.915g, 91.3%).

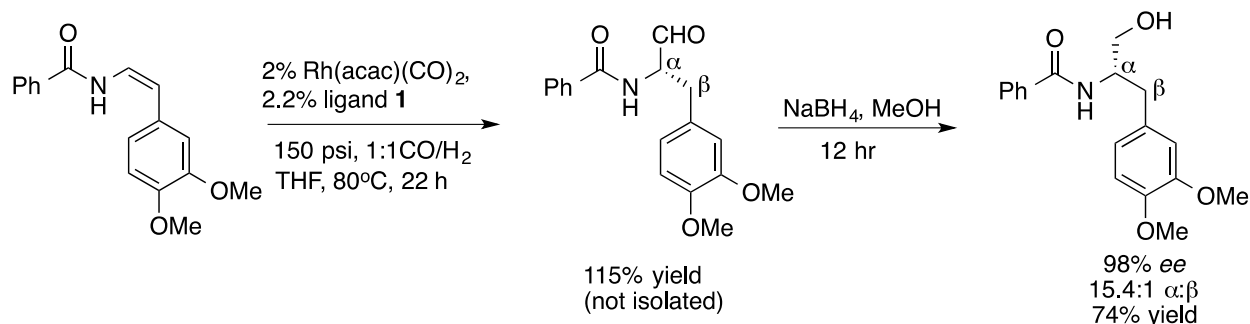


Enamide formation: The enamide was synthesized by the general procedure reported above, starting from 3.915g (24.17 mmol) of the alkyne. After the typical extractive workup and removal of the solvent under vacuum, the crude mixture was left overnight. Upon standing, the desired product precipitated out, and the dark liquid impurities were dissolved in EtOAc (the product does not dissolve in EtOAc). The product was separated using filtration, and the solids were washed with EtOAc. The product was recrystallized from a mixture of DCM and hexane four times to yield 0.8624g of light green crystals (12.6% yield). Characterization data are consistent with previously reported results.³¹

¹H NMR (500 MHz, Chloroform-d) δ 8.37 (d, J = 11.0 Hz, 1H), 7.80 – 7.73 (m, 2H), 7.58 – 7.50 (m, 1H), 7.50 – 7.41 (m, 2H), 7.16 (dd, J = 11.1, 9.4 Hz, 1H), 6.94 (d, J = 2.1 Hz, 2H), 6.83 (d, J = 1.5 Hz, 1H), 5.85 (d, J = 9.4 Hz, 1H), 3.92 (s, 3H), 3.89 (s, 3H).

¹³C NMR (126 MHz, Chloroform-d) δ 164.19, 149.51, 148.13, 133.41, 132.15, 128.87, 128.51, 127.02, 121.75, 119.99, 111.73, 111.29, 110.94, 55.98, 55.93.

HRMS (ESI-TOF) m/z: [M+H]⁺ calcd for C₁₇H₁₇NO₃ 284.1282; found 284.1279.



AHF and reduction: 0.5 mL of 20 mM Rh(acac)(CO)₂ solution in THF was combined with 1.1 mL of 20 mM ligand solution in THF with about 50% potency. The mixture was stirred in a pressure bottle under 150 psi of syngas (1:1 H₂/CO) at 70-80 °C for 1hr, then the entire mixture was removed via syringe and injected into another pressure bottle containing 0.1418g (0.5 mmol) of the olefin. The mixture was pressurized to 155 psi of syngas, submerged in an 80 °C oil bath, and stirred at a high rate to ensure sufficient gas-liquid mixing for 22 hours. The crude mixture was passed through a short pad of silica, rinsed with THF. Then the mixture was concentrated in vacuum to give the aldehyde (>100% crude yield).

The crude aldehyde was dissolved in MeOH, and excess NaBH₄ was added to the solution at 0 °C, and the resulting mixture was stirred overnight. The crude material was purified using small-scale flash column chromatography (60% EtOAc in hexane) to give 0.116g of the alcohol product (74% yield from enamide).

Aldehyde:

¹H NMR (500 MHz, 3:1 Toluene-d₈:CDCl₃) δ 9.39 (s, 1H), 7.64 (d, J = 7.5 Hz, 2H), 7.27 (t, J = 7.3 Hz, 1H), 7.19 (t, J = 7.5 Hz, 2H), 6.62 (d, J = 5.1 Hz, 1H), 6.59 – 6.51 (m, 3H), 4.61 (q, J = 6.1 Hz, 1H), 3.59 (s, 4H), 3.55 (s, 3H), 3.13 – 2.99 (m, 2H). ¹³C NMR (126

MHz, 3:1 Toluene-d₈:CDCl₃) δ 198.95, 167.39, 149.71, 148.80, 134.21, 132.23, 129.05 (2C), 128.64, 127.50 (2C), 121.84, 113.13, 111.88, 60.79, 56.027, 55.961, 34.86.

HRMS (ESI-TOF) m/z: [M+H]⁺ calcd for C₁₈H₁₉NO₄ 314.1387; found 314.1392.

Alcohol:

¹H NMR (500 MHz, Chloroform-d) δ 7.71 – 7.66 (m, 2H), 7.52 – 7.46 (m, 1H), 7.45 – 7.37 (m, 2H), 6.83 – 6.76 (m, 3H), 6.46 (d, J = 7.4 Hz, 1H), 4.42 – 4.25 (m, 1H), 3.86 (s, 3H), 3.83 (s, 3H), 3.82 – 3.68 (m, 2H), 2.95 (d, J = 7.2 Hz, 2H), 2.91 (br. s, 1H). ¹³C NMR (126 MHz, Chloroform-d) δ 168.15, 149.25, 148.01, 134.38, 131.85, 131.82, 130.18, 128.75, 127.03, 121.37, 112.40, 111.46, 64.35, 56.04, 55.99, 53.48, 36.70.

HRMS (ESI-TOF) m/z: [M+H]⁺ calcd for C₁₈H₂₁NO₄ 316.1544; found 316.1550.

Separation by HPLC: Chiralpak IA, 10% 2-propanol / 90% hexane, 1.2 mL/min flow, ambient temperature, λ=220 nm. tr (alpha isomer) = 12.7 min (major, S), 15.7 min (minor, R). tr (beta isomer) = 23.5 min (minor), 24.9 min (major).

2.5. References

1. For hydroformylation reviews, see: (a) Agbossou, F.; Carpentier, J. F.; Mortreaux, A. *Chem. Rev.* **1995**, *95*, 2485-2506. (b) Claver, C.; van Leeuwen, P. W. N. M. *Rhodium Catalyzed Hydroformylation*; Kluwer Academic Publishers: Dordrecht, The Netherlands, 2000. (c) Wiese, K. D.; Obst, D. *Top. Organomet. Chem.* **2006**, *18*, 35–64. (d) Franke, R.; Selent, D.; Börner, A. *Chem. Rev.* **2012**, *112*, 5675–5732. (e) Whiteker, G.T.; Cogley, C.J. *Top. Organomet. Chem.* **2012**, *42*, 35–46. For reviews of asymmetric hydroformylation, see: (f) Klosin, J.; Landis, C. R. *Acc. Chem. Res.* **2007**, *40*, 1251–1259. (g) Breit, B. *Top. Curr. Chem.* **2007**, *279*, 139–172. (h) Gual, A.; Godard, C.; Castillon, S.; Claver, C. *Tetrahedron: Asymmetry* **2010**, *21*, 1135 – 1146.
2. (a) Sakai, N.; Mano, S.; Nozaki, K.; Takaya, H. *J. Am. Chem. Soc.* **1993**, *115*, 7033–7034. (b) Sakai, N.; Nozaki, K.; Takaya, H. *J. Chem. Soc., Chem. Commun.* **1994**, 395-396. (c) Nanno, T.; Sakai, N.; Nozaki, K.; Takaya, H. *Tetrahedron: Asymmetry* **1995**, *6*, 2583-2591. (d) Nozaki, K.; Sakai, N.; Nanno, T.; Higashijima, T.; Mano, S.; Horiuchi, T.; Takaya, H. *J. Am. Chem. Soc.* **1997**, *119*, 4413– 4423. (e) Horiuchi, T.; Ohta, T.; Shirakawa, E.; Nozaki, K.; Takaya, H. *J. Org. Chem.* **1997**, *62*, 4285–4292. (f) Nozaki, K.; Li, W.; Horiuchi, T.; Takaya, H. *Tetrahedron Lett.* **1997**, *38*, 4611–4614.
3. Babin, J. E.; Whiteker, G. T. World Patent, WO 9303839, 1993.
4. Yan, Y.; Zhang, X. *J. Am. Chem. Soc.* **2006**, *128*, 7198-7202.
5. Fernandez-Perez, H.; Benet-Buchholz, J.; Vidal-Ferran, A. *Org Lett.* **2013**, *15*, 3634-3637.

6. Zhang, X. W.; Cao, B. N.; Yan, Y. J.; Yu, S. C.; Ji, B. M.; Zhang, X. M. *Chem.—Eur. J.* **2010**, *16*, 871-877.
7. (a) Lightburn, T. E.; Dombrowski, M. T.; Tan, K. L. *J. Am. Chem. Soc.* **2008**, *130*, 9210–9211. (b) Grünanger, C. U.; Breit, B. *Angew. Chem., Int. Ed.* **2008**, *47*, 7346–7349. (c) Grünanger, C. U.; Breit, B. *Angew. Chem., Int. Ed.* **2010**, *49*, 967–970. (d) ¹ (e) Sun, X.; Frimpong, K.; Tan, K. L. *J. Am. Chem. Soc.* **2010**, *132*, 11841–11843. (f) Joe, C. L.; Tan, K. L. *J. Org. Chem.* **2011**, *76*, 7590-7596. (g) Usui, I.; Nomura, K.; Breit, B. *Org. Lett.* **2011**, *13*, 612–615. (h) Ueki, Y.; Ito, H.; Usui, I.; Breit, B. *Chem. Eur. J.* **2011**, *17*, 8555-8558. (i) Joe, C. L.; Blaisdell, T. P.; Geoghan, A. F.; Tan, K. L. *J. Am. Chem. Soc.* **2014**, *136*, 8556-8559.
8. (a) Clark, T. P.; Landis, C. R.; Freed, S. L.; Klosin, J.; Abboud, K. A. *J. Am. Chem. Soc.* **2005**, *127*, 5040–5042. (b) Watkins, A. L.; Hashiguchi, B. G.; Landis, C. R. *Org. Lett.* **2008**, *10*, 4553-4556. (c) McDonald, R. I.; Wong, G. W.; Neupane, R. P.; Stahl, S. S.; Landis, C. R. *J. Am. Chem. Soc.* **2010**, *132*, 14027-14029. (d) Watkins, A. L.; Landis, C. R. *Org. Lett.* **2011**, *13*, 164-167. (e) Risi, R. M.; Burke, S. D. *Org. Lett.* **2012**, *14*, 1180 – 1182. (f) Risi, R.M.; Burke, S. D. *Org. Lett.* **2012**, *14*, 2572 – 2575. (g) Adint, T. T.; Wong, G. W.; Landis, C. R. *J. Org. Chem.* **2013**, *78*, 4231–4238. (h) Adint, T. T.; Landis, C. R. *J. Am. Chem. Soc.* **2014**, *136*, 7943-7953.
9. Clemens, A. J. L.; Burke, S. D. *J. Org. Chem.* **2012**, *77*, 2983-2985.
10. Ho, S.; Bucher, C.; Leighton, J. L. *Angew. Chem., Int. Ed.* **2013**, *52*, 6757-6761.
11. Wang, X.; Buchwald, S. L. *J. Org. Chem.* **2013**, *78*, 3429-3433. Wang, X.; Buchwald, S. L. *J. Am. Chem. Soc.* **2011**, *133*, 19080–19083.

12. Doucet, H.; Martin-Vaca, B.; Bruneau, C.; Dixneuf, P. H. *J. Org. Chem.* **1995**, *60*, 7247-7255.
13. Gooßen, L. J.; Paetzold, J.; Koley, D. *Chem. Commun.* **2003**, 706-707.
14. Gooßen, L. J.; Salih, K. S. M.; Blanchot, M. *Angew. Chem. Int. Ed.* **2008**, *47*, 8492.
15. (a) Chen, X.; Chen, J.; De Paolis, M.; Zhu, J.; *J. Org. Chem.* **2005**, *70*, 4397-4408
(b) De Paolis, M.; Chen, X.; Zhu, J. *Synlett* **2004**, 729-731.
16. Myers, A. G.; Zhong, B.; Movassaghi, M.; Kung, D. W.; Lanman, B. A.; Kwon, S. *Tetrahedron Lett.* **2000**, *41*, 1359-1362.
17. Knowles, W. S. *Acc. Chem. Res.* **1983**, *16*, 106-112.
18. See supporting information for synthesis and references to procedures utilized.
19. Butyl, $-(\text{CH}_2)_2\text{Ph}$, $-(\text{CH}_2)_3\text{Cl}$, $-\text{CH}_2\text{Cy}$, and Ph substituted benzamides were reported in: Gooßen, L. J.; Salih, K. S. M.; Blanchot, M. *Angew. Chem. Int. Ed.* **2008**, *47*, 8492. (*Z*)-*N*-(5-cyanopent-1-en-1-yl)benzamide was reported in: Honjo, T.; Phipps, R.J.; Rauniyar, V.; Toste, F.D.; *Angew. Chem. Int. Ed.* **2012**, *51*, 9684-9688.
20. Das, U.K.; Bhattacharjee, M. *J. Organomet. Chem.* **2012**, *700*, 78-82.
21. Chattopadhyay, A.; Mamdapur, V.R. *J. Org. Chem.* **1995**, *60*, 585-587.
22. Egri, G.; Baitz-Gacs, E.; Poppe, L. *Tetrahedron: Asymmetry* **1996**, *5*, 1437-1448.

23. (a) Kadyrov, R.; Koenigs, R. M.; Brinkmann, C.; Voigtlaender, D.; Rueping, M. *Angew. Chem. Int. Ed.* **2009**, *48*, 7556-7559; (b) Martynow, J. G.; Józwik, J.; Szelejewski, W.; Achmatowicz, O.; Kutner, A. et al. *Eur. J. Org. Chem.* **2007**, 689-703.
24. Pan, H.; Xie, Y.; Liua, M.; Shi, Y. *RSC Adv.* **2014**, *4*, 2389-2392.
25. Silver, M. S.; Haskell, J. H. *J. Med. Chem.* **1989**, *32*, 1253-1259.
26. Myers, A. G.; Kung, D. W.; Zhong, B.; Movassaghi, M.; Kwon, S. *J. Am. Chem. Soc.*, **1999**, *121*, 8401–8402.
27. Jiang, H.; Sun, L.; Yuan, S.; Lu, W.; Wan, W.; Zhu, S.; Hao, J. *Tetrahedron* **2012**, *13*, 2858-2862.
28. Jiang, H.; Yan, L.; Xu, M.; Lu, W.; Cai, Y.; Wan, W.; Yao, J.; Wu, S.; Zhu, S.; Hao, J. *J. Org. Chem.* **2013**, *78*, 4261–4269.
29. Liu, X.; Xia, Q.; Zhang, Y.; Chen, C.; Chen W. *J. Org. Chem.* **2013**, *78*, 8531-8536.
30. Rosiak, A.; Frey, W.; Christoffers, J. *Eur. J. Org. Chem.* **2006**, 4044–4054.
31. Wendlandt, A.E.; Stahl, S.S. *Org. Biomol. Chem.* **2012**, *10*, 3866.

Chapter 3

Condensation Oligomers with Sequence Control but without Coupling Reagents and
Protecting Groups via Asymmetric Hydroformylation and Hydroacyloxylation

Chapter 3 is published in

Foarta, F. and Landis, C. R. *J. Org. Chem.* **2016**, 136, 14583 - 14588

3.1. Introduction

A fundamental challenge in synthesizing sequence-specific oligomers, such as α - and β -peptides or oligoesters, is the waste generated by coupling reagents and protecting groups. Is it possible to devise a scheme by which achiral starting materials are transformed into sequence-specific oligomers with catalytic introduction of all stereogenic centers and near 100% atom economy?

Consider oligoesters, which are important model compounds for the analysis and design of high molecular weight polyester materials or as model foldamers that lack hydrogen bonding capability along the backbone and are readily degradable by hydrolysis.² Considerable effort has been placed on generating structurally diverse oligoesters with reliable control of monomer sequence, molecular weight and tacticity.³ Current strategies to access sequence defined oligoesters rely on stoichiometric coupling reagents and orthogonal protecting group strategies⁴ that are inspired by the solid phase synthesis of oligopeptides.⁵ Obvious drawbacks of such methods include low atom economy, limited compatibility with other functional groups, or challenging stereoselective syntheses of monomers. Alternative strategies to generate oligoesters via efficient, low-waste and scalable processes are highly desirable. Asymmetric hydroformylation (AHF) has emerged as a powerful catalytic and atom-efficient process that can address these challenges. Herein we describe an alternative approach to the synthesis of oligo(2-hydroxyacid)s that employs AHF methodology and two other transformations, aldehyde oxidation and alkyne hydroacyloxylation, in an iterative fashion. The resulting oligoesters, oligo(2-hydroxyacid)s, share the same backbone as poly(lactic acid), a biodegradable and biocompatible polyester with numerous industrial and biomedical applications.⁶

AHF is a catalytic stereoselective carbon-carbon bond forming reaction that generates chiral aldehydes from alkenes, CO and H₂.⁷ Several chiral ligands enable this transformation efficiently.⁸ We previously have reported that the chiral Bisdiazaphos⁹ ligand (Figure 3.1) shows remarkable activity, enantio- and regioselectivity in the AHF of a variety of alkenes under mild conditions.¹⁰ The high level of synthetic versatility accessible at the aldehyde stage makes AHF an attractive disconnection strategy in organic synthesis. Notable recent syntheses of Patulolide C¹¹, Garner's aldehyde,¹² the Prelog-Djerassi lactone,¹³ the macrolide Dictyostatin,¹⁴ γ -chiral α,β -unsaturated carbonyl compounds and vinylogous ester oligomers¹⁵ demonstrate the utility of AHF.

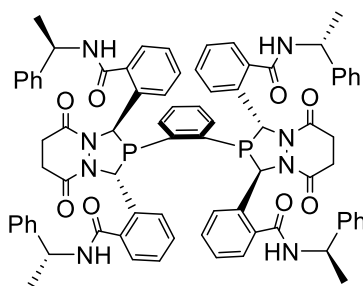
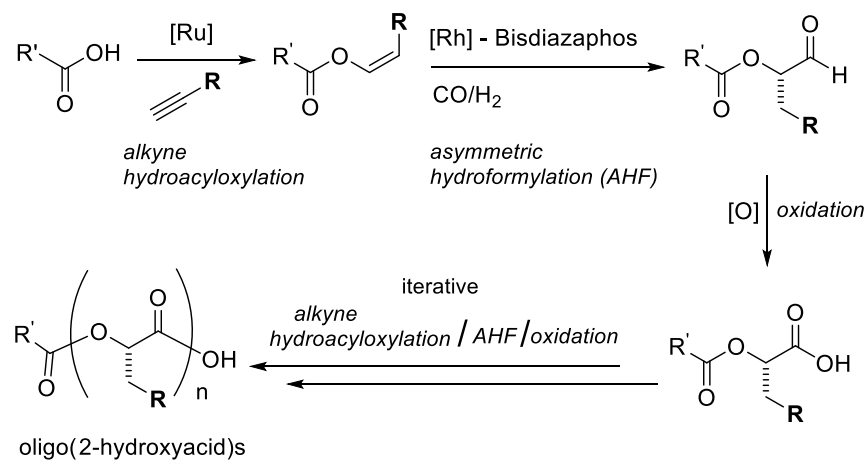


Figure 3.1. (S,S,S)-Bisdiazaphos ligand used in AHF

We recently reported the regio- and enantioselective Rh-BisDiazaphos catalyzed AHF of 1,2-disubstituted alkenes, specifically Z-enamides and Z-enol esters¹⁶. AHF of these substrates generates the corresponding α -functionalized chiral aldehydes with high conversion (53-100%), regioselectivity (5.7:1 to 99:1 $\alpha:\beta$), enantioselectivity (84-99% *ee*) and functional group compatibility. Ru-catalyzed alkyne hydroamidation¹⁷ and hydroacyloxylation¹⁸ provide catalytic, economical access to Z-enamides and Z-enol esters, respectively.



Scheme 3.1. Synthetic strategy for coupling reagent and protecting group free synthesis of sequence specific oligoesters

We report herein that Rh-BisDiazaphos catalyzed AHF of (Z)-enol esters provides sequence specific chiral oligo(2-hydroxyacid)s as part of an iterative sequence comprising enol ester formation, AHF and aldehyde oxidation. This catalytic and atom-economical approach to oligoester synthesis avoids drawbacks of common methods, such as in high amounts of waste, tedious separations, and difficult scale-up that result from coupling reagents and protection / deprotection strategies.

Our synthetic strategy to generate oligo(2-hydroxyacid)s is depicted in Scheme 3.1. The reaction sequence involves Ru-catalyzed addition of carboxylic acids to alkynes to yield (Z)-enol esters, Rh-BisDiazaphos catalyzed AHF of the (Z)-enol esters to give α -functionalized chiral aldehydes, and oxidation of the aldehydes to produce new chiral α -functionalized chiral carboxylic acids. Oligo(2-hydroxyacid)s can be formed via multiple

iterations of this three-step reaction sequence, with each iteration adding one new monomer unit. The side chain of each monomer is tailored by choosing from a variety of readily available alkynes. The stereochemistry of each monomer is determined by the chirality of the AHF catalyst. All organic starting materials are achiral and readily available. The methodology is demonstrated for four iterations to generate a tetramer of four unique monomer units in a single sequence (Scheme 3.2).

3.2. Results and Discussion

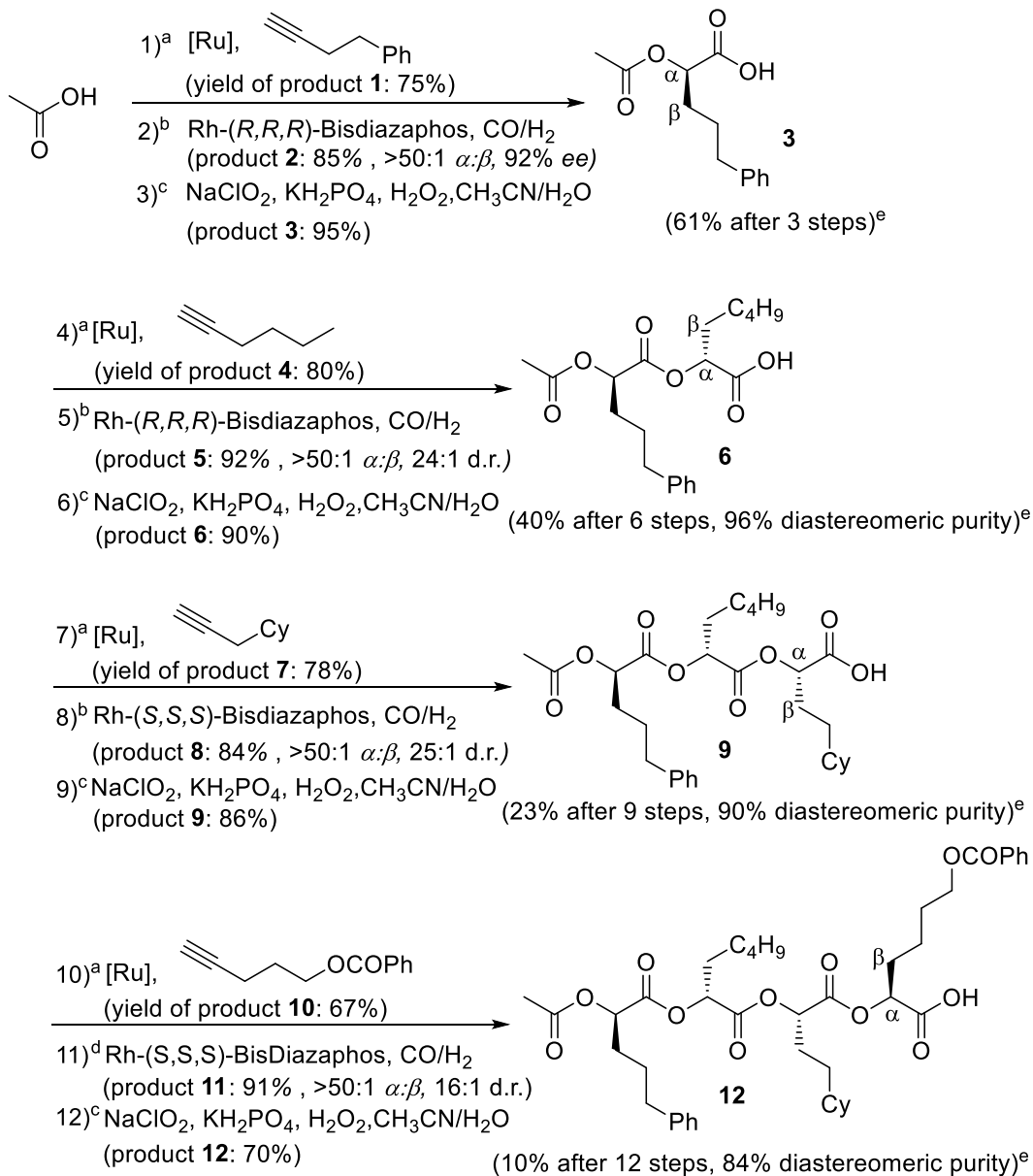
The alkyne hydroacyloxylation reaction^{18a} in the presence of 5% Ru(methallyl)₂dppb (dppb = 1,4-Bis(diphenylphosphino)butane) affords, after 16 h at 45 °C in THF, the corresponding (Z)-enol ester products **1**, **4**, **7** and **10** (Scheme 3.2) with conversion greater than 90%, isolated yields between 67-80%, and Z selectivity higher than 90% (commonly observed by-products are the E isomer and the 1,1-disubstituted alkene regioisomer). We note that not all alkynes undergo successful hydroacyloxylation; replacing 3-cyclohexyl propyne with phenylacetylene in step 7 led to less than 10% formation of the desired Z product. Signals in the 6-8 ppm region of ¹H NMR spectrum suggest alkyne oligomerization as major pathway. Replacing 5-benzoyloxy-1-pentyne in step 10 with 5-methoxypent-1-yne gave, however, comparable high conversion.

The (Z)-enol esters undergo successful AHF. At 0.3-0.5% Rh(acac)(CO)₂ (acac = acetylacetonate) and 0.36-0.6% (1.2 eq.) of (S,S,S) or (R,R,R)-BisDiazaphos and 150 psig of 1:1 CO/H₂ at 65 °C in THF for 12 h, the corresponding α-functionalized chiral aldehydes **2**, **5**, **8** and **11** are generated with excellent regioselectivity (>50:1 α:β), diastereoselectivity (between 16:1 and 25:1) and conversion (95-100%). AHF studies

performed with both enantiomers of BisDiazaphos in steps 5 and 8 indicate that stereinduction is predominantly catalyst controlled.

Oxidation of the aldehydes afforded the corresponding carboxylic acids **3**, **6**, **9** and **312** in 70% to 95% yield under Pinnick¹⁹ oxidation conditions without epimerization. Although Pinnick oxidation uses stoichiometric reagents, emerging catalytic aldehyde oxidation methods have the potential to improve the efficiency of this step.²⁰

Tetramer **12** was obtained in 10% overall isolated yield and 84% diastereomeric purity after 4 iterations (12 steps total) and was characterized by NMR spectroscopy (¹H, quantitative and non-quantitative ¹³C, Tocsy1D, Cosy, HSQC, HMBC) and ESI-MS. The absolute configuration of each stereocenter in the major diastereomer was monitored by optical rotation after each AHF step. The observed preference for Rh to insert at the Re face of the alkene when the (S,S,S) enantiomer of BisDiazaphos is used is consistent with previous observations.^{9b, 10c}

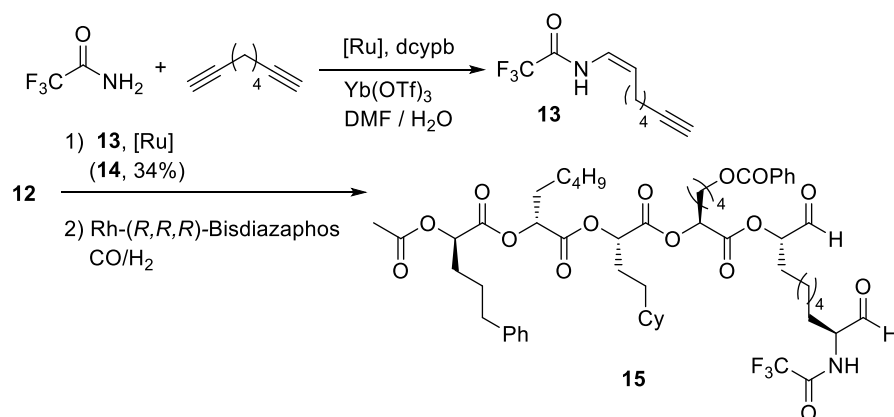


Scheme 3.2. Synthesis of a tetramer via the proposed iterative alkyne hydroacyloxylation / AHF / oxidation sequence

^aConditions: Ru(methallyl)₂dppb (5 mol%), carboxylic acid (1 eq.), alkyne (1.5 eq.), THF, 45 °C, 16 - 24 h. Reported yields represent isolated yields. ^bConditions: Rh(acac)(CO)₂ (0.3 mol%), (*S,S,S*)- or (*R,R,R*) - BisDiazaphos (0.36 mol%), 150 psig 1:1 CO / H₂, 65 °C, 12 h, THF, [enol ester] = 1.5 M. Reported yields represent isolated yields. Regioselectivity was determined by crude ¹H NMR integrations. Enantiomeric excess (for **2**) was

determined by NaBH₄ reduction of the aldehyde, followed by chiral HPLC analysis. Diastereomeric ratios (for **5**, **8**, **11**) were determined by ¹H NMR and quantitative ¹³C integrations of the aldehyde signals. ^cConditions: aldehyde (1 eq.), KH₂PO₄ (4 eq), H₂O₂ (4.1 eq), NaClO₂ (4 eq), CH₃CN, H₂O, 10 °C to room temperature, 3 h. Reported yields represent isolated yields. ^d0.5 mol% Rh(acac)(CO)₂, 0.6 mol% (S,S,S)-BisDiazaphos. ^eReported yields represent isolated yields. Diastereomeric purity was determined by ¹³C integrations of the aldehyde signals. dppb = 1,4-Bis(diphenylphosphino)butane, acac = acetylacetonate

Hydroacyloxylation / AHF enables novel ligations. For example, connection of tetramer carboxylic acid **12** to a carboxamide can be effected via a diyne linker.²¹ This ligation began with hydroamidation^{17a} of one end of 1,7-octadiyne with trifluoroacetamide to generate the (Z)-enamide **13** (Scheme 3.3).^{22,23} The pendant alkyne of **13** was then joined to tetramer **12** by hydroacyloxylation to generate the di-unsaturated enol ester/enamide **14**. AHF of (Z)-enol ester and the (Z)-enamide functionalities yielded the di-aldehyde **15** with greater than 95% conversion. The two aldehyde groups provide sites for further transformations.



Scheme 3.3. Demonstration of coupling between the synthesized tetramer and a carboxamide using a diyne linker. dcy pb = 1,4-bis(dicyclohexylphosphino)butane; [Ru] = bis(2-methallyl)cycloocta-1,5-diene-ruthenium(II)

3.3 Conclusions

This work establishes, as a proof-of-concept, that short oligoesters can be synthesized with sequence-specificity and stereocontrol in the absence of coupling agents or protection/deprotection steps. The main limitation at this stage is low overall yield, a result of unoptimized isolation and purification procedures after the Pinnick oxidation and hydroacyloxylation²⁴ steps. As in the development of chemical syntheses of peptides, it is likely that growth of oligomers on solid-phase supports²⁵ partially can mitigate these problems. Improved efficiency of the catalytic hydroacyloxylation and the enantioselectivity of the AHF also would enable higher yields and diastereomeric purity. At the current stage of development, the AHF/oxidation/hydroacyloxylation sequence may be most effective for making fragments for convergent syntheses rather than long, linear sequences.

In summary, this paper demonstrates the novel generation of oligo(2-hydroxyacid)s via iterative AHF / oxidation / alkyne hydroacyloxylation reaction sequence. Significantly this approach begins with achiral starting materials, avoids coupling reagents, features sequence specificity and atom economical C–C and C–O bond forming reactions, with introduction of all stereocenters by enantioselective catalysis. Key to this sequence is efficient AHF which provides high stereo (up to 25:1 d.r.) and regiocontrol (>50:1) at low catalyst loadings (0.3-0.5%) and mild pressures (150 psi CO/H₂). This strategy represents an attractive method for making 2-hydroxyacid esters. A similar strategy can, in principle, be applied to the synthesis of peptides and other sequence specific oligomers. However, α -peptide synthesis via hydroamidation-AHF currently is limited by a lack of atom-efficient methods for converting α -chiral aldehydes to the corresponding α -chiral carboxamides.

3.4. Experimental section

General

All steps involving enol ester synthesis and AHF were carried out under moisture and oxygen free conditions using standard Schlenk and glove box techniques. The oxidation step and all work-up procedures were performed in air. Dry and oxygen-free THF solvent was collected from a solvent column system that uses activated alumina. Anhydrous DMF solvent was sparged with N₂ and stored in a N₂ filled glove box. Acetic acid was distilled before use. All chemicals were purchased and used without further purification. BisDiazaphos ligands were prepared as reported in literature^{9a}. All alkynes were degassed by sparging with N₂ before use. Reactors were assembled as previously reported²⁶.

Regiomer ratios, diastereomer ratios and conversion were determined by proton ^1H NMR spectroscopy on crude reaction mixtures. ^1H chemical shifts are referenced to tetramethylsilane in CDCl_3 . ^{13}C chemical shifts are referenced to residual solvent peak. ^{19}F chemical shifts are referenced to tetramethylsilane in the proton spectrum using the unified scale. Splitting patterns in ^1H NMR spectra are reported as singlet (s), doublet (d), triplet (t), quartet (q), pentet (p) doublet of doublets (dd), doublet of triplets (dt), triplet of doublets (td), broad (br) and multiplet (m). Mass spectra were collected using electrospray ionization or atmospheric solids analysis probe - mass spectrometry (for **13** only), and a TOF analyzer. Flash column chromatography was performed on Silicycle Siliaflash P60 silica gel 40-63 μm and 230-400 mesh and TLC spots were visualized using a UV lamp at 254 nm. Absolute configuration of the chiral centers was determined by monitoring optical rotation at each aldehyde stage for all monomers and by LiAlH_4 reduction of the aldehyde at the monomer and dimer stages.

General procedure for enol ester synthesis^{18a}

$\text{Ru}(\text{methallyl})_2\text{dppb}$ (5 mol%) and dry and degassed THF (1.5 mL) were combined in an oven-dried Schlenk flask equipped with a stir bar inside a N_2 glove box. Inside a fume hood, the carboxylic acid (1 eq, 2 mmol) was added to the reaction flask via syringe as a solution in dry and degassed THF (0.5 mL), followed by neat alkyne (1.5 eq, 3 mmol). The solution was immersed in an oil bath and allowed to stir at 45°C for 24 h under N_2 . After reaction is complete, the reaction mixture is passed through a pad of silica in a fritted glass funnel, the silica washed with 20% EtOAc/hexanes (200 mL) and the dark yellow oil residue is purified via silica gel flash column chromatography with 10% EtOAc/hexanes as eluent.

(Z)-4-phenylbut-1-en-1-yl acetate (**1**). All characterization data is in accordance with previously reported data¹⁶.

(Z)-hex-1-en-1-yl (*R*)-2-acetoxy-5-phenylpentanoate (**4**). started with 1.47 mmol **3**. 80%, 0.37 g colorless oil. ¹H NMR 20:1 Z/E (500 MHz, Chloroform-*d*) δ 7.28 (m, 2H), 7.22 – 7.15 (m, 3H), 6.97 (dt, *J* = 6.3, 1.6 Hz, 1H), 5.10 (dd, *J* = 6.9, 5.7 Hz, 1H), 4.94 (td, *J* = 7.5, 6.3 Hz, 1H), 2.74 – 2.55 (m, 2H), 2.14 (s, 3H), 2.10 (qd, *J* = 7.3, 1.4 Hz, 2H), 1.96 – 1.88 (m, 2H), 1.83 – 1.72 (m, 2H), 1.40 – 1.22 (m, 4H), 0.89 (t, *J* = 7.0 Hz, 3H). ¹³C NMR (126 MHz, CDCl₃) δ 170.4, 167.4, 141.4, 133.6, 128.4, 128.35, 126.0, 115.5, 71.7, 35.2, 31.1, 30.5, 26.8, 24.1, 22.2, 20.6, 13.9. HRMS-(ESI) for C₁₉H₂₆O₄ [M+NH₄]⁺: calculated 336.2170, found 336.2170

(Z)-3-cyclohexylprop-1-en-1-yl (*R*)-2-(((*R*)-2-acetoxy-5-phenylpentanoyl)oxy)heptanoate (**7**). started with 0.96 mmol **6**. 78%, 0.36 g colorless oil, 22:1 Z/E ¹H NMR (500 MHz, Chloroform-*d*) δ 7.30 – 7.24 (m, 2H), 7.21 – 7.16 (m, 3H), 6.99 (dt, *J* = 6.3, 1.5 Hz, 1H), 5.15 (t, *J* = 6.2 Hz, 1H), 5.07 (dd, *J* = 8.1, 4.6 Hz, 1H), 4.97 (q, *J* = 7.5 Hz, 1H), 2.73 – 2.60 (m, 2H), 2.13 (s, 3H), 2.05 – 1.87 (m, 6H), 1.86 – 1.76 (m, 2H), 1.74 – 1.58 (m, 5H), 1.51 – 1.38 (m, 2H), 1.37 – 1.27 (m, 5H), 1.27 – 1.08 (m, 3H), 0.96 – 0.87 (m, 5H). ¹³C NMR (126 MHz, CDCl₃) δ 170.5, 169.8, 167.1, 141.6, 134.1, 128.38, 128.35, 125.9, 114.2, 72.4, 71.8, 37.7, 35.4, 33.0, 32.98, 32.1, 31.3, 31.0, 30.6, 26.8, 26.5, 26.3, 24.5, 22.4, 20.6, 14.0. HRMS-(ESI) for C₂₉H₄₂O₆ [M+NH₄]⁺: calculated 504.3320, found 504.3317

(4*R*,7*R*,10*S*, *Z*)-10-(2-cyclohexylethyl)-2,5,8,11-tetraoxo-7-pentyl-4-(3-phenylpropyl)-3,6,9,12-tetraoxaheptadec-13-en-17-yl benzoate (**10**). The alkyne for step 10 was synthesized according to a known procedure starting from the alcohol precursor 4-pentyn-

1-ol. All characterization data is in accordance with previous report²⁷. Started with 0.36 mmol **9**. Purification of **10** via silica gel chromatography using 20% EtOAc/hexanes. 67%, 0.173 g yellow oil, 20:1 Z/E. **¹H NMR** (500 MHz, Chloroform-*d*) δ 8.07 – 7.98 (m, 2H), 7.58 – 7.51 (m, 1H), 7.43 (t, $J = 7.8$ Hz, 2H), 7.30 – 7.23 (m, 2H), 7.20 – 7.14 (m, 3H), 7.03 (dt, $J = 6.3, 1.6$ Hz, 1H), 5.18 (t, $J = 6.2$ Hz, 1H), 5.12 – 5.05 (m, 2H), 5.01 (td, $J = 7.4, 6.2$ Hz, 1H), 4.34 (t, $J = 6.5$ Hz, 2H), 2.73 – 2.58 (m, 2H), 2.31 (qd, $J = 7.5, 1.6$ Hz, 2H), 2.11 (s, 3H), 2.05 – 1.74 (m, 10H), 1.71 – 1.59 (m, 5H), 1.47 – 1.38 (m, 2H), 1.36 – 1.08 (m, 10H), 0.95 – 0.81 (m, 5H). **¹³C NMR** (126 MHz, CDCl₃) δ 170.4, 169.5, 169.2, 166.7, 166.5, 141.6, 134.4, 132.9, 130.4, 129.6, 128.4, 125.9, 114.0, 72.8, 72.5, 71.8, 64.3, 37.1, 35.4, 33.2, 32.9, 32.5, 31.3, 31.0, 30.6, 28.5, 28.2, 26.9, 26.5, 26.21, 26.18, 24.5, 22.4, 21.2, 20.6, 14.0. **HRMS-(ESI)** for C₄₂H₅₆O₁₀ [M+NH₄]⁺: calculated 738.4212, found 738.4214

General procedure for asymmetric hydroformylation.

An oven-dried glass pressure bottle equipped with a stir bar is charged with THF 20 mM stock solutions of Rh(acac)(CO)₂ (0.3% catalyst loading, 150.37 μ L) and BisDiazaphos ligand (0.36%, 180.44 μ L) inside an N₂ glove box and then attached to a reactor. Inside a fume hood, the reactor is subjected to three pressurizing (150 psig) - depressurizing (20 psig) cycles, then pressurized to 150 psig and immersed in an oil bath set to 65 °C. After at least 30 min of catalyst pre-activation, the reactor is removed from the oil bath, allowed to cool down for five minutes and depressurized down to 10-20 psig. The alkene (1.00 mmol) is injected into the reactor as a solution in THF (amount of THF adjusted so that alkene concentration in the reactor is 0.8 M) via a gas-tight syringe and the reactor is then pressurized to 150 psig and immersed in the oil bath. Good gas-liquid mixing is

ensured by vigorous stirring with the stir bar constantly breaking the gas-liquid interface. After the reaction is complete, the reactor is allowed to cool down for 30 min and then depressurized. Crude ^1H NMR spectra are obtained by adding CDCl_3 directly to the crude THF solution. Reaction mixture is passed through a pad of silica gel and washed with 20% EtOAc in hexanes (200 mL) to remove residual catalyst.

(R)-(+)-1-oxo-5-phenylpentan-2-yl acetate (**2**). All characterization data is in accordance with previously reported data¹⁶. $[\alpha]_{\text{D}}^{20}$ +18.8 (c 1.00, CHCl_3). For determination of absolute configuration: the aldehyde was reduced with LiAlH_4 in dry THF at 0°C warming to room temperature for 24 h total reaction time, followed by slow addition of MeOH, sat aq. NH_4Cl and extraction with ethyl acetate of the resulting 5-Phenyl-1,2-Pentanediol $[\alpha]_{\text{D}}^{20}$ +0.8 (c 1.00, CHCl_3). Lit. $[\alpha]_{\text{D}}^{20}$ -13.6 (c 1.00, CHCl_3) for (S)-4-Phenyl-1,2-Butanediol²⁸

(R)-1-oxoheptan-2-yl (*R*)-2-acetoxy-5-phenylpentanoate (**5**). started with 1.17 mmol **4**. 92%, 0.38 g colorless oil. ^1H NMR (500 MHz, Chloroform-*d*) δ 9.45 (s, 1H), 7.28 (t, J = 7.5 Hz, 2H), 7.22 – 7.15 (m, 3H), 5.07 (dd, J = 7.8, 4.9 Hz, 2H), 2.74 – 2.61 (m, 2H), 2.12 (s, 3H), 2.03 – 1.92 (m, 2H), 1.90 – 1.67 (m, 4H), 1.45 – 1.36 (m, 2H), 1.36 – 1.24 (m, 4H), 0.93 – 0.85 (m, 3H). ^{13}C NMR (126 MHz, CDCl_3) δ 197.3, 170.6, 169.9, 141.5, 128.41, 128.40, 126.0, 78.8, 72.0, 35.3, 31.3, 30.7, 28.5, 26.8, 24.4, 22.3, 20.6, 13.9. HRMS-(ESI) for $\text{C}_{20}\text{H}_{28}\text{O}_5$ $[\text{M}+\text{NH}_4]^+$: calculated 366.2275, found 366.2278. $[\alpha]_{\text{D}}^{20}$ +25.8 (c 1.00, CHCl_3). For determination of absolute configuration (R, R): the aldehyde was reduced with LiAlH_4 in dry THF at 0°C warming to room temperature for 30 h total reaction time, followed by slow addition of MeOH, sat aq. NH_4Cl and extraction with ethyl acetate of the resulting mixture of 5-Phenyl-1,2-Pentanediol and 1,2-heptanediol. Optical rotation

of this mixture of diols was compared with a prepared mixture of the same two diols of (R) configuration and known optical rotation value.

(S)-4-cyclohexyl-1-oxobutan-2-yl (*R*)-2-(((*R*)-2-acetoxy-5-phenylpentanoyl)oxy)heptanoate (**8**). started with 0.5 mmol **7**. 84%, 0.217 g colorless oil. **¹H NMR** (500 MHz, Chloroform-*d*) δ 9.48 (s, 1H), 7.27 (dd, *J* = 8.6, 6.5 Hz, 2H), 7.18 (t, *J* = 6.9 Hz, 3H), 5.14 (t, *J* = 6.2 Hz, 1H), 5.07 (dd, *J* = 8.1, 4.5 Hz, 1H), 4.97 (dd, *J* = 8.8, 4.5 Hz, 1H), 2.72 – 2.61 (m, 2H), 2.12 (s, 3H), 2.02 – 1.60 (m, 13H), 1.48 – 1.11 (m, 12H), 0.94 – 0.84 (m, 5H). **¹³C NMR** (126 MHz, CDCl₃) δ 198.0, 170.5, 169.9, 169.6, 141.6, 128.39, 128.38, 126.0, 79.3, 72.7, 71.8, 37.3, 35.3, 33.2, 33.0, 32.3, 31.3, 31.0, 30.5, 26.8, 26.5, 26.3, 26.22, 26.20, 24.5, 22.4, 20.6, 14.0. **HRMS-(ESI)** for C₃₀H₄₄O₇ [M+NH₄]⁺: calculated 534.3425, found 534.3427. **$[\alpha]_D^{20}$** +6.6 (*c* 1.00, CHCl₃).

(4R,7R,10S,13S)-10-(2-cyclohexylethyl)-13-formyl-2,5,8,11-tetraoxo-7-pentyl-4-(3-phenylpropyl)-3,6,9,12-tetraoxaheptadecan-17-yl benzoate (**11**). 0.5% Rh(acac)(CO)₂, 0.6% (*S,S,S*)-BisDiazaphos. Started with 0.24 mmol **10**. 92%, 0.17 g yellow oil. **¹H NMR** (500 MHz, Chloroform-*d*) δ 9.45 (s, 1H), 8.08 – 7.98 (m, 2H), 7.54 (dt, *J* = 7.0, 1.7 Hz, 1H), 7.47 – 7.38 (m, 2H), 7.32 – 7.22 (m, 2H), 7.22 – 7.08 (m, 3H), 5.14 (t, *J* = 6.3 Hz, 1H), 5.11 – 5.03 (m, 3H), 4.32 (t, *J* = 6.5 Hz, 2H), 2.71 – 2.59 (m, 2H), 2.11 (s, 3H), 2.02 – 1.55 (m, 16H), 1.49 – 1.38 (m, 2H), 1.37 – 1.08 (m, 13H), 0.94 – 0.80 (m, 5H). **¹³C NMR** (126 MHz, CDCl₃) δ 197.5, 170.5, 169.6, 169.5, 169.3, 166.5, 141.6, 132.9, 130.3, 129.6, 128.4, 125.9, 78.7, 73.2, 72.6, 71.8, 64.4, 37.2, 35.3, 33.3, 33.0, 32.6, 31.3, 31.0, 30.5, 29.7, 28.6, 28.3, 28.2, 26.9, 26.5, 26.2, 26.2, 24.5, 22.4, 21.5, 20.6, 14.0. **HRMS-(ESI)** for C₄₃H₅₈O₁₁ [M+Na]⁺: calculated 773.3872, found 773.3870. **$[\alpha]_D^{20}$** -2.8 (*c* 1.00, CHCl₃).

General procedure for aldehyde oxidation.

The aldehyde (1 eq, 3.1 mmol), CH₃CN (7.64 mL), H₂O (7.43 mL), KH₂PO₄ (4 eq, 12.4 mmol, 1.67 g) and 30% H₂O₂ (4.1 eq, 12.71 mmol, 1.44 g 30% solution) were combined in a round bottom flask in this order. The reaction flask was cooled to 10°C and NaClO₂ (4 eq, 12.4 mmol, 1.11 g) was added dropwise as a solution in H₂O (7.64 mL). The solution was stirred vigorously for 3 h, while allowing it to warm up to room temperature. After reaction is complete, sodium sulfite is added for quenching, followed by 1M HCl (20 mL) and the aqueous mixture is extracted with dichloromethane (30 mL x 5). Two additional extractions of the aqueous mixture with EtOAc were performed after synthesis of **9** and **12**. The organic layers are combined, dried over MgSO₄ and solvent removed in vacuo to afford the carboxylic acid product as a yellow oil. Note: All acetonitrile needs to be removed before the enol ester formation step to avoid catalyst poisoning.

(R)-2-acetoxy-5-phenylpentanoic acid (**3**). started with 3.1 mmol **2**. 95%, 0.7 g colorless oil. ¹H NMR (400 MHz, Chloroform-*d*) δ 7.34 – 7.24 (m, 2H), 7.24 – 7.15 (m, 3H), 5.03 (dd, *J* = 7.1, 5.4 Hz, 1H), 2.66 (dd, *J* = 8.5, 6.7 Hz, 2H), 2.14 (s, 3H), 1.96 – 1.87 (m, 2H), 1.78 (p, *J* = 7.3 Hz, 2H). ¹³C NMR (126 MHz, CDCl₃) δ 176.0, 170.9, 141.5, 128.5, 128.4, 126.1, 71.8, 35.3, 30.5, 26.9, 20.6. HRMS-(ESI) for C₁₃H₁₆O₄ [M-H]⁻: calculated 235.0975, found 235.0978. **Separation by HPLC** (supports no epimerization of the chiral center during oxidation): CHIRALPAK 1A (AD-H), 5% iPrOH/hexanes, 0.5 ml/min, ambient temperature, 220 nm, *t*_R 8.8 min (minor, (S)), 10.1 min (major, (R))

(R)-2-(((*R*)-2-acetoxy-5-phenylpentanoyl)oxy)heptanoic acid (**6**). started with 0.54 mmol **5**. 90%, 0.175 g yellow oil. ¹H NMR (500 MHz, Chloroform-*d*) δ 8.82 (br, 1H), 7.26 (t, *J* = 7.5 Hz, 2H), 7.22 – 7.14 (m, 3H), 5.16 – 4.96 (m, 2H), 2.67 – 2.60 (m, 2H), 2.12 (s, 3H),

2.01 – 1.84 (m, 4H), 1.79 (p, $J = 7.3, 6.7$ Hz, 2H), 1.48 – 1.40 (m, 2H), 1.34 – 1.27 (m, 4H), 0.90 (t, $J = 6.7$ Hz, 3H). $^{13}\text{C NMR}$ (126 MHz, CDCl_3) δ 175.4, 170.8, 169.9, 141.6, 128.37, 128.35, 125.9, 72.3, 71.9, 35.3, 31.2, 30.8, 30.5, 26.7, 24.6, 22.3, 20.6, 14.0.

HRMS-(ESI) for $\text{C}_{20}\text{H}_{28}\text{O}_6$ $[\text{M}+\text{NH}_4]^+$: calculated 382.2225, found 382.2224

(S)-2-(((*R*)-2-(((*R*)-2-acetoxy-5-phenylpentanoyl)oxy)heptanoyl)oxy)-4-

cyclohexylbutanoic acid (9). started with 0.42 mmol **8**. 86%, 0.19 g, colorless oil. $^1\text{H NMR}$ (500 MHz, Chloroform-*d*) δ 7.31 – 7.23 (m, 2H), 7.18 (dd, $J = 8.2, 6.5$ Hz, 3H), 5.17 (t, $J = 6.2$ Hz, 1H), 5.06 (ddd, $J = 8.3, 5.6, 4.3$ Hz, 2H), 2.73 – 2.59 (m, 2H), 2.12 (s, 3H), 2.04 – 1.75 (m, 8H), 1.74 – 1.60 (m, 6H), 1.47 – 1.37 (m, 2H), 1.36 – 1.09 (m, 9H), 0.93 – 0.84 (m, 5H). $^{13}\text{C NMR}$ (126 MHz, CDCl_3) δ 174.9, 170.6, 169.7, 169.2, 141.6, 128.4, 126.0, 72.7, 72.6, 71.9, 37.2, 35.3, 33.2, 33.0, 32.5, 31.3, 31.0, 30.6, 28.5, 27.0, 26.5, 26.24, 26.21, 24.5, 22.4, 20.6, 14.0. **HRMS-(ESI)** for $\text{C}_{30}\text{H}_{44}\text{O}_8$ $[\text{M}+\text{NH}_4]^+$: calculated 550.3375, found 550.3369

(2S,5S,8R,11R)-2-(4-(benzoyloxy)butyl)-5-(2-cyclohexylethyl)-4,7,10,13-tetraoxo-8-

pentyl-11-(3-phenylpropyl)-3,6,9,12-tetraoxatetradecanoic acid (12). started with 0.22 mmol **11**. 70% yield, 120 mg yellow oil. $^1\text{H NMR}$ (500 MHz, Chloroform-*d*) δ 8.05 – 8.02 (m, 2H), 7.54 (t, $J = 7.4$ Hz, 1H), 7.43 (t, $J = 7.6$ Hz, 2H), 7.29 – 7.23 (m, 2H), 7.19 – 7.14 (m, 3H), 5.18 – 5.10 (m, 2H), 5.09 – 5.05 (m, 2H), 4.33 (t, $J = 6.4$ Hz, 2H), 2.64 (td, $J = 9.1, 6.3$ Hz, 2H), 2.11 (s, 3H), 2.02 – 1.75 (m, 10H), 1.72 – 1.58 (m, 6H), 1.47 – 1.36 (m, 2H), 1.36 – 1.05 (m, 13H), 0.93 – 0.81 (m, 5H). $^{13}\text{C NMR}$ (126 MHz, CDCl_3) δ 173.5, 169.6, 168.6, 168.3, 168.0, 165.6, 140.6, 131.9, 129.2, 128.5, 127.3, 124.9, 71.8, 71.6, 71.1, 70.8, 63.4, 36.1, 34.3, 32.2, 31.9, 31.3, 30.2, 30.0, 29.49, 29.45, 28.7, 27.3, 27.1,

25.9, 25.5, 25.2, 23.4, 21.3, 20.6, 19.5, 12.9. **HRMS-(ESI)** for $C_{43}H_{58}O_{12}$ $[M+NH_4]^+$: calculated 784.4267, found 784.4269

Procedures and characterization data for enamide synthesis and AHF (Scheme 3.3)

(4*R*,7*R*,10*S*,13*S*)-10-(2-cyclohexylethyl)-2,5,8,11-tetraoxo-7-pentyl-4-(3-phenylpropyl)-13-((((1*Z*,7*Z*)-8-(2,2,2-trifluoroacetamido)octa-1,7-dien-1-yl)oxy)carbonyl)-3,6,9,12-tetraoxaheptadecan-17-yl benzoate (**14**). Ru(methallyl)₂dppb (6 mol%, 6 mg) and 0.5 mL dry and degassed THF were combined in an oven-dried Schlenk flask equipped with a stir bar inside a N₂ glove box. Inside a fume hood, the tetramer carboxylic acid **12** (1 eq, 120 mg, 0.16 mmol) was added to the reaction flask via syringe as a solution in 0.5 mL dry and degassed THF, followed by neat alkyne **13** (1.5 eq, 0.0623 mL, 0.24 mmol). The solution was immersed in an oil bath and allowed to stir at 45°C for 48 h under N₂. After reaction is complete, the reaction mixture is passed through a pad of silica in a fritted glass funnel, washed with 20% EtOAc in hexanes (450 mL) and solvent removed in vacuo. The yellow oil residue is purified via silica gel flash column chromatography with 20% EtOAc/hexanes as eluent to give the product as a viscous yellow oil in 34% yield (54 mg) in 7:1 *Z/E* ratio. **¹H NMR** (500 MHz, Chloroform-*d*) δ 8.07 – 7.95 (m, 2H), 7.56 (td, *J* = 7.4, 1.6 Hz, 1H), 7.44 (t, *J* = 7.7 Hz, 2H), 7.31 – 7.23 (m, 2H), 7.18 (dd, *J* = 7.9, 6.1 Hz, 3H), 6.95 (dd, *J* = 6.4, 1.7 Hz, 1H), 6.63 (t, *J* = 10.8, 8.9 Hz, 1H), 5.19 – 5.11 (m, 1H), 5.11 – 4.99 (m, 4H), 4.92 (q, *J* = 7.2 Hz, 1H), 4.36 – 4.29 (m, 2H), 2.72 – 2.52 (m, 2H), 2.11 (s, 3H), 2.08 – 1.74 (m, 15H), 1.73 – 1.55 (m, 8H), 1.48 – 1.36 (m, 6H), 1.35 – 1.08 (m, 10H), 0.95 – 0.82 (m, 5H). **¹³C NMR** (126 MHz, CDCl₃) δ 170.5, 169.6, 169.3, 169.1, 167.8, 166.7, 166.6, 154.5, 141.6, 134.0, 133.0, 132.97, 130.2, 129.5, 128.4,

128.35, 125.9, 118.8, 117.0, 115.2, 72.8, 72.6, 72.2, 71.8, 64.4, 37.2, 35.3, 33.3, 32.9, 32.5, 31.3, 31.0, 30.54, 30.46, 28.44, 28.42, 28.1, 27.0, 26.5, 26.2, 25.5, 24.5, 24.1, 22.4, 21.5, 20.6, 14.00. **HRMS-(ESI)** for C₅₃H₇₀F₃NO₁₃ [M+NH₄]⁺: calculated 1003.5138, found 1003.5144

(Z)-2,2,2-trifluoro-*N*-(oct-1-en-7-yn-1-yl)acetamide (**13**).

synthesized according to a modified known procedure^{17a}: In an oven-dried 50 mL Schlenk flask equipped with a magnetic stir bar inside a nitrogen-filled glovebox, *bis*(2-methylallyl)(COD)ruthenium(II) (5%, 240 mg), 1,4-*bis*(dicyclohexylphosphino)butane (6%, 405 mg), ytterbium triflate (4%, 372 mg), and trifluoroacetamide (1 eq., 15 mmol, 1.7 g) were combined, and anhydrous DMF (22 mL) was added. In a fume hood on a Schlenk line, degassed 1,7-octadiyne (2 eq., 30.0 mmol, 4.1 mL) was added via syringe, followed by degassed H₂O (1.62 mL). The dark red solution was stirred for 24 h at 60 °C in an oil bath. The mixture was then poured into saturated aqueous sodium bicarbonate solution (100 mL). This mixture was extracted with ethyl acetate (3x50 mL), the combined organic layers were washed with water (5x50 mL) and brine (1x50 mL), dried over magnesium sulfate, filtered, and the volatiles were removed in vacuo. The dark brown oil was purified twice by flash column chromatography on silica gel with 10% EtOAc in hexanes for the first column and 5% EtOAc in hexanes for the second column. The product was obtained as a bright yellow oil in 20% yield, 0.53 g. **¹H NMR** (400 MHz, Chloroform-*d*) δ 7.62 (s, 1H), 6.66 (dd, *J* = 10.8, 9.0 Hz, 1H), 5.08 (q, *J* = 7.9 Hz, 1H), 2.26 – 2.19 (m, 2H), 2.15 – 2.04 (m, 2H), 1.97 (t, *J* = 2.7 Hz, 1H), 1.59 (h, *J* = 3.6, 2.8 Hz, 4H). **¹³C NMR** (126 MHz, CDCl₃) δ 154.1, 118.9, 116.8, 114.6, 84.0, 68.8, 28.0, 27.6,

25.3, 18.2. ^{19}F NMR (377 MHz, CDCl_3) δ -75.66. **HRMS-(ASAP-MS)** for $\text{C}_{10}\text{H}_{12}\text{F}_3\text{NO}$
[M+H] $^+$: calculated 220.0944, found 220.0944

(4R,7R,10S,13S)-10-(2-cyclohexylethyl)-13-((((2S)-1,10-dioxo-9-(2,2,2-trifluoroacetamido)decan-2-yl)oxy)carbonyl)-2,5,8,11-tetraoxo-7-pentyl-4-(3-phenylpropyl)-3,6,9,12-tetraoxaheptadecan-17-yl benzoate (15).

Procedure modified from the general hydroformylation procedure due to the small amount of sample: Two oven-dried glass pressure bottles each equipped with a stir bar and two reactors are brought into a N_2 filled glovebox. One pressure bottle is charged with THF 100 mM stock solution of $\text{Rh}(\text{acac})(\text{CO})_2$ (25.35 μL stock solution, 5% catalyst loading) and 20 mM stock solution of (S,S,S)-BisDiazaphos (152.11 μL stock solution, 6 % ligand loading) and then attached to a reactor. The second pressure bottle is charged with the viscous enol ester/enamide substrate (50 mg) as a mixture in 0.5 mL dry THF. After all the THF is removed (under vacuo inside the glove box), the pressure bottle is attached to a reactor. Inside a fume hood, the reactor containing the catalyst mixture is subjected to three pressurizing (150 psig) - depressurizing (20 psig) cycles, then pressurized to 150 psig and immersed in an oil bath set to 65 $^\circ\text{C}$. After 30 min of catalyst pre-activation, the reactor is removed from the oil bath, allowed to cool down for five minutes and depressurized down to 10-20 psig. The catalyst solution is then transferred to the second reactor containing the substrate using a syringe. The reactor containing now the substrate and the catalyst solution is then pressurized to 150 psig and immersed in the oil bath. Good gas-liquid mixing is ensured by vigorous stirring with the stir bar constantly breaking the gas-liquid interface. After 3 h at 65 $^\circ\text{C}$, the reactor is allowed to cool down for 30 min and then depressurized. Crude ^1H NMR spectra are obtained by adding CDCl_3 directly to

the crude THF solution. Reaction mixture is passed through a pad of silica gel and washed with 20% EtOAc in hexanes to remove residual catalyst. Recovered after silica pad: 30 mg combined weight, yellow oil, higher than 95% conversion of the starting material to a di-aldehyde (determined by ^1H and ^{13}C NMR). Due to the small amount of sample, **15** could not be isolated and its diastereomeric purity could not be unambiguously determined. ^1H NMR (500 MHz, Chloroform-*d*) δ 9.58 (s, 1H), 9.46 (s, 1H), 8.04 (d, $J = 7.5$ Hz, 2H), 7.55 (t, $J = 7.5$ Hz, 1H), 7.44 (t, $J = 7.7$ Hz, 2H), 7.27 (t, $J = 7.6$ Hz, 2H), 7.17 (d, $J = 7.5$ Hz, 3H), 5.19 – 4.98 (m, 5H), 4.64 – 4.53 (m, 1H), 4.38 – 4.30 (m, 2H), 2.73 – 2.58 (m, 2H), 2.11 (s, 3H), 2.09 – 1.57 (m, 20H), 1.52 – 1.07 (m, 20H), 0.93 – 0.81 (m, 8H). ^{13}C NMR (126 MHz, CDCl_3) δ 196.0, 195.6, 169.5, 168.6, 168.3, 168.2, 168.0, 156.3, 140.6, 131.9, 129.2, 128.5, 127.3, 124.9, 115.8, 77.7, 71.8, 71.53, 71.48, 70.8, 63.5, 57.9, 36.1, 34.3, 32.3, 31.9, 31.5, 30.6, 30.2, 30.0, 29.5, 27.7, 27.5, 27.4, 27.3, 27.2, 27.1, 25.9, 25.5, 25.2, 25.17, 23.6, 23.5, 21.6, 21.4, 20.6, 19.5, 12.9. **HRMS-(ESI)** for $\text{C}_{55}\text{H}_{74}\text{F}_3\text{NO}_{15}$ $[\text{M}+\text{NH}_4]^+$: calculated 1063.5349, found 1063.5334

3.5 References

1. Worthy, A. D.; Joe, C. L.; Lightburn, T. E.; Tan, K. L., *Journal of the American Chemical Society* **2010**, *132* (42), 14757-14759.
2. (a) Hatada, K.; Kitayama, T.; Ute, K.; Nishiura, T., *Macromol. Rapid Commun.* **2004**, *25* (16), 1447-1477; (b) Sudesh, K.; Abe, H.; Doi, Y., *Prog. Polym. Sci.* **2000**, *25* (10), 1503-1555.
3. (a) Franz, N.; Kreutzer, G.; Klok, H. A., *Synlett* **2006**, (12), 1793-1815; (b) Albert, M.; Seebach, D.; Duchardt, E.; Schwalbe, H., *Helv. Chim. Acta* **2002**, *85* (2), 633-658;

- (c) Lutz, J. F.; Ouchi, M.; Liu, D. R.; Sawamoto, M., *Science* **2013**, *341* (6146), 628-+;
- (d) Badi, N.; Lutz, J. F., *Chem. Soc. Rev.* **2009**, *38* (12), 3383-3390; (e) Solleder, S. C.; Meier, M. A. R., *Angew.Chem.Int.Ed.* **2014**, *53* (3), 711-714; (f) Ito, S.; Noguchi, M.; Nozaki, K., *Chem. Commun.* **2012**, *48* (85), 10481-10483; (g) Nakatani, K.; Ogura, Y.; Koda, Y.; Terashima, T.; Sawamoto, M., *J. Am. Chem. Soc.* **2012**, *134* (9), 4373-4383;
- (h) Pacini, A.; Caricato, M.; Ferrari, S.; Capsoni, D.; de Ilarduya, A. M.; Munoz-Guerra, S.; Pasini, D., *J. Polym. Sci., Part A: Polym. Chem.* **2012**, *50* (22), 4790-4799; (i) Rubinshtein, M.; James, C. R.; Young, J. L.; Ma, Y. J.; Kobayashi, Y.; Gianneschi, N. C.; Yang, J., *Org. Lett.* **2010**, *12* (15), 3560-3563.
4. (a) Binauld, S.; Damiron, D.; Connal, L. A.; Hawker, C. J.; Drockenmuller, E., *Macromol. Rapid Commun.* **2011**, *32* (2), 147-168; (b) Franz, N.; Menin, L.; Klok, H. A., *Eur. J. Org. Chem.* **2009**, (31), 5390-5405.
5. Merrifield, R. B., *Angew. Chem. Int. Ed. Engl* **1985**, *24* (10), 799-810.
6. (a) Yu, Y.; Zou, J.; Cheng, C., *Polymer Chemistry* **2014**, *5* (20), 5854-5872; (b) Tsuji, H.; Eto, T.; Sakamoto, Y., *Materials* **2011**, *4* (8), 1384-1398; (c) Kim, S.-H.; Sim, Y.-K.; Kim, B.-T.; Kim, Y. H.; Kim, Y.-J.; Park, S.; Lee, H., *Tetrahedron: Asymmetry* **2011**, *22* (14–15), 1499-1504.
7. (a) Wu, X.-F.; Fang, X.; Wu, L.; Jackstell, R.; Neumann, H.; Beller, M., *Acc. Chem. Res.* **2014**, *47* (4), 1041-1053; (b) Chikkali, S. H.; van der Vlugt, J. I.; Reek, J. N. H., *Coord. Chem. Rev.* **2014**, *262* (0), 1-15; (c) Franke, R.; Selent, D.; Börner, A., *Chem. Rev.* **2012**, *112* (11), 5675-5732; (d) Whiteker, G.; Cobley, C., Applications of Rhodium-Catalyzed Hydroformylation in the Pharmaceutical, Agrochemical, and Fragrance Industries. In *Organometallics as Catalysts in the Fine Chemical Industry*,

Beller, M.; Blaser, H.-U., Eds. Springer Berlin Heidelberg: 2012; Vol. 42, pp 35-46; (e) Gual, A.; Godard, C.; Castellón, S.; Claver, C., *Tetrahedron: Asymmetry* **2010**, *21* (9–10), 1135-1146; (f) Breit, B., Recent Advances in Alkene Hydroformylation. In *Metal Catalyzed Reductive C–C Bond Formation*, Krische, M., Ed. Springer Berlin Heidelberg: 2007; Vol. 279, pp 139-172; (g) Klosin, J.; Landis, C. R., *Acc. Chem. Res.* **2007**, *40* (12), 1251-1259.

8. (a) Allmendinger, S.; Kinuta, H.; Breit, B., *Adv. Synth. Catal.* **2015**, *357* (1), 41-45; (b) Fernández-Pérez, H.; Benet-Buchholz, J.; Vidal-Ferran, A., *Org. Lett.* **2013**, *15* (14), 3634-3637; (c) Nozaki, K.; Sakai, N.; Nanno, T.; Higashijima, T.; Mano, S.; Horiuchi, T.; Takaya, H., *J. Am. Chem. Soc.* **1997**, *119* (19), 4413-4423; (d) Sakai, N.; Nozaki, K.; Takaya, H., *J. Chem. Soc., Chem. Commun.* **1994**, (4), 395-396; (e) Yan, Y.; Zhang, X., *J. Am. Chem. Soc.* **2006**, *128* (22), 7198-7202; (f) Joe, C. L.; Blaisdell, T. P.; Geoghan, A. F.; Tan, K. L., *J. Am. Chem. Soc.* **2014**, *136* (24), 8556-8559; (g) Grünanger, C. U.; Breit, B., *Angew. Chem. Int. Ed.* **2008**, *47* (38), 7346-7349; (h) Breit, B., *Acc. Chem. Res.* **2003**, *36* (4), 264-275.

9. (a) Adint, T. T.; Wong, G. W.; Landis, C. R., *J. Org. Chem.* **2013**, *78* (9), 4231-4238; (b) Clark, T. P.; Landis, C. R.; Freed, S. L.; Klosin, J.; Abboud, K. A., *J. Am. Chem. Soc.* **2005**, *127* (14), 5040-5042.

10. (a) Watkins, A. L.; Landis, C. R., *Org. Lett.* **2011**, *13* (1), 164-167; (b) McDonald, R. I.; Wong, G. W.; Neupane, R. P.; Stahl, S. S.; Landis, C. R., *J. Am. Chem. Soc.* **2010**, *132* (40), 14027-14029; (c) Watkins, A. L.; Hashiguchi, B. G.; Landis, C. R., *Org. Lett.* **2008**, *10* (20), 4553-4556.

11. (a) Risi, R. M.; Maza, A. M.; Burke, S. D., *J. Org. Chem.* **2015**, *80* (1), 204-216;
(b) Risi, R. M.; Burke, S. D., *Org. Lett.* **2012**, *14* (4), 1180-1182.
12. Clemens, A. J. L.; Burke, S. D., *J. Org. Chem.* **2012**, *77* (6), 2983-2985.
13. Risi, R. M.; Burke, S. D., *Org. Lett.* **2012**, *14* (10), 2572-2575.
14. Ho, S.; Bucher, C.; Leighton, J. L., *Angew. Chem. Int. Ed.* **2013**, *52* (26), 6757-6761.
15. Wong, G. W.; Landis, C. R., *Angew. Chem. Int. Ed.* **2013**, *52* (5), 1564-1567.
16. Abrams, M. L.; Foarta, F.; Landis, C. R., *J. Am. Chem. Soc.* **2014**, *136* (41), 14583-14588.
17. (a) Gooßen, L. J.; Salih, K. S. M.; Blanchot, M., *Angew. Chem. Int. Ed.* **2008**, *47* (44), 8492-8495; (b) Huang, L.; Arndt, M.; Gooßen, K.; Heydt, H.; Gooßen, L. J., *Chem. Rev.* **2015**, *115* (7), 2596-2697; (c) Goossen, L. J.; Blanchot, M.; Brinkmann, C.; Goossen, K.; Karch, R.; Rivas-Nass, A., *J. Org. Chem.* **2006**, *71* (25), 9506-9509.
18. (a) Doucet, H.; Martin-Vaca, B.; Bruneau, C.; Dixneuf, P. H., *J. Org. Chem.* **1995**, *60* (22), 7247-7255; (b) Chary, B. C.; Kim, S., *J. Org. Chem.* **2010**, *75* (22), 7928-7931; (c) Gooßen, L. J.; Rodríguez, N.; Gooßen, K., *Angew. Chem. Int. Ed.* **2008**, *47* (17), 3100-3120; (d) Bruneau, C.; Dixneuf, P. H., *Angew. Chem. Int. Ed.* **2006**, *45* (14), 2176-2203; (e) Hua, R.; Tian, X., *J. Org. Chem.* **2004**, *69* (17), 5782-5784; (f) Goossen, L. J.; Paetzold, J.; Koley, D., *Chem. Commun.* **2003**, (6), 706-707; (g) Doucet, H.; Derrien, N.; Kabouche, Z.; Bruneau, C.; Dixneuf, P. H., *J. Organomet. Chem.* **1998**, *551* (1-2), 151-157; (h) Wei, S. P.; Pedroni, J.; Meissner, A.; Lumbroso, A.; Drexler, H. J.; Heller, D.; Breit, B., *Chem. Eur. J.* **2013**, *19* (36), 12067-12076.

19. Bal, B. S.; Childers, W. E.; Pinnick, H. W., *Tetrahedron* **1981**, 37 (11), 2091-2096.
20. Miles, K. C.; Abrams, M. L.; Landis, C. R.; Stahl, S. S., *Org. Lett.* **2016**, 18 (15), 3590-3593.
21. Pattabiraman, V. R.; Bode, J. W., *Nature* **2011**, 480 (7378), 471-479.
22. (a) Sharp, P. P.; Banwell, M. G.; Renner, J.; Lohmann, K.; Willis, A. C., *Org. Lett.* **2013**, 15 (11), 2616-2619; (b) Gupta, S.; Agarwal, P. K.; Saifuddin, M.; Kundu, B., *Tetrahedron Lett.* **2011**, 52 (44), 5752-5757.
23. Hydroamidation of a diyne has been reported before in related Cu and Au systems. The Ru-promoted enamide synthesis reported in Scheme 3 initially generates both mono-coupled product 10 and corresponding bis-coupled product in a 3.3:1 mixture. Separation of this mixture via silica gel chromatography affords clean 10 in 20% isolated yield. The use of 2 eq. diyne in the attempt to favour predominant formation of 10 appeared to inhibit the reaction. At 2, 4 and 8 eq. diyne, 50%, 25% and 12% of trifluoroacetamide reacted respectively.
24. Purification of the enol esters via silica gel chromatography was necessary in order to remove residual Ru. Traces of Ru were observed to inhibit AHF and lead to either no conversion of starting material or, in some cases, Z/ E isomerization.
25. (a) Vougioukalakis, G. C., *Chem. Eur. J.* **2012**, 18 (29), 8868-8880; (b) Paquette, L. A.; Schloss, J. D.; Efremov, I.; Fabris, F.; Gallou, F.; Mendez-Andino, J.; Yang, J., *Org. Lett.* **2000**, 2 (9), 1259-1261.
26. Wong, G. W. A. T. T. L., C.R., *Org. Synth.* **2012**, 89, 243-254.
27. Stevens, B. D.; Nelson, S. G., *J. Org. Chem.* **2005**, 70 (11), 4375-4379.

28. (a) Kadyrov, R.; Koenigs, R. M.; Brinkmann, C.; Voigtlaender, D.; Rueping, M., *Angew.Chem.Int.Ed.* **2009**, *48* (41), 7556-7559; (b) Martynow, J. G.; Jozwik, J.; Szelejewski, W.; Achmatowicz, O.; Kutner, A.; Wisniewski, K.; Winiarski, J.; Zegrocka-Stendel, O.; Golebiewski, P., *Eur. J. Org. Chem.* **2007**, (4), 689-703.

Chapter 4

Enantioenriched α -Tetrasubstituted Aldehydes

via Rhodium-Bisphosphine Catalyzed Asymmetric Hydroformylation

4.1. Introduction

Stereoselective synthesis of tetrasubstituted stereogenic centers remains a formidable challenge in organic synthesis, despite their prevalence in numerous drug candidates and natural products. Tetrasubstituted aldehydes are attractive synthetic intermediates due to the versatility of the aldehyde functionality. Existing stereoselective methods to generate enantioenriched α -tetrasubstituted aldehydes include organocatalytic methods¹, chiral auxiliary-controlled² or Pd-catalyzed asymmetric alkylations³, reactions of prochiral enol derivatives⁴ or stereocontrolled cycloadditions⁵. These methods generally suffer from limited scope, lack of predictability or cost-efficiency. An alternative strategy for generating enantioenriched α -tetrasubstituted aldehydes is branched selective asymmetric hydroformylation (AHF) of 1,1'-disubstituted alkenes (Figure 4.1).

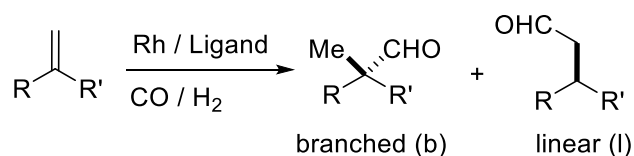


Figure 4.1 AHF of 1,1'-disubstituted alkenes

Hydroformylation is a long-standing commodity process in the synthesis of linear aldehydes from alkenes, carbon monoxide and dihydrogen⁶. Unlike linear hydroformylation, AHF is underdeveloped in the synthesis of branched, chiral aldehydes, which serve as useful synthons in the production of pharmaceuticals and fine chemicals. Effective AHF has been demonstrated for various monosubstituted⁷, and to a lesser

extent, disubstituted alkenes⁸. Notable chiral ligand systems for selective alkene AHF include BisDiazaphos⁹ (**L1**), Ph-BPE (**L2**), Chiraphos (**L3**), DIOP (**L4**), BINAP (**L5**), P-chirogenic ligands such as QuinoxP* (**L6**), among others (Figure 4.3)¹⁰.

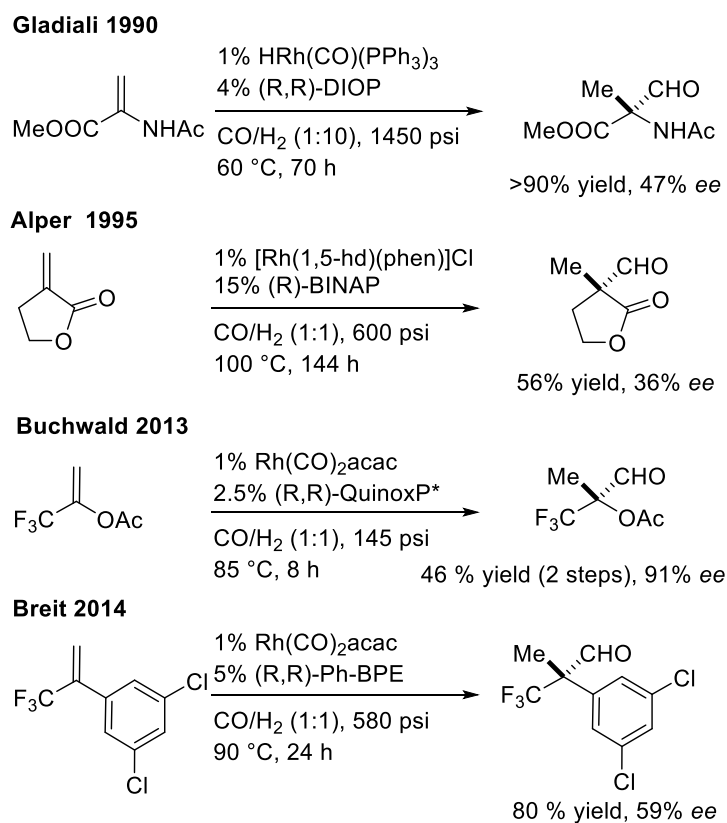


Figure 4.2 Previous examples of AHF of 1,1'-disubstituted alkenes

Despite the large volume of literature on enantioselective hydroformylation, there are only four examples where a 1,1'-disubstituted alkene undergoes stereoselective branched hydroformylation¹¹. AHF of 1,1'-alkenes is generally slow compared to mono- or 1,2-disubstituted alkenes and generally favors linear selectivity (according to Keuleman's

rule). Examples of branched selective AHF of 1,1'-alkenes are scarce. Gladiali¹², Alper¹³ and Breit¹⁴ reported AHF of N-acylamino acrylate, α -methylene- γ -butyrolactone and 1,3-dichloro-5-(3,3,3-trifluoroprop-1-en-2-yl)benzene respectively (Figure 4.2). These reactions proceeded with high branched selectivity, but they required high pressures and displayed modest enantioselectivities. In addition, significant amount of alkene hydrogenation was reported as a common side reaction, especially in the case of acrylate derivatives. Buchwald¹⁵, and more recently Zhang¹⁶, reached high enantioselectivity (up to 91% ee) with 1-(trifluoromethyl)-ethenyl acetate at mild conditions. Herein, we report highly selective and practical AHF of various 1,1'-disubstituted alkenes to generate enantioenriched α -tetrasubstituted aldehydes.

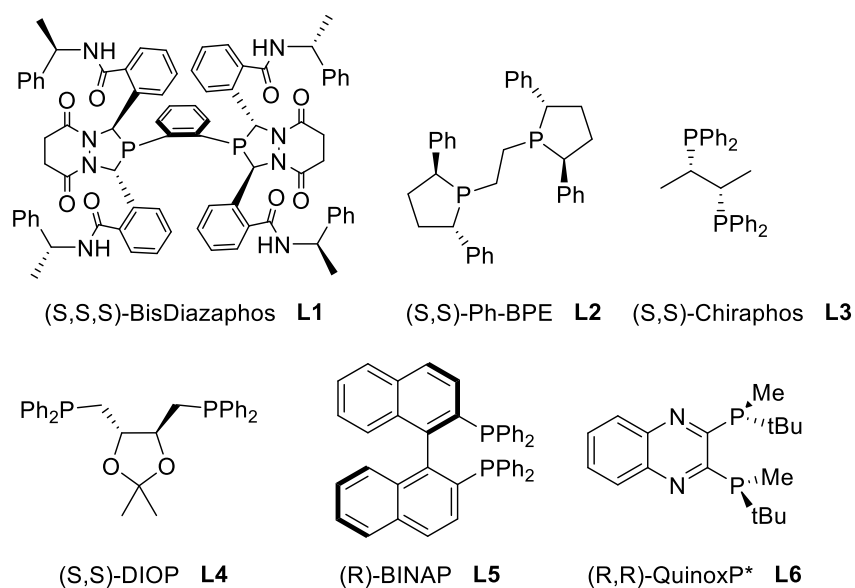
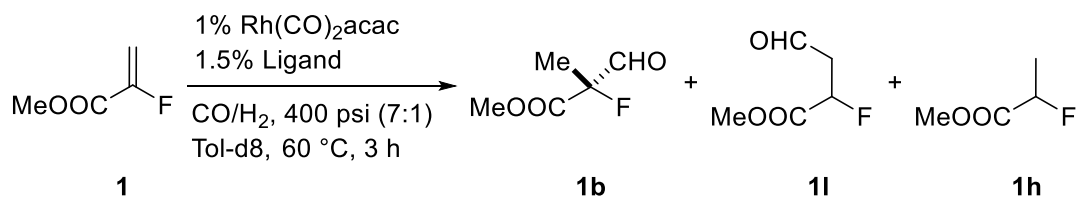


Figure 4.3 Chiral ligands for AHF

Based on previous AHF results, alkenes bearing electron withdrawing groups through the sigma framework, such as enol esters, enamides, vinyl arenes, vinyl fluorides or acrylates, tend to favor the branched regioisomer in AHF and override the general steric preference for the linear regioisomer. We hypothesized that a similar strategy could lead to branched selective AHF of 1,1'-disubstituted alkenes.

4.2. Results and discussion

Initial studies focused on methyl 2-fluoroacrylate **1**, a commercially available alkene that is expected to favor branched selectivity due to its electron withdrawing substituents. In order to investigate the effect of ligand structure on hydroformylation, ligands **L1** through **L6** were investigated in the AHF of **1** in the presence of Rh(CO)₂acac precursor at 400 psi CO/H₂ (7:1), at 60 °C (Table 4.1). A gas mixture rich in CO was used in order to minimize competing alkene hydrogenation. Under these conditions, **L1** and **L2** displayed the highest regio and enantioselectivity, with **L1** giving the fastest rates. **L4** and **L6** afforded high branch selectivity, but modest enantioselectivity, while **L3** and **L5** showed no appreciable conversion of starting material. Given these results, only **L1** and **L2** ligands were used for the remaining of our studies.

Table 4.1. Ligand screening in the AHF of Methyl 2-fluoroacrylate

Entry	Ligand	% conversion ^b			% ee (1b) ^c
		1b	1l	1h	
1. ^a	L1	96	<1	3	85
2. ^a	L2	55	<1	5	84
3.	L3	<1	0	0	-
4.	L4	55	<1	1	40
5.	L5	<1	0	0	-
6.	L6	18	<1	<1	71

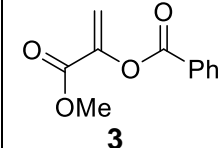
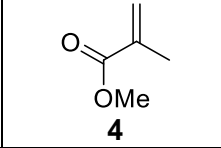
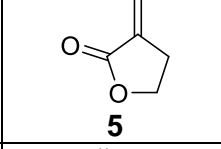
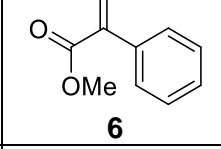
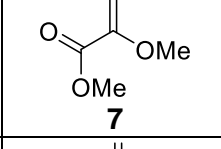
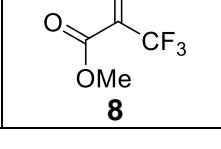
^a THF as solvent ^b determined via ¹H NMR of crude mixture ^c determined via chiral GC of crude mixture

The effect of CO/H_2 ratios and temperature on AHF of methyl 2-fluoroacrylate were examined in Table 4.2. Higher CO partial pressures (entry 1 versus entry 2) and lower temperatures (entry 3) lead to higher hydroformylation to hydrogenation ratios. A slight increase in enantioselectivity is observed at lower temperatures (Table 4.2). Results obtained at milder pressures, such as 150 psi (entry 1), reveal very little erosion of selectivity compared to higher pressures. Hence, the rest of our studies are conducted at

Other α -substituted acrylates, many of these commercially available, have been investigated in AHF. While α -substituted aldehydes, especially β -dicarbonyls, are generally susceptible to racemization, tetrasubstituted aldehydes are non-enolizable. This advantage expands the synthetic potential of the aldehyde products.

The acrylates **1-8** were tested in the presence of both (S,S,S)-BisDiazaphos (**L1**) and (S,S)-Ph-BPE (**L2**). Entries 2 and 3 proceed with excellent branched selectivity in just 2 h in the presence of Rh/**L1** displaying 73% and 16% ee respectively. Results with Rh/**L2** are modest. The substrate scope is not limited to alkenes bearing two electron withdrawing groups. Hydroformylation of the less electronically activated methyl methacrylate¹⁹ (entry 4) and α -methylene- γ -butyrolactone **5** (entry 5) proceeds with excellent regioselectivity in the presence of Rh/Ph-BPE. Unlike Alper's previous report, where only 36% ee was achieved in the AHF of **5**, the Rh/Ph-BPE catalyst system affords the highest reported enantioselectivity to date for this alkene, 95% ee, also at milder conditions. AHF of phenyl acrylate (entry 6) proceeds predominantly with branch selectivity in the presence of Rh/**L1** (60% conversion to branched aldehyde after 24 h), but with poor enantiocontrol (13% ee). Rh/**L2** gives predominantly hydrogenation under the same conditions. The methoxy acrylate in entry 7 proceeds with excellent branched selectivity and enantioselectivity (90% ee with both ligands), both only 79% and 55% of starting material reacted after 72 h in the presence of **L1** and **L2** respectively.

Other electron deficient alkenes afford branch selective AHF (Table 4.4). AHF of 1-(trifluoromethyl)ethenyl acetate, thoroughly investigated by Buchwald previously¹⁵, affords high selectivity with both Rh/**L1** and **L2** (entry 1). AHF of 1-Cyanovinyl Acetate (entry 2) proceeds with excellent branched selectivity (95% conversion to branched

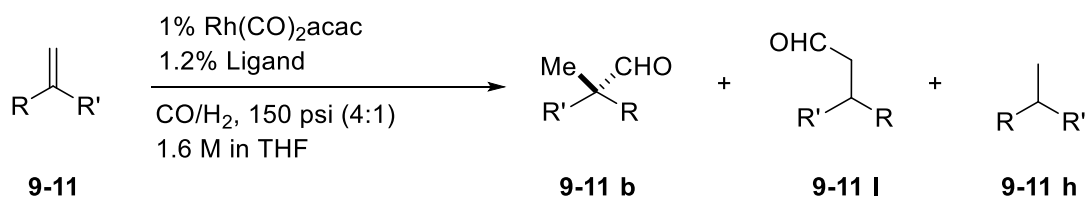
3.		L1 L2	2	>99 (80) 31 ^f	<1 <1	<1 10	16 0
4.		L1 L2	24	60 ^f 87 ^f (74)	16 2	<1 3	n/a
5. ^g		L1 L2	24	39 ^e 93 (78)	15 2	<1 5	25 95
6.		L1 L2	24	65 ^f (51) 15	14 1	21 80	13 nd
7.		L1 L2	72	73 ^f (61) 53 ^f	5 1	<1 <1	90 89
8. ^d		L1	2	43	<1	66	15

^a determined via crude ¹H NMR versus mesitylene ^b isolated yield in parenthesis after 2 steps (AHF, followed by Wittig olefination) ^c determined via GC analysis of crude mixture or by ¹H NMR after diastereomeric imine formation with a chiral amine ^d 350 psi CO / 50 psi H₂ ^e remaining mass balance is isomerization of the starting material to a trisubstituted alkene ^f remaining mass balance is unreacted starting material ^g at 40 °C

Results vary widely across different substrates, but a general trend is that very electron deficient alkenes with small substituents lead to best rates, regio and enantioselectivities. In addition, comparing relative rates for entries 4 and 5 in Table 4.3, as well as entry 3 in Table 4.4, it is worth noting that strained cyclic alkenes tend to be good candidates for AHF. Furthermore, overall, ligand **L1** is faster than **L2**, although **L2** shows better

selectivity for alkyl substituted acrylates, such as methyl methacrylate (entry 4) and alpha-methylene-gamma-butyrolactone (entry 5).

Table 4.4. AHF of other 1,1'-disubstituted alkenes

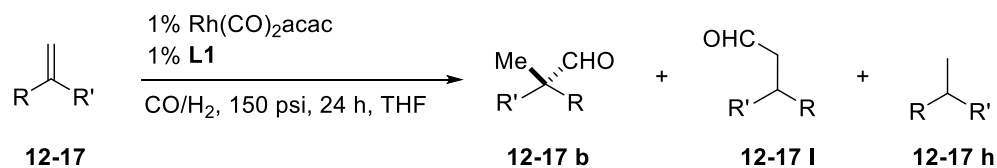


Entry	Alkene	L	Time (h)	%conversion ^a			% ee (b) ^c
				b ^b	l	h	
1.	 9	L1 L2	24	83 ^d (71) 97 ^d	1 1	3 <1	85 92
2.	 10	L1 L2	2	95 (77) 5	0 0	5 5	61 nd
3.	 11	L1 L2	2	98 98	1 <1	1 1	40 71

^adetermined via ¹H NMR versus mesitylene ^b isolated yield in parenthesis after 2 steps (AHF, followed by Wittig olefination) ^c % ee determined via chiral GC of crude mixture ^dremaining mass balance is unreacted starting material

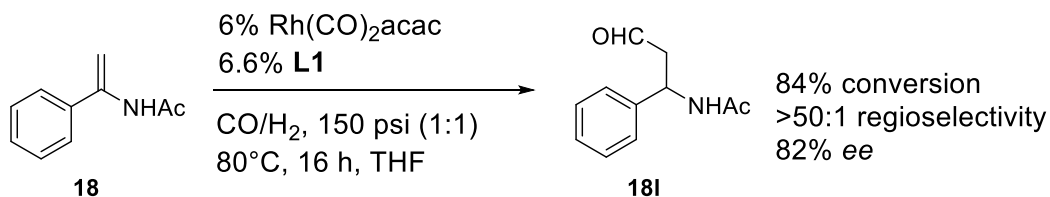
A difficulty associated with AHF of alkenes **1-10** is that the aldehyde products are unstable to common purification methods, such as silica gel chromatography or distillation. Therefore, the crude aldehydes **1-10b** were reacted with an ylide,

material undergoes competing polymerization. Entries 2 and 3 reveal how small structural changes can lead to reversal of selectivity. While 2-phenyl-acrylic acid methyl ester **6** afforded predominantly the branched aldehyde, the addition of a methyl (**13**, entry 2) or trifluoromethyl (**14**, entry 3) in the *ortho* position affords the linear aldehyde only. Entry 4 did not undergo productive hydroformylation. Unlike other α -substituted enol esters, such as **2**, **9** and **10**, which show high branched selectivity in AHF, 1-acetoxy-1-phenylethene **15** afforded less than 5% branched aldehyde. The crude mixture revealed loss of acetic acid accompanied by the branched and linear AHF products of styrene via a possible β -acetoxy elimination pathway. Entry 5 proceeds with linear selectivity. Replacing the acrylate functionality with an enone (**17**, entry 6) proved unsuccessful in AHF. Hydrogenation was the only reaction observed.

Table 4.6. Substrates that do not yield tetrasubstituted aldehydes

Entry	Alkene	%conversion ^a			Entry	Alkene	%conversion ^a		
		b	l	h			b	l	h
1.		28	3	20	4.		<5	<1	0
2.b,c		0	10	2	5.b		0	20	0
3.b		0	10	<1	6.b		0	0	27

^adetermined via ¹H NMR crude mixture ^bthe rest of mass balance is unreacted starting material ^cAHF in toluene-d₈, 20 h; This compound is unreactive in the presence of (S,S)-Ph-BPE at 300 psi 5:1 CO/H₂, 19 h, <1% conversion of starting material

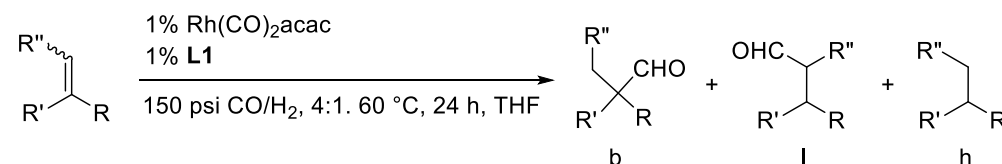


Dissertation, Leigh Abrams

Scheme 4.1. Linear selective AHF of N-(1-phenylvinyl) acetamide

Although branched selectivity is not always favored, the alternative linear selective pathway could also lead to useful products. For example, AHF of N-(1-phenylvinyl) acetamide **18** (Scheme 4.1) affords the linear aldehyde **18l** with 84% conversion and 82% ee. Although no tetrasubstituted aldehyde was detected, these results suggest that an alternative linear AHF pathway to generate aldehydes with β -chirality could be generated effectively with proper optimization. The aldehyde **18l** is valuable as precursor to enantioenriched β^3 -amino acids, such as N-acetyl- β -phenylalanine.

Table 4.7. Attempts to form tetrasubstituted aldehydes via AHF of trisubstituted alkenes



Entry	Trisubstituted Alkene	%conversion ^a		
		b	l	h
1.	 19	<1	0	0
2.	 20	<1	0	0
3. ^b	 21	0	0	>99

^adetermined via ¹H NMR crude mixture; the rest of mass balance is unreacted starting material ^b300 psi 5:1 CO/H₂

One of the limitations in the AHF of 1,1-disubstituted alkenes is that the products are limited to a methyl group. Given the fast AHF rates of some 1,1'-disubstituted alkenes, such as **1** and **2**, it seemed possible that tetrasubstituted aldehydes could form via AHF of electronically activated trisubstituted alkenes under the same conditions. Attempts to form tetrasubstituted aldehydes were unsuccessful (Table 4.7). Entries 1 and 2 showed no appreciable conversion of starting material, whereas entry 3 formed solely the hydrogenation product. The observed hydrogenation product in entry 3 suggests that alkene insertion occurs, but CO migratory insertion does not proceed competitively with hydrogenation. In general, formation of hydroformylation versus hydrogenation product might be controlled by the rate of CO migratory insertion. Therefore, we looked at catalyst speciation of preformed $\text{Rh(H)(CO)}_2\text{(L)}$ catalyst under noncatalytic conditions using NMR.

4.3. Catalyst Speciation via Low Temperature NMR

Alkene hydrogenation is present as a side reaction in the AHF of 1,1'-alkenes. The presence of the hydrogenated alkene side-product suggests a relatively slow CO migratory insertion step, that leads to competitive trapping by H_2 of a rhodium alkyl intermediate (Figure 4.4). Such a scenario suggests that this competition would allow the alkyl intermediate to accumulate in high enough concentration to be detected by NMR, in the absence of hydrogen.

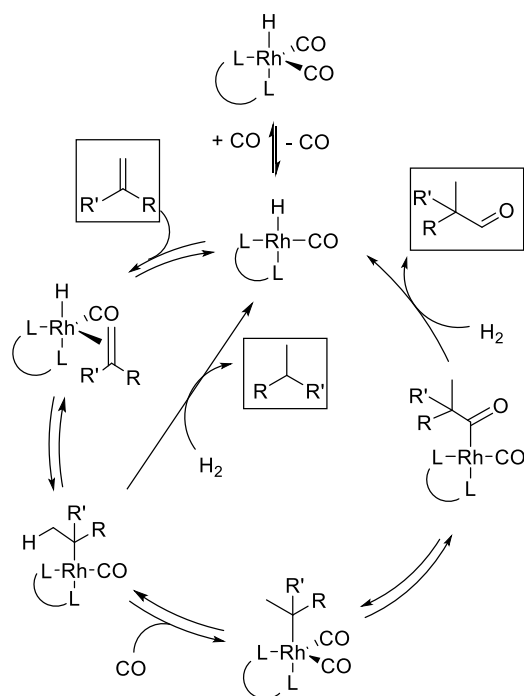


Figure 4.4. Mechanistic model for the observed alkene hydrogenation during the branched hydroformylation pathway

Monitoring the reaction between preformed $[Rh(H)(CO)_2(L7)]$ **22** and 10 equiv **1** by $^{31}P\{^1H\}$ in the absence of H_2 , at 0 °C, 1 atm CO, with passive gas-liquid mixing in a standard NMR tube, revealed **22** being consumed and replaced by two major species with two distinct P resonances each (Figure 4.5)²⁰. The NMR metrics are dd at 71 ppm ($^1J_{P-Rh} = 80$ Hz, $^2J_{P-P} = 21$ Hz) and ddd at 60 ppm ($^1J_{P-Rh} = 167$ Hz, $^2J_{P-P} = 21$ Hz, $^4J_{P-F} = 12$ Hz) for one species and ddd at 75 ppm ($^1J_{P-Rh} = 81$ Hz, $^2J_{P-P} = 11$ Hz, $^4J_{P-F} = 36$ Hz) and ddd at 43 ppm ($^1J_{P-Rh} = 143$ Hz, $^2J_{P-P} = 11$ Hz, $^4J_{P-F} = 29$ Hz) for the second species. The resonances at 71 and 60 ppm were assigned as rhodium branched acyl species **23_{acyl}** and the resonances at 75 and 43 ppm as rhodium branched alkyl species **23_{alkyl}**. The larger ^{31}P chemical shift difference between the downfield and upfield resonances in

the case of **23_{alkyl}** is consistent with a stronger trans difference for an alkyl versus an acyl. The $^1J_{P-Rh}$ values of 80 and 143 Hz for the alkyl and 81 and 167 Hz for the acyl, respectively are consistent with both intermediates being five-coordinate trigonal bipyramidal complexes. ^{19}F , $^{19}F\{^1H\}$ and $^{19}F\{^{31}P\}$ NMR experiments distinguish between branched and linear isomers. The presence of a quartet, $^3J_{F-H} = 21$ Hz and 23 Hz for acyl and alkyl respectively, is consistent with branched complexes, and not linear. In addition to these two species, minor resonances are visible at 74 and 42 ppm, both ddd, slightly upfield from **23_{alkyl}** resonances. The resemblance in chemical shift and coupling constants to **23_{alkyl}** made us assign this minor species as the diastereomer of **23_{alkyl}**.

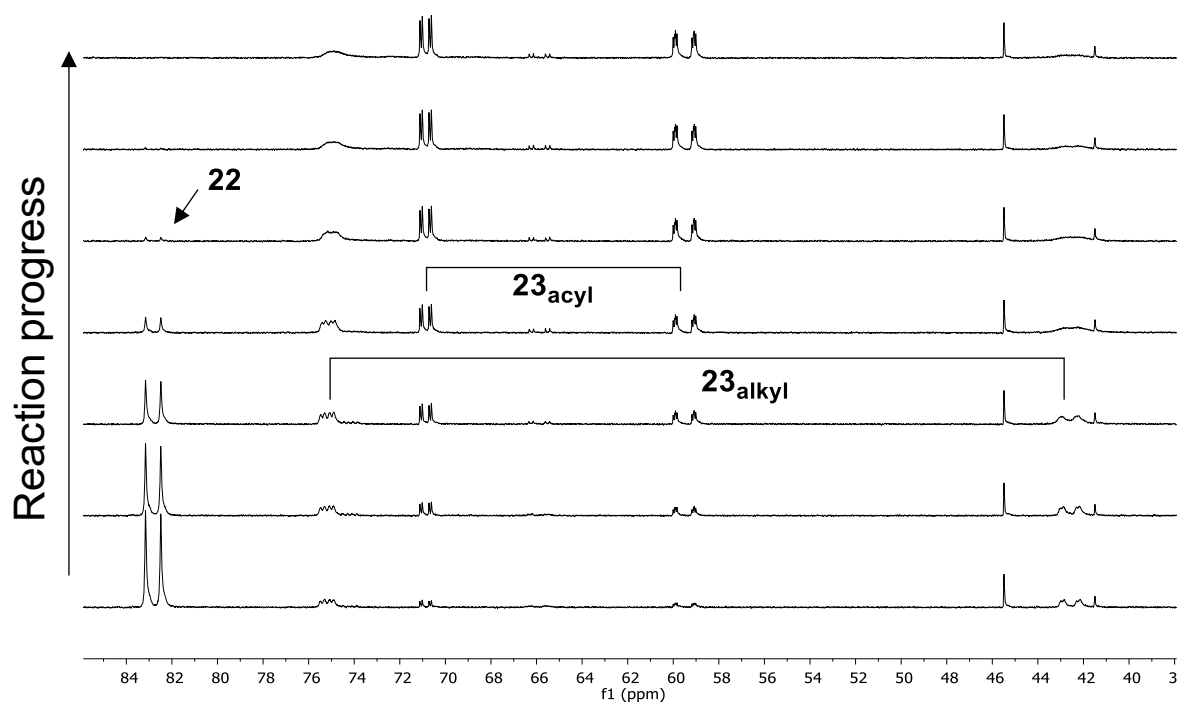
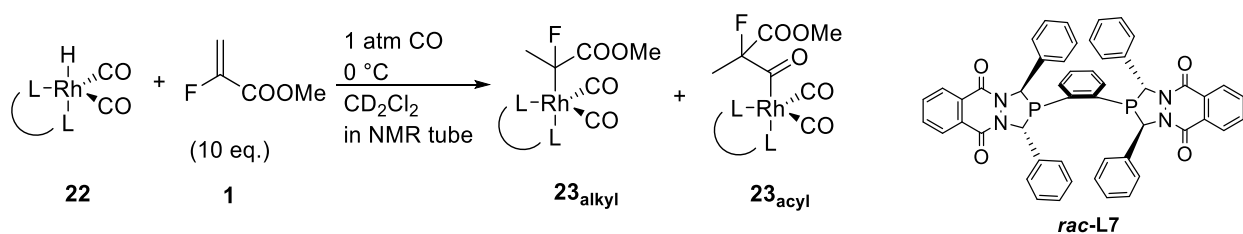


Figure 4.5. $^{31}\text{P}\{^1\text{H}\}$ monitoring the reaction between $[\text{Rh}(\text{H})(\text{CO})_2(\text{rac-L7})]$ **22** with methyl 2-fluoroacrylate **1** (10 equiv.) at 0 °C, under 1 atm CO, CD_2Cl_2 . Spectra every 3.5 min

Under realistic AHF conditions, **L7** is slower than **L1**, but both ligands display similar selectivity (1% Rh/**L7**, CO/ H_2 150 psi 1:1, 40 °C, 3 h, [methyl 2-fluoroacrylate] = 1.4 M in CH_2Cl_2 : 17% conversion of starting material, >50:1 branch to linear, 11:1 AHF to hydrogenation)

The reaction progress in Figure 4.5 shows **22** being consumed and replaced by the alkyl intermediate **23_{alkyl}**, which then slowly converts into the acyl **23_{acyl}**. Complete conversion does not occur. As the reaction progresses and the acyl intermediate is formed, CO is being consumed. While the exact concentration of CO in solution is unknown, we anticipate the reaction would not go to completion. As CO is being depleted, the ^{31}P alkyl resonances become broader as the reaction progresses at 0°C. When reaction is cooled down to -30 °C, the alkyl and the minor peak, assigned as the other diastereomer, are clearly distinguished in approximately 3:1 ratio (Figure 4.6). Bubbling with CO at -30 °C leads to sharp peaks (Figure 4.6), suggesting that the observed broadness is facilitated by decrease of CO concentration in solution as the reaction progresses. The peak broadening could be consistent with CO loss from a five-coordinate alkyl dicarbonyl species to form a four-coordinate alkyl monocarbonyl species as the available CO in solution is depleted. After more CO is added, reaction progress while temperature is raised from -30 °C to room temperature reveals that the major alkyl diastereomer gets converted into the acyl faster than the minor diastereomer.(Figure 4.7).

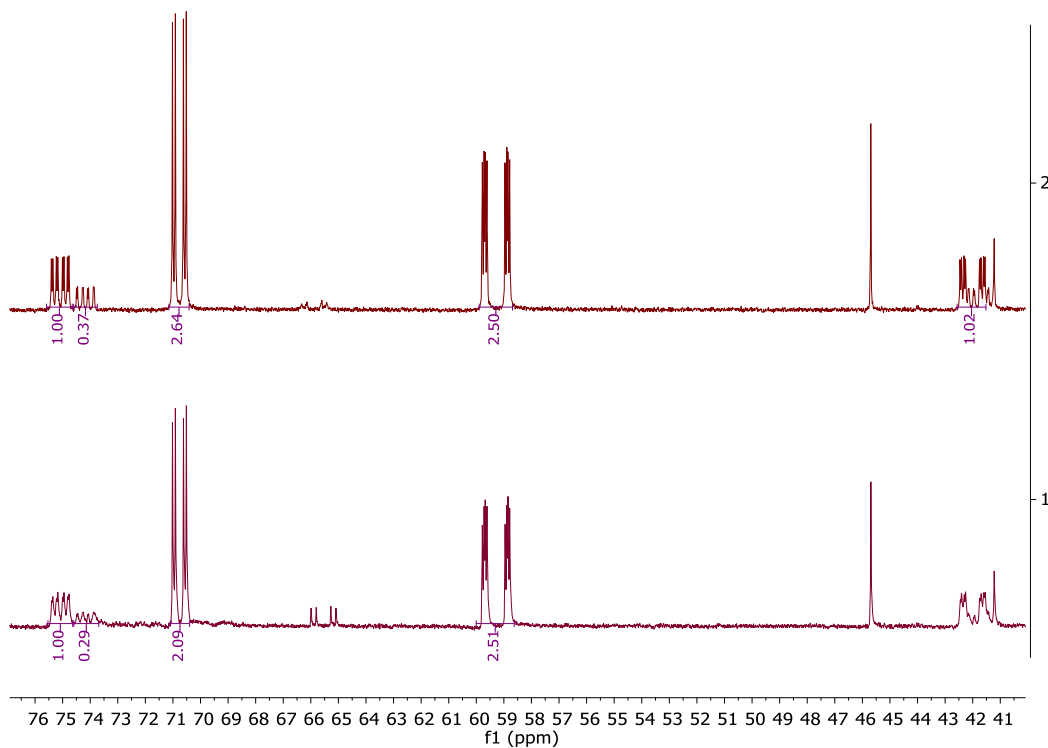


Figure 4.6 $^{31}\text{P}\{^1\text{H}\}$ of **23**_{alkyl} (43 and 75 ppm) and **23**_{acyl} (60 and 71 ppm); bottom spectrum: at -30 °C, before bubbling with CO; upper spectrum: at -30 °C, after bubbling with CO

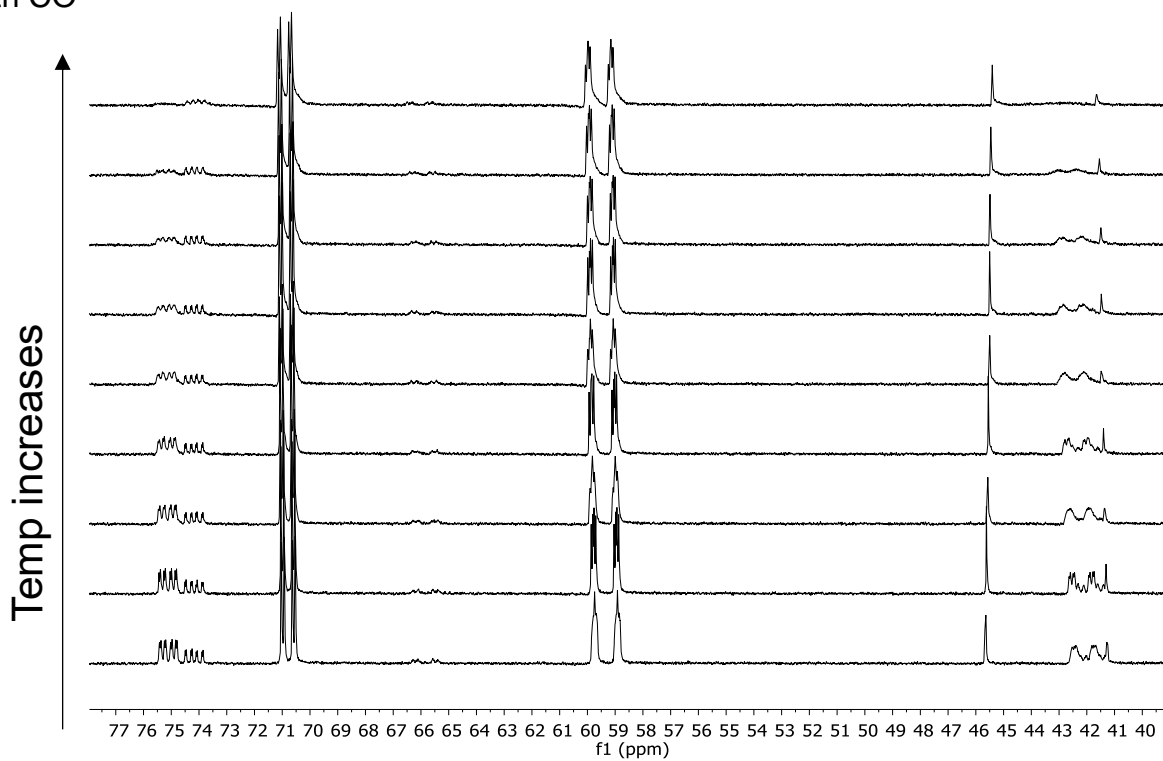


Figure 4.7 $^{31}\text{P}\{^1\text{H}\}$ monitoring the reaction between $[\text{Rh}(\text{H})(\text{CO})_2(\text{rac-L7})]$ **22** (83 ppm, 20 mM) with **1** (10 equiv.) while temperature increases from -30°C to room temperature. Spectra every 3.5 min

The two alkyl and acyl intermediates presented herein are the first tertiary alkyl and acyl examples to be directly observed by NMR during hydroformylation of a 1,1'-alkene. Our group has previously reported the detection of intermediates by NMR for several monosubstituted alkenes²⁰. In that report, acyl species were most commonly observed, while the interception of alkyl species was rare. A few alkyl species could be detected in small amounts under special circumstances, such as low CO concentration or π -allyl stabilization (the latter in the case of butadiene). The tertiary alkyl observed during hydroformylation of methyl 2-fluoroacrylate is not only visible in appreciable amount, but its presence persists, suggesting a slow conversion of the alkyl into the acyl that would allow alkene hydrogenation to become competitive.

4.4. Deuterioformylation of a linear selective alkene

Analysis of the product mixture in the AHF of 2-(2-methylphenyl)-acrylic acid methyl ester **13** reveals exclusive conversion of the starting material to the linear aldehyde **13I**. No branched aldehyde is detected under these reaction conditions. We can envision two general scenarios: one where only the linear rhodium-alkyl intermediate forms which goes on to form the observed linear aldehyde, and a second scenario where both linear and branched alkyl intermediates are formed, but only the linear one can go on to form the aldehyde, while the branched alkyl undergoes only beta-hydride elimination.

Deuterioformylation of **13** is used to probe the reversibility of the branched alkyl intermediate. This technique has been used before to probe reversibility of intermediates for 1,1-diphenylethene²¹, as well as other monosubstituted examples²². Incorporation of deuterium into unconverted substrate at the terminal vinyl position indicates reversible formation of the branched alkyl intermediate. Analysis of the crude deuterioformylation mixture at partial substrate conversion (3%) reveals two major products: the expected deuterated linear aldehyde, and the deuterated alkene, in an approximate ratio of 1.2:1. This suggests that the branched rhodium-alkyl intermediate is formed, but this intermediate is more likely to undergo β -hydride elimination than migratory insertion, consistent with the observed formation of linear aldehyde.

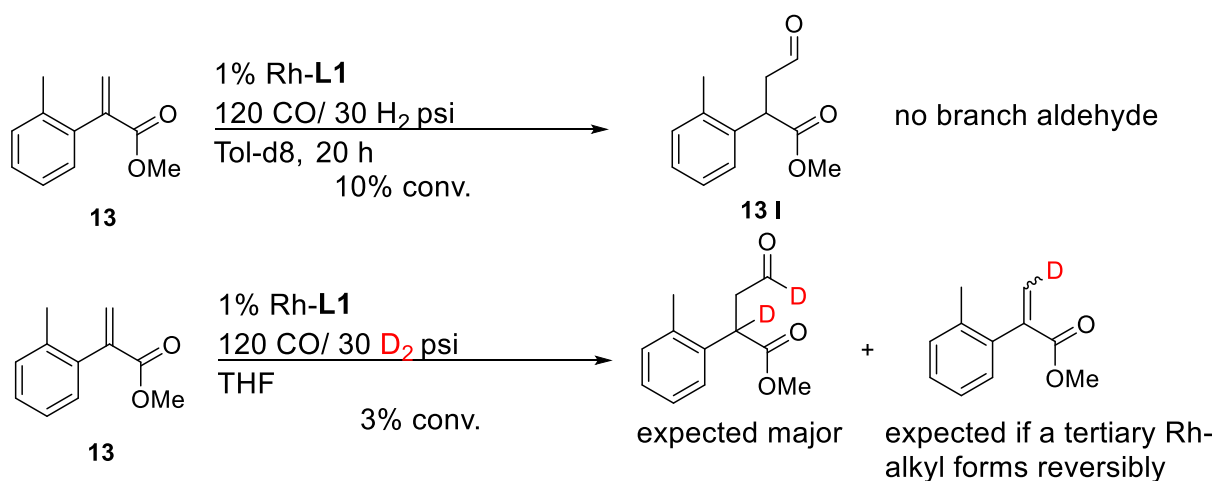


Figure 4.8. Linear selective hydroformylation (top scheme) and deuterioformylation (bottom scheme) of **13**

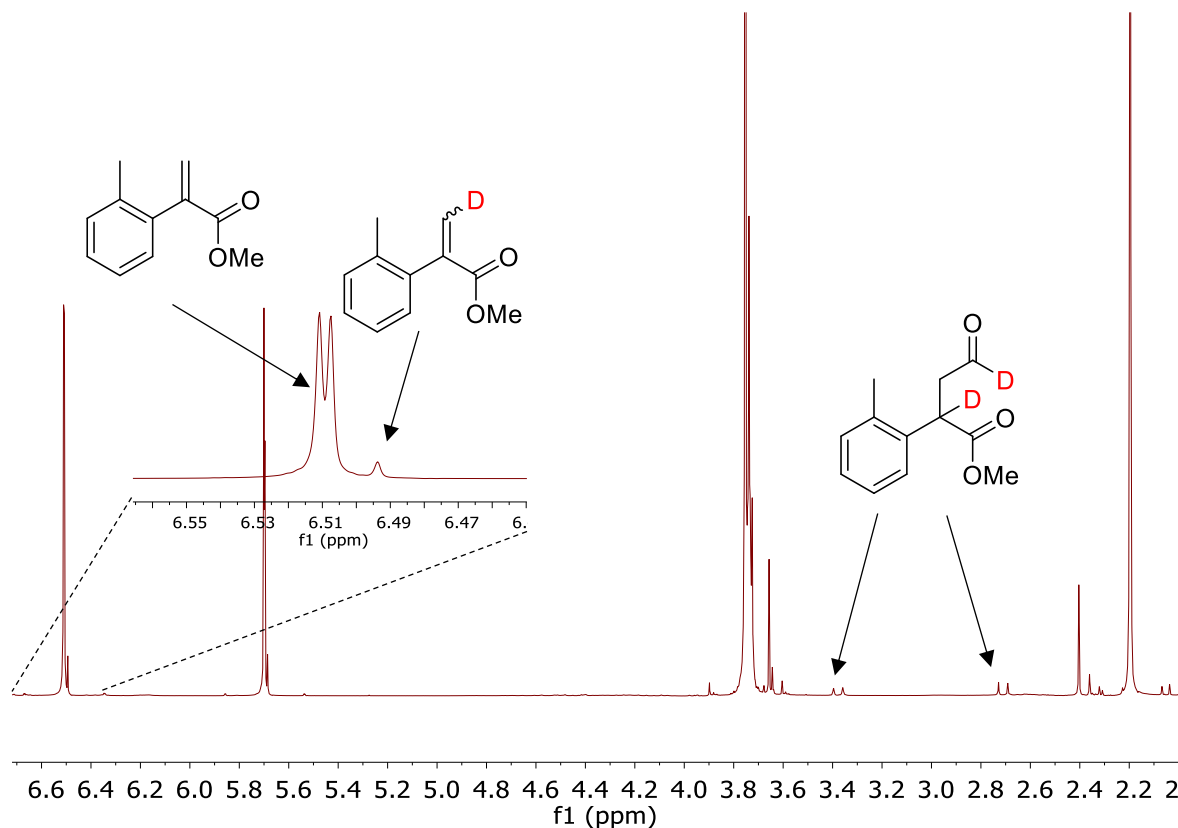


Figure 4.9. ^1H NMR (CDCl_3) of crude deuterioformylation of 2-(2-methylphenyl)-acrylic acid methyl ester **13** at partial substrate conversion

4.5. Conclusions

Tetrasubstituted stereogenic centers are prevalent in a lot of drug candidates and natural products. Tetrasubstituted aldehydes are useful synthetic intermediates due to the versatile aldehyde functionality, but their synthesis is a challenging task. Branched-selective asymmetric hydroformylation of 1,1'-disubstituted alkenes represents a direct, catalytic route to enantioenriched tetrasubstituted aldehydes.

The results herein show that fast, selective hydroformylation occurs to produce tetrasubstituted aldehydes for various 1,1'-alkenes bearing electron withdrawing groups.

Alpha-substituted acrylates and acetates are particularly reactive. In some cases, unprecedented rates (up to 50 turnovers / hour) and selectivities (up to 95% ee and >50:1 branched selectivity) are obtained at mild conditions (150 psi, 60 °C) in the presence of rhodium – BisDiazaphos or rhodium – (S, S)-Ph-BPE catalysts.

One of the competing reactions is alkene hydrogenation, predominantly in the case of acrylate derivatives. Our model is that alkene insertion occurs to form a branched alkyl intermediate, but a relatively slow CO migratory insertion step leads to competitive trapping by H₂ of this alkyl intermediate. Based on this model, higher CO partial pressures and lower H₂ partial pressures would favor hydroformylation over hydrogenation. Thus, we were able to minimize the amount of hydrogenation by running the reactions at 150 psi rich in CO (4:1 CO:H₂).

This notion of a sluggish CO insertion was further investigated by monitoring the reaction between Rh(H)(CO)₂(**L7**) and methyl 2-fluoroacrylate by NMR, in the absence of hydrogen. When Rh(H)(CO)₂(**L7**) was reacted with methyl 2-fluoroacrylate, an alkyl intermediate formed, but this intermediate only slowly converted into an acyl. This observation is consistent with the model that alkene insertion occurs, but the alkyl intermediate is slow to undergo CO migratory insertion to form an acyl.

Overall, this work demonstrates that tetrasubstituted aldehydes can be formed via hydroformylation of 1,1'-alkenes, with useful selectivities and rates, and at mild conditions. This method provides a direct route to unique highly functionalized tetrasubstituted aldehydes from inexpensive α -acrylate and acetate precursors, some of them commercially available.

4.6. Experimental

4.6.1 General

Dry and oxygen-free tetrahydrofuran (Sigma) and toluene (Sigma) solvents were collected from solvent columns that use activated alumina. The following reagents and solvents were used as received. Ethyl acetate, hexane, dichloromethane, toluene-d₈, dichloromethane-d₂, acetonitrile-d₃, α -methylene- γ -butyrolactone **5**, methyl methacrylate **4**, (carbethoxymethylene)triphenylphosphorane, mesitylene were purchased from Sigma. methyl 2-fluoroacrylate **1**, 1-(trifluoromethyl)-ethenyl acetate **9** and (S)-(+)-1-Methoxy-2-propylamine were obtained from Alfa Aesar, and 1-Cyanovinyl Acetate **10** from TCI. (S,S)-Ph-BPE (**L2**) was purchased from Strem Chemicals. Synthesis gas (1:1 CO:H₂) and CO gas were obtained from Airgas. AHF reactions were run in glass pressure bottles purchased from Ace Glass Inc. Reactors were assembled as previously reported²³. **L1**, **L7**, Rh(acac)(**L7**) and Rh(H)(CO)₂(**L7**) were synthesized as previously reported^{20b}.

Alkenes **2**²⁴, **3**²⁵, **6**²⁶, **7**²⁷, **11**²⁸, **13**²⁶, **14**²⁶, **15**²⁹, **17**³⁰, **19**³¹, **20**³² were synthesized according to literature procedures.

NMR spectra were acquired on Bruker Avance III 400 and 500 spectrometers. Chemical shifts are reported in ppm. ¹H NMR chemical shifts are referenced to tetramethylsilane (for CDCl₃) or to residual solvent (for toluene-d₈ or dichloromethane-d₂). ¹³C chemical shifts are referenced to residual solvent. Splitting patterns in ¹H NMR are reported as singlet (s), doublet (d), triplet (t), quartet (q), doublet of doublets (dd) and multiplet (m). GC data was obtained on chiral BetaDex 225 column on a Shimadzu analytical GC-2010 Plus equipped with an FID detector. ESI mass spectrometry data were collected on a

Thermo Q Exactive™ Plus spectrometer. Optical rotation was obtained on a Randolph digital polarimeter using a 1 mL cell with 0.5 dm path length at room temperature. Absolute configuration is determined for (S)-2-methyl-3-oxo-2-phenylpropanoate **6b** and (R)-2-fluoro-2-methyl-propanoic acid by comparison to reported literature values. The sign of optical rotation is reported for products after Wittig olefination. Silica gel flash column chromatography was performed on Silicycle Siliaflash P60 230-400 mesh, 40-63 μm . Conversion and regioselectivity were determined by crude ^1H NMR. Isolated yields are reported after 2 steps: AHF, followed by Wittig olefination of the crude AHF mixture with (carbethoxymethylene)triphenylphosphorane.

4.6.2. Experimental Procedures and Characterization Data

General Procedure for Asymmetric Hydroformylation (150 psi or less)

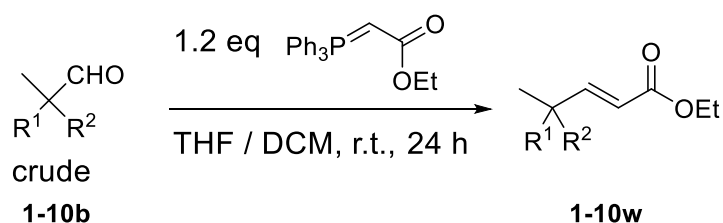
An oven-dried 30 mL glass pressure bottle equipped with a stir bar is charged with THF 100 mM stock solution of $\text{Rh}(\text{acac})(\text{CO})_2$ (1% catalyst loading, 300 μL) and THF 40 mM stock solution of ligand (**L1** or **L2**) (1.2%, 900 μL) inside a N_2 glove box and then attached to a reactor. Inside a fume hood, the reactor is subjected to three pressurization (150 psig) - depressurization (20 psig) cycles with syngas, then pressurized to 150 psig syngas and placed in an oil bath at 60 $^\circ\text{C}$ for 30 min to 1 h. The reactor is allowed to cool down for five minutes and depressurized to 10 psig. The alkene (3.00 mmol) and mesitylene standard (1/3 eq, 140 μl , 1 mmol) are injected into the reactor using a syringe as a solution in THF (amount of THF adjusted to reach 1.6 M alkene concentration). The reactor is then pressurized-depressurized 3 times with CO, pressurized to 90 psig CO, followed by 60 psig syngas and placed in the oil bath set at the desired temperature. The mixture is stirred vigorously, with the stir bar frequently breaking the gas-liquid interface for good

gas-liquid mixing. After the reaction is complete, the reactor is allowed to cool down for 30 min and then depressurized. An aliquot of the crude mixture is used for ^1H NMR and chiral GC analysis. Since the aldehydes proved unstable during chromatographic or distillation methods, these products were derivatized via Wittig olefination for isolation and full characterization purposes.

General Procedure for Asymmetric Hydroformylation (>150 psi)

A CAT24 reactor is charged with THF or toluene 100 mM stock solution of $\text{Rh}(\text{acac})(\text{CO})_2$ (1% catalyst loading, 48 μL), THF or toluene 20 mM stock solution of ligand (1.2%, 264 μL) and alkene (0.48 mmol) inside a N_2 glove box and sealed. Inside a fume hood, the reactor is pressurized, heated at the desired temperature, while stirring at 700 rpm. When reaction complete, the reactor is allowed to cool down for 30 min and then depressurized. Crude mixture is analyzed by ^1H NMR and chiral GC analysis.

General Procedure for Wittig olefination of the aldehydes:



The crude aldehydes **1-10b** is transferred to a 50 mL oven-dried Schlenk flask. Under a flow of N_2 , (carbethoxymethylene)triphenylphosphorane (1.2 eq, 1.25 g, 3.6 mmol) is added as a solution in dichloromethane (7 mL) at room temperature. The mixture is allowed to stir at room temperature overnight under N_2 . The mixture is concentrated

under vacuo and purified via silica gel chromatography using 20% EtOAc/hexanes as eluent to afford the products **1-10w** as colorless oils.

General Procedure for Low Temperature Noncatalytic Experiments

The experiments were performed by a previously reported method^{20b}.

An oven-dried 15 mL glass pressure bottle equipped with a stir bar is charged with Rh(acac)(**L7**) (60 mg) and 1 mL CD₂Cl₂ inside a N₂ glove box and then attached to a reactor. Inside a fume hood, the reactor is subjected to three pressurization (150 psig) - depressurization (20 psig) cycles with syngas, then pressurized to 150 psig syngas and placed in an oil bath at 60 °C for 3 h. The reactor is allowed to cool down for five minutes and depressurized to 10 psig. The reactor is pressurized-depressurized 5 times with CO to ensure removal of H₂, then depressurized to 15 psig. The reactor was connected to an oven-dried septum-capped NMR tube via a cannula and the system was purged with CO for 2 min. The solution in the pressure bottle was then transferred to the NMR tube via same cannula. The NMR tube septum was sealed with parafilm. The NMR spectrometer was cooled to 0 °C and an initial spectrum was obtained of the Rh(H)(**L7**)(CO)₂ solution. The tube was ejected from the spectrometer and methyl 2-fluoroacrylate **1** (18.26 μL) was injected quickly using a gas tight syringe. The tube was inverted 3 times, quickly returned to the spectrometer and ³¹P spectra collected right away.

General Procedure for Deuterioformylation

An oven-dried 15 mL glass pressure bottle equipped with a stir bar is charged with THF 100 mM stock solution of Rh(acac)(CO)₂ (1% catalyst loading, 56.76 μL) and THF 30 mM

stock solution of **L1** (1.2%, 189.2 μL) inside a N_2 glove box and then attached to a reactor. Inside a fume hood, the reactor is subjected to three pressurization (100 psig) - depressurization (20 psig) cycles with CO , then pressurized with 120 psig CO and 30 psig D_2 and placed in an oil bath at $60\text{ }^\circ\text{C}$ for 1 h. The reactor is allowed to cool down for five minutes and depressurized to 10 psig. The alkene 2-(2-methylphenyl)-acrylic acid methyl ester **13** (0.57 mmol, 100 mg) and 1,4-Bis(trimethylsilyl)benzene standard (1/10 eq, 6.31 mg) are injected into the reactor using a syringe as a solution in THF (amount of THF adjusted to reach 1.6 M alkene concentration). The reactor is then pressurized-depressurized 3 times with CO , pressurized to 120 psig CO , followed by 30 psig D_2 and placed in the oil bath set at $60\text{ }^\circ\text{C}$ for 19 h. The mixture is stirred vigorously, with the stir bar frequently breaking the gas-liquid interface for good gas-liquid mixing. After the reaction is complete, the reactor is allowed to cool down for 30 min and then depressurized. An aliquot of the crude mixture is used for NMR analysis.

Characterization Data

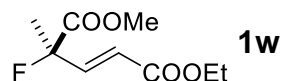


^1H NMR (500 MHz, Chloroform- d) δ 9.65 (d, $J = 5.7$ Hz, 1H), 3.85 (s, 3H), 1.70 (d, $J = 21.6$ Hz, 3H). ^{19}F NMR (377 MHz, Chloroform- d) δ -167.30.

Chiral separation via GC: $80\text{ }^\circ\text{C}$, hold 6 min, ramp $2\text{ }^\circ\text{C}/\text{min}$ to $90\text{ }^\circ\text{C}$, hold 6 min, ramp $2\text{ }^\circ\text{C}/\text{min}$ to $100\text{ }^\circ\text{C}$, hold 6 min, ramp $2\text{ }^\circ\text{C}/\text{min}$ to $110\text{ }^\circ\text{C}$, hold 5 min, ramp $3\text{ }^\circ\text{C}/\text{min}$ to $120\text{ }^\circ\text{C}$, hold 5 min, t_{R} (S) 14.8 min, t_{R} (R) 21.1 min.

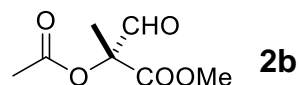
The crude aldehyde was oxidized to a carboxylic acid via a previously reported procedure³³, and the sign of optical rotation, $[\alpha]^{20}_{\text{D}} = +19.4$ ($c = 1.00$, MeOH), was

compared to that of previously reported³⁴ (S)-(-)- α -fluoro- α -methylmalonic acid monoethyl ester, $[\alpha]_D^{20} = -22.5$ ($c = 2.20$, MeOH).



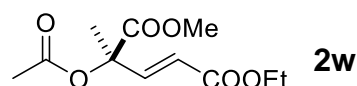
¹H NMR (500 MHz, Chloroform-*d*) δ 7.01 (dd, $J = 20.2, 15.7$ Hz, 1H), 6.19 (d, $J = 15.7$ Hz, 1H), 4.22 (d, $J = 7.5$ Hz, 2H), 3.82 (s, 3H), 1.72 (d, $J = 21.4$ Hz, 3H), 1.31 (t, $J = 7.2$ Hz, 3H). ¹³C NMR (126 MHz, Chloroform-*d*) δ 169.59 (d, $J = 25.9$ Hz), 165.50, 143.43 (d, $J = 20.6$ Hz), 121.82 (d, $J = 10.0$ Hz), 93.05 (d, $J = 189.8$ Hz), 60.92, 53.16, 24.08 (d, $J = 23.8$ Hz), 14.19. ¹⁹F NMR (377 MHz, Chloroform-*d*) δ -158.20.

HRMS-(ESI) for C₉H₁₃FO₄ [M+Na]⁺: calculated 227.0690, found 227.0690



¹H NMR (500 MHz, Chloroform-*d*) δ 9.87 (s, 1H), 3.83 (s, 3H), 2.17 (s, 3H), 1.60 (s, 3H).

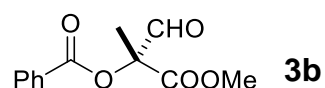
Chiral separation via GC: 50 °C, ramp 2 °C/min to 100 °C, hold 2 min, ramp 6 °C/min to 150 °C, hold 2 min t_R (major) 12.7 min, t_R (minor) 14.9 min.



¹H NMR (500 MHz, Chloroform-*d*) δ 7.16 (d, $J = 15.9$ Hz, 1H), 6.04 (d, $J = 15.9$ Hz, 1H), 4.21 (q, $J = 7.1$ Hz, 2H), 3.76 (s, 3H), 2.13 (s, 3H), 1.68 (s, 3H), 1.30 (t, $J = 7.1$ Hz, 3H).

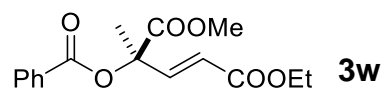
^{13}C NMR (126 MHz, CDCl_3) δ 170.3, 169.5, 165.8, 144.9, 121.7, 79.2, 61.0, 53.2, 23.6, 21.1, 14.3

HRMS-(ESI) for $\text{C}_{11}\text{H}_{16}\text{O}_6$ $[\text{M}+\text{NH}_4]^+$: calculated 262.1281, found 262.1283



^1H NMR (500 MHz, Chloroform- d) δ 10.00 (s, 1H), 8.21 – 7.94 (m, 2H), 7.69 – 7.56 (m, 1H), 7.47 (t, $J = 7.8$ Hz, 2H), 3.85 (s, 3H), 1.75 (s, 3H).

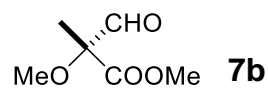
Chiral separation via GC: 80 $^\circ\text{C}$, then ramp 1 $^\circ\text{C}/\text{min}$ to 185 $^\circ\text{C}$, hold 1 min, t_{R} (major) 76.7 min, t_{R} (minor) 77.1 min.



^1H NMR (500 MHz, Chloroform- d) δ 8.07 (dd, $J = 8.1, 1.5$ Hz, 2H), 7.65 – 7.56 (m, 1H), 7.47 (t, $J = 7.7$ Hz, 2H), 7.31 (d, $J = 15.9$ Hz, 1H), 6.15 (d, $J = 15.9$ Hz, 1H), 4.22 (q, $J = 7.2$ Hz, 2H), 3.78 (s, 3H), 1.83 (s, 3H), 1.30 (t, $J = 7.2$ Hz, 3H). ^{13}C NMR (126 MHz, CDCl_3) δ 170.1, 165.6, 164.8, 144.9, 133.6, 129.9, 129.2, 128.5, 121.6, 79.4, 60.8, 53.0, 23.6, 14.2.

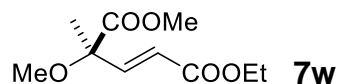
HRMS-(ESI) for $\text{C}_{16}\text{H}_{18}\text{O}_6$ $[\text{M}+\text{NH}_4]^+$: calculated 324.1442, found 324.1441

$[\alpha]_{\text{D}}^{20} = +5.6$ ($c = 1.00$, CHCl_3)



^1H NMR (500 MHz, Chloroform-*d*) δ 9.62 (s, 1H), 3.81 (s, 3H), 3.42 (s, 3H), 1.53 (s, 3H).

Chiral separation via GC: 80 °C, hold 8 min, ramp 3 °C/min to 100 °C, hold 8 min, ramp 5 °C/min to 120 °C, hold 4 min, t_{R} (minor) 13.9 min, t_{R} (major) 15.0 min.

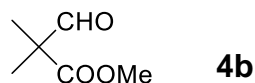


^1H NMR (500 MHz, Chloroform-*d*) δ 7.03 (d, $J = 15.8$ Hz, 1H), 6.13 (d, $J = 15.8$ Hz, 1H), 4.22 (q, $J = 7.1$ Hz, 2H), 3.79 (s, 3H), 3.33 (s, 3H), 1.55 (s, 3H), 1.30 (t, $J = 7.1$ Hz, 3H).

^{13}C NMR (126 MHz, CDCl_3) δ 171.9, 166.0, 146.4, 122.3, 80.1, 60.7, 52.9, 52.7, 22.9, 14.2.

HRMS-(ESI) for $\text{C}_{10}\text{H}_{16}\text{O}_5$ $[\text{M}+\text{Na}]^+$: calculated 239.0890, found 239.0891

$[\alpha]_{\text{D}}^{20} = +234$ ($c = 1.00$, CHCl_3)

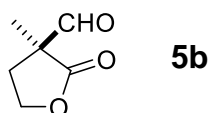


^1H NMR (400 MHz, Chloroform-*d*) δ 9.66 (s, 1H), 2.27 (s, 3H), 1.36 (s, 6H).



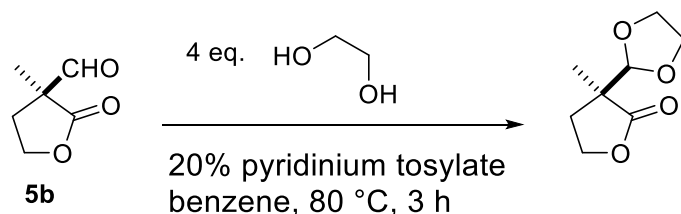
^1H NMR (400 MHz, Chloroform-*d*) δ 7.11 (d, $J = 16.0$ Hz, 1H), 5.85 (d, $J = 16.0$ Hz, 1H), 4.20 (q, $J = 7.2$ Hz, 2H), 3.70 (s, 3H), 1.36 (s, 6H), 1.30 (t, $J = 7.2$ Hz, 3H). ^{13}C NMR (101 MHz, CDCl_3) δ 175.3, 166.5, 151.3, 119.7, 60.5, 52.4, 44.6, 24.5, 14.2.

HRMS-(ESI) for $\text{C}_{10}\text{H}_{16}\text{O}_4$ $[\text{M}+\text{Na}]^+$: calculated 223.0941, found 223.0939

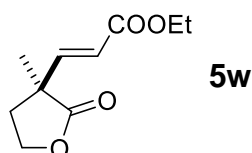


^1H NMR (400 MHz, Chloroform-*d*) δ 9.57 (s, 1H), 4.42 – 4.24 (m, 2H), 2.84 (ddd, $J = 13.1$, 7.8, 5.3 Hz, 1H), 2.07 (ddd, $J = 13.2$, 7.7 Hz, 1H), 1.53 (s, 3H).

Chiral separation via ^1H NMR after diastereomeric imine formation with (S)-(+)-1-Methoxy-2-propylamine as previously reported³⁵ and by chiral GC after protection of the aldehyde with ethylene glycol as previously reported³⁶.



Chiral separation via GC: 100 °C, ramp 1 °C/min to 180 °C, hold 2 min, ramp 6 °C/min to 200 °C, hold 2 min, t_R (minor) 41.1 min, t_R (major) 41.4 min.



^1H NMR (500 MHz, Chloroform-*d*) δ 6.96 (d, $J = 15.8$ Hz, 1H), 5.96 (d, $J = 15.9$ Hz, 1H), 4.38 – 4.25 (m, 2H), 4.21 (q, $J = 7.1$ Hz, 2H), 2.47 – 2.37 (m, 1H), 2.29 – 2.20 (m, 1H), 1.44 (s, 3H), 1.30 (t, $J = 7.1$ Hz, 3H). ^{13}C NMR (126 MHz, CDCl_3) δ 178.0, 165.8, 146.9, 122.0, 65.1, 60.8, 45.1, 35.4, 22.5, 14.2.

HRMS-(ESI) for $\text{C}_{10}\text{H}_{14}\text{O}_4$ $[\text{M}+\text{Na}]^+$: calculated 221.0784, found 221.0784

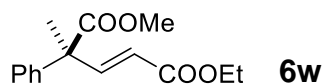
$[\alpha]^{20}_{\text{D}} = +109.4$ ($c = 1.00$, CHCl_3)



^1H NMR (500 MHz, Chloroform-*d*) δ 9.87 (s, 1H), 7.43 – 7.38 (m, 2H), 7.37 – 7.31 (m, 1H), 7.26 – 7.15 (m, 2H), 3.81 (s, 3H), 1.69 (s, 3H).

Chiral separation via ^1H NMR after diastereomeric imine formation with (S)-(+)-1-Methoxy-2-propylamine as previously reported³⁵. One drop of acetic acid was added to the NMR tube for fast imine formation.

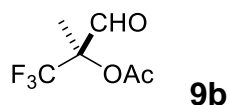
$[\alpha]^{20}_{\text{D}} = -22.6$ ($c = 1.00$, CHCl_3), literature: (R)-methyl 2-methyl-3-oxo-2-phenylpropanoate, $[\alpha]^{20}_{\text{D}} = +102.1$ ($c = 0.45$, CHCl_3 ; 77% ee)



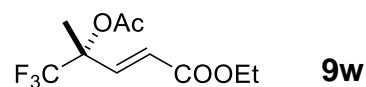
^1H NMR (500 MHz, Chloroform-*d*) δ 7.48 (d, $J = 16.0$ Hz, 1H), 7.36 – 7.30 (m, 2H), 7.29 – 7.24 (m, 1H), 7.24 – 7.20 (m, 2H), 5.83 (d, $J = 16.0$ Hz, 1H), 4.21 (q, $J = 7.2$ Hz, 2H), 3.71 (s, 3H), 1.70 (s, 3H), 1.29 (t, $J = 7.2$ Hz, 3H). ^{13}C NMR (126 MHz, CDCl_3) δ 173.9, 166.3, 150.1, 141.6, 128.7, 127.4, 126.4, 121.5, 60.6, 53.3, 52.7, 23.4, 14.2.

HRMS-(ESI) for $\text{C}_{15}\text{H}_{18}\text{O}_4$ $[\text{M}+\text{NH}_4]^+$: calculated 280.1543, found 280.1540

$[\alpha]^{20}_{\text{D}} = -2.2$ ($c = 1.00$, CHCl_3)

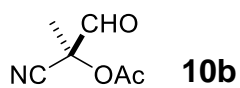


characterization data agrees with previously reported data¹⁵



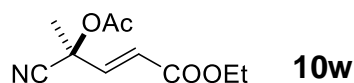
^1H NMR (500 MHz, Chloroform-*d*) δ 6.89 (d, $J = 16.0$ Hz, 1H), 6.08 (d, $J = 15.9$ Hz, 1H), 4.22 (q, $J = 7.1$ Hz, 2H), 2.12 (s, 3H), 1.83 (s, 3H), 1.31 (t, $J = 7.2$ Hz, 3H). ^{13}C NMR (126 MHz, Chloroform-*d*) δ 168.28, 164.98, 140.68, 125.60, 124.70 (q, $J = 287.0$ Hz), 79.85 (q, $J = 32.0$ Hz), 61.07, 21.49, 17.31, 14.16.

HRMS-(ESI) for $\text{C}_{10}\text{H}_{13}\text{F}_3\text{O}_4$ $[\text{M}+\text{Na}]^+$: calculated 277.0658, found 277.0657



^1H NMR (400 MHz, Chloroform-*d*) δ 9.37 (s, 1H), 2.24 (s, 3H), 1.76 (s, 3H).

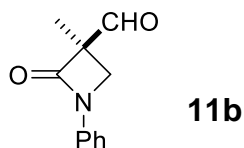
Chiral separation via GC: 110 °C, hold 5 min, ramp 1.5 °C/min to 150 °C, hold 4 min, ramp 5 °C/min to 180 °C, hold 2 min, t_{R} (major) 27.2 min, t_{R} (minor) 27.9 min.



^1H NMR (400 MHz, Chloroform-*d*) δ 6.78 (d, $J = 15.7$ Hz, 1H), 6.33 (d, $J = 15.7$ Hz, 1H), 4.23 (q, $J = 7.2$ Hz, 2H), 2.14 (s, 3H), 1.85 (s, 3H), 1.31 (t, $J = 7.1$ Hz, 3H). ^{13}C NMR (101 MHz, CDCl_3) δ 168.3, 164.9, 141.6, 124.2, 116.5, 69.8, 61.2, 26.4, 20.8, 14.1.

HRMS-(ESI) for $\text{C}_{10}\text{H}_{13}\text{NO}_4$ $[\text{M}+\text{Na}]^+$: calculated 234.0737, found 234.0734

$[\alpha]_{\text{D}}^{20} = -18.6$ ($c = 1.00$, CHCl_3)



^1H NMR (400 MHz, Chloroform- d) δ 9.72 (s, 1H), 7.41 – 7.33 (m, 5H), 4.13 (d, J = 6.2 Hz, 1H), 3.49 (d, J = 6.2 Hz, 1H), 1.65 (s, 3H)

Chiral separation via GC: 80 °C, hold 5 min, ramp 1 °C/min to 170 °C, ramp 4 °C/min to 190 °C, hold 3 min, t_R (major) 94.7 min, t_R (minor) 92.9 min.

4.7. References

1. (a) Desmarchelier, A.; Coeffard, V.; Moreau, X.; Greck, C., *Tetrahedron* **2014**, *70* (15), 2491-2513; (b) Lalonde, M. P.; Chen, Y. G.; Jacobsen, E. N., *Angew.Chem.Int.Ed.* **2006**, *45* (38), 6366-6370; (c) Quintard, A.; Alexakis, A., *Chem. Commun.* **2010**, *46* (23), 4085-4087.
2. Vargas-Diaz, M. E.; Joseph-Nathan, P.; Tamariz, J.; Zepeda, L. G., *Org. Lett.* **2007**, *9* (1), 13-16.
3. Trost, B. M.; Xu, J. Y.; Reichle, M., *J. Am. Chem. Soc.* **2007**, *129* (2), 282-283.
4. DeBergh, J. R.; Spivey, K. M.; Ready, J. M., *J. Am. Chem. Soc.* **2008**, *130* (25), 7828-+.
5. Snyder, S. A.; Corey, E. J., *J. Am. Chem. Soc.* **2006**, *128* (3), 740-742.
6. (a) Franke, R.; Selent, D.; Börner, A., *Chem. Rev.* **2012**, *112* (11), 5675-5732; (b) Whiteker, G.; Cobley, C., Applications of Rhodium-Catalyzed Hydroformylation in the Pharmaceutical, Agrochemical, and Fragrance Industries. In *Organometallics as*

Catalysts in the Fine Chemical Industry, Beller, M.; Blaser, H.-U., Eds. Springer Berlin Heidelberg: 2012; Vol. 42, pp 35-46.

7. (a) Watkins, A. L.; Hashiguchi, B. G.; Landis, C. R., *Org. Lett.* **2008**, *10* (20), 4553-4556; (b) McDonald, R. I.; Wong, G. W.; Neupane, R. P.; Stahl, S. S.; Landis, C. R., *J. Am. Chem. Soc.* **2010**, *132* (40), 14027-14029; (c) Risi, R. M.; Burke, S. D., *Org. Lett.* **2012**, *14* (10), 2572-2575.
8. Abrams, M. L.; Foarta, F.; Landis, C. R., *J. Am. Chem. Soc.* **2014**, *136* (41), 14583-14588.
9. Clark, T. P.; Landis, C. R.; Freed, S. L.; Klosin, J.; Abboud, K. A., *J. Am. Chem. Soc.* **2005**, *127* (14), 5040-5042.
10. (a) Yan, Y.; Zhang, X., *J. Am. Chem. Soc.* **2006**, *128* (22), 7198-7202; (b) Joe, C. L.; Blaisdell, T. P.; Geoghan, A. F.; Tan, K. L., *J. Am. Chem. Soc.* **2014**, *136* (24), 8556-8559; (c) Klosin, J.; Landis, C. R., *Acc. Chem. Res.* **2007**, *40* (12), 1251-1259; (d) Sakai, N.; Mano, S.; Nozaki, K.; Takaya, H., *J. Am. Chem. Soc.* **1993**, *115* (15), 7033-7034.
11. Deng, Y. C.; Wang, H.; Sun, Y. H.; Wang, X., *ACS Catal.* **2015**, *5* (11), 6828-6837.
12. Gladiali, S.; Pinna, L., *Tetrahedron-Asymmetry* **1990**, *1* (10), 693-696.
13. Lee, C. W.; Alper, H., *J. Org. Chem.* **1995**, *60* (3), 499-503.
14. Fanfoni, L.; Diab, L.; Smejkal, T.; Breit, B., *Chimia* **2014**, *68* (6), 371-377.
15. Wang, X.; Buchwald, S. L., *J. Org. Chem.* **2013**, *78* (7), 3429-3433.

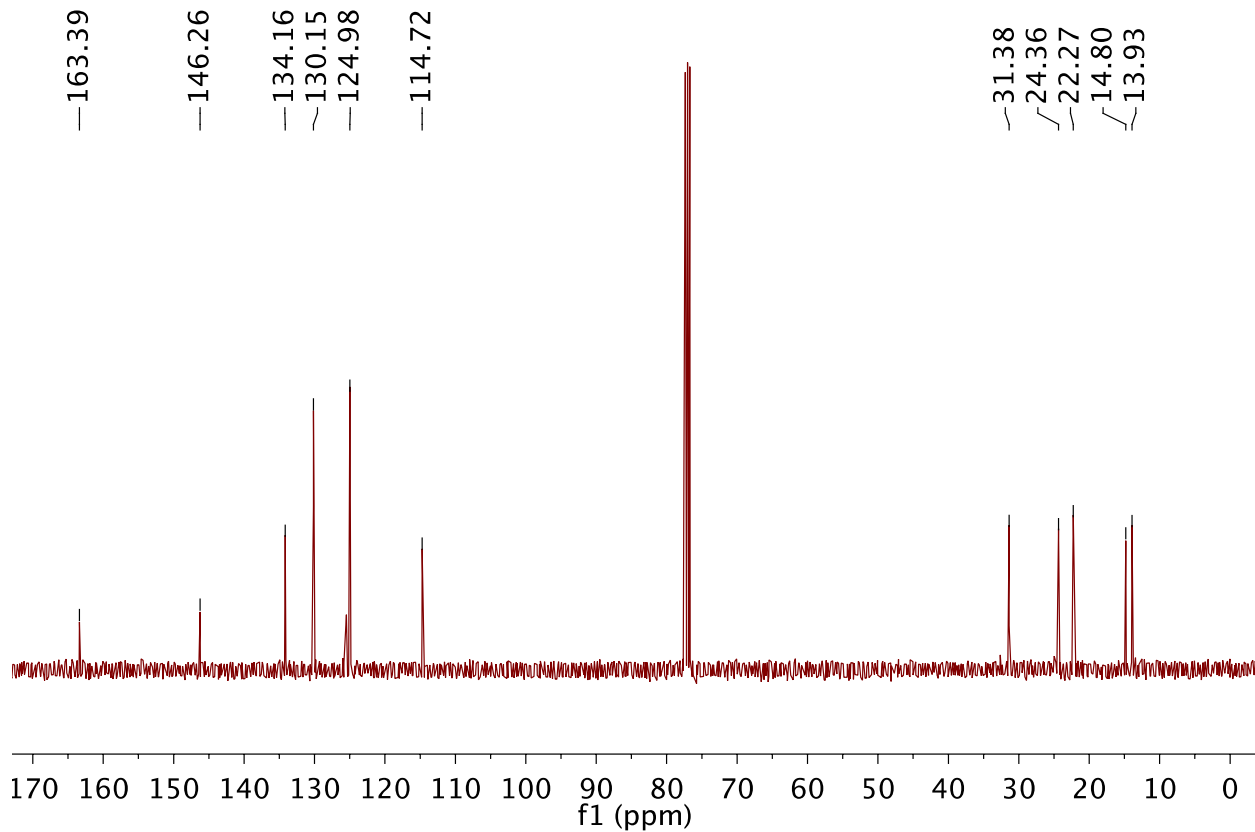
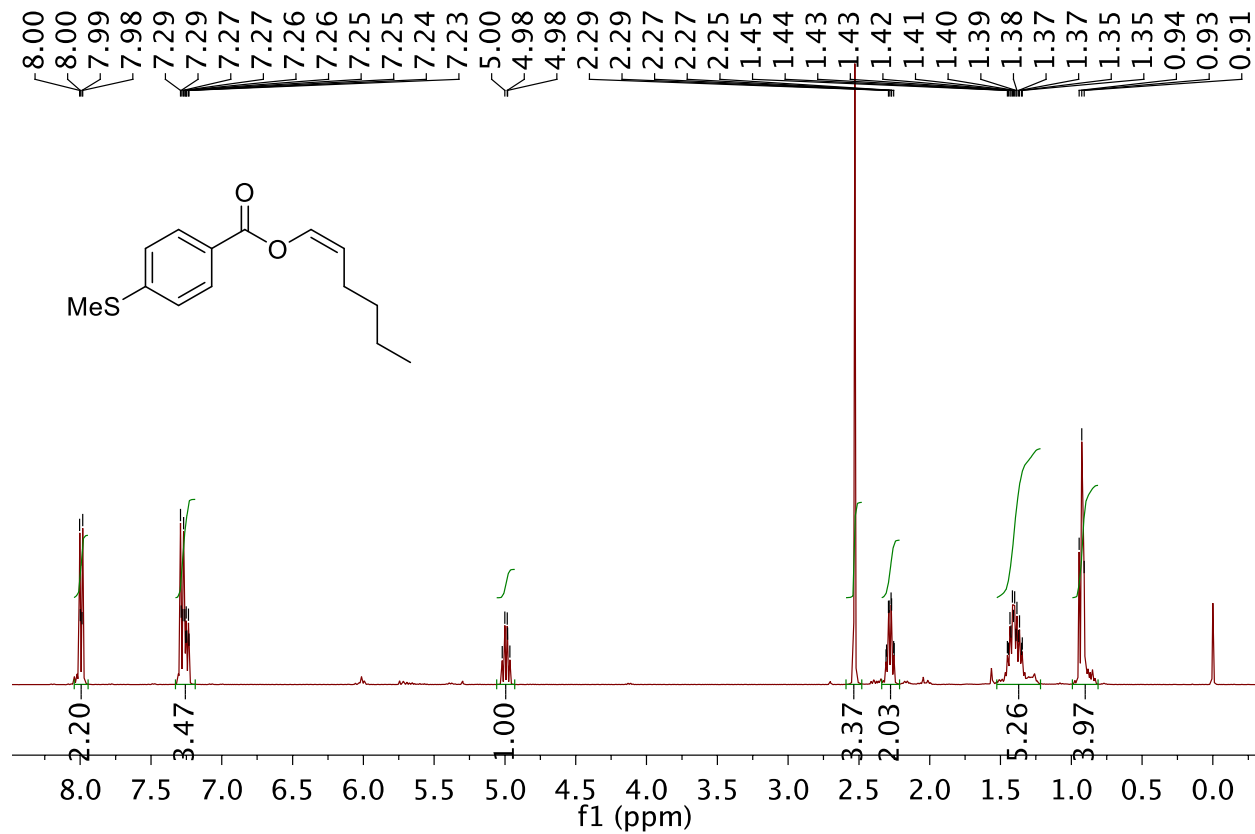
16. Tan, R. C.; Zheng, X.; Qu, B.; Sader, C. A.; Fandrick, K. R.; Senanayake, C. H.; Zhang, X. M., *Org. Lett.* **2016**, *18* (14), 3346-3349.
17. (a) Schulte, M. L.; Lindsley, C. W., *Org. Lett.* **2011**, *13* (20), 5684-5687; (b) Liang, T.; Neumann, C. N.; Ritter, T., *Angew.Chem.Int.Ed.* **2013**, *52* (32), 8214-8264.
18. Shibatomi, K.; Kitahara, K.; Okimi, T.; Abe, Y.; Iwasa, S., *Chem. Sci.* **2016**, *7* (2), 1388-1392.
19. Clarke, M. L.; Roff, G. L., *Chem. Eur. J.* **2006**, *12* (31), 7978-7986.
20. (a) Nelsen, E. R.; Brezny, A. C.; Landis, C. R., *J. Am. Chem. Soc.* **2015**, *137* (44), 14208-14219; (b) Nelsen, E. R.; Landis, C. R., *J. Am. Chem. Soc.* **2013**, *135* (26), 9636-9639.
21. (a) Lazzaroni, R.; Settambolo, R.; Rocchiccioli, S.; Paganelli, S.; Marchetti, M., *J. Organomet. Chem.* **2005**, *690* (7), 1699-1704; (b) Lazzaroni, R.; UccelloBarretta, G.; Scamuzzi, S.; Settambolo, R.; Caiazza, A., *Organometallics* **1996**, *15* (21), 4657-4659.
22. Watkins, A. L.; Landis, C. R., *J. Am. Chem. Soc.* **2010**, *132* (30), 10306-10317.
23. Wong, G. W. A. T. T. L., C.R., *Org. Synth.* **2012**, *89*, 243-254.
24. Zhang, Z. X.; Ma, B. C.; Zhu, Q. Q.; Ding, Y.; Wang, C. M.; Song, W. F., *Synth. Commun.* **2012**, *42* (20), 3053-3060.
25. Herrera, R.; Jimenez-Vazquez, H. A.; Modelli, A.; Jones, D.; Soderberg, B. C.; Tamariz, J., *Eur. J. Org. Chem.* **2001**, (24), 4657-4669.
26. Pietruszka, J.; Scholzel, M., *Adv. Synth. Catal.* **2012**, *354* (4), 751-756.

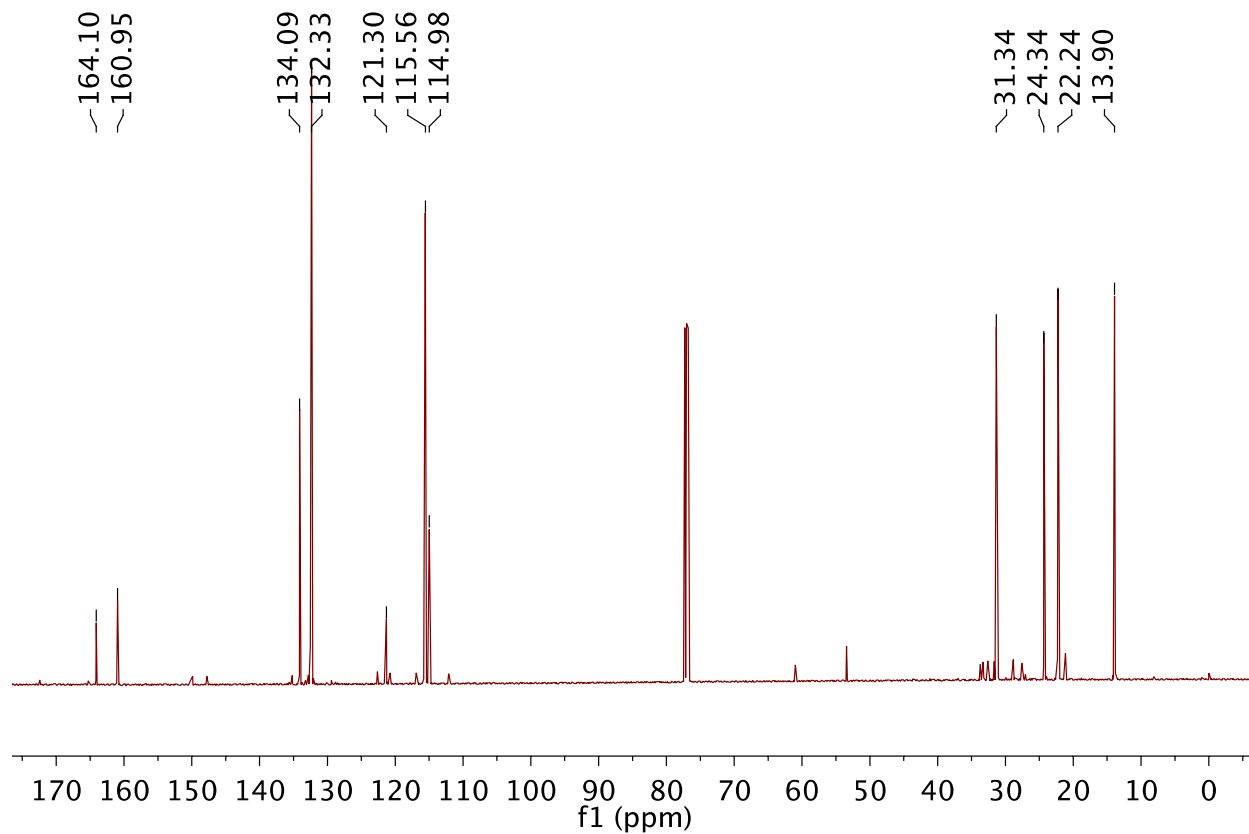
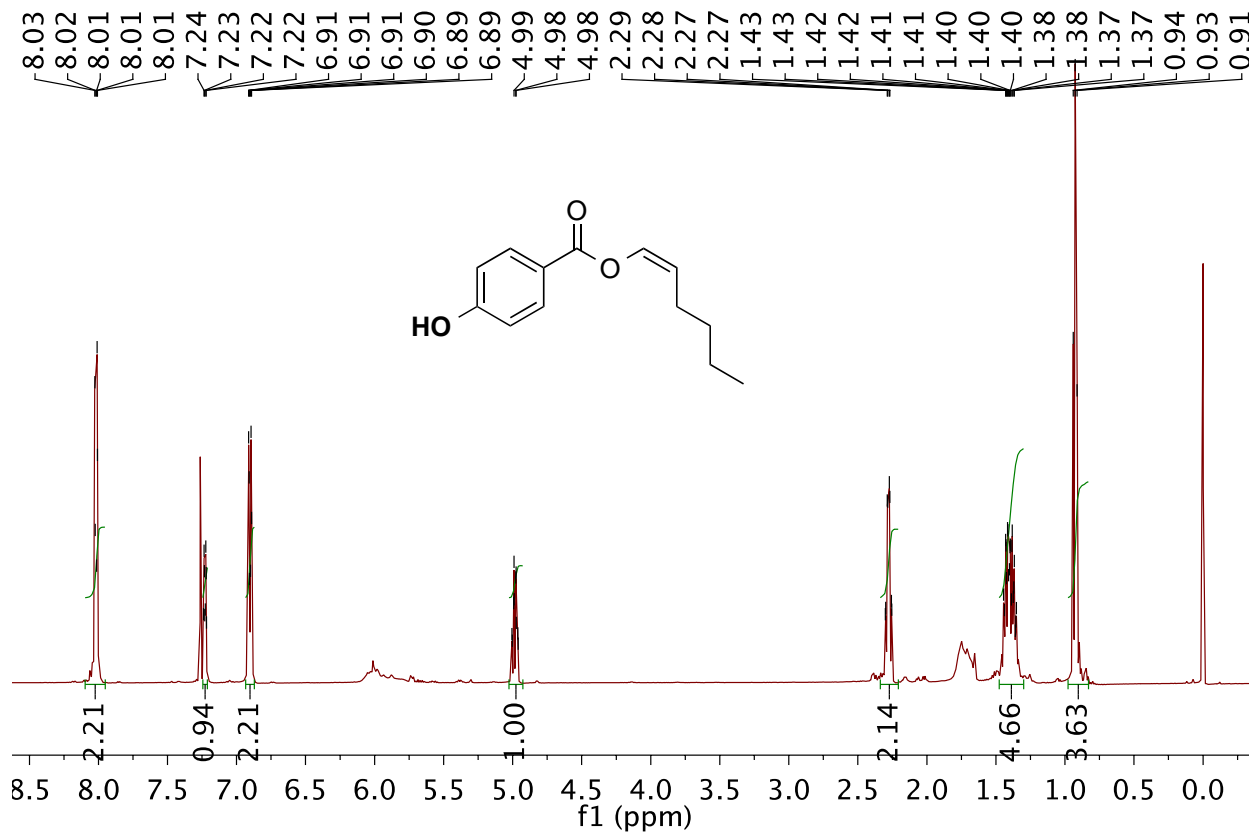
27. Chen, B. F.; Tasi, M. R.; Yang, C. Y.; Chang, J. K.; Chang, N. C., *Tetrahedron* **2004**, *60* (45), 10223-10231.
28. Li, W.; Liu, C.; Zhang, H.; Ye, K. Y.; Zhang, G. H.; Zhang, W. Z.; Duan, Z. L.; You, S. L.; Lei, A. W., *Angew.Chem.Int.Ed.* **2014**, *53* (9), 2443-2446.
29. Berkessel, A.; Sebastian-Ibarz, M. L.; Muller, T. N., *Angew.Chem.Int.Ed.* **2006**, *45* (39), 6567-6570.
30. Sun, T.; Zhang, X. M., *Adv. Synth. Catal.* **2012**, *354* (17), 3211-3215.
31. Monnin, J., *Helv. Chim. Acta* **1956**, *39* (6), 1721-1724.
32. Rousee, K.; Bouillon, J. P.; Couve-Bonnaire, S.; Pannecoucke, X., *Org. Lett.* **2016**, *18* (3), 540-543.
33. Foarta, F.; Landis, C. R., *J. Org. Chem.* **2016**, *81* (22), 11250-11255.
34. Kitazume, T.; Murata, K.; Ikeya, T., *J. Fluorine Chem.* **1986**, *32* (2), 233-238.
35. Chi, Y.; Peelen, T. J.; Gellman, S. H., *Org. Lett.* **2005**, *7* (16), 3469-3472.
36. Sterzycki, R., *Synthesis-Stuttgart* **1979**, (9), 724-725.

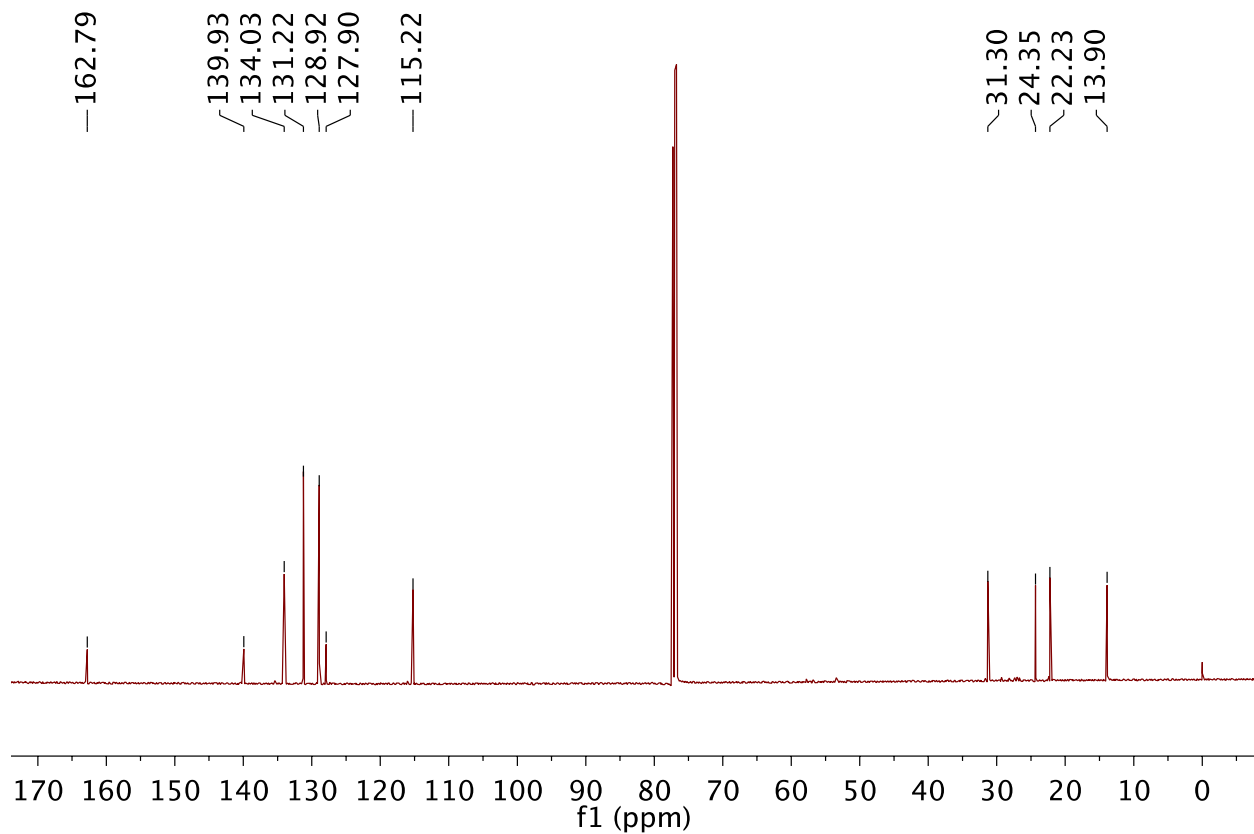
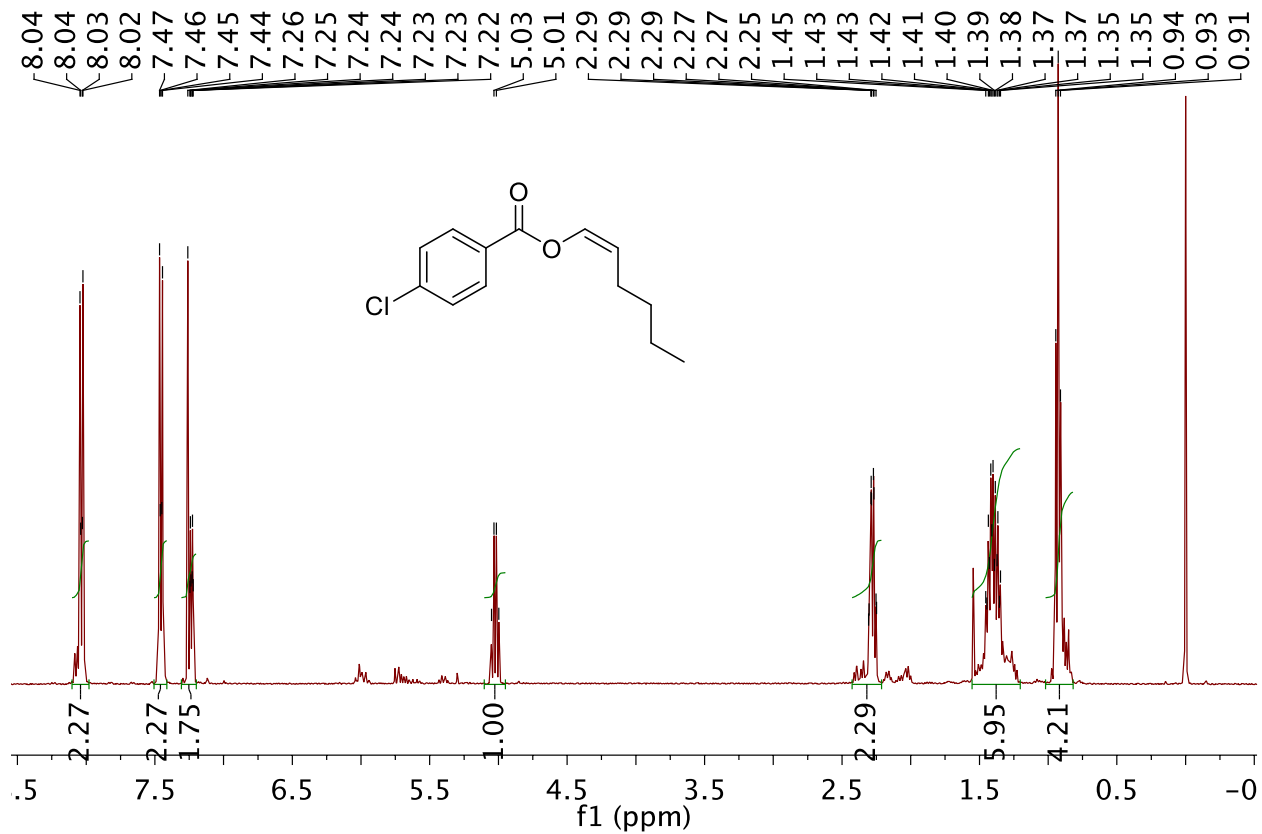
Appendix

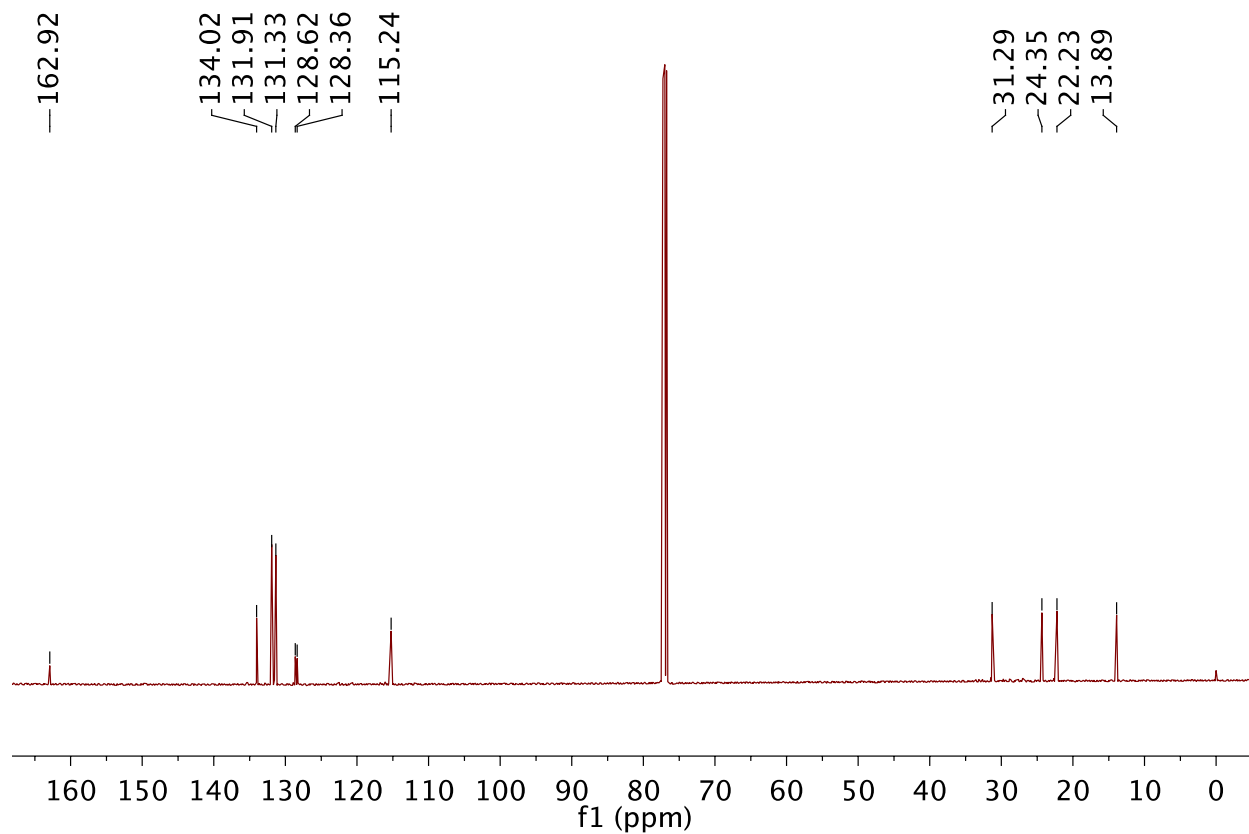
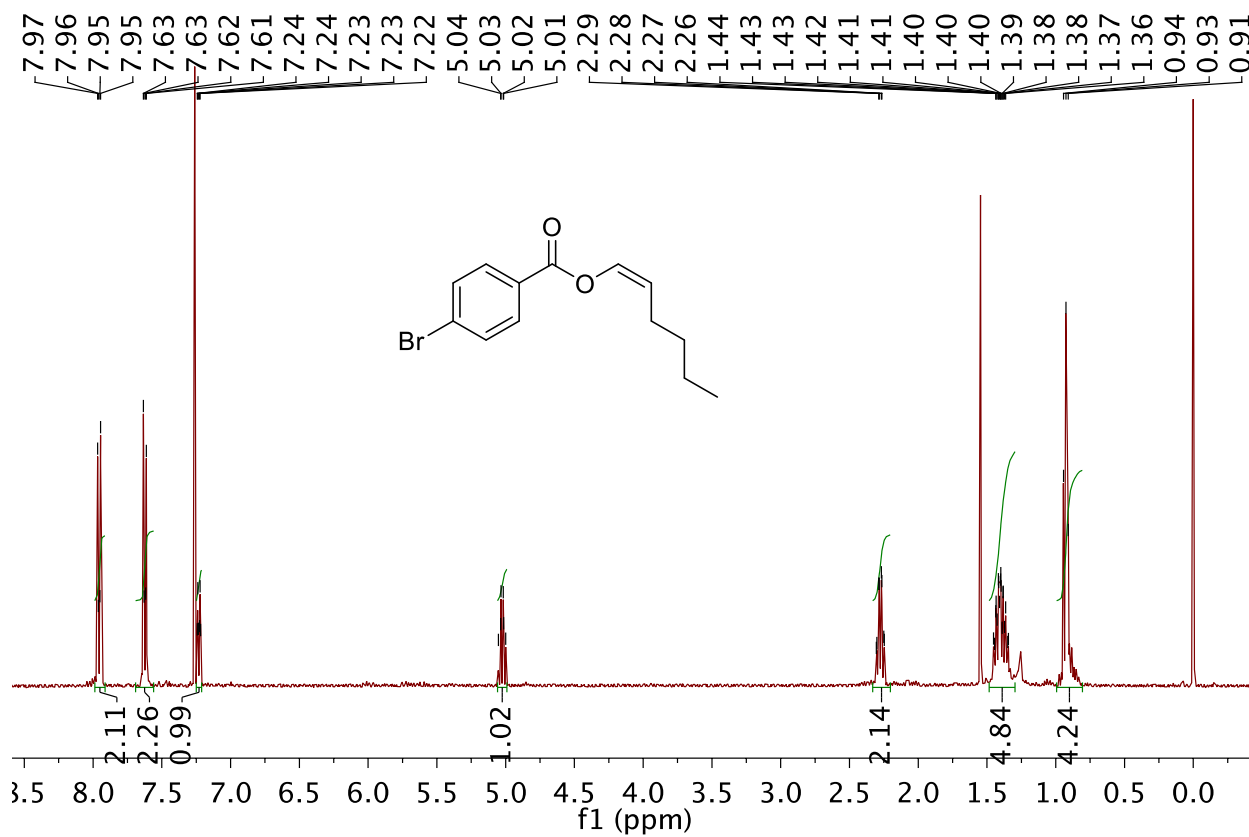
Spectra and Supporting Data for Chapters 2-4

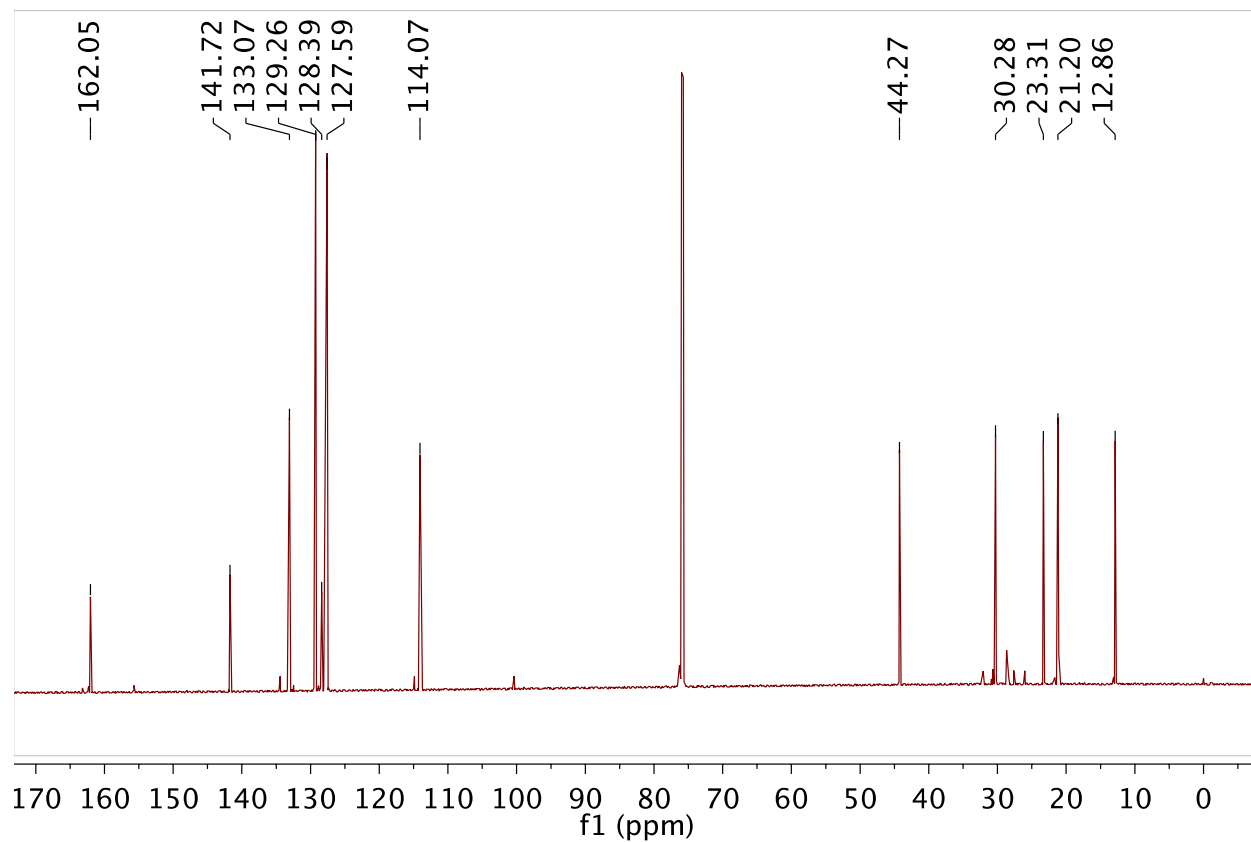
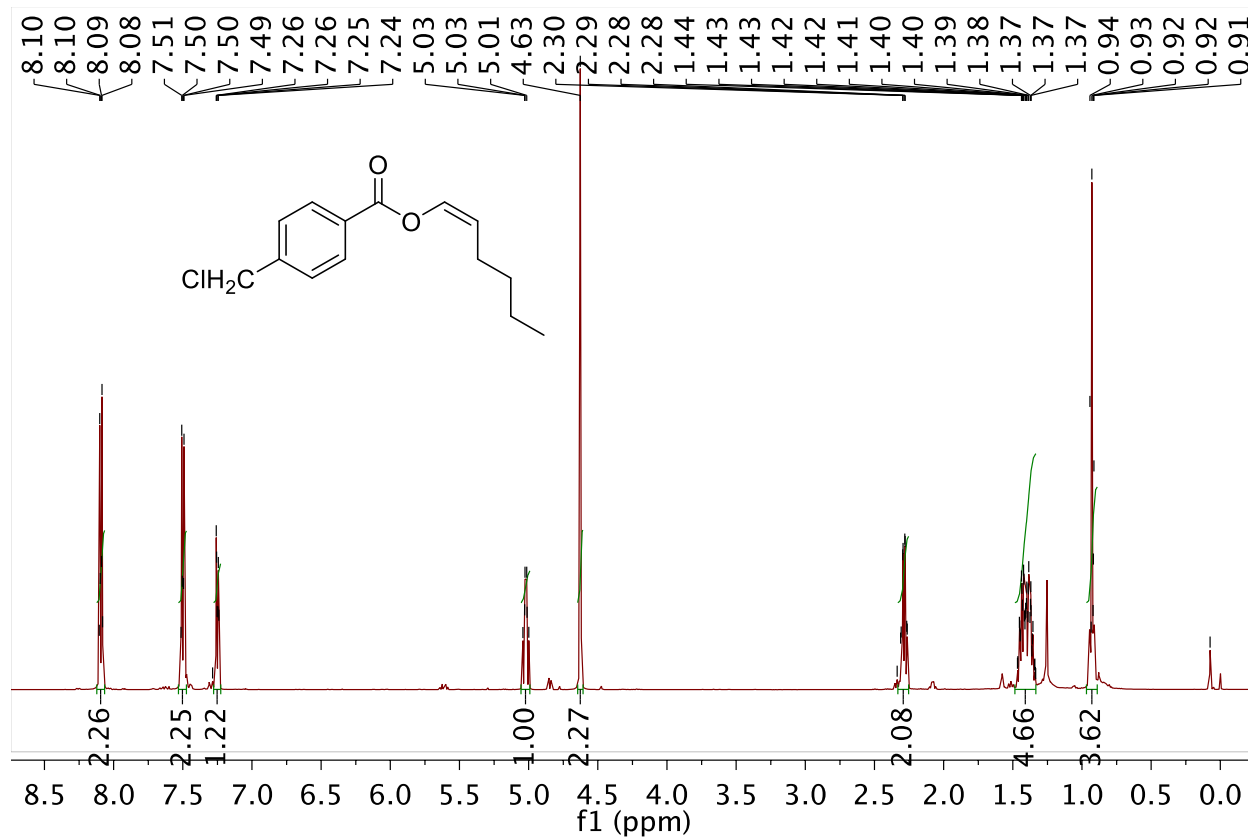
NMR Spectra for Chapter 2

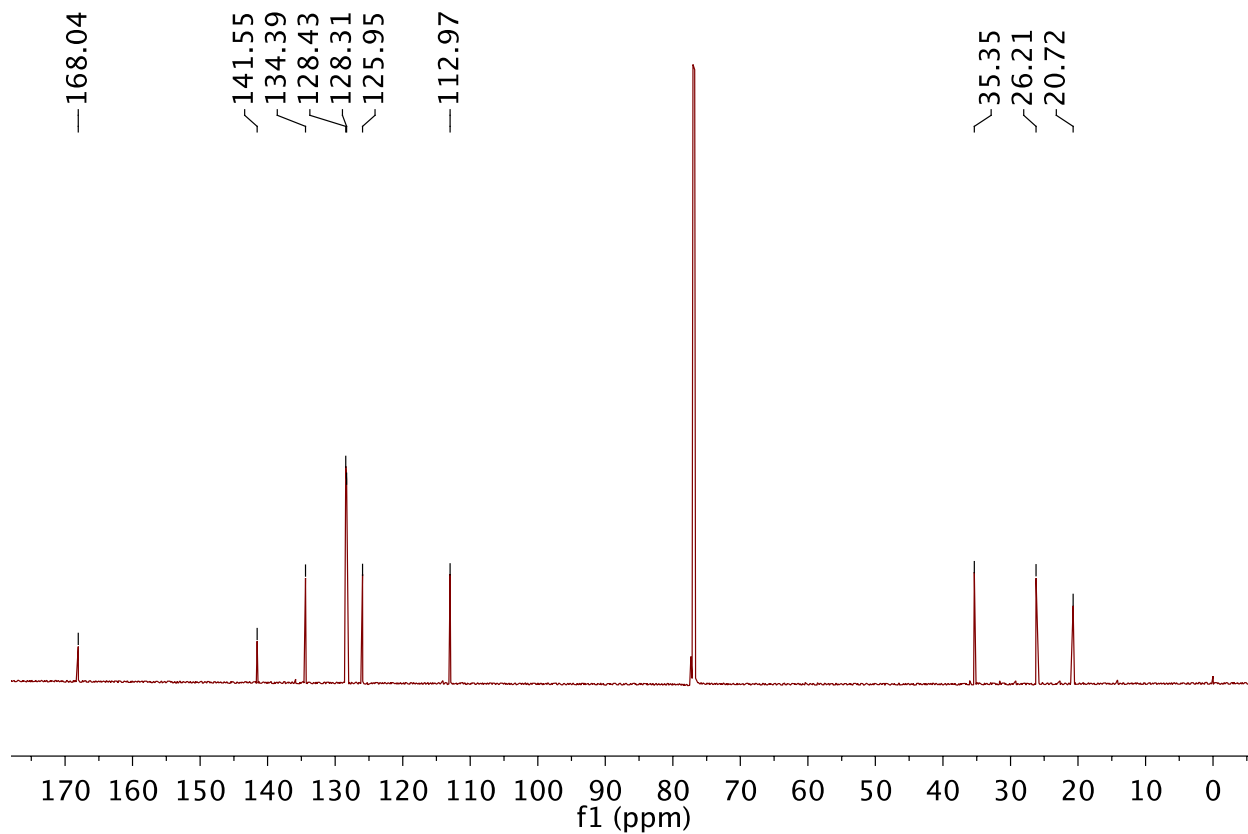
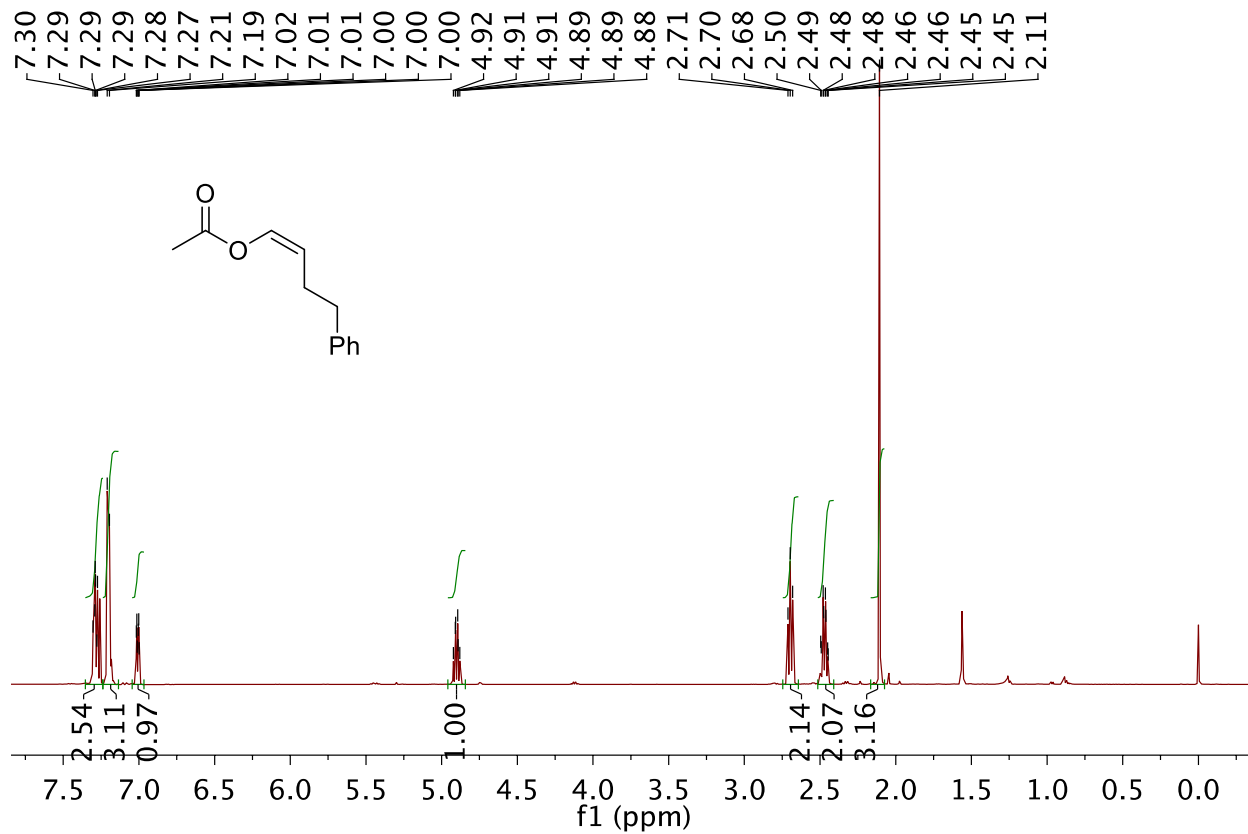


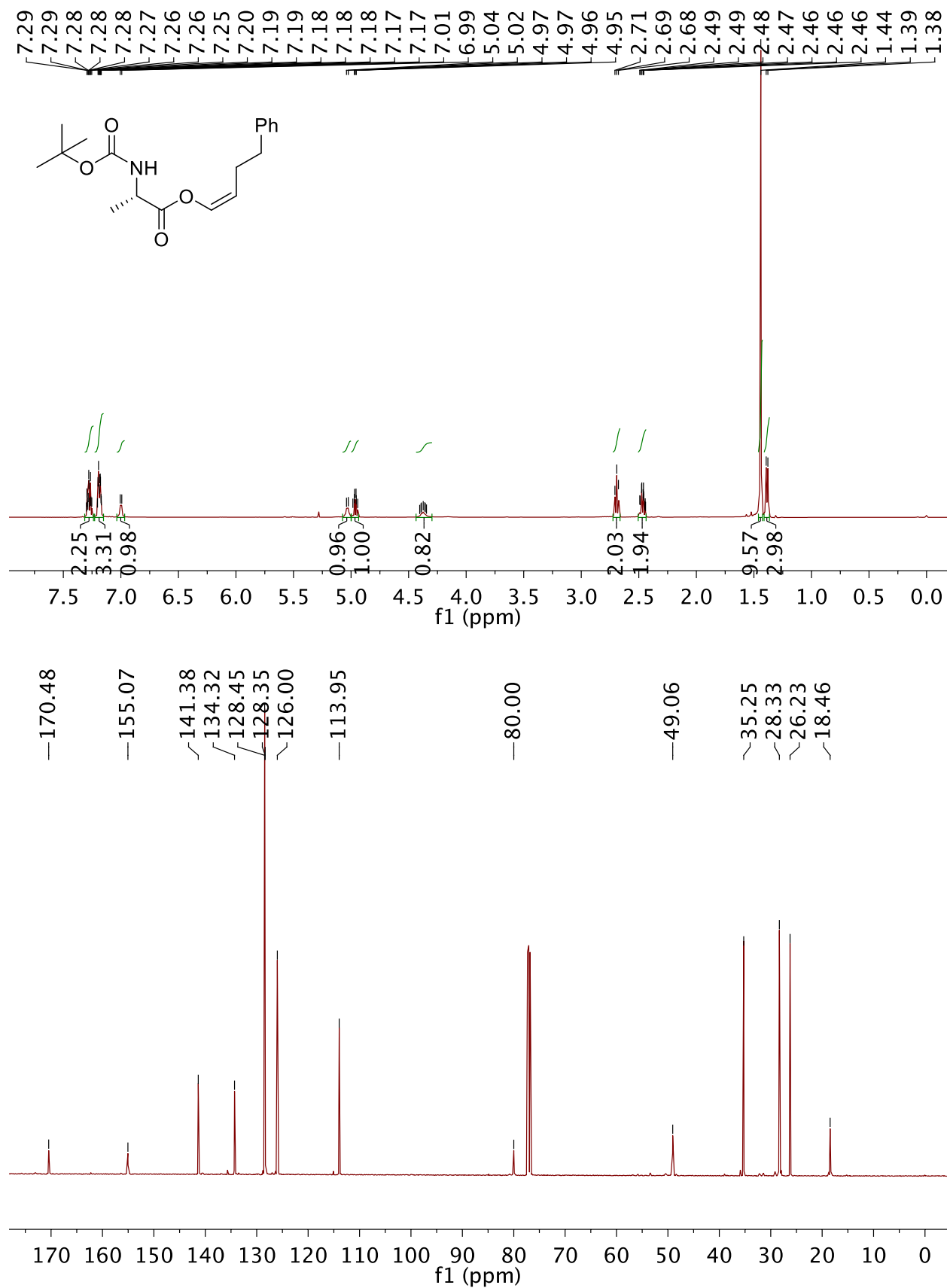


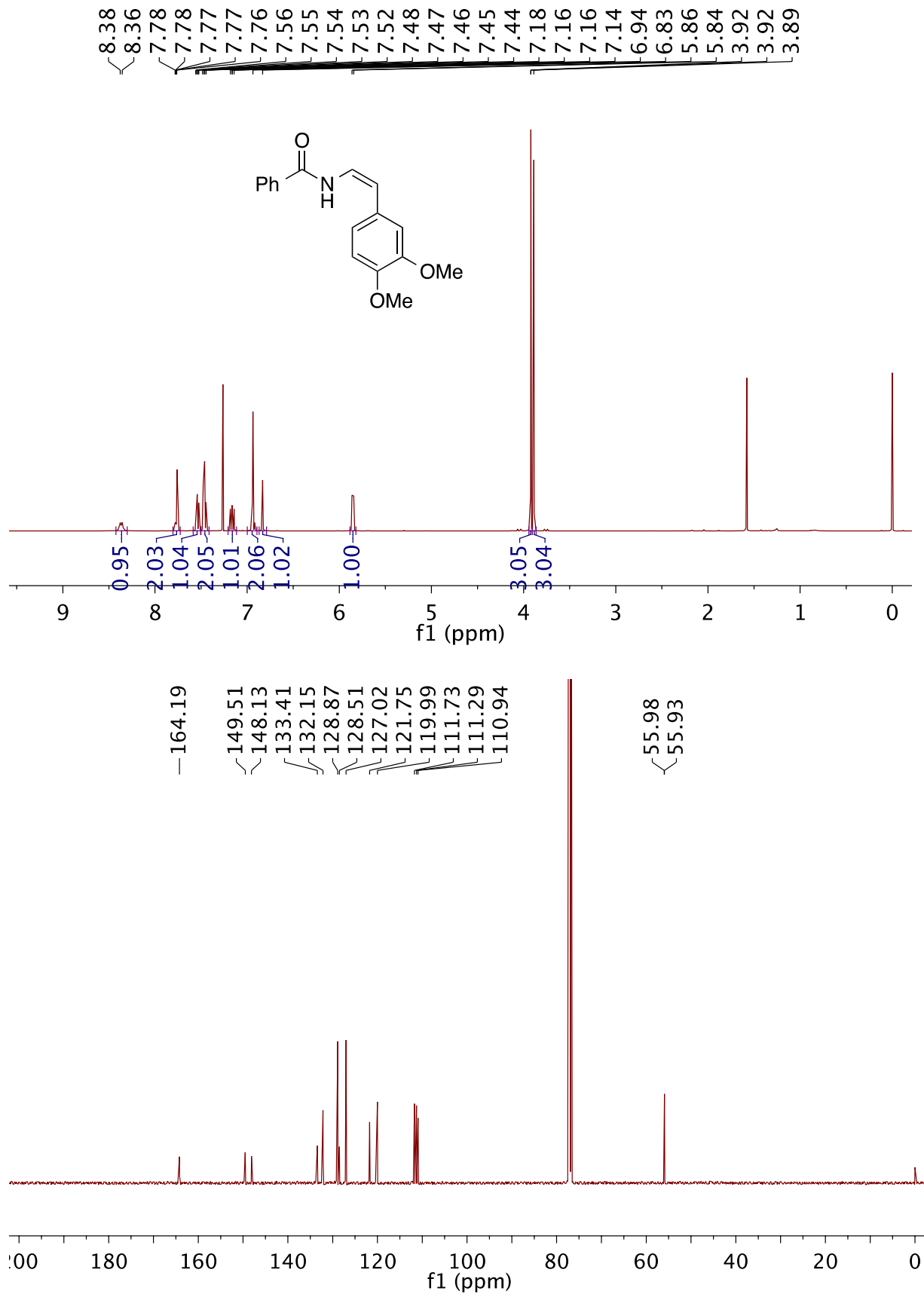


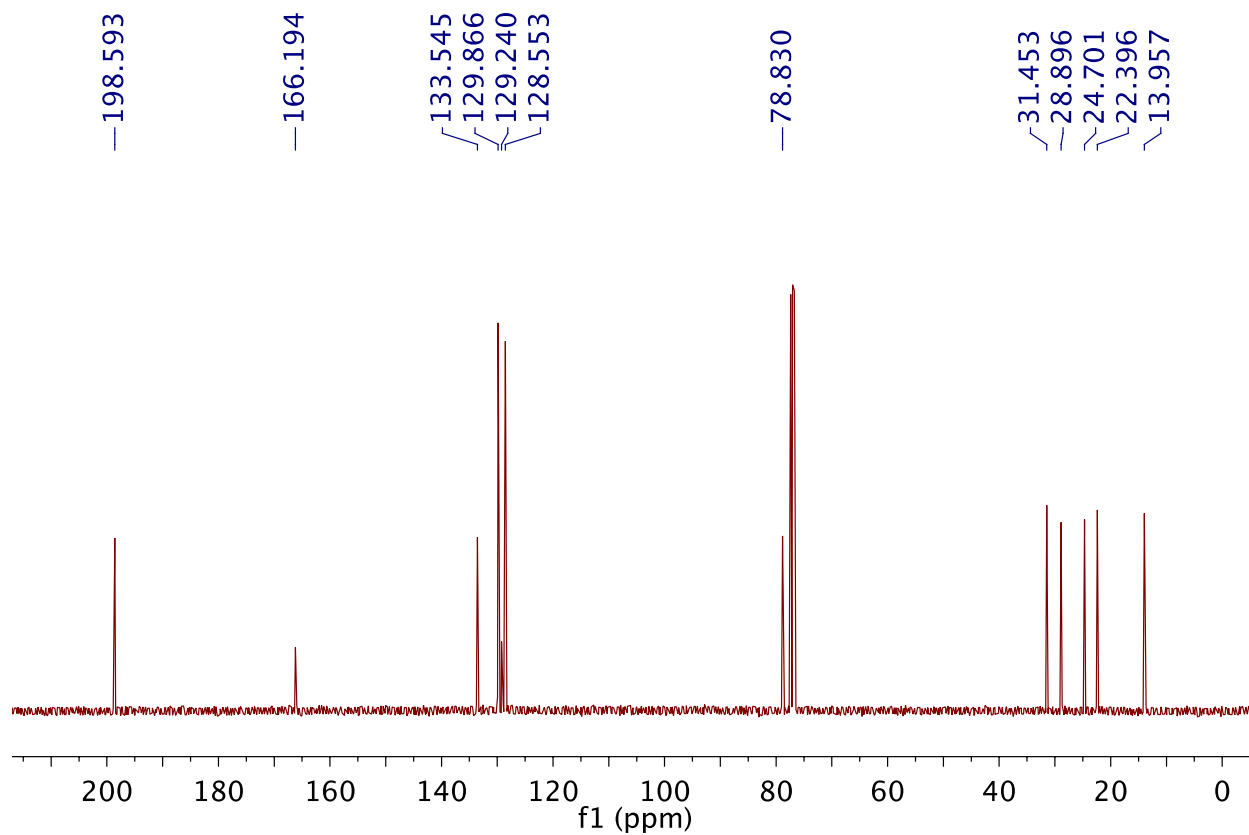
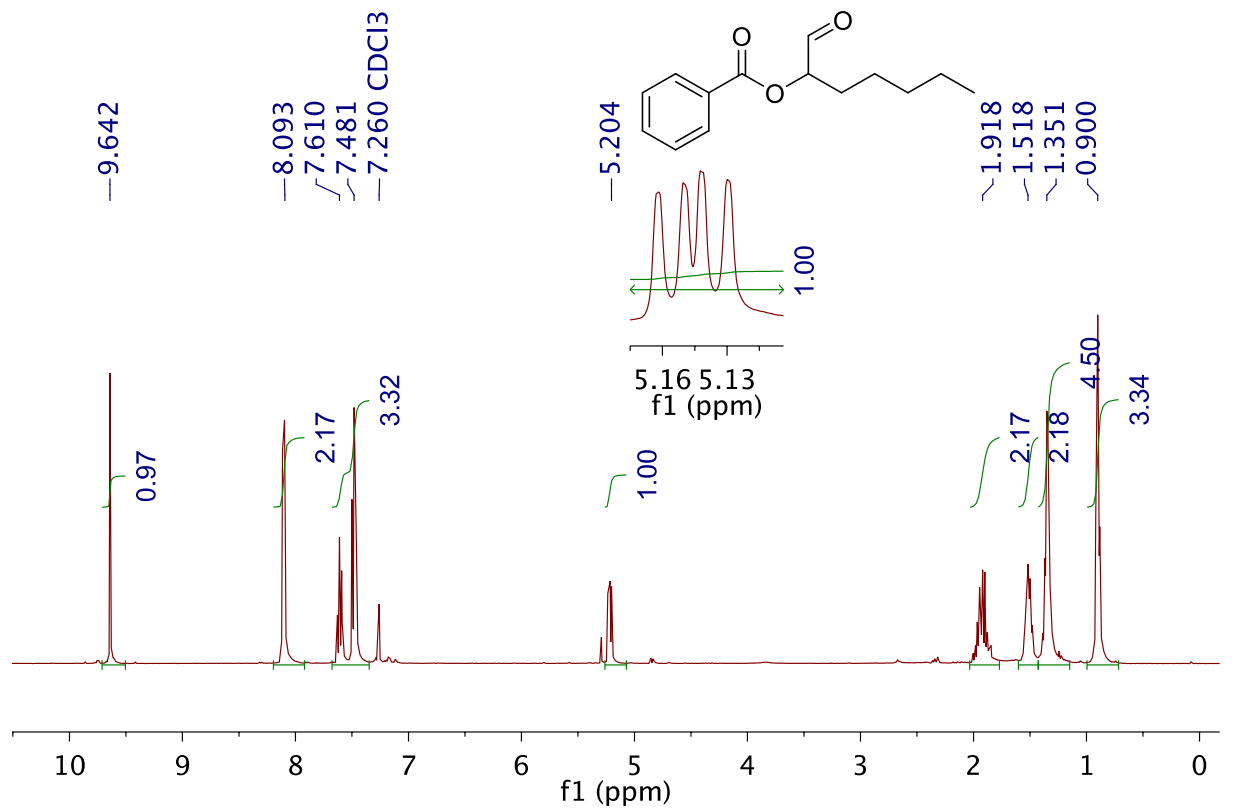


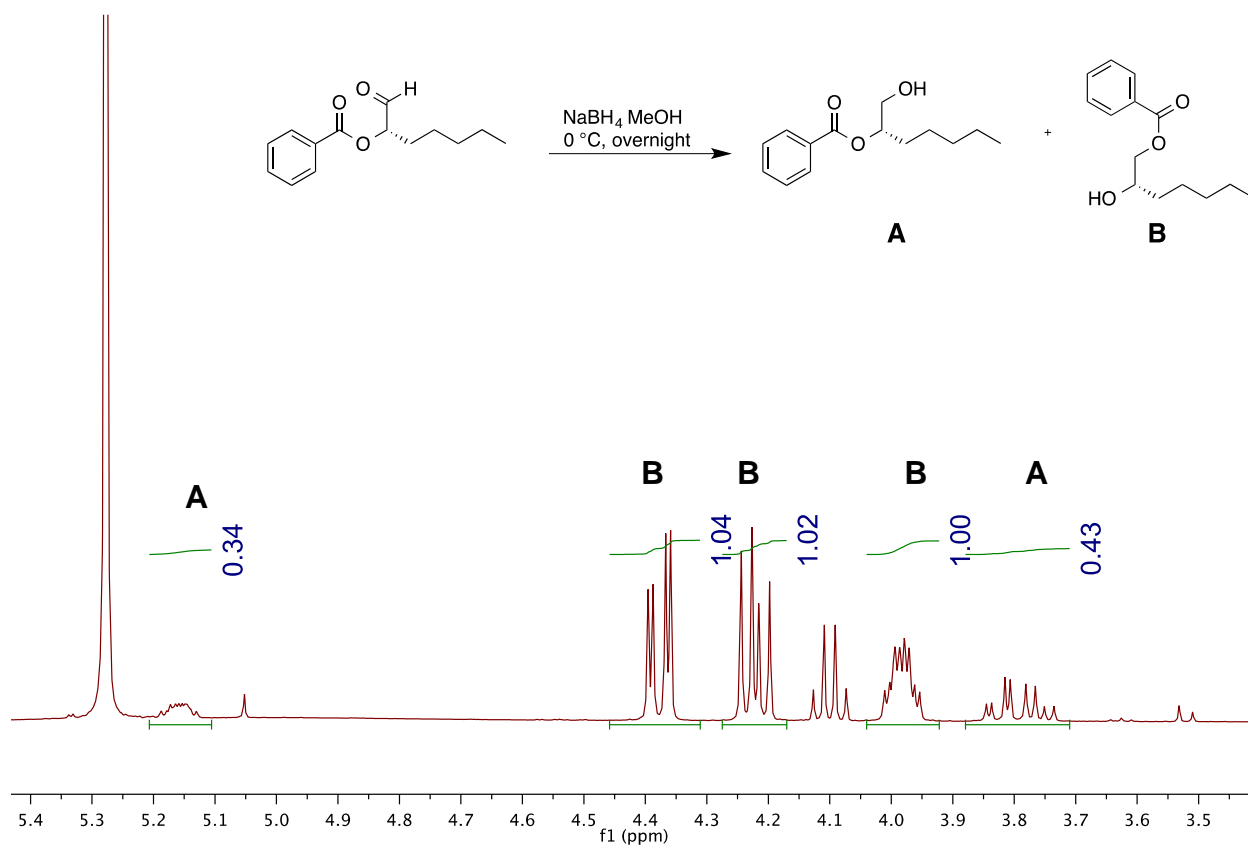
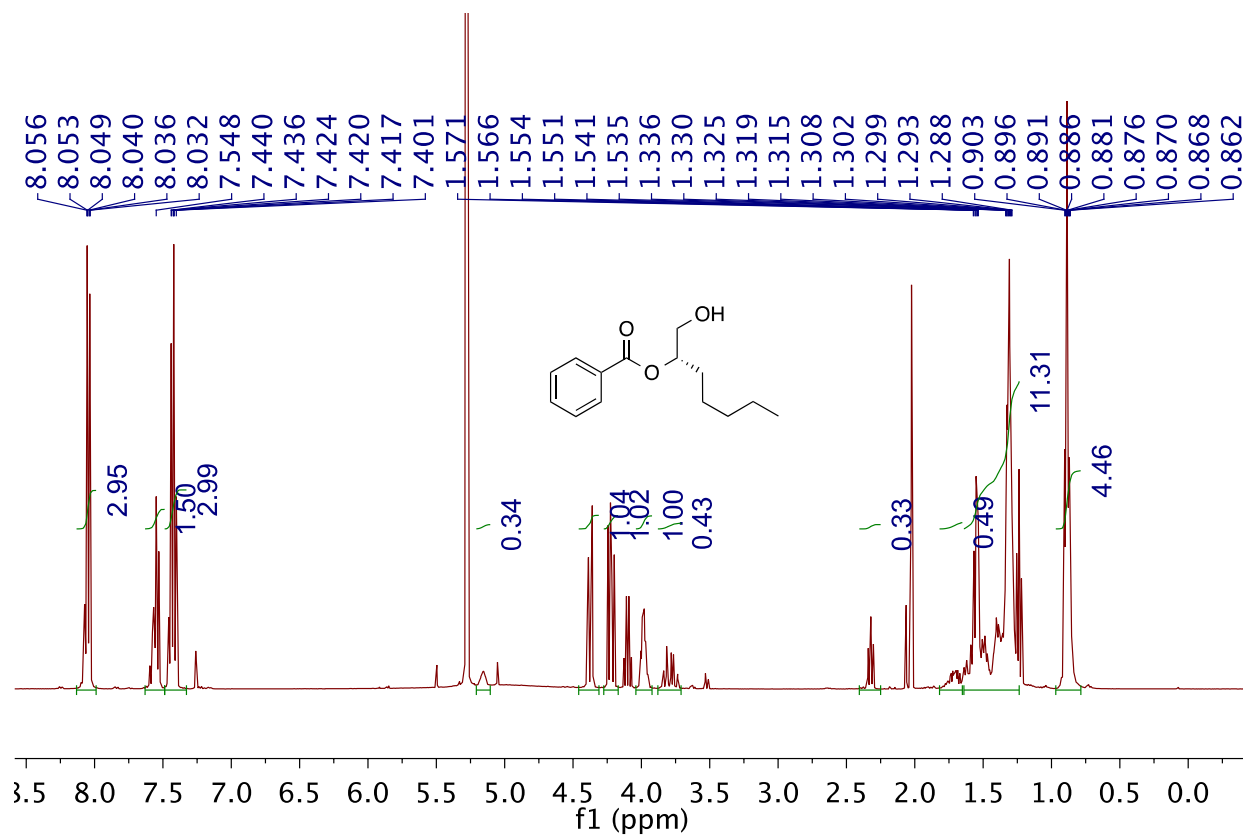


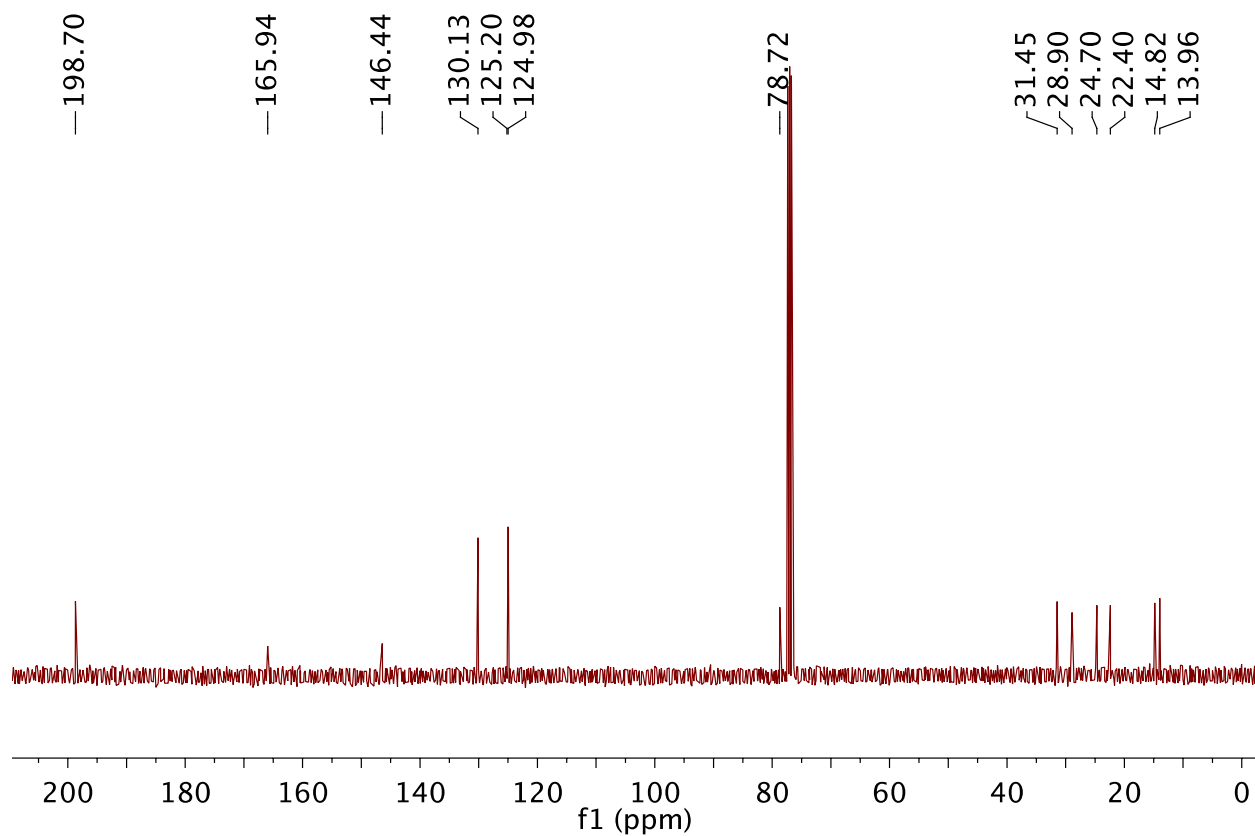
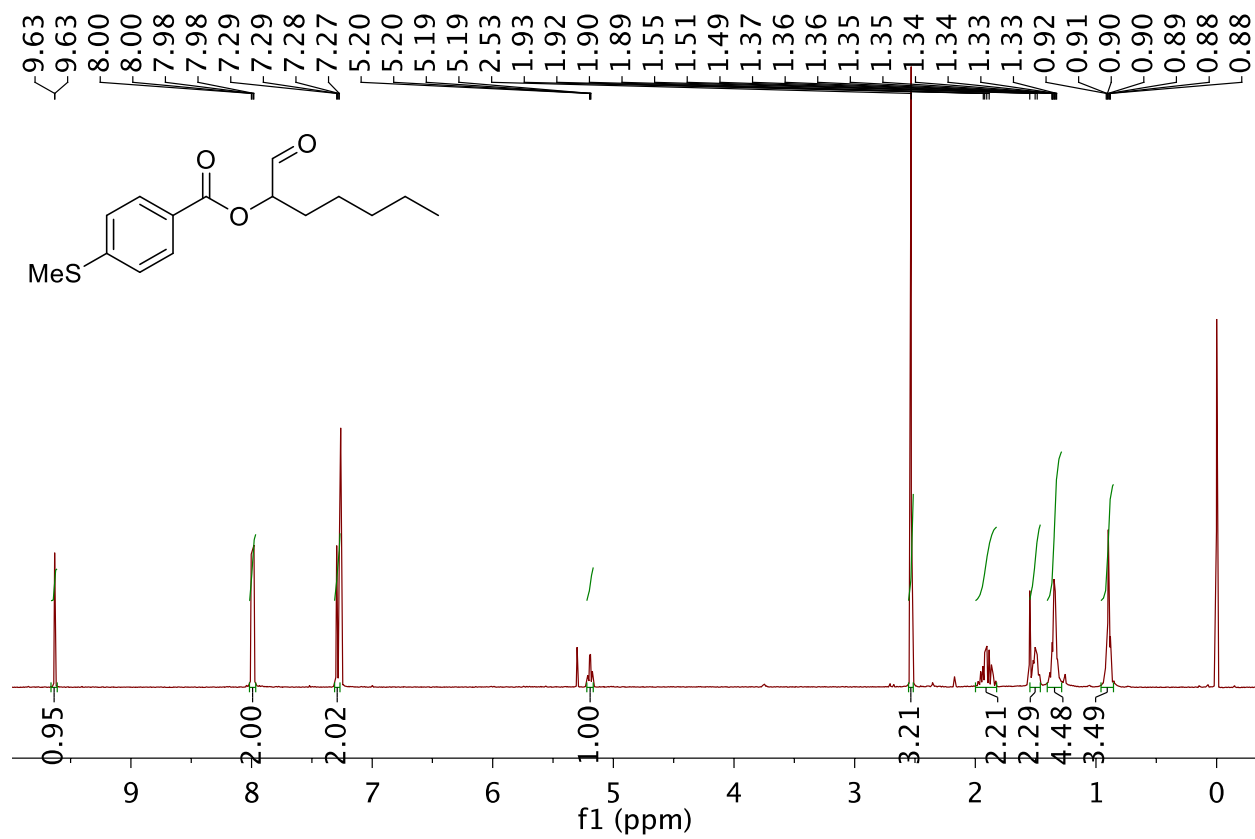


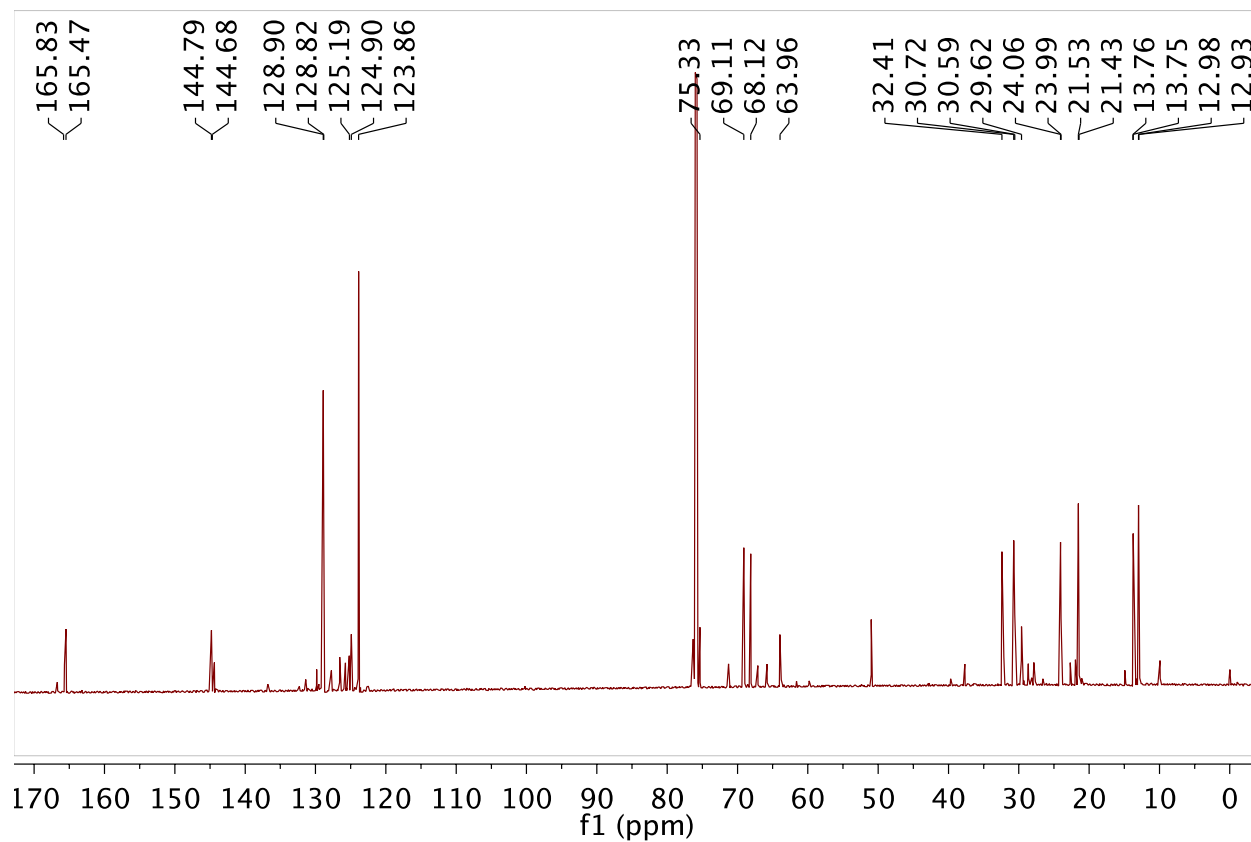
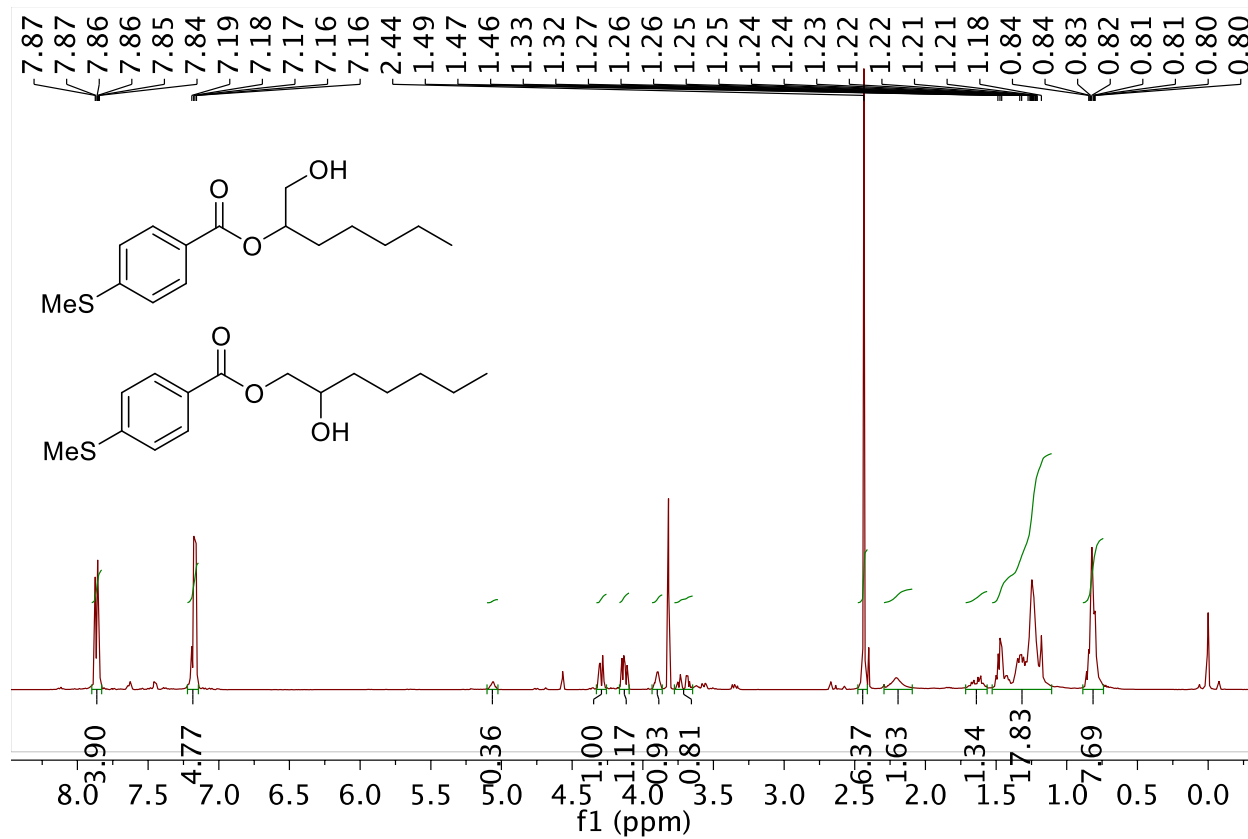


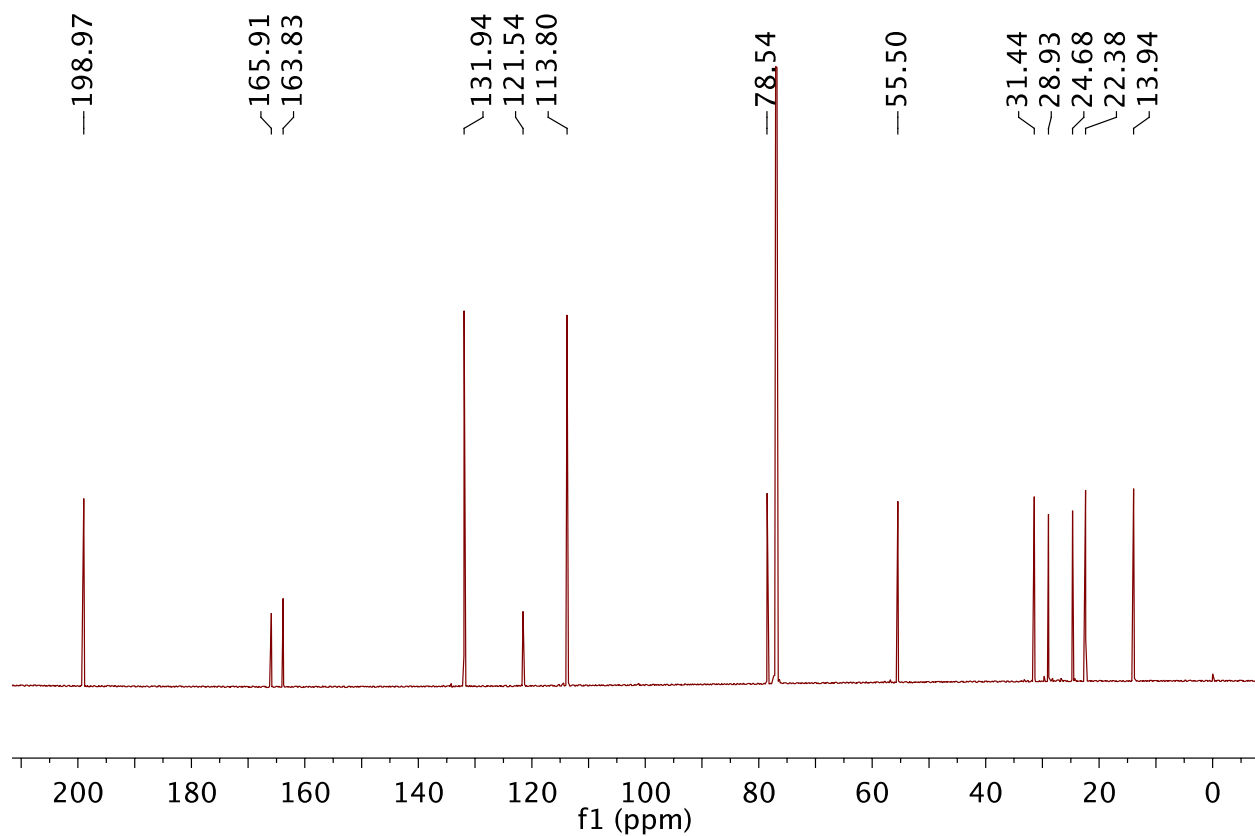
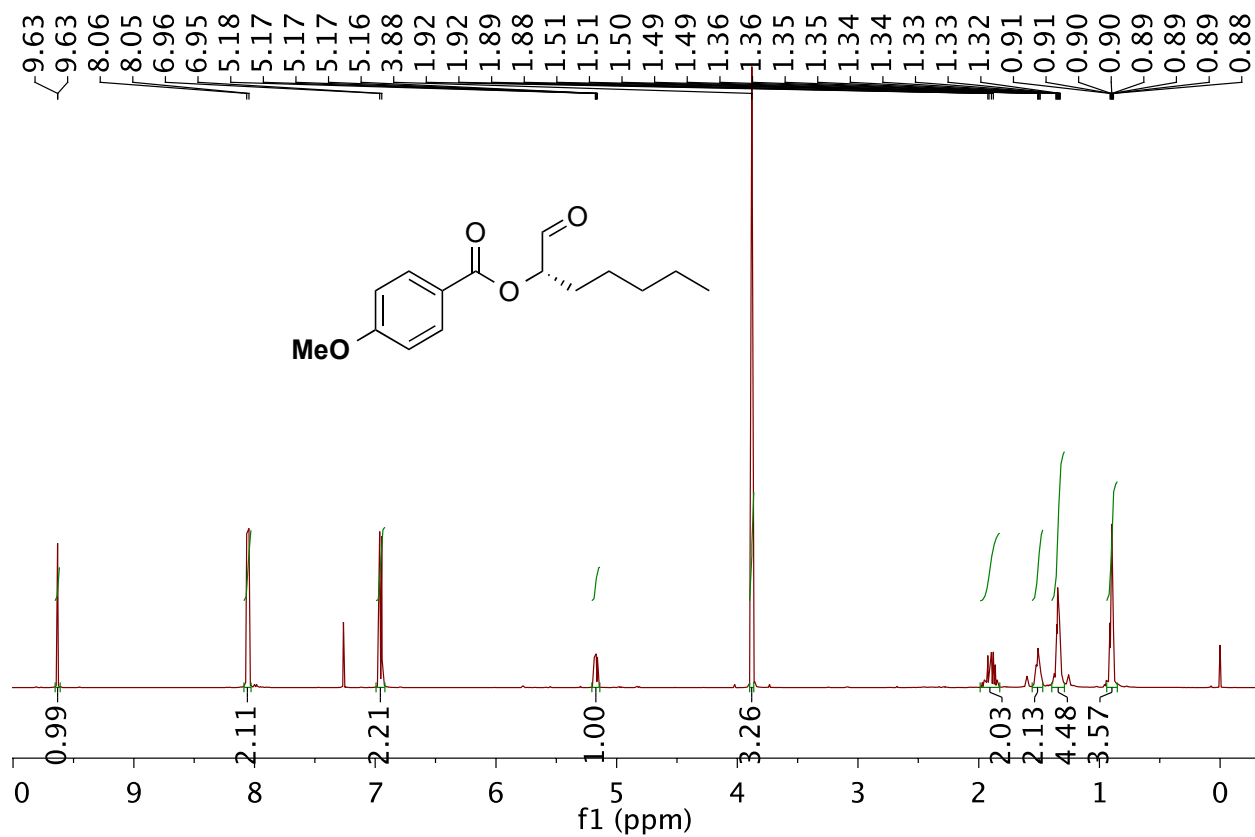


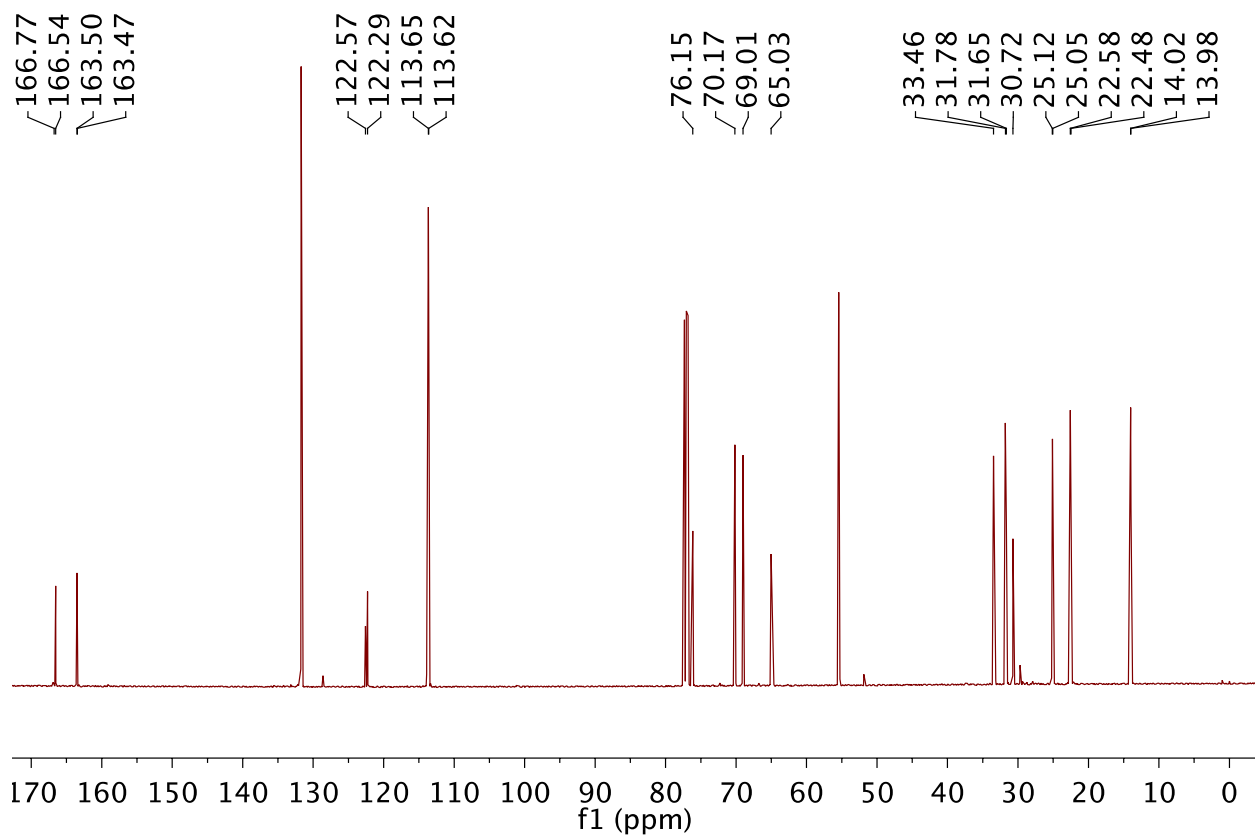
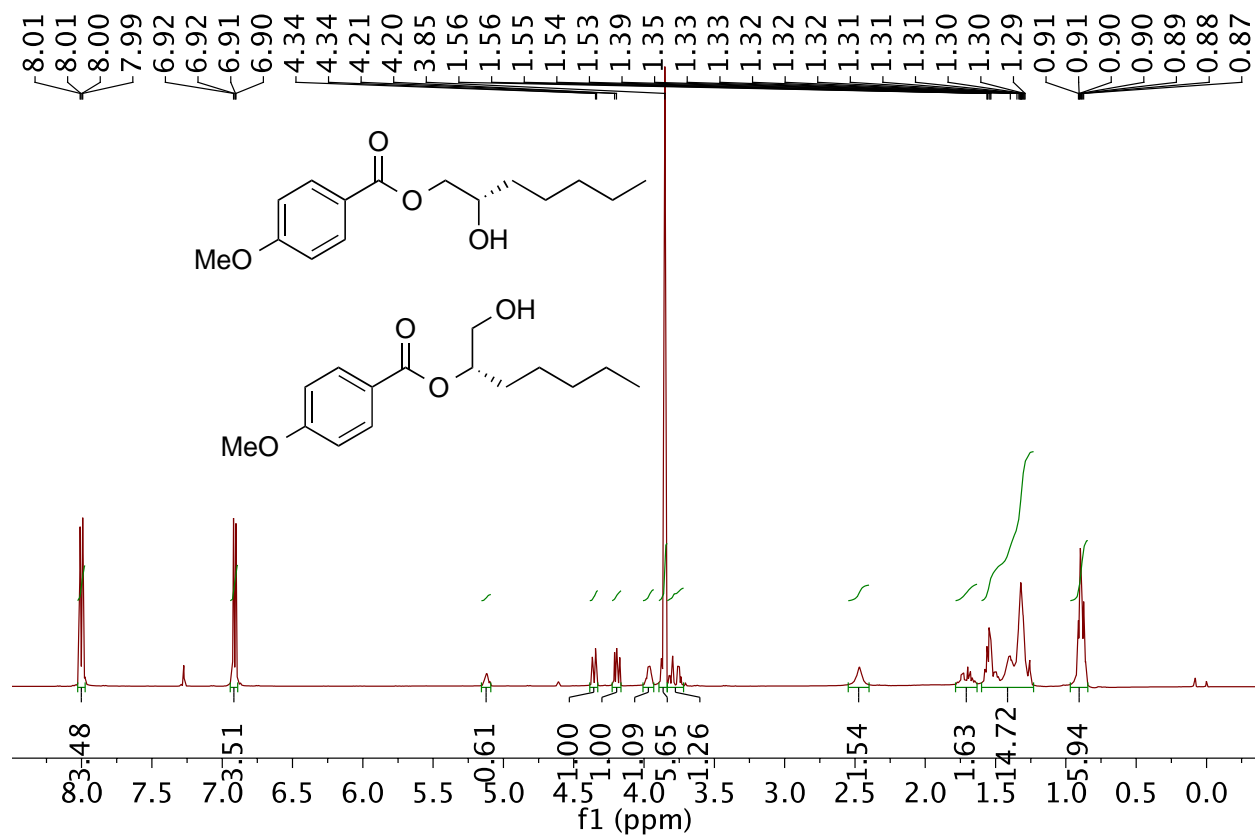


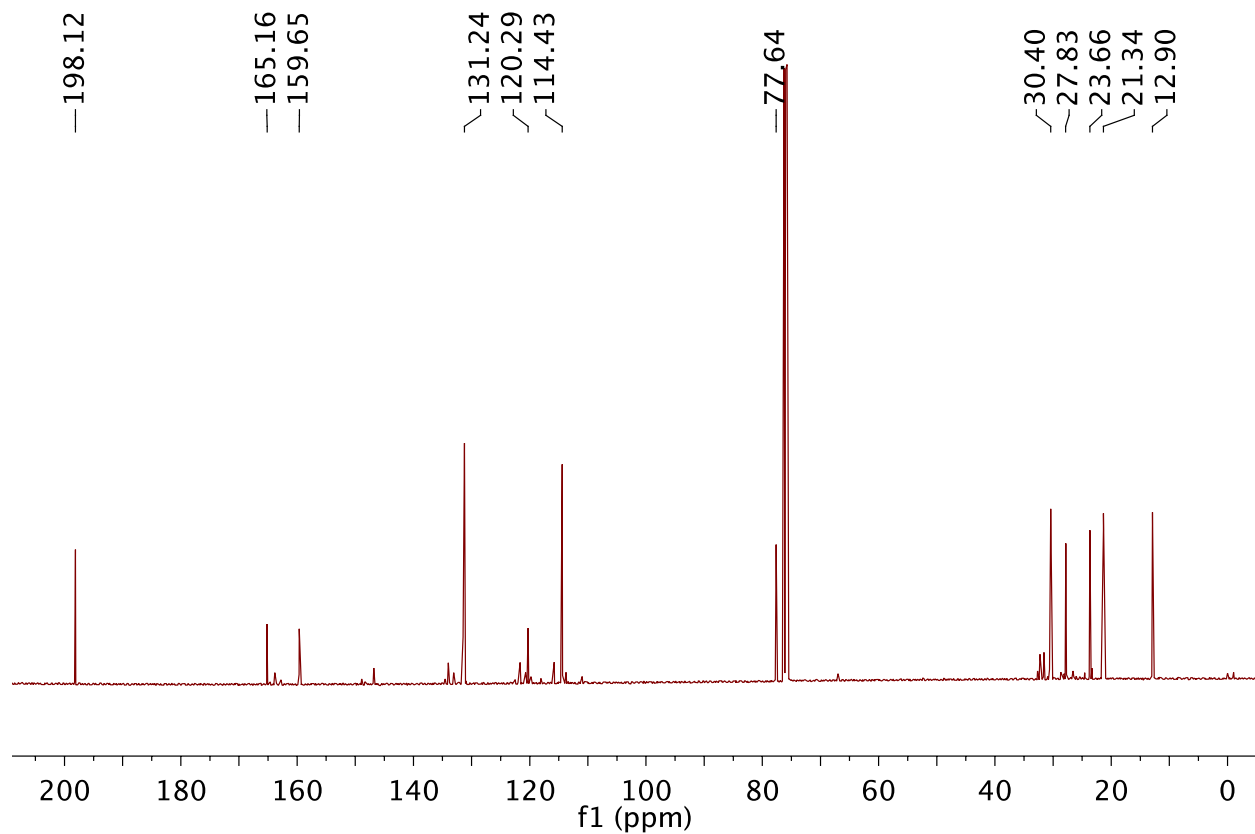
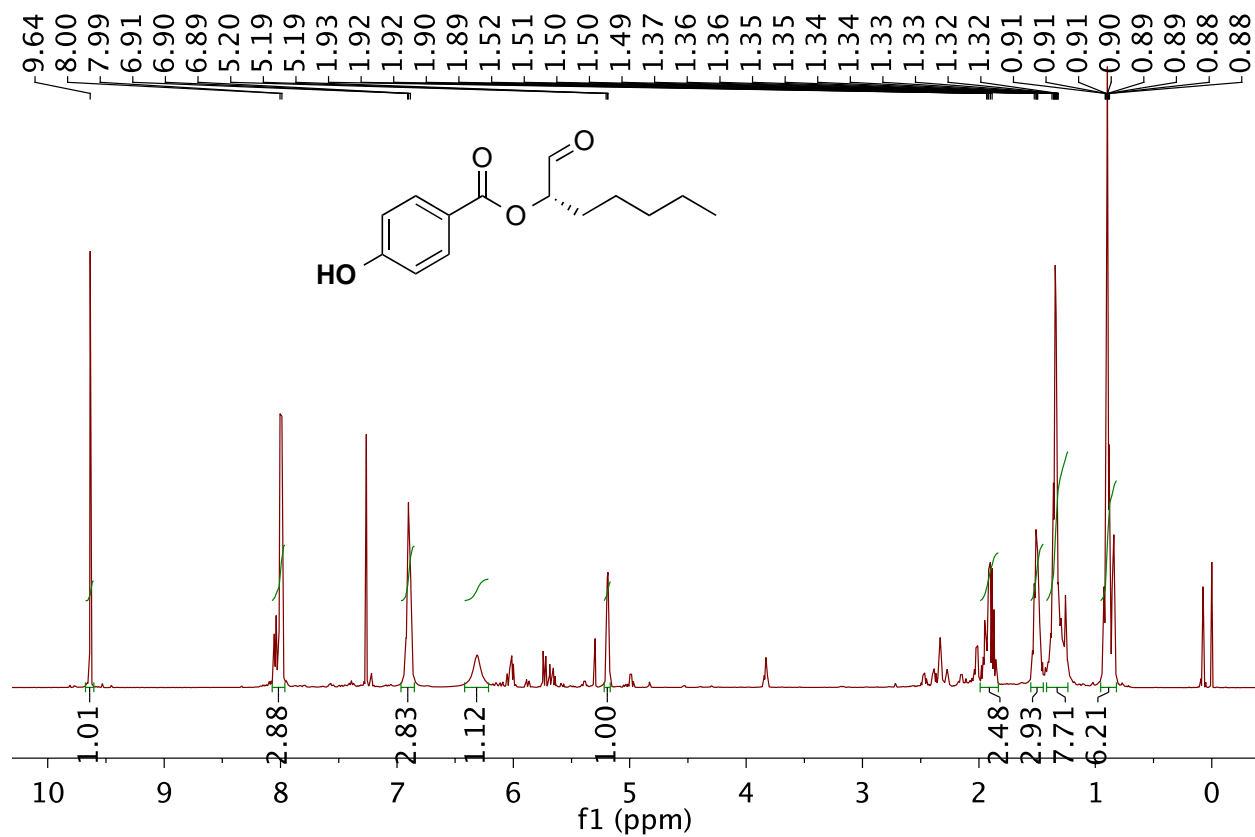


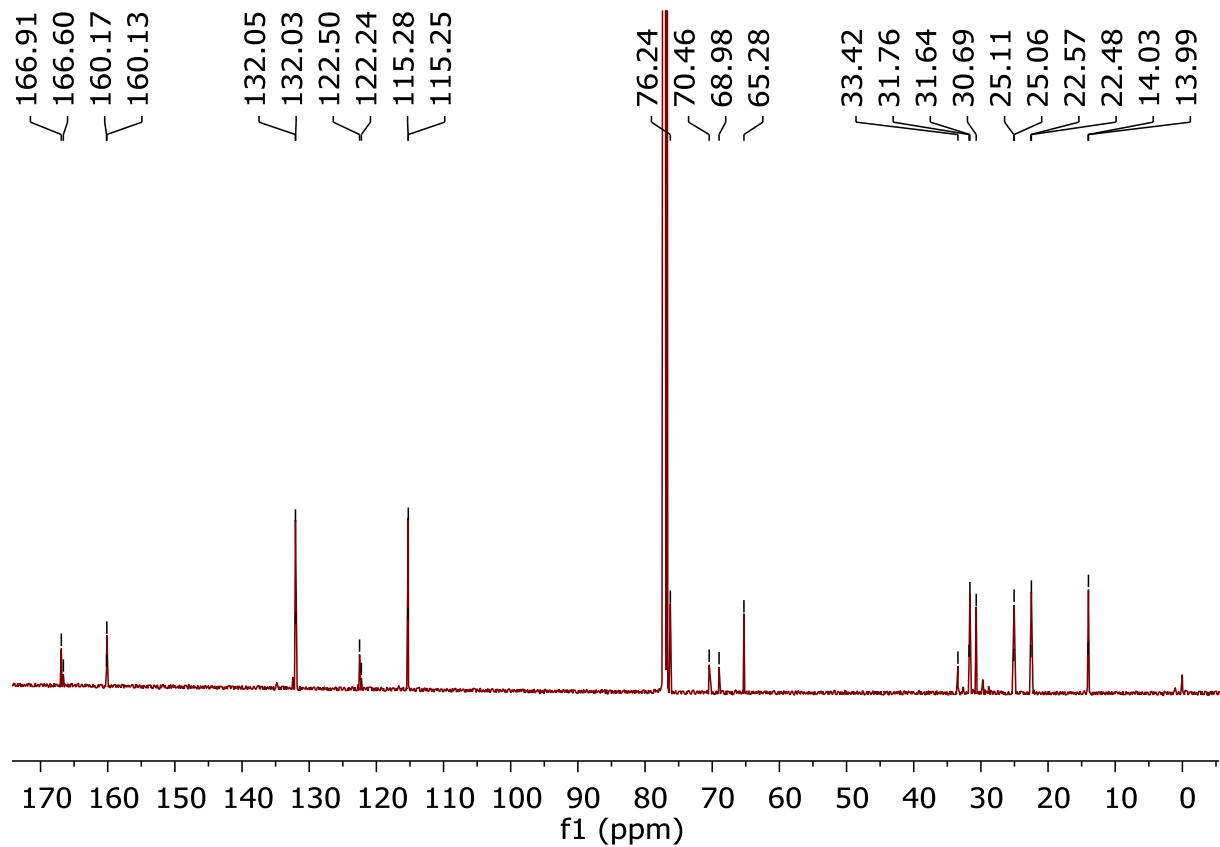
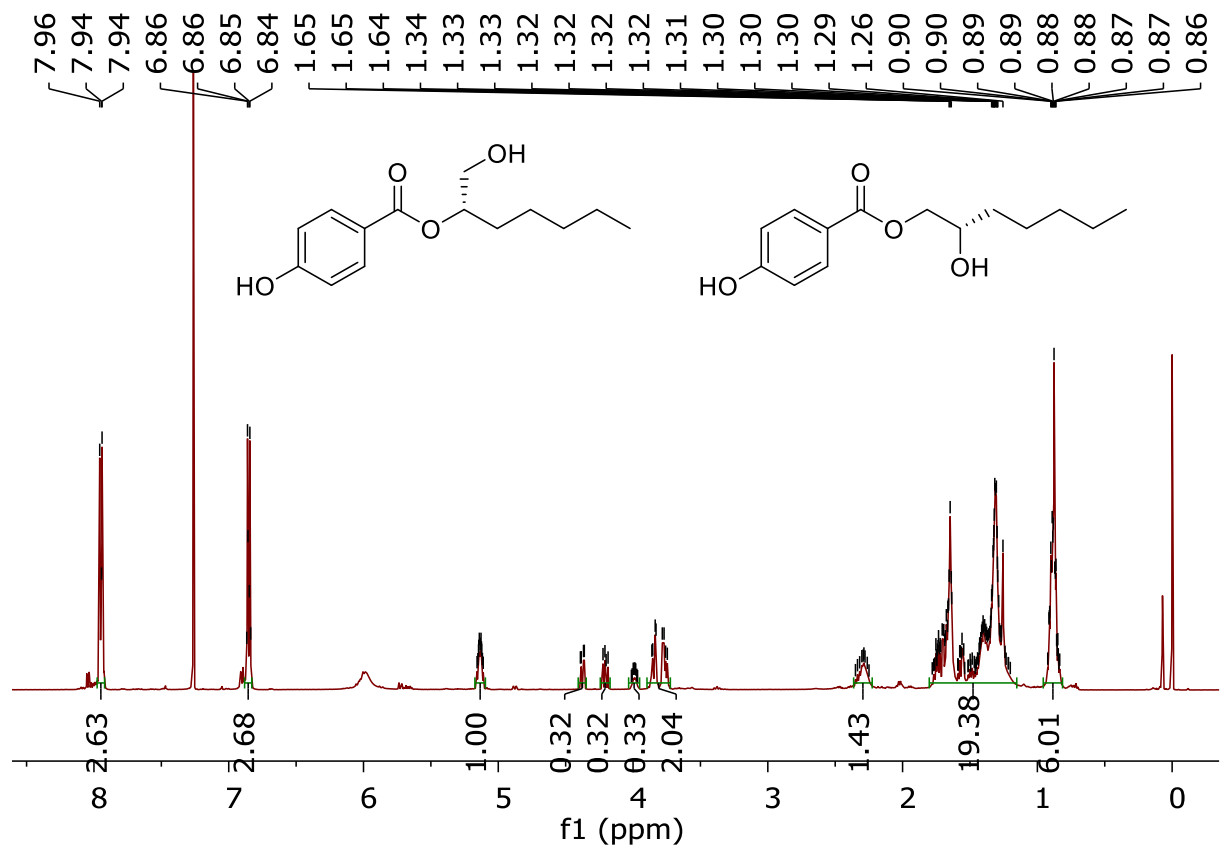


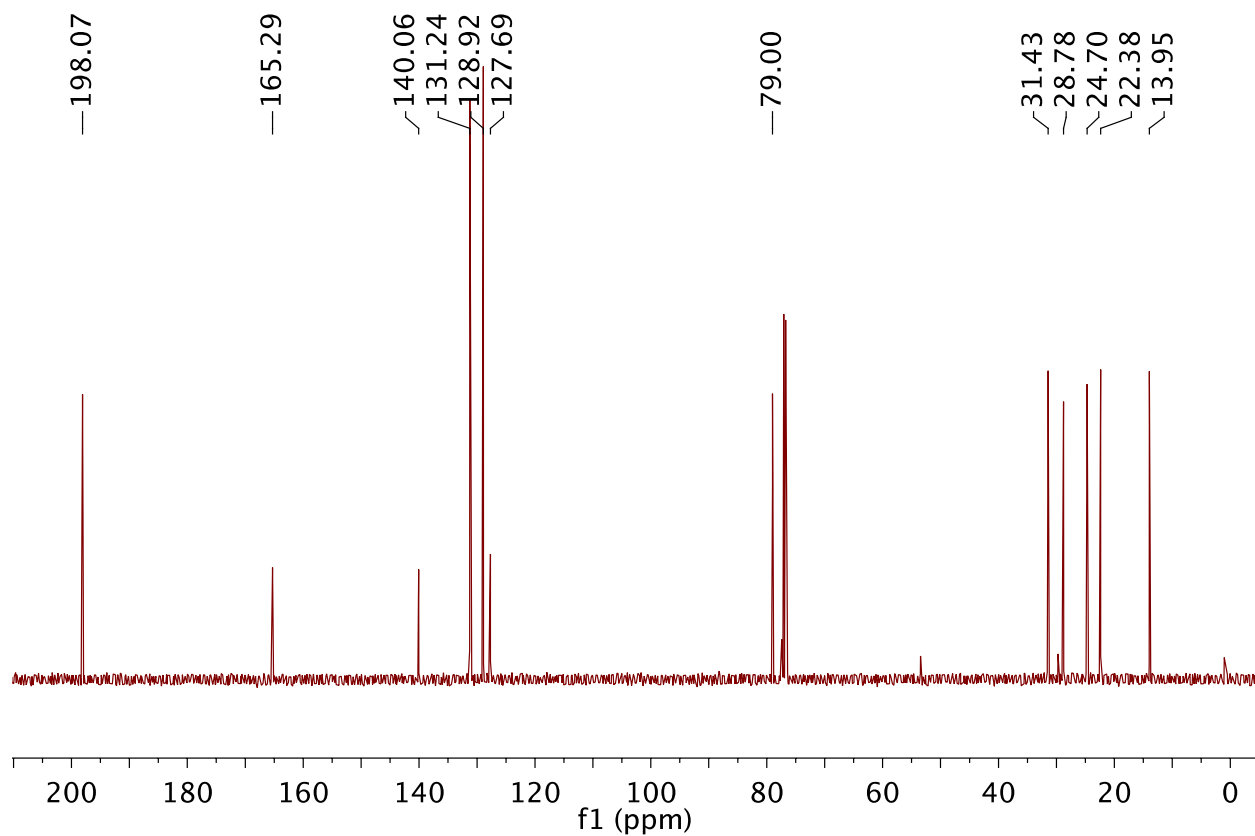
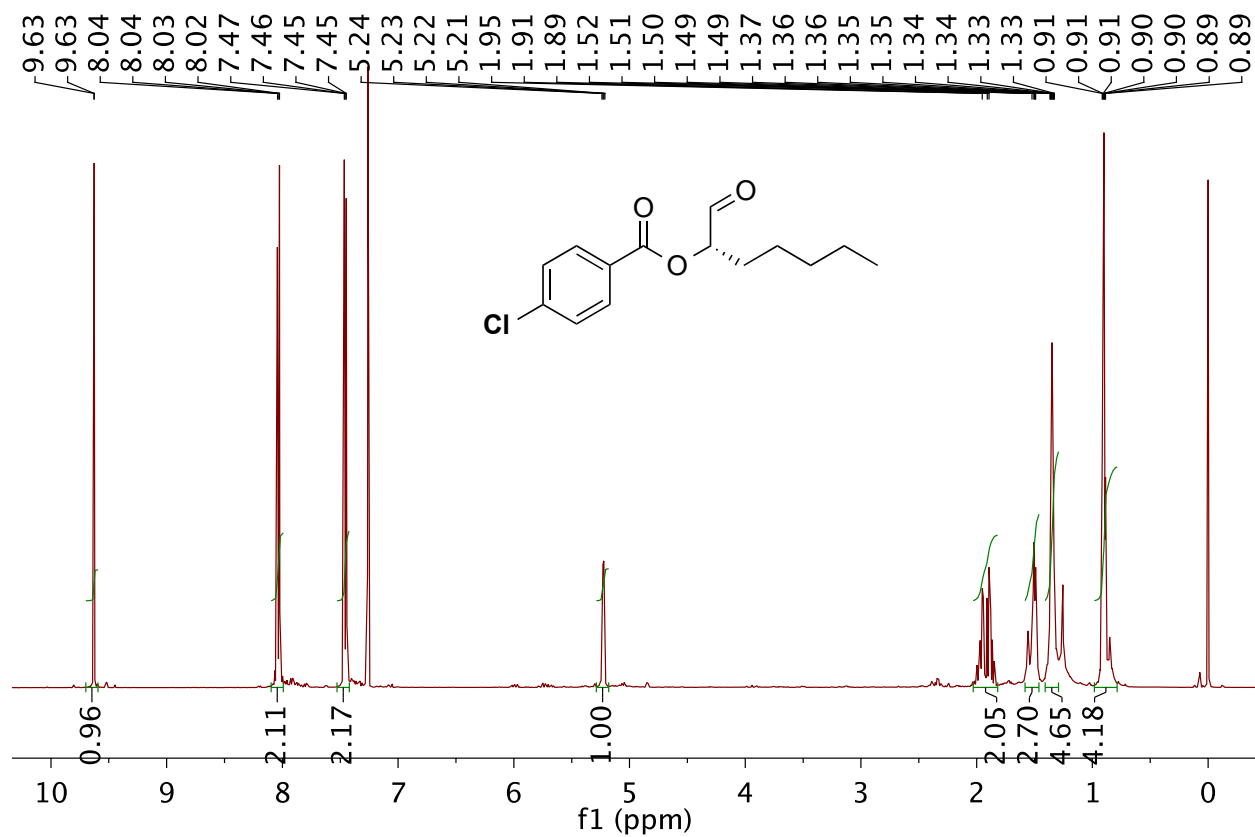


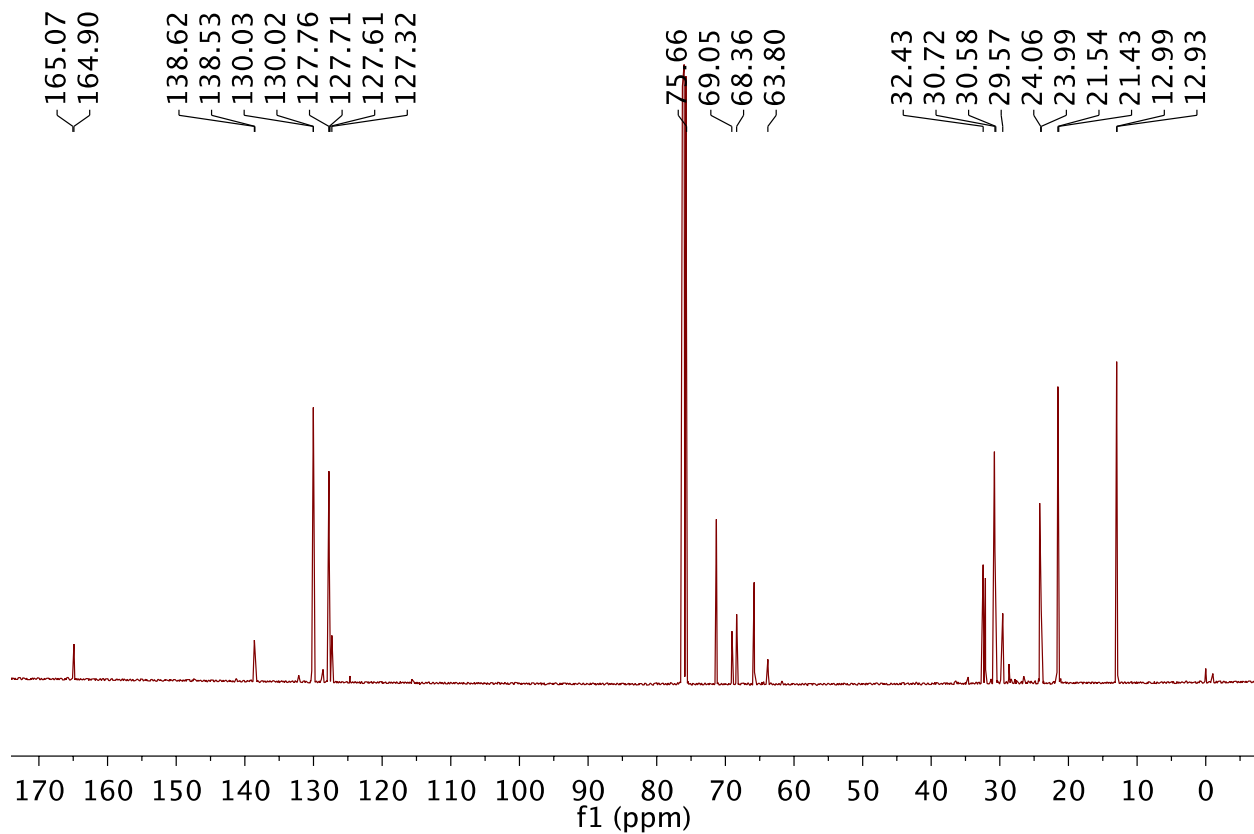
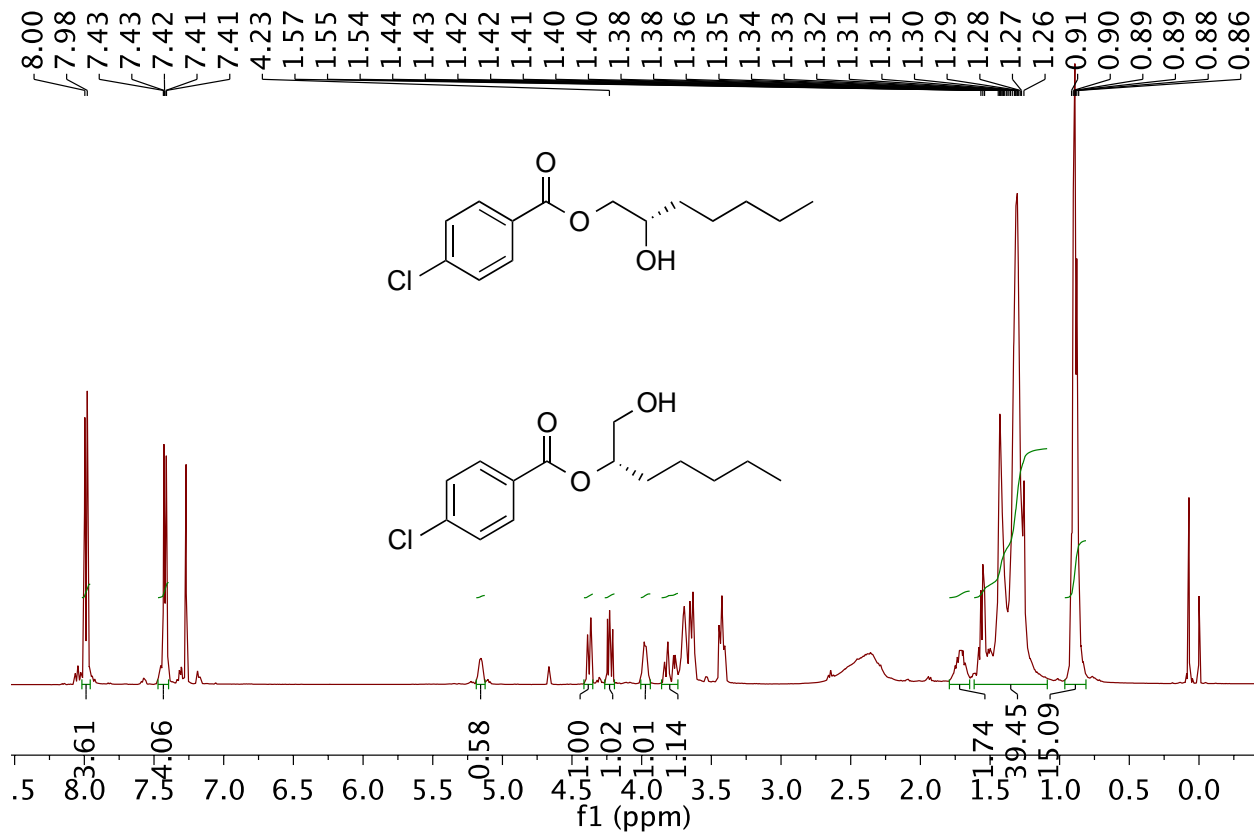


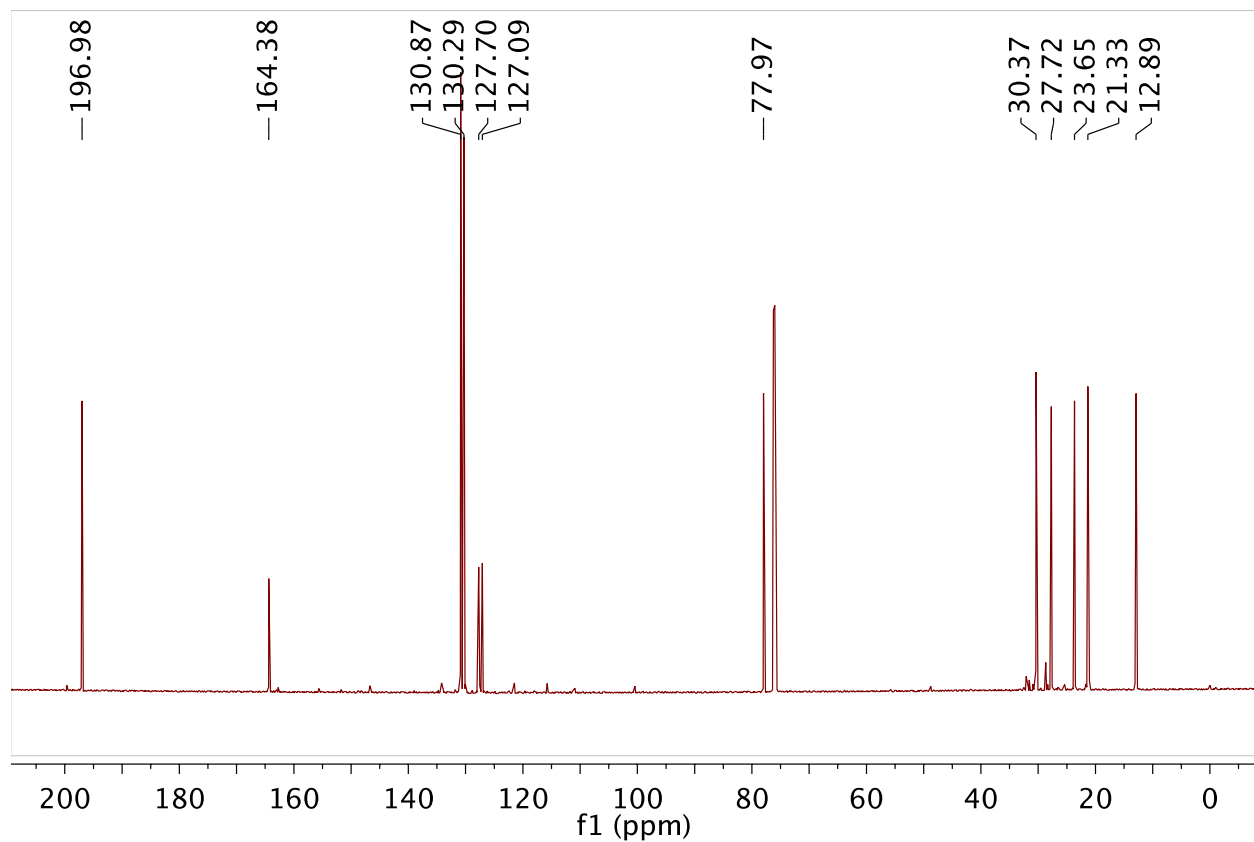
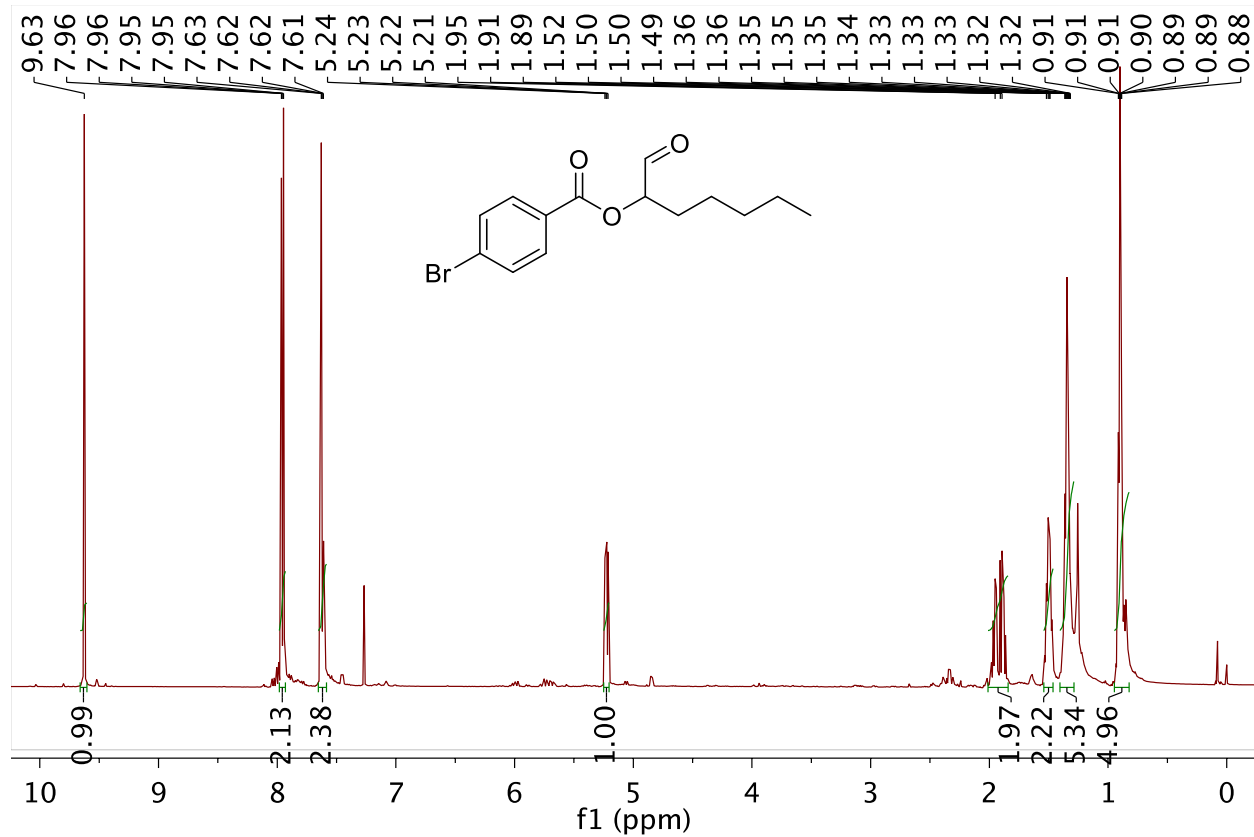


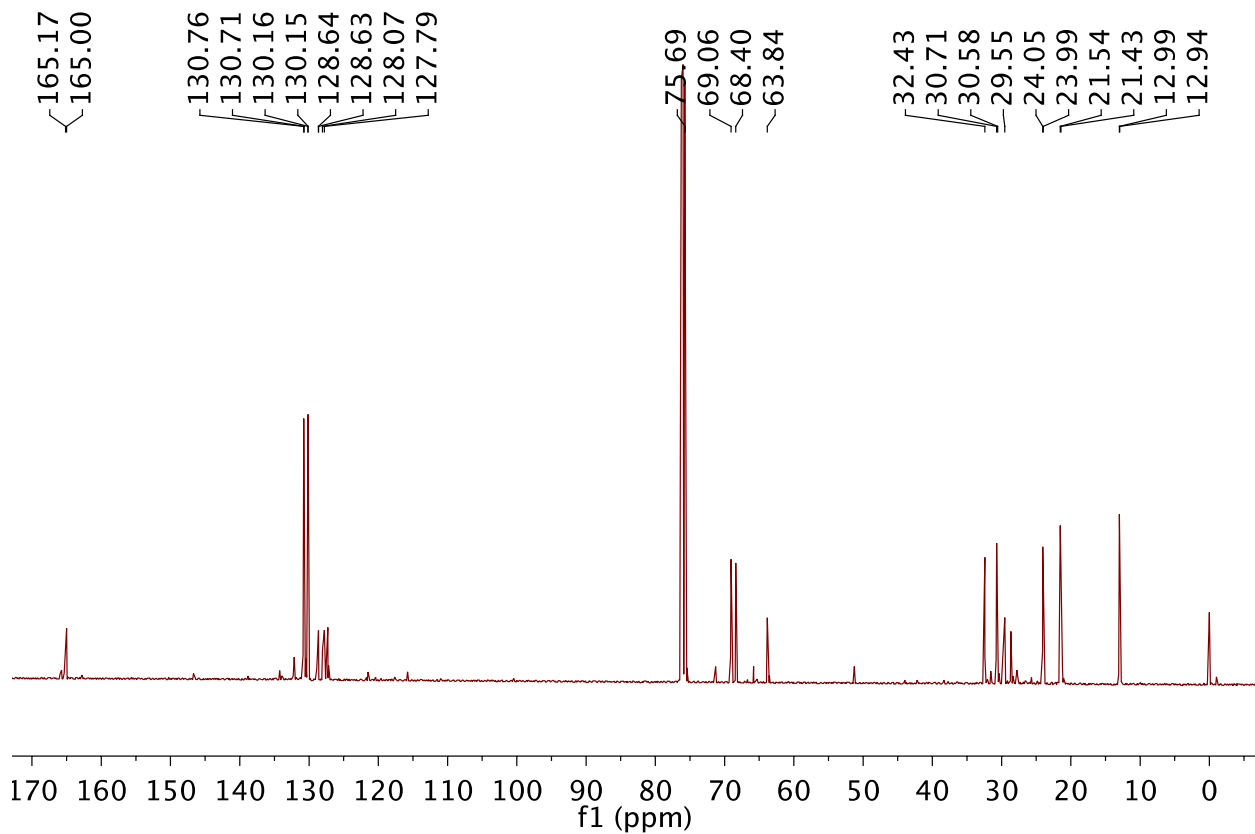
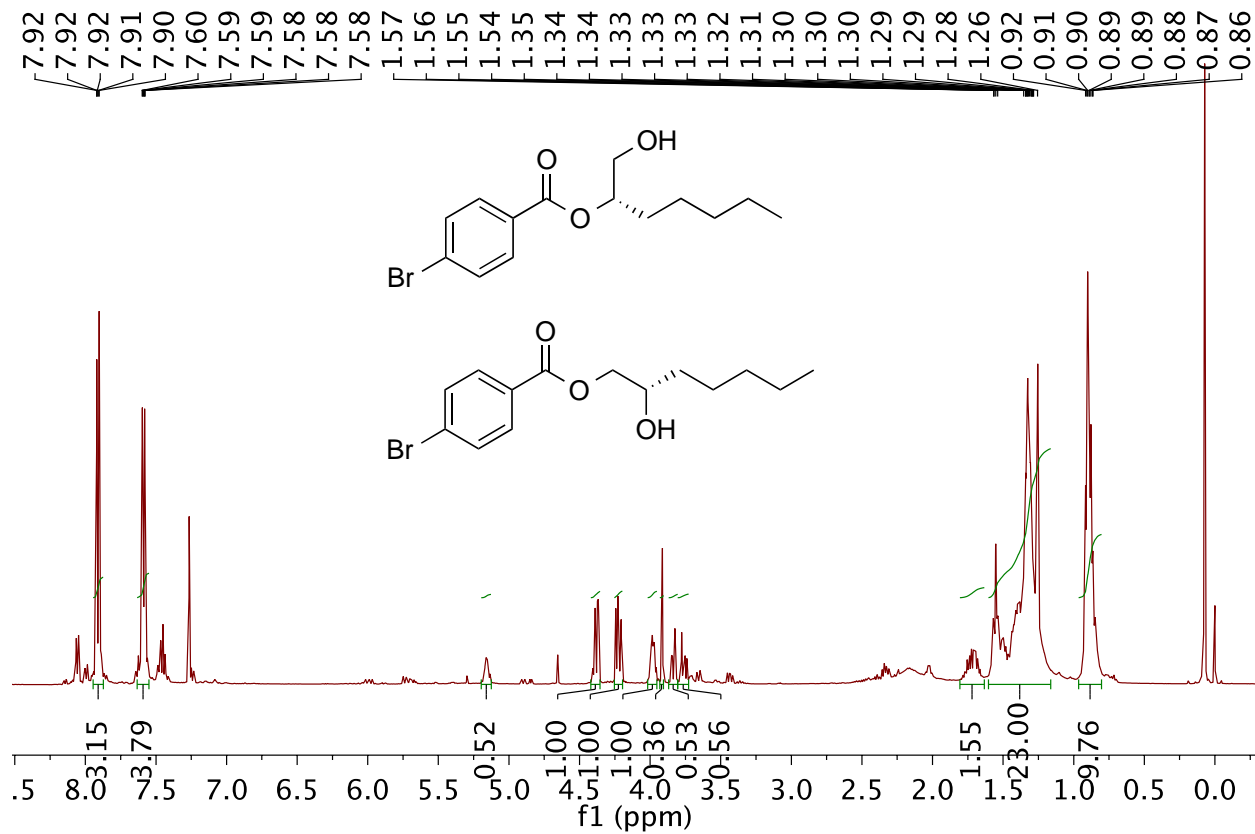


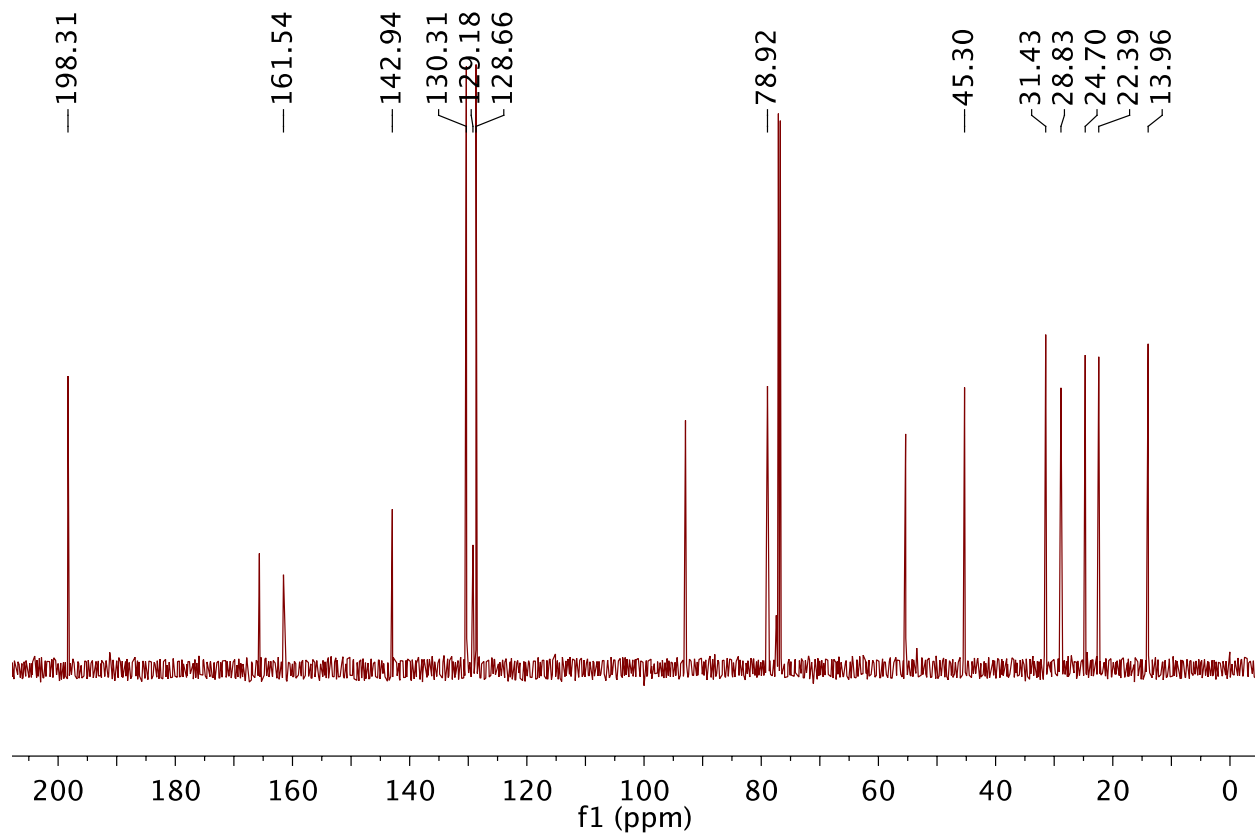
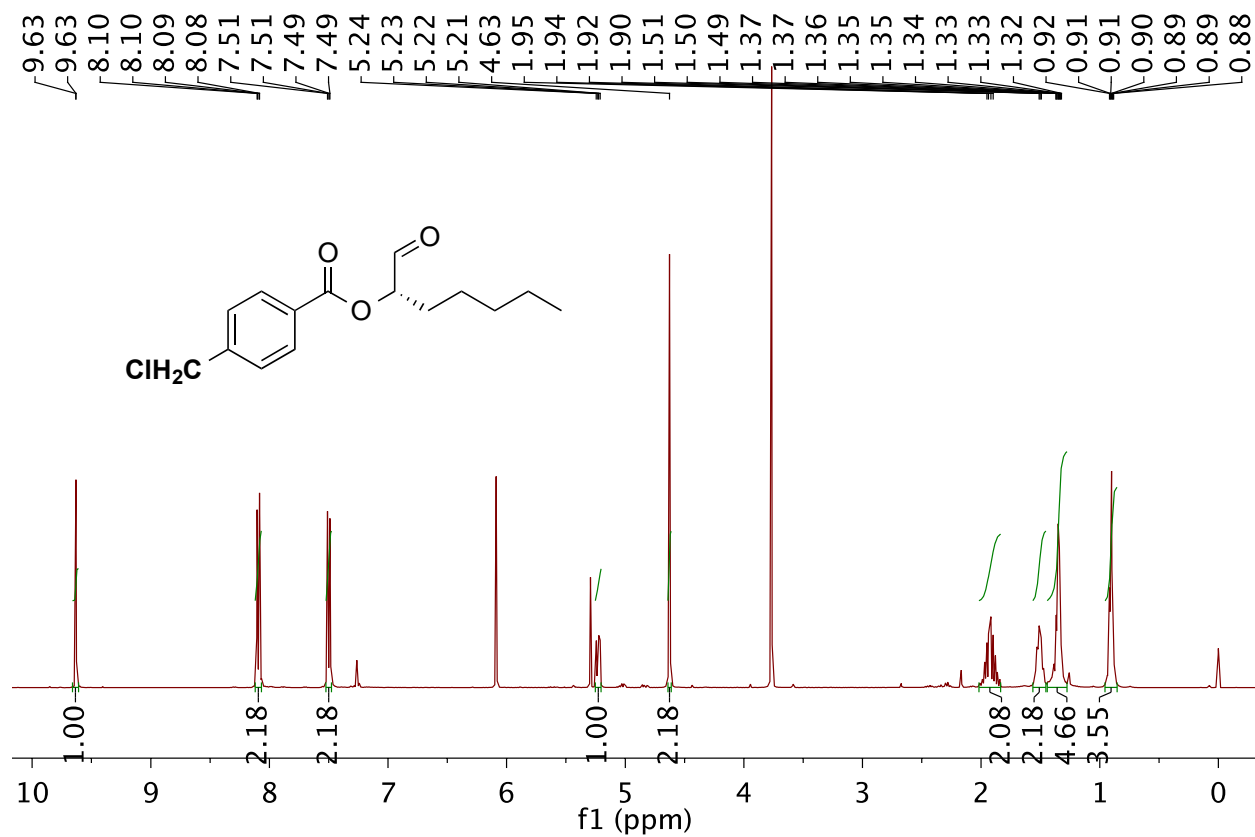


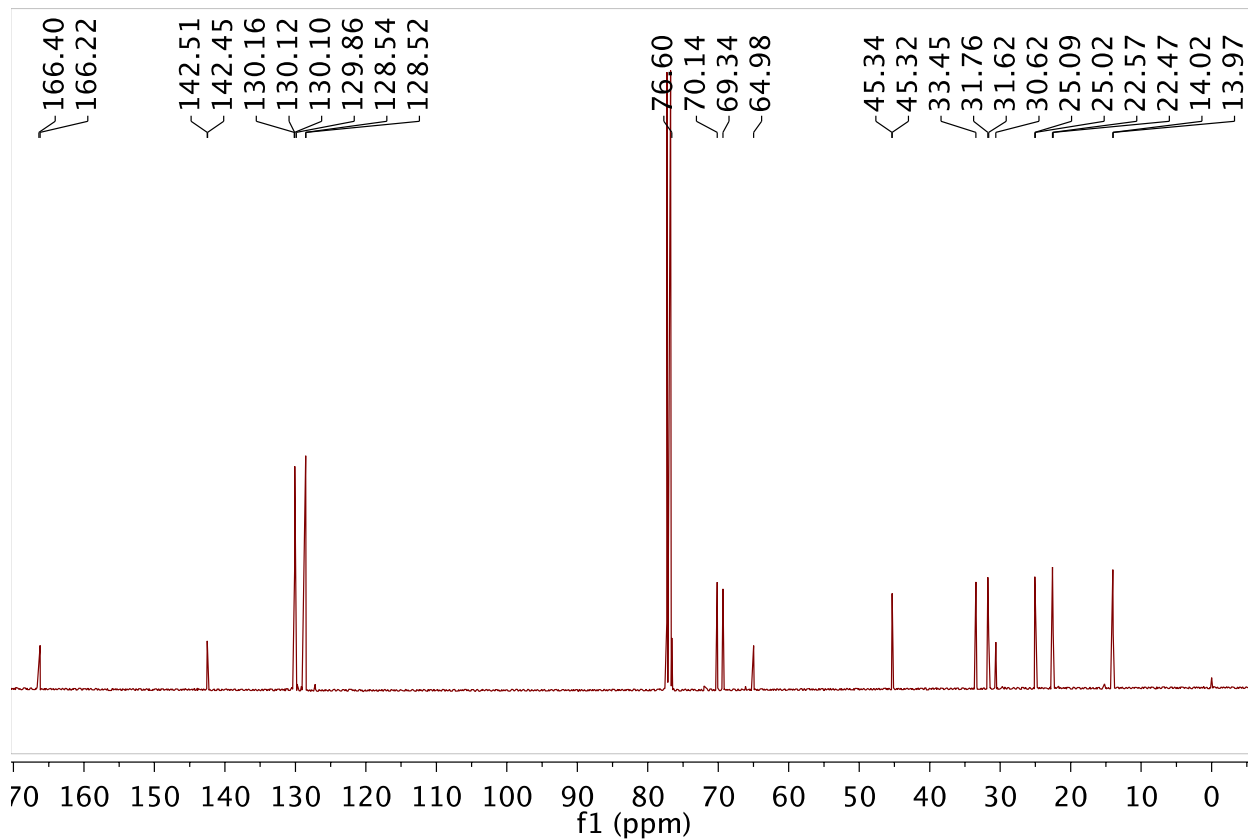
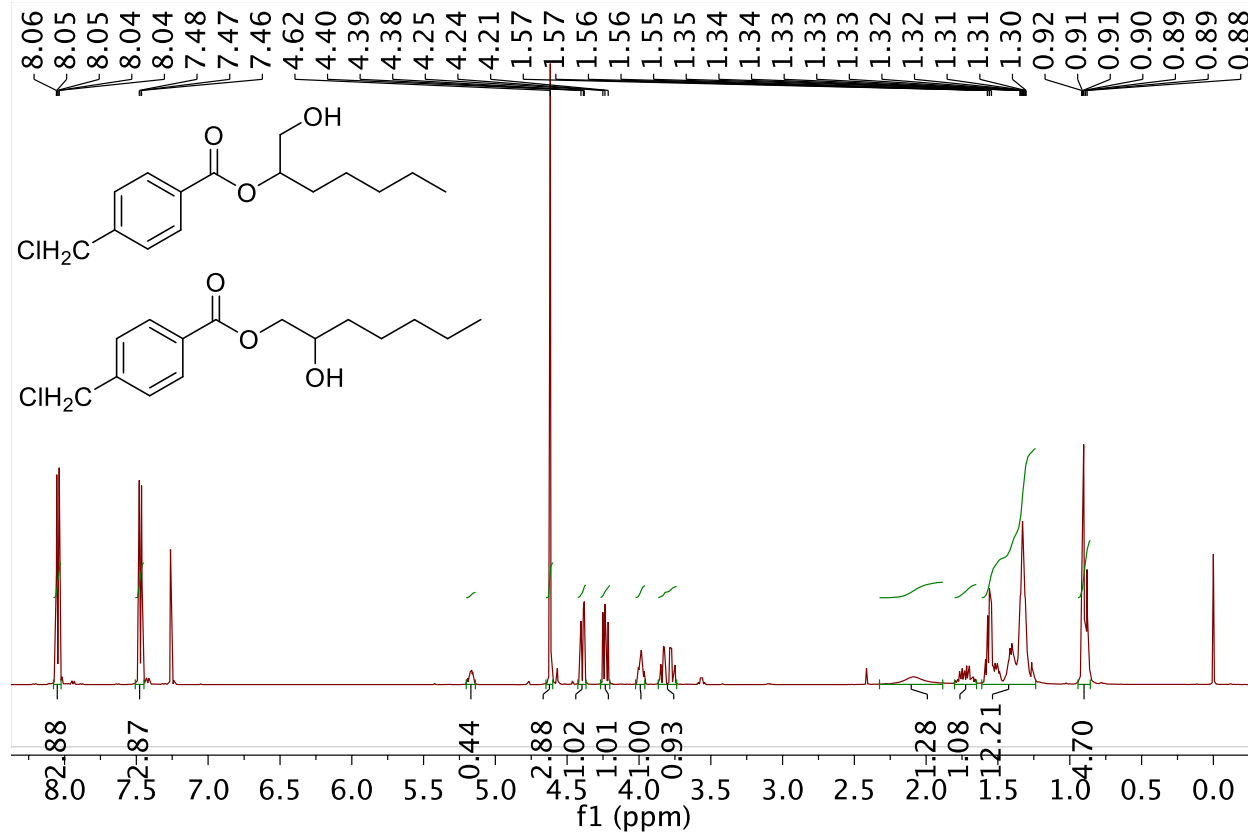


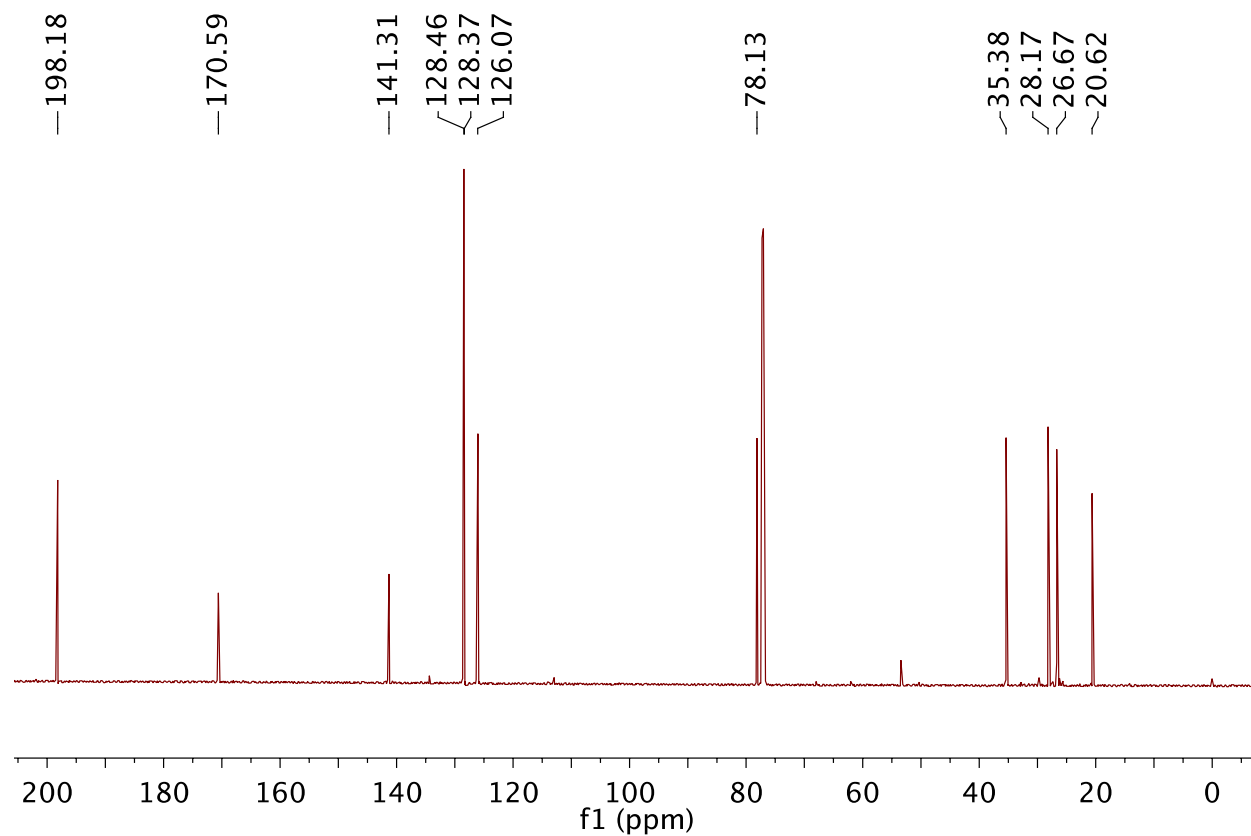
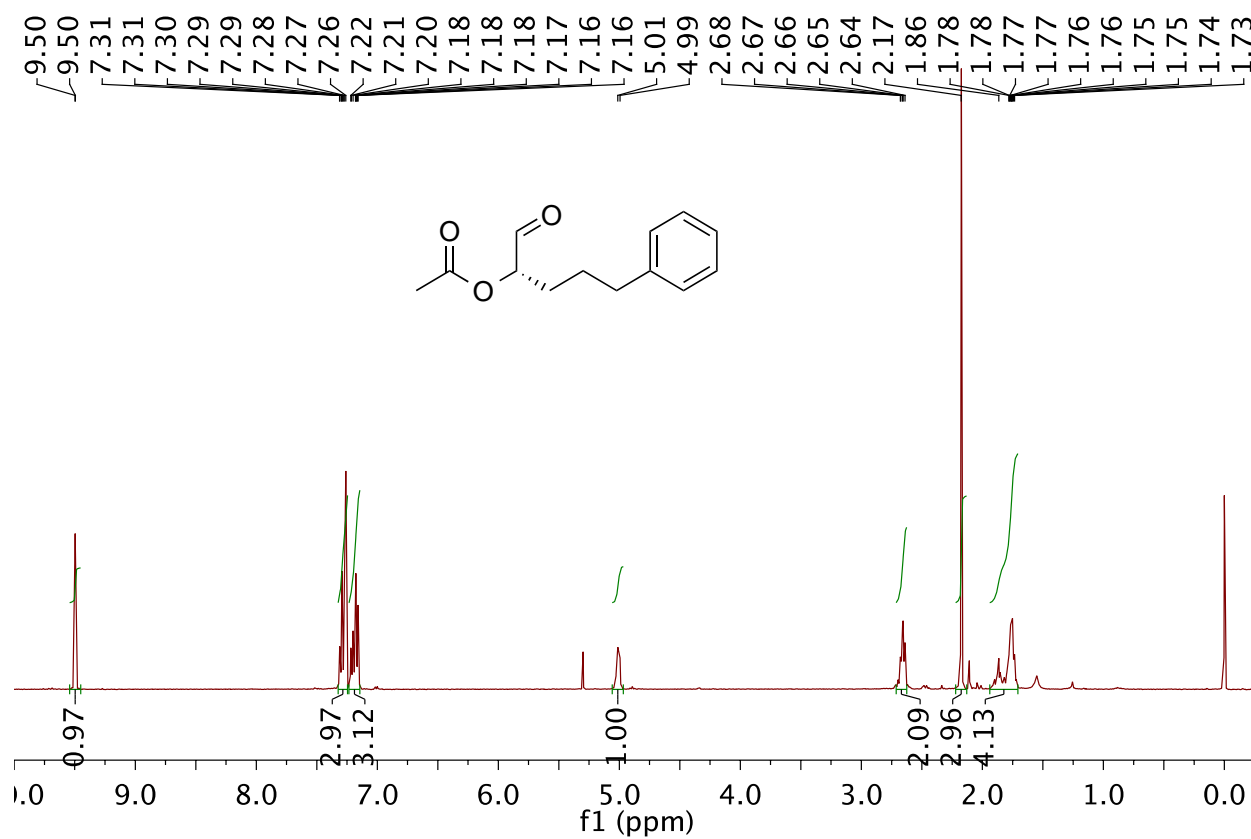


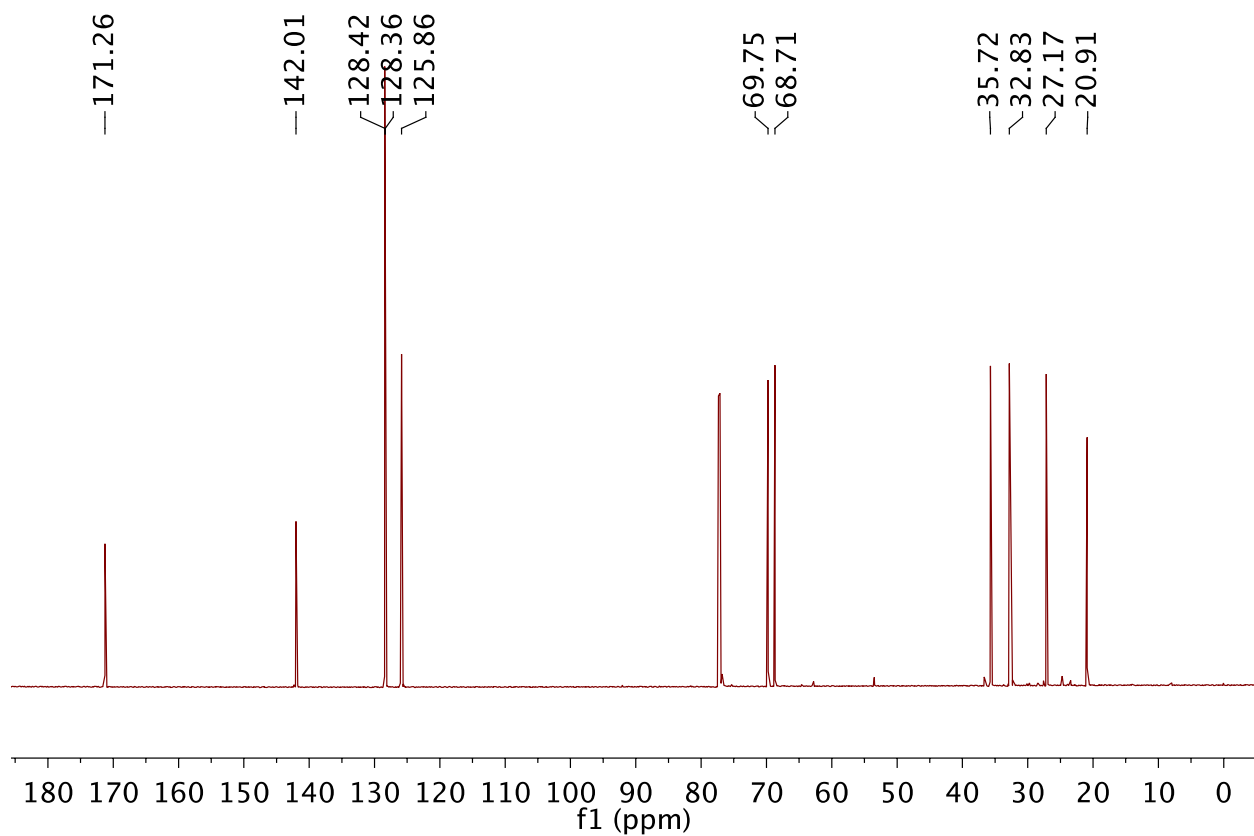
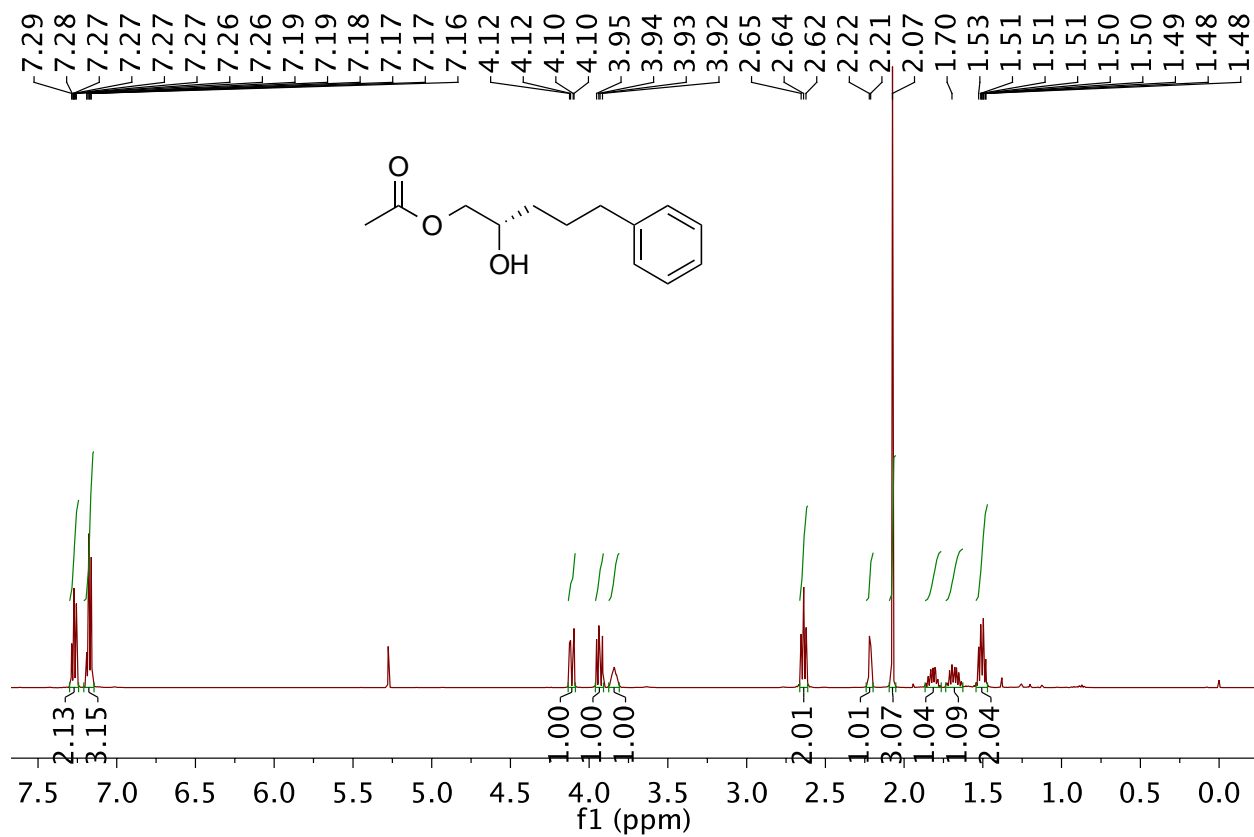


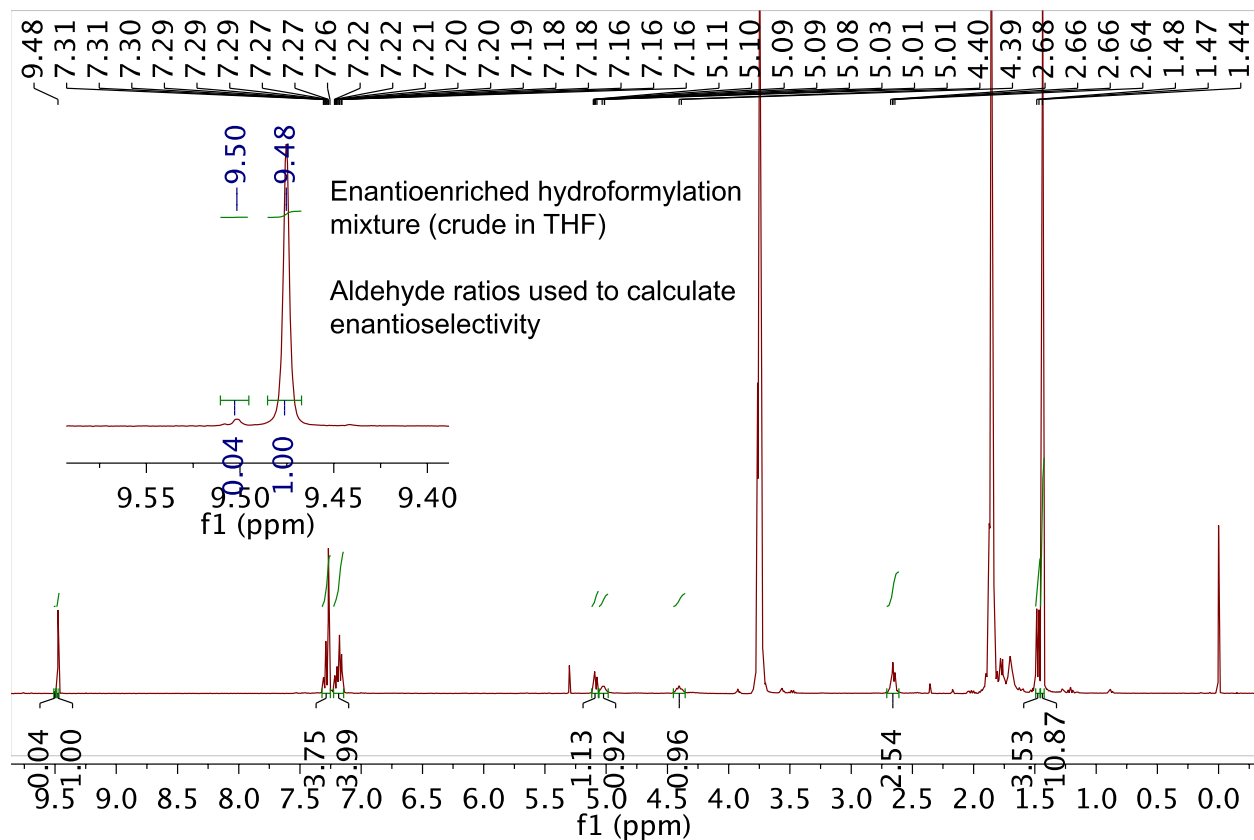
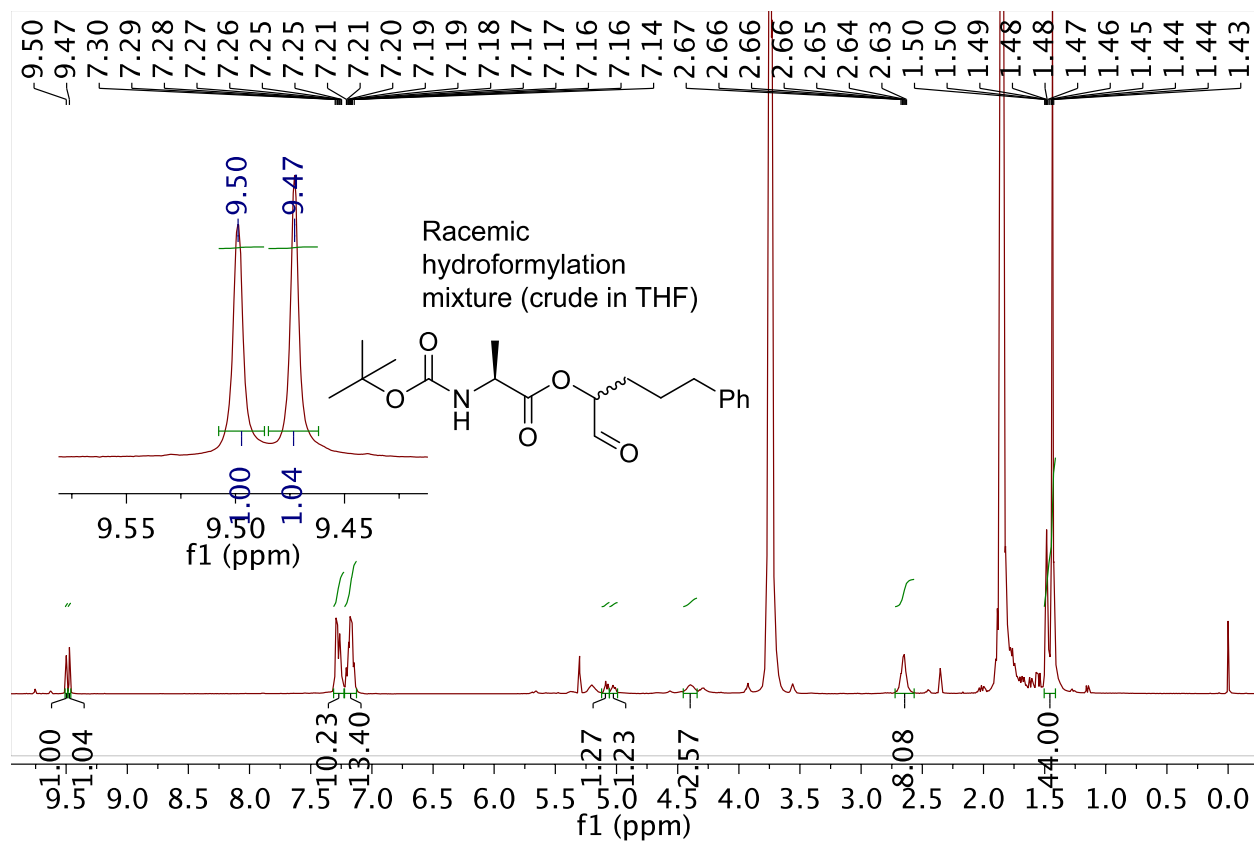


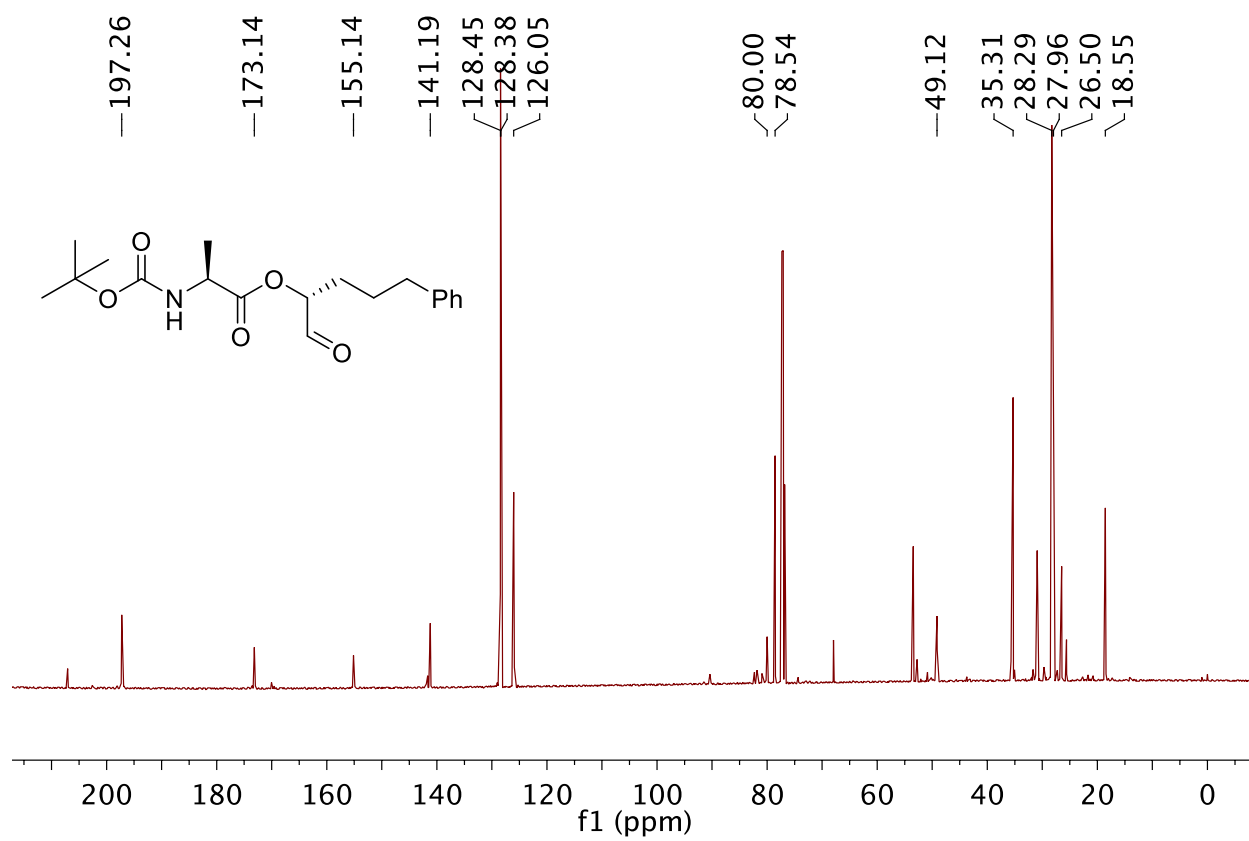


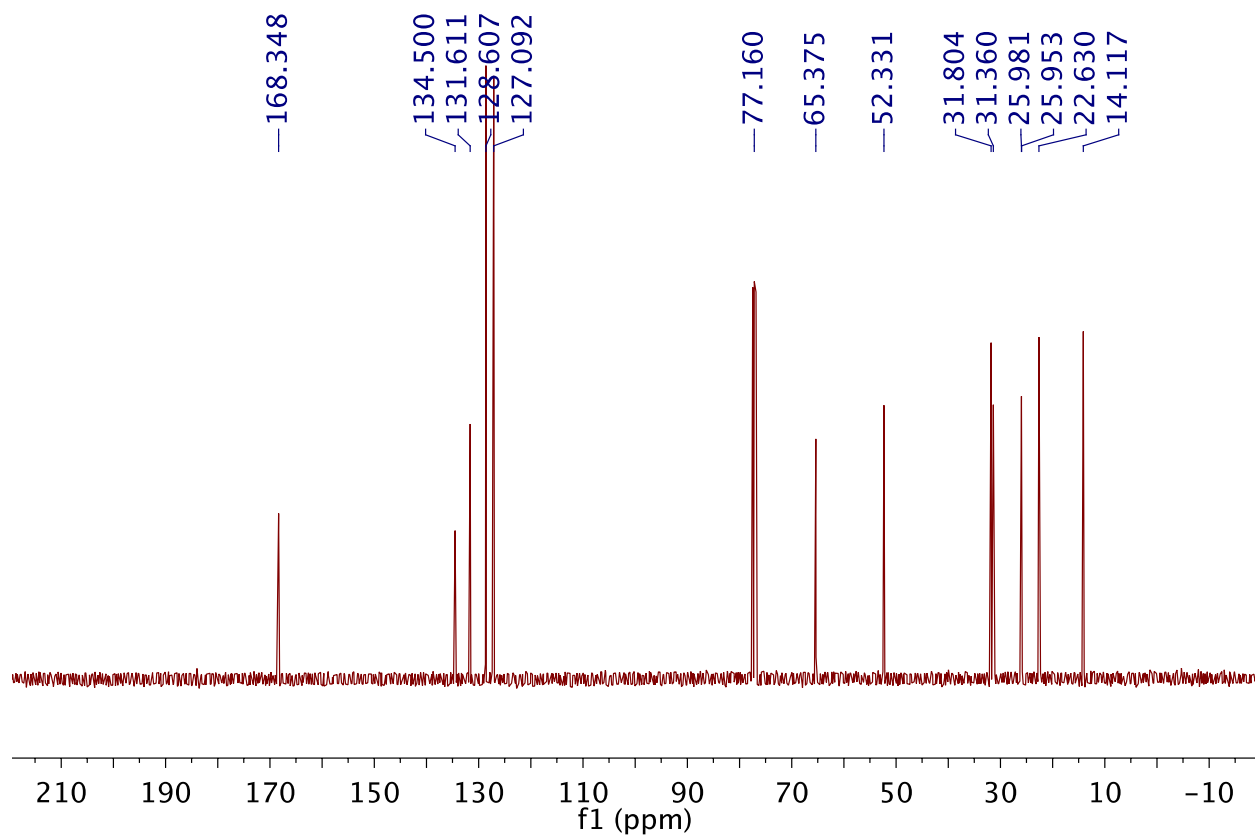
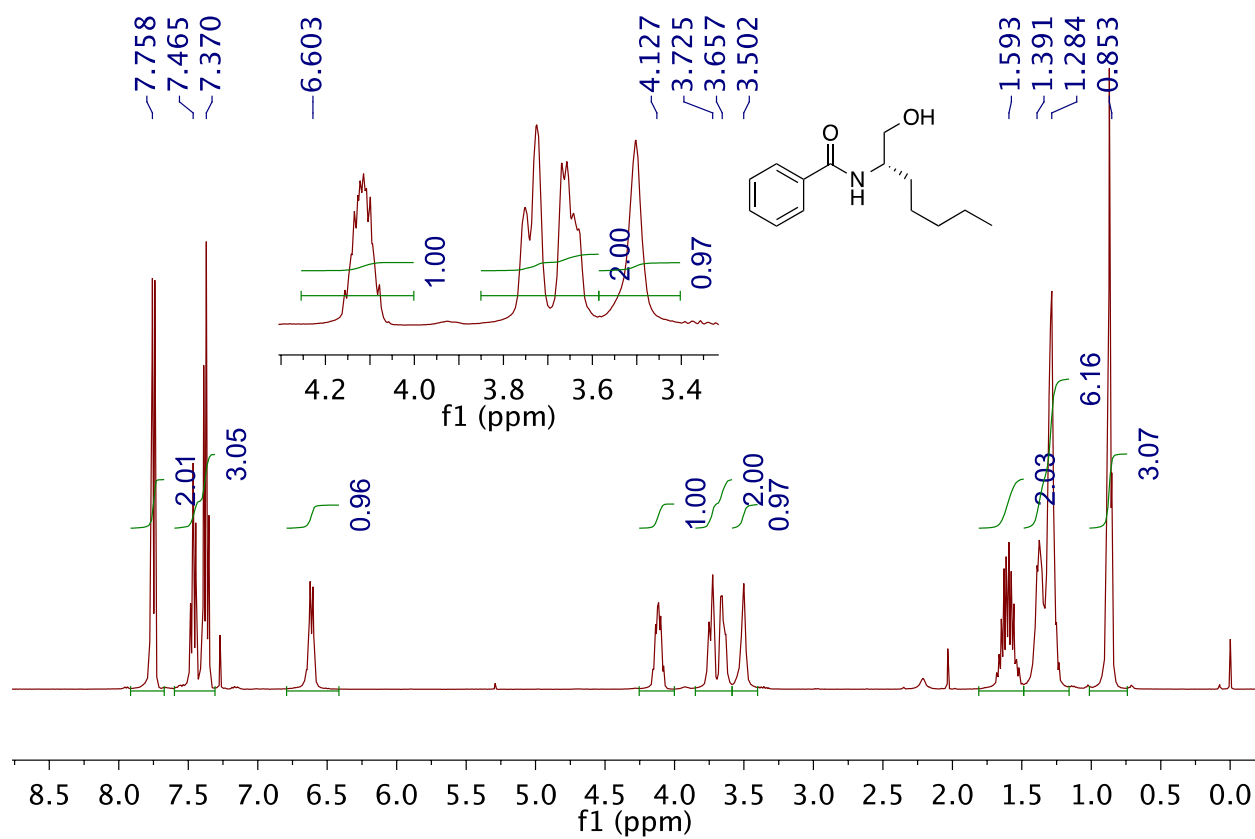


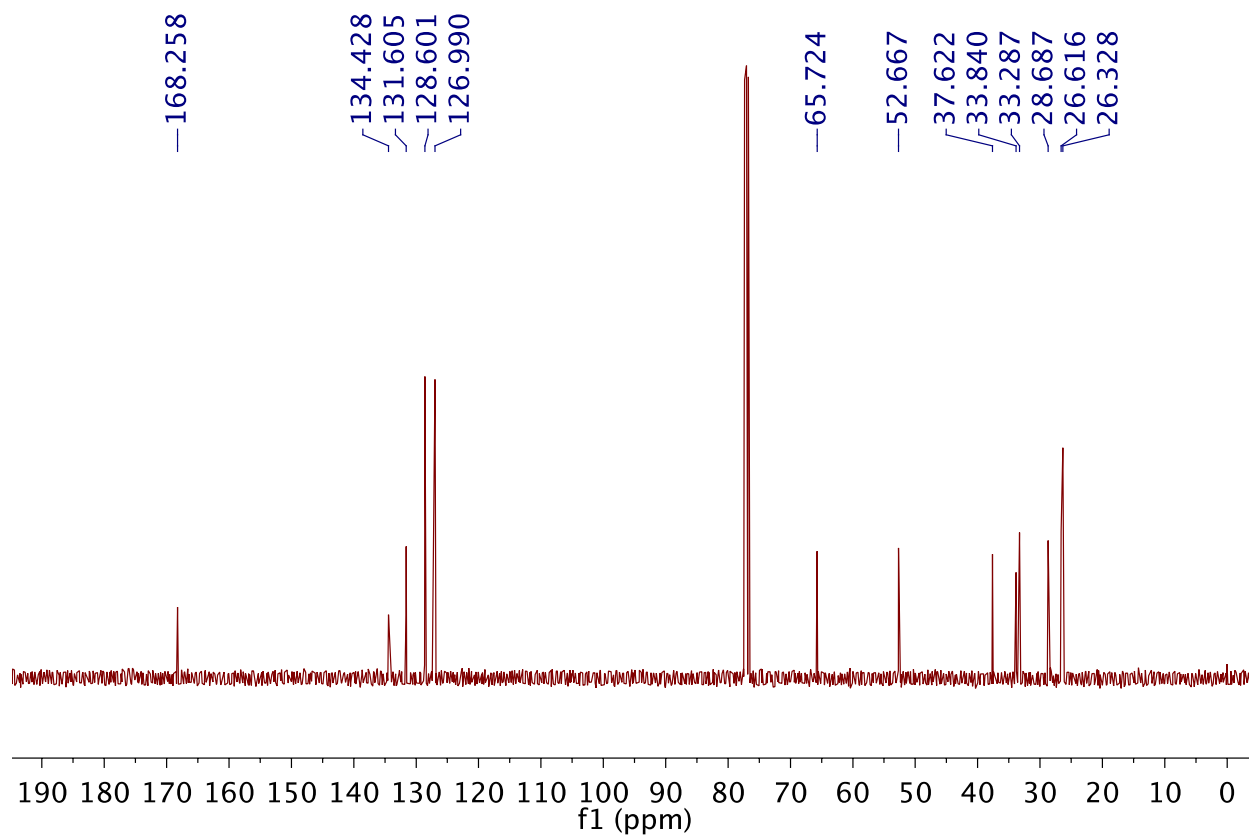
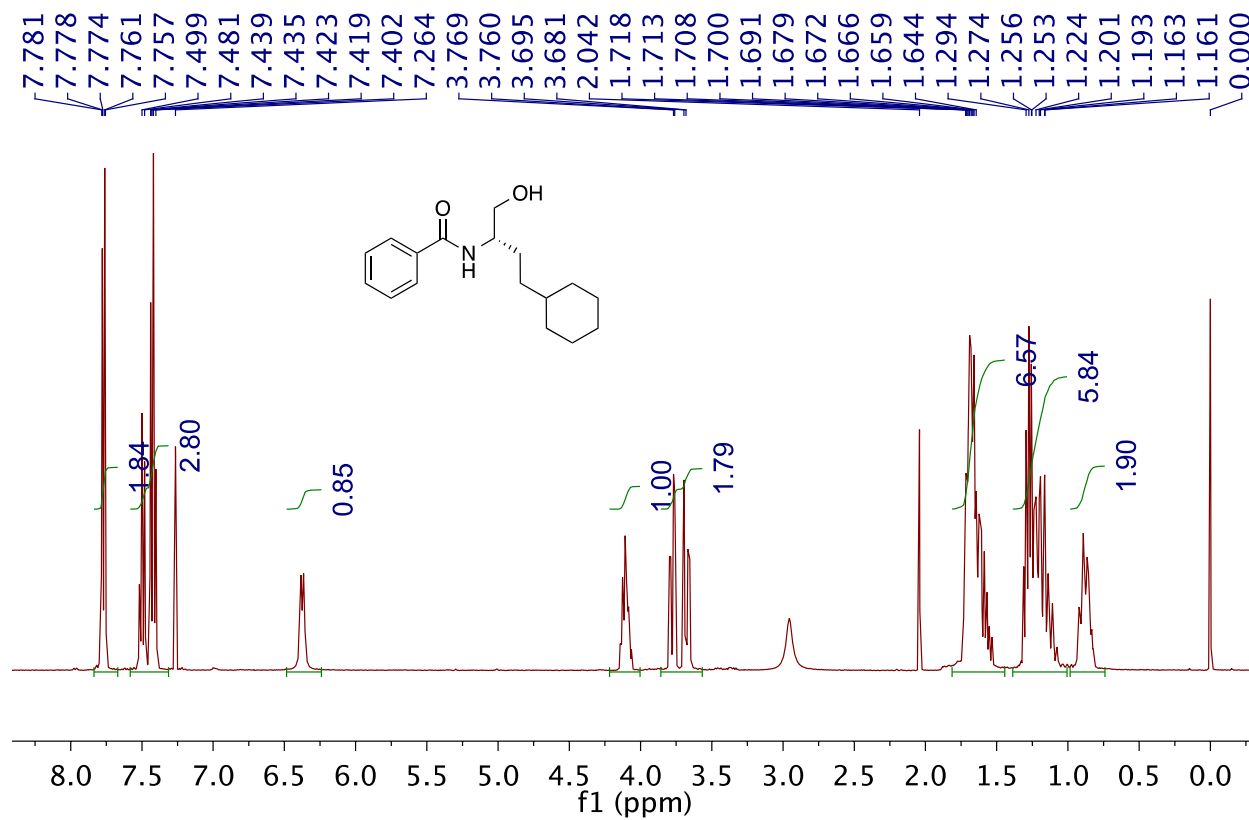


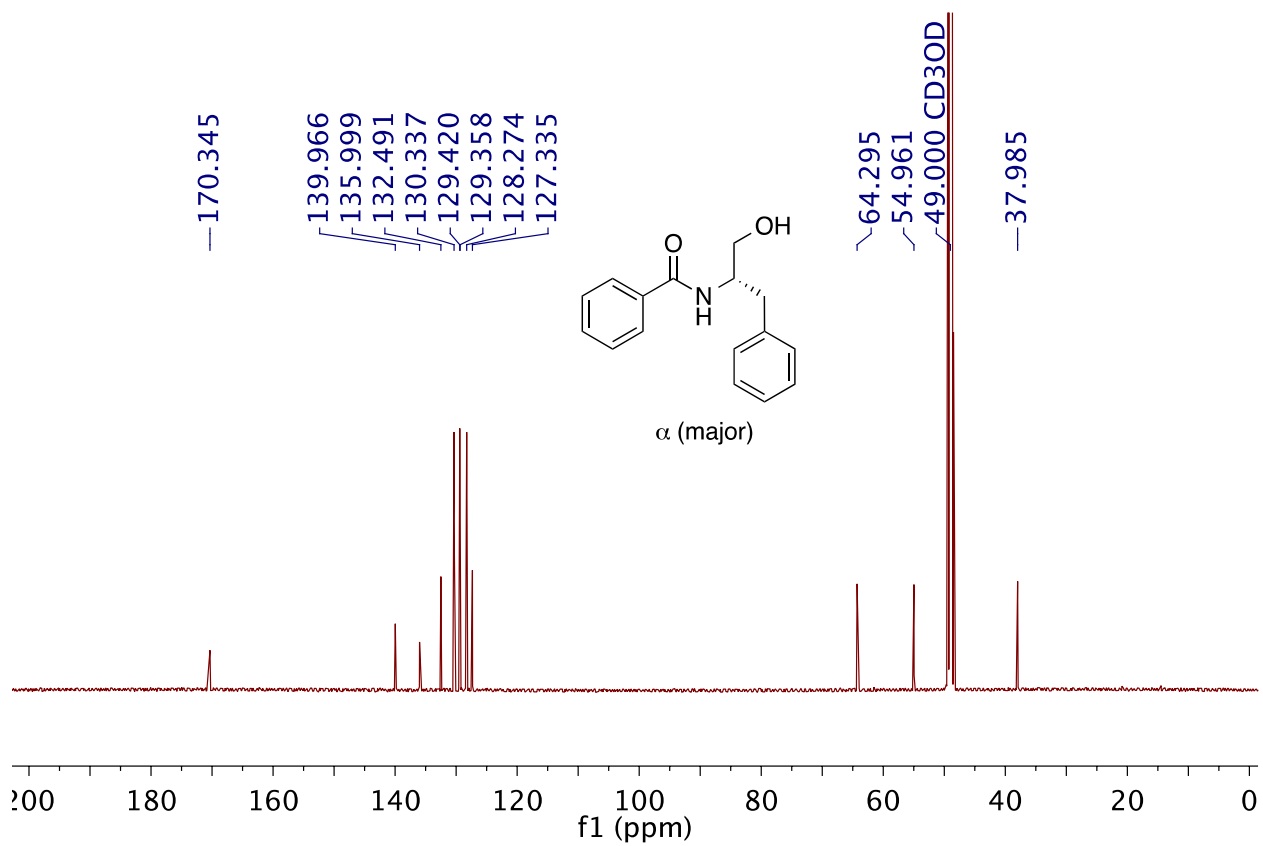
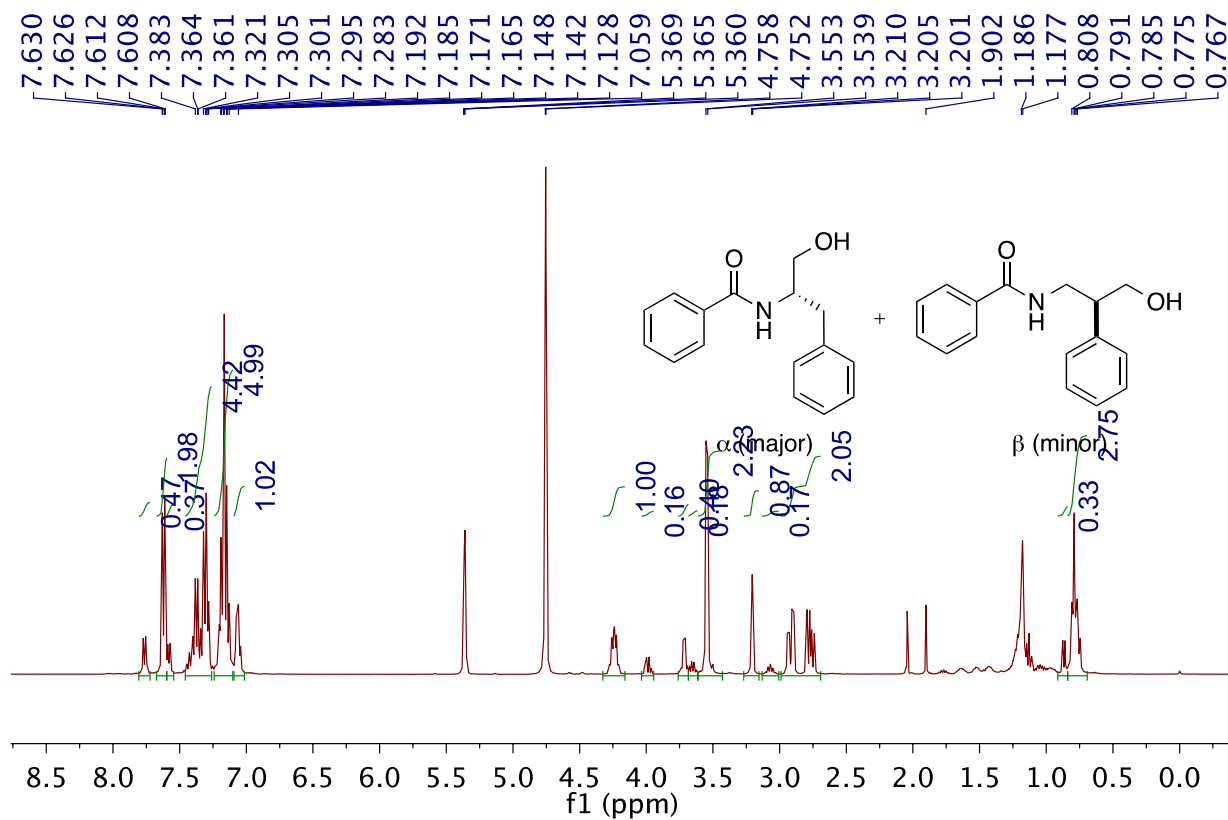


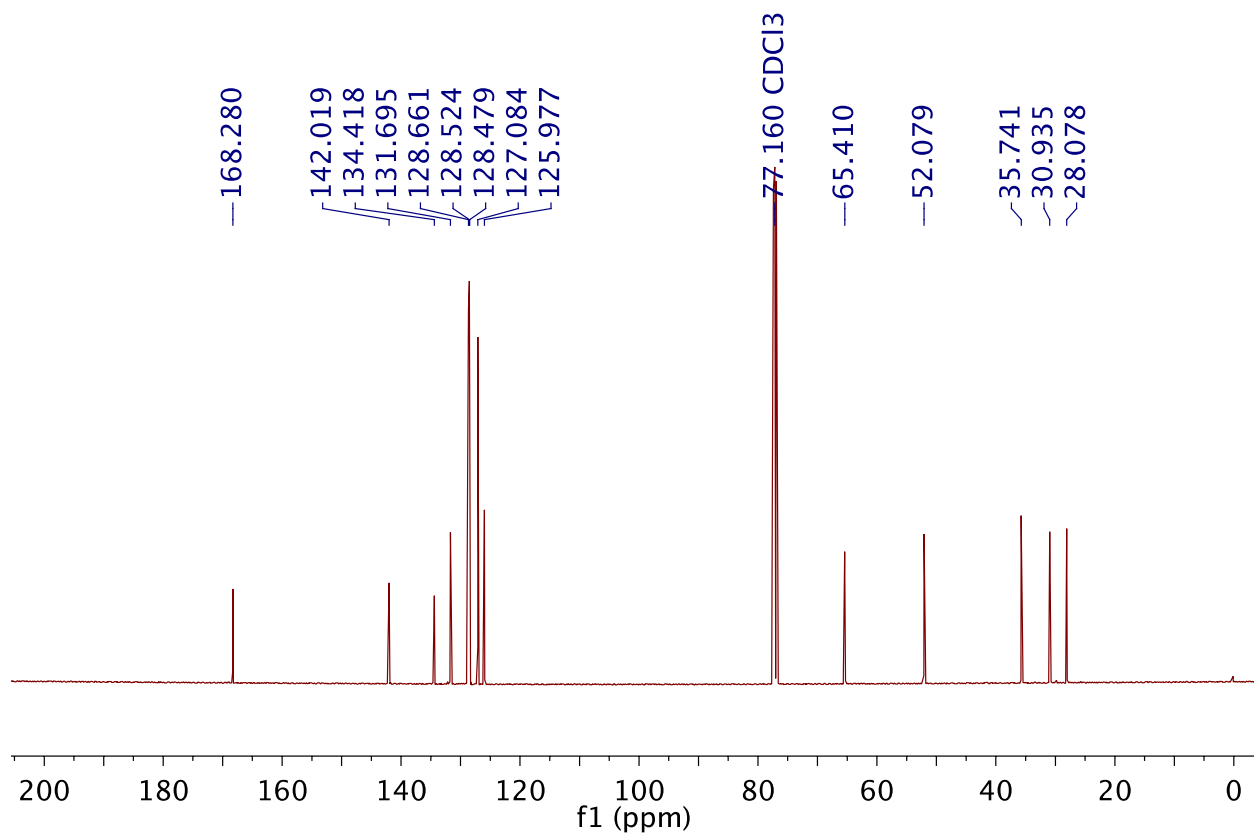
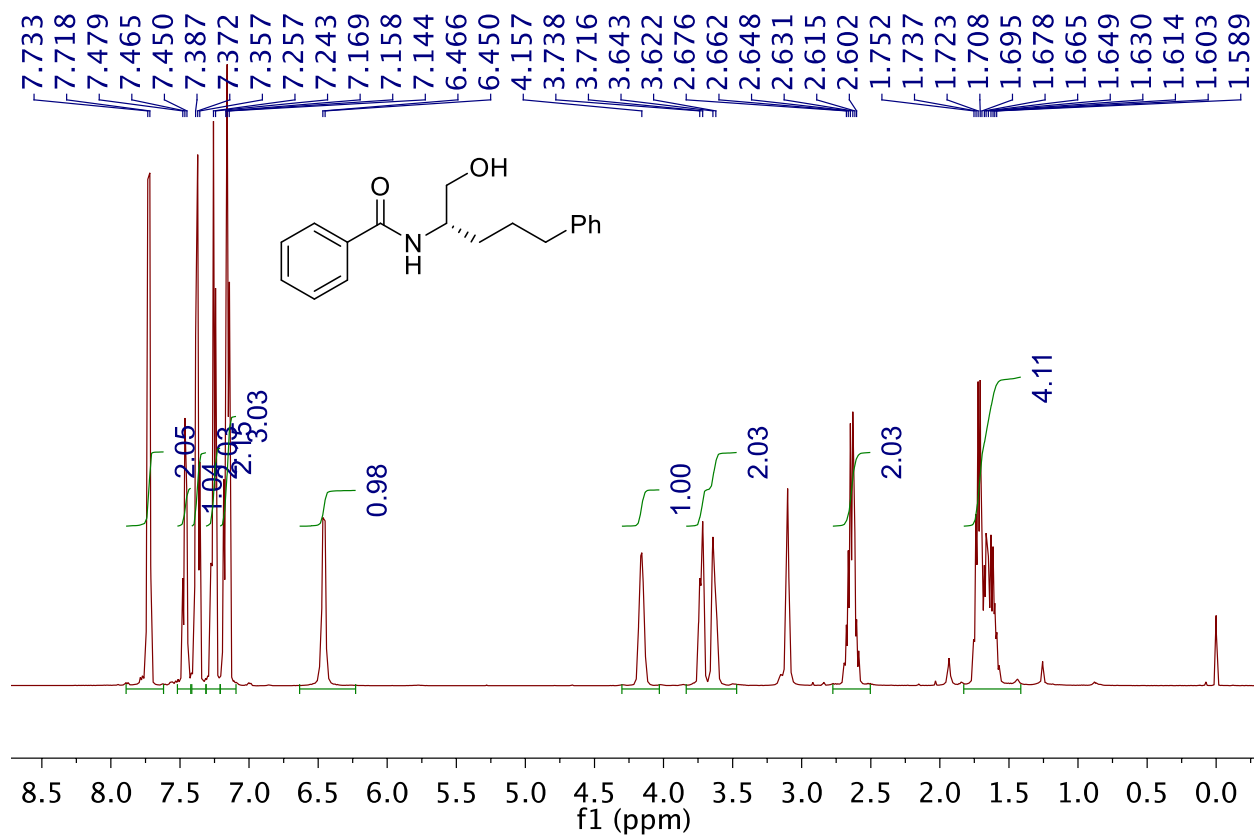


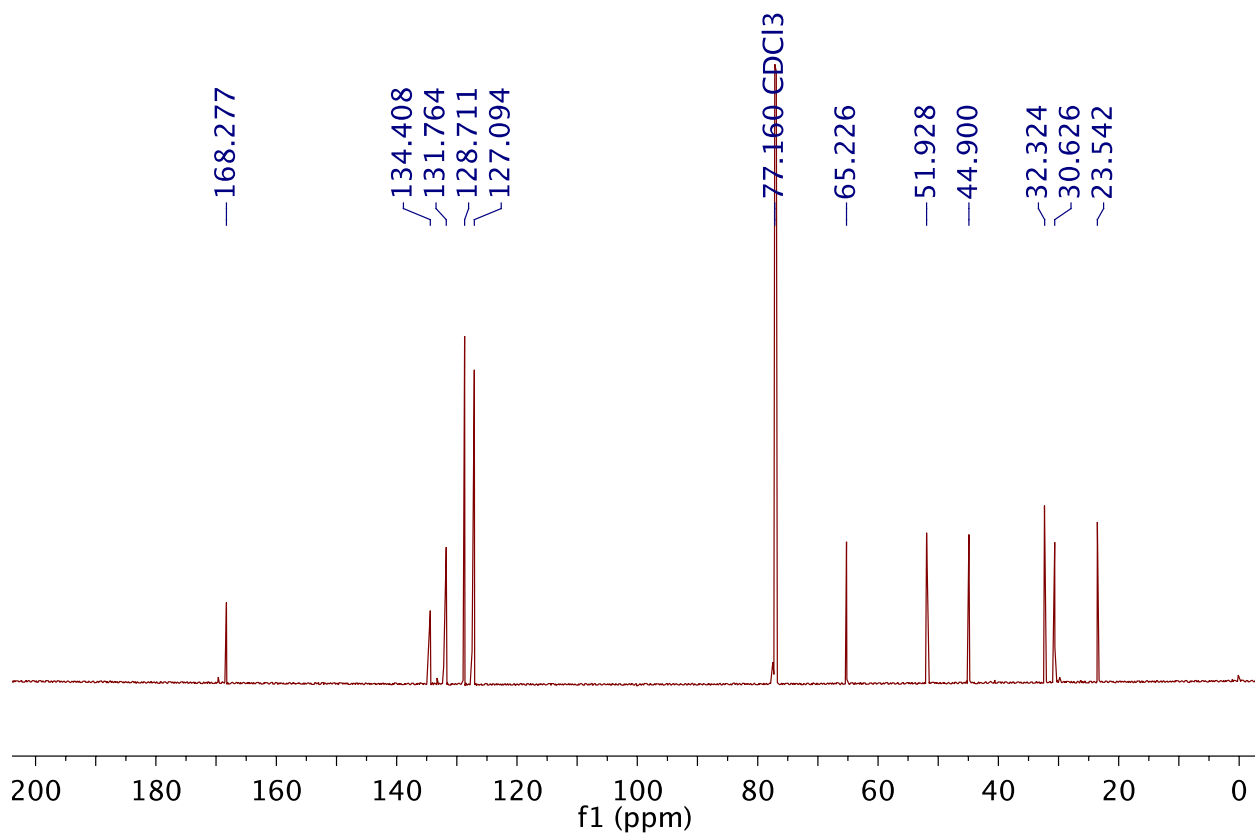
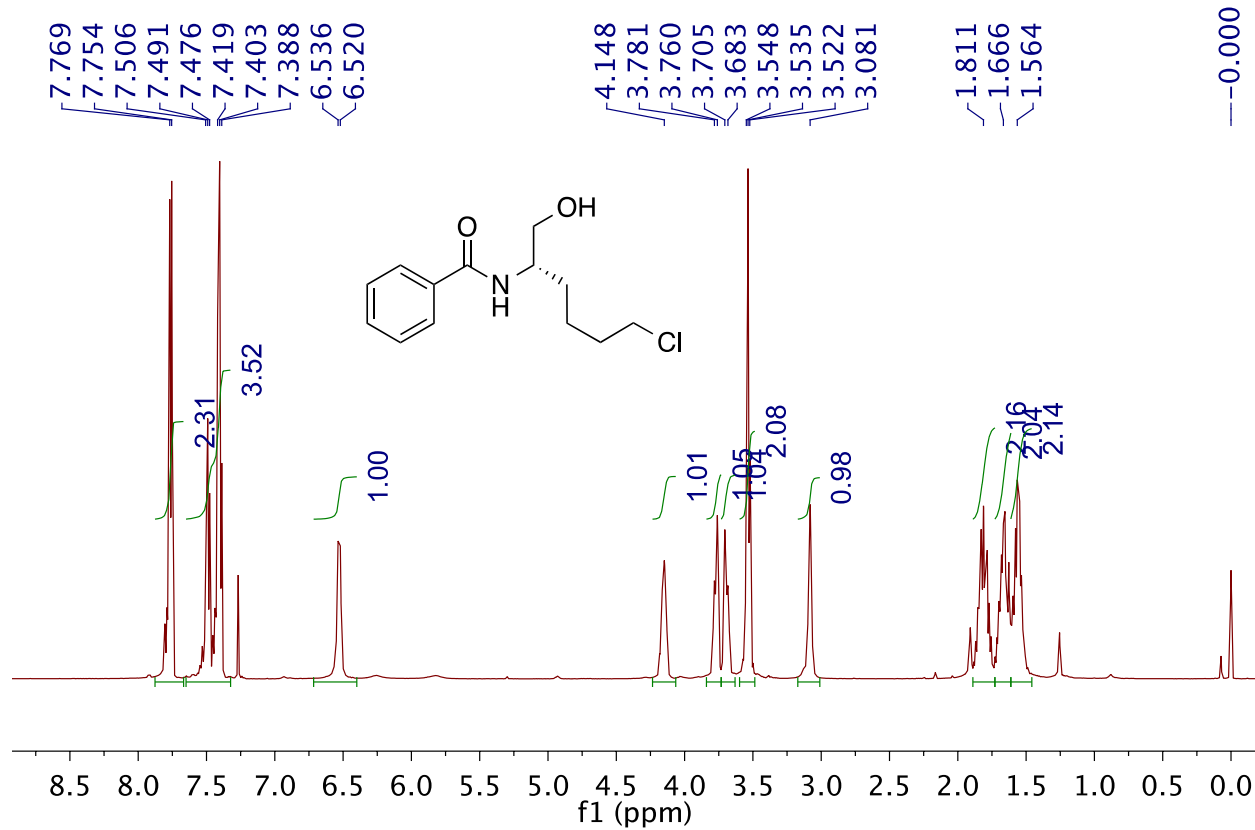


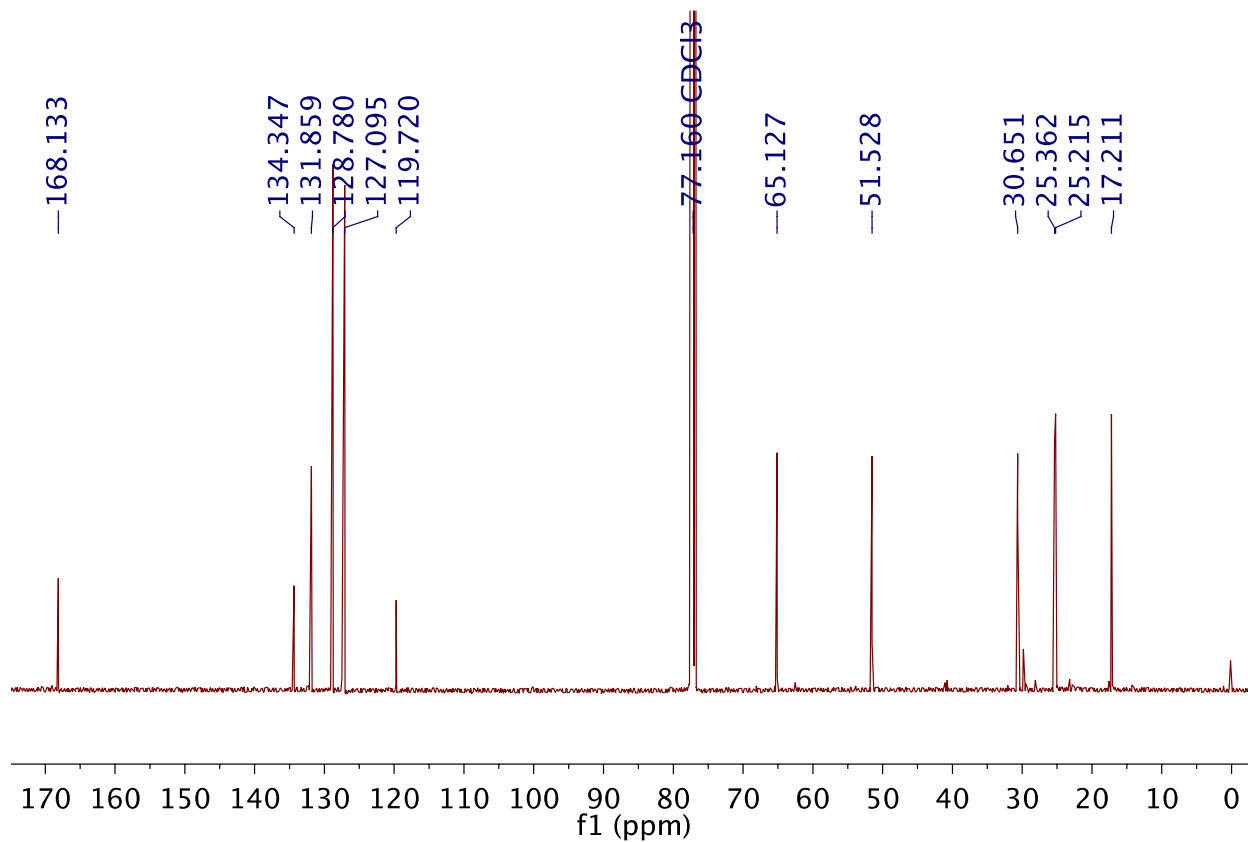
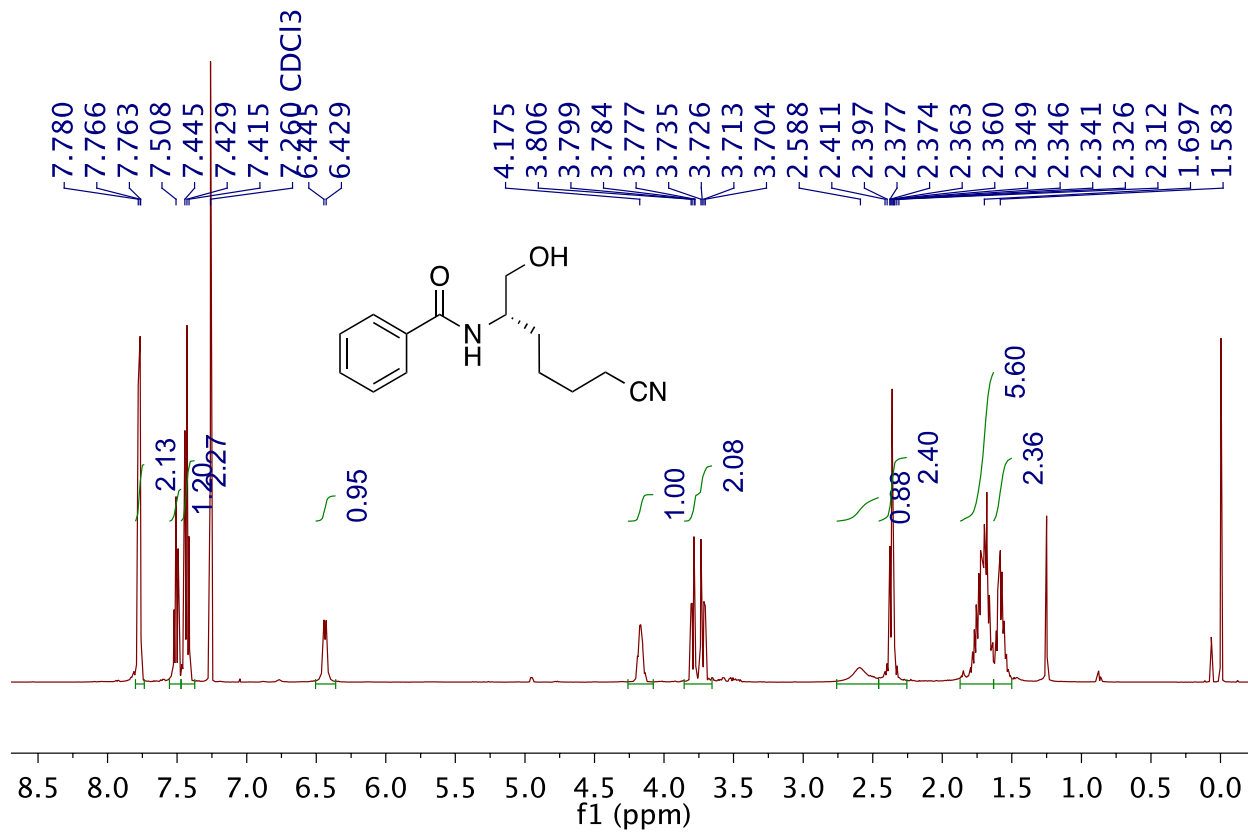


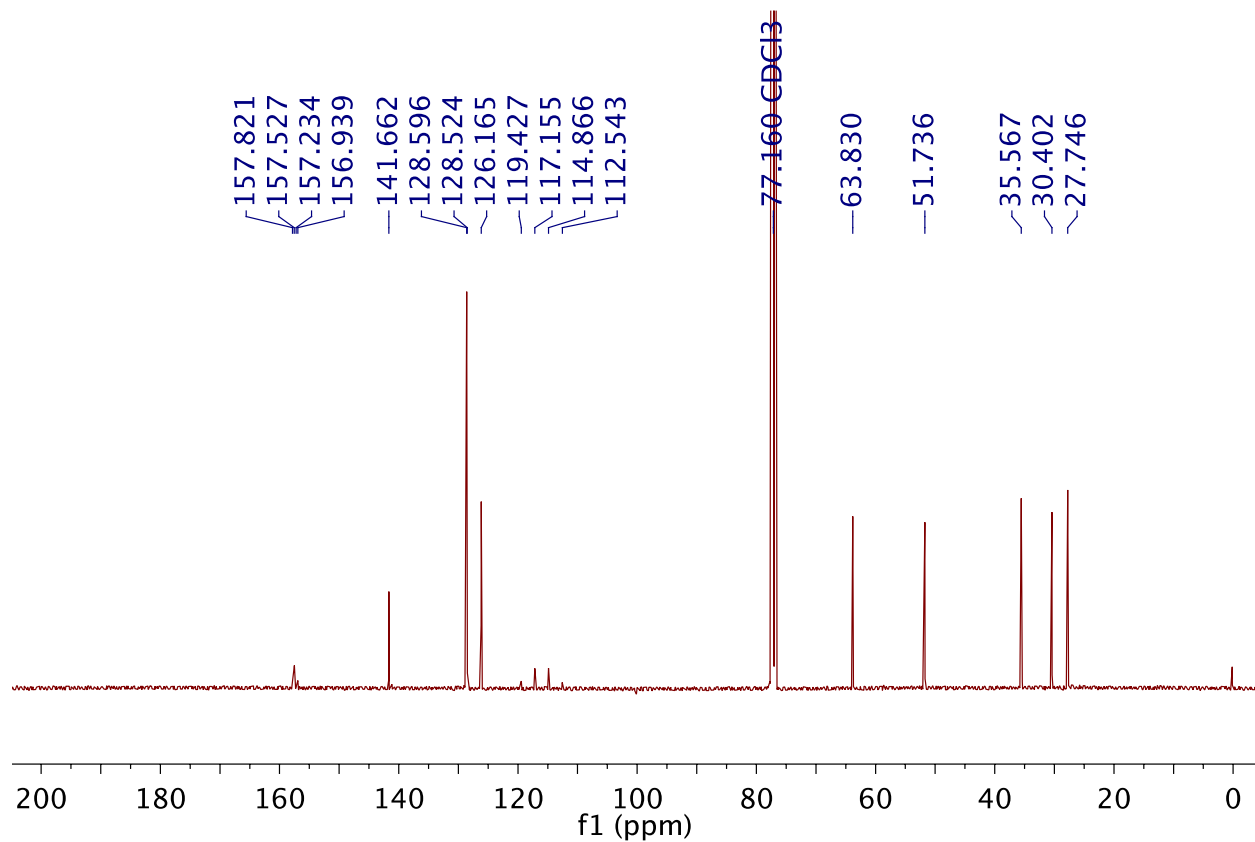
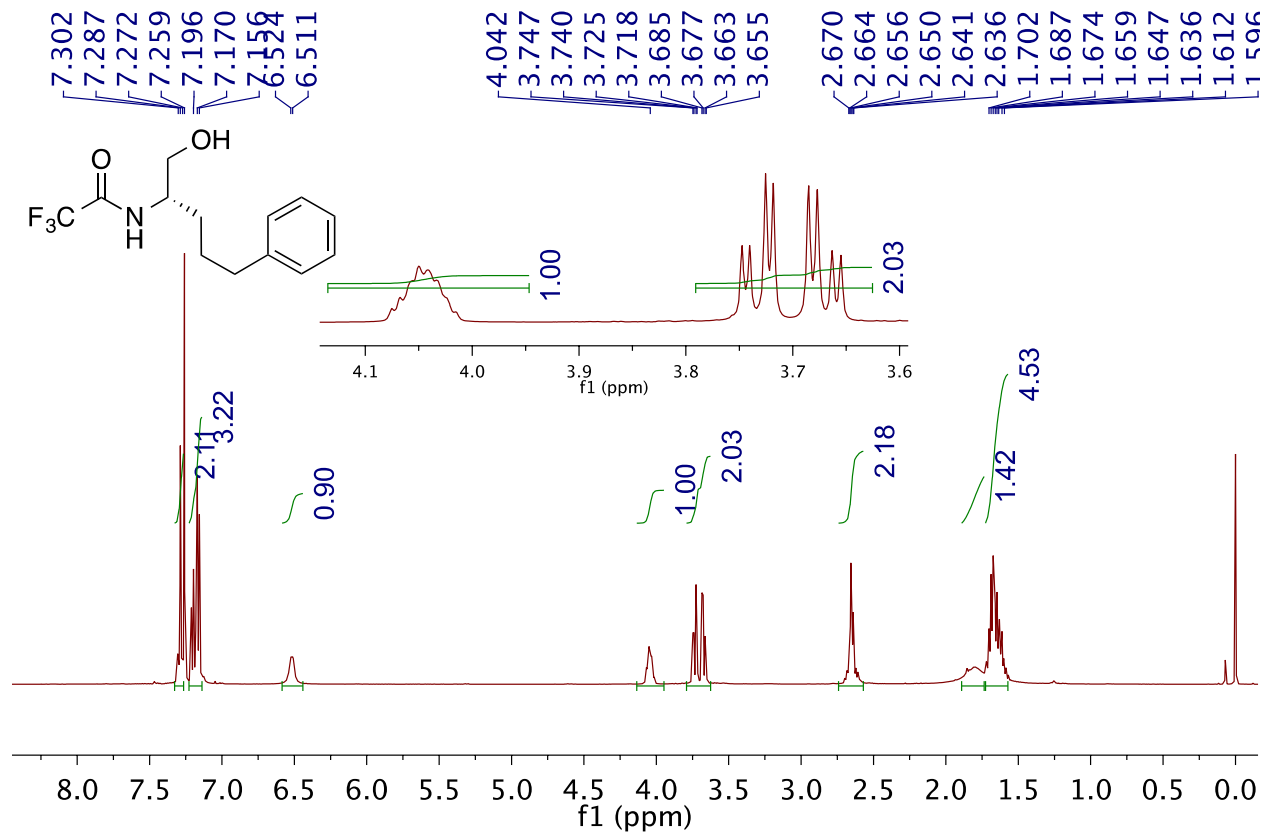


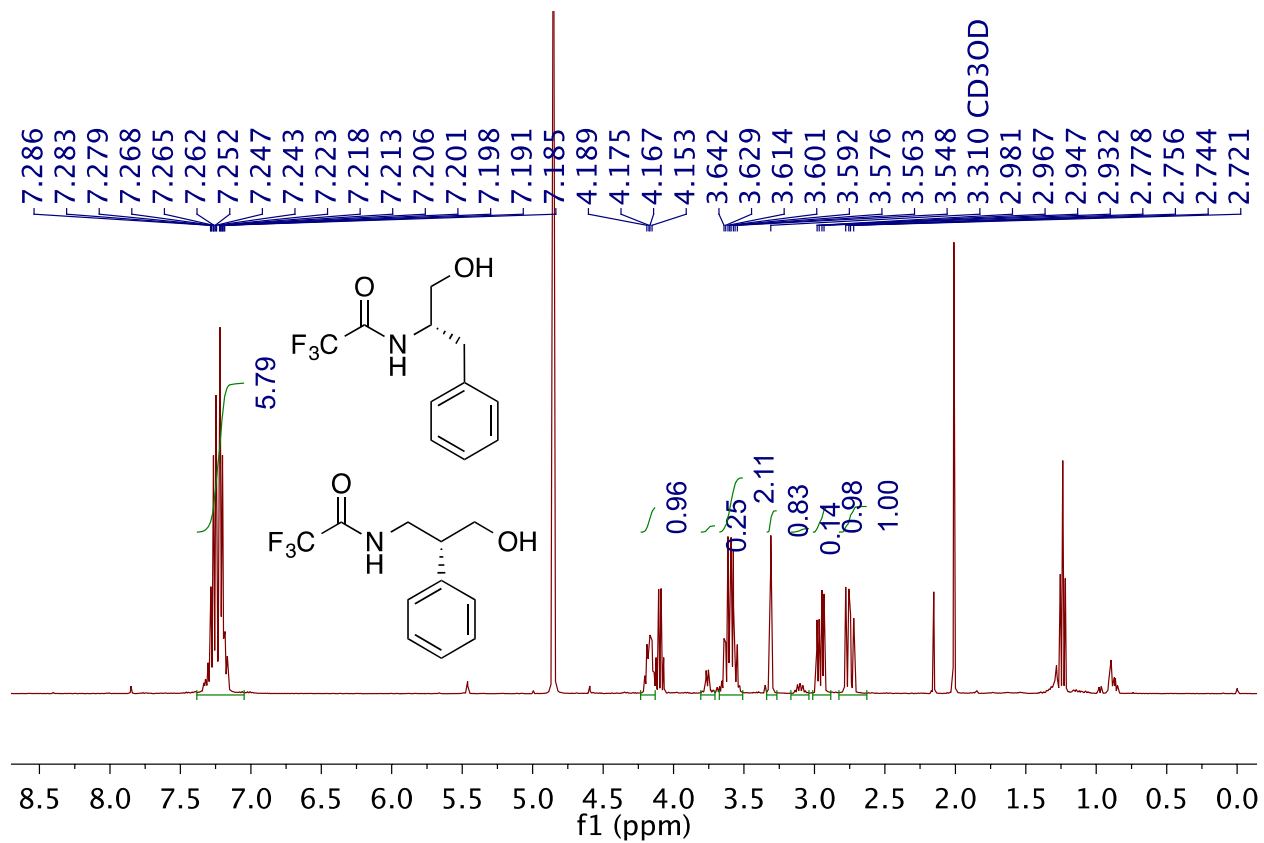


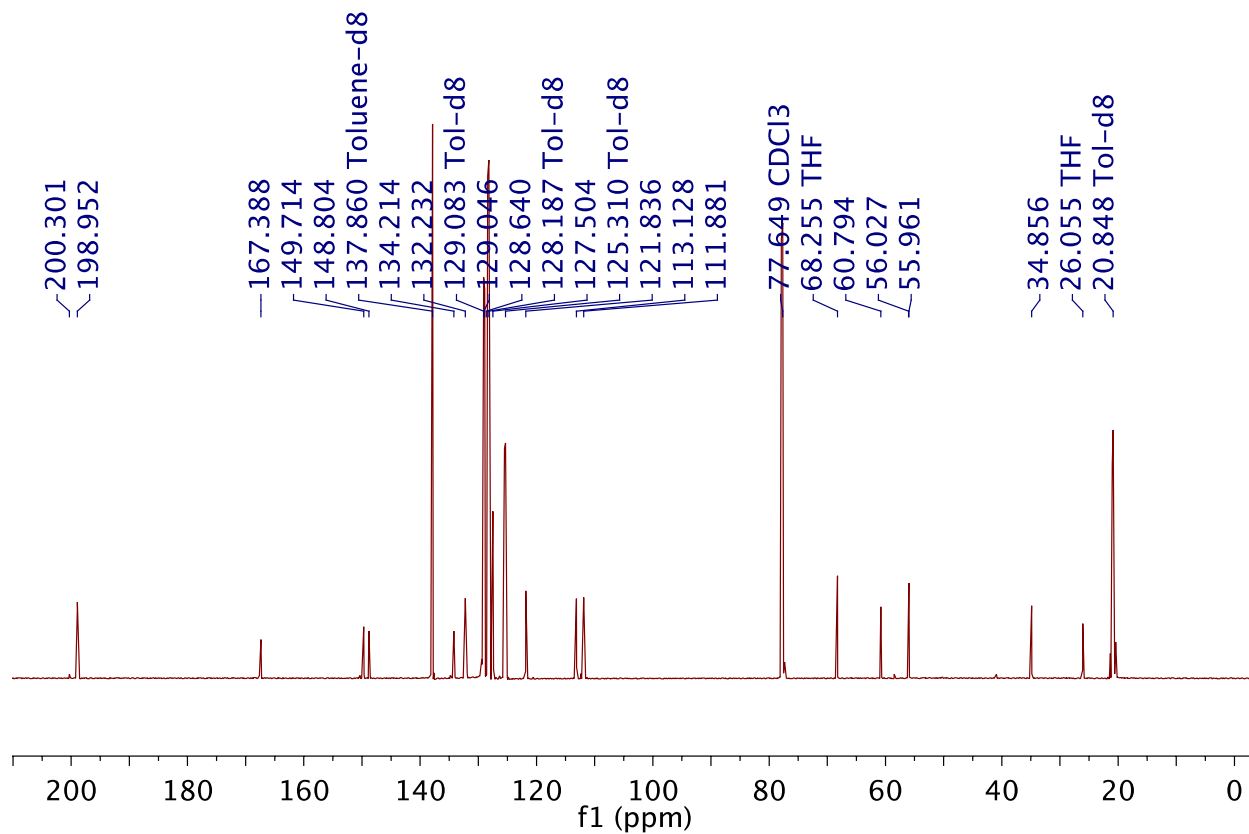
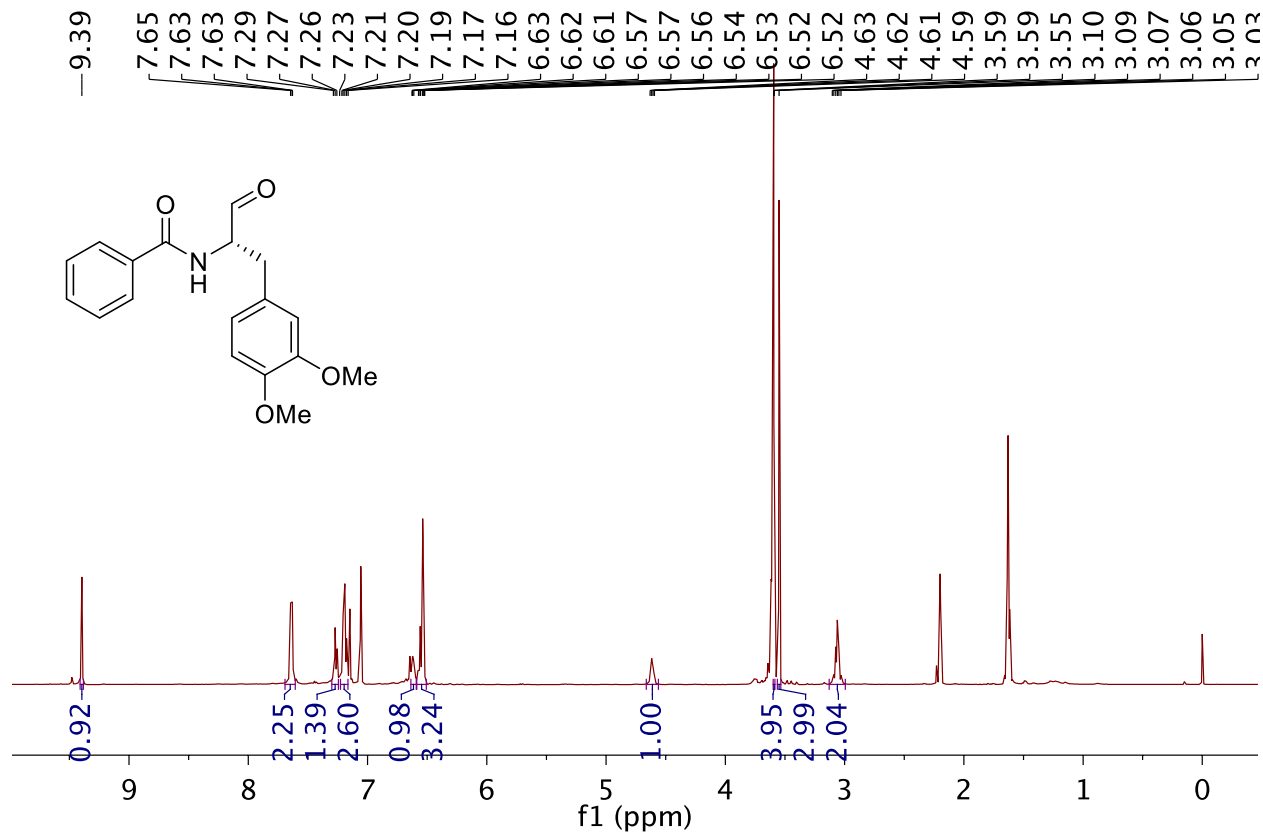




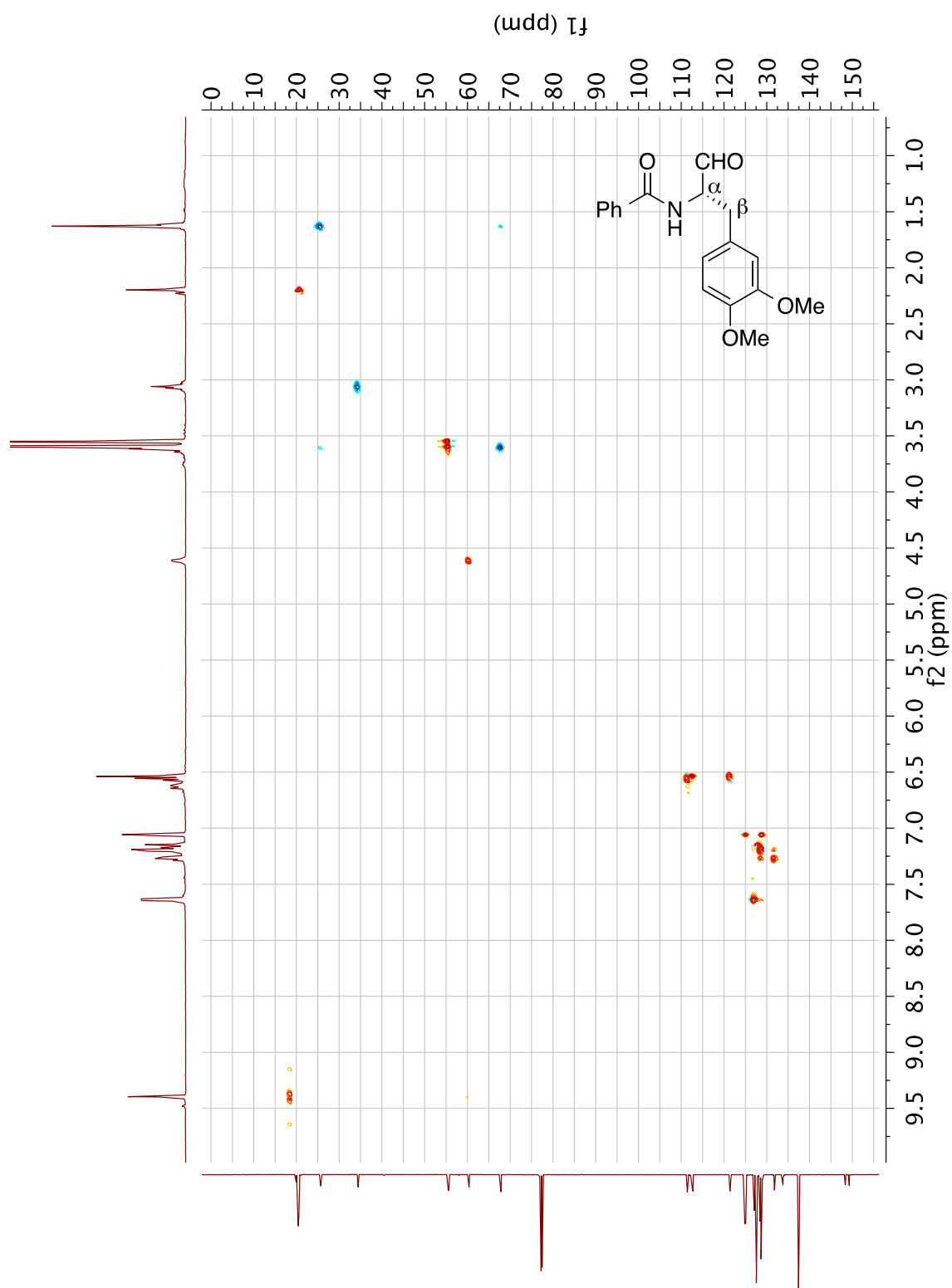


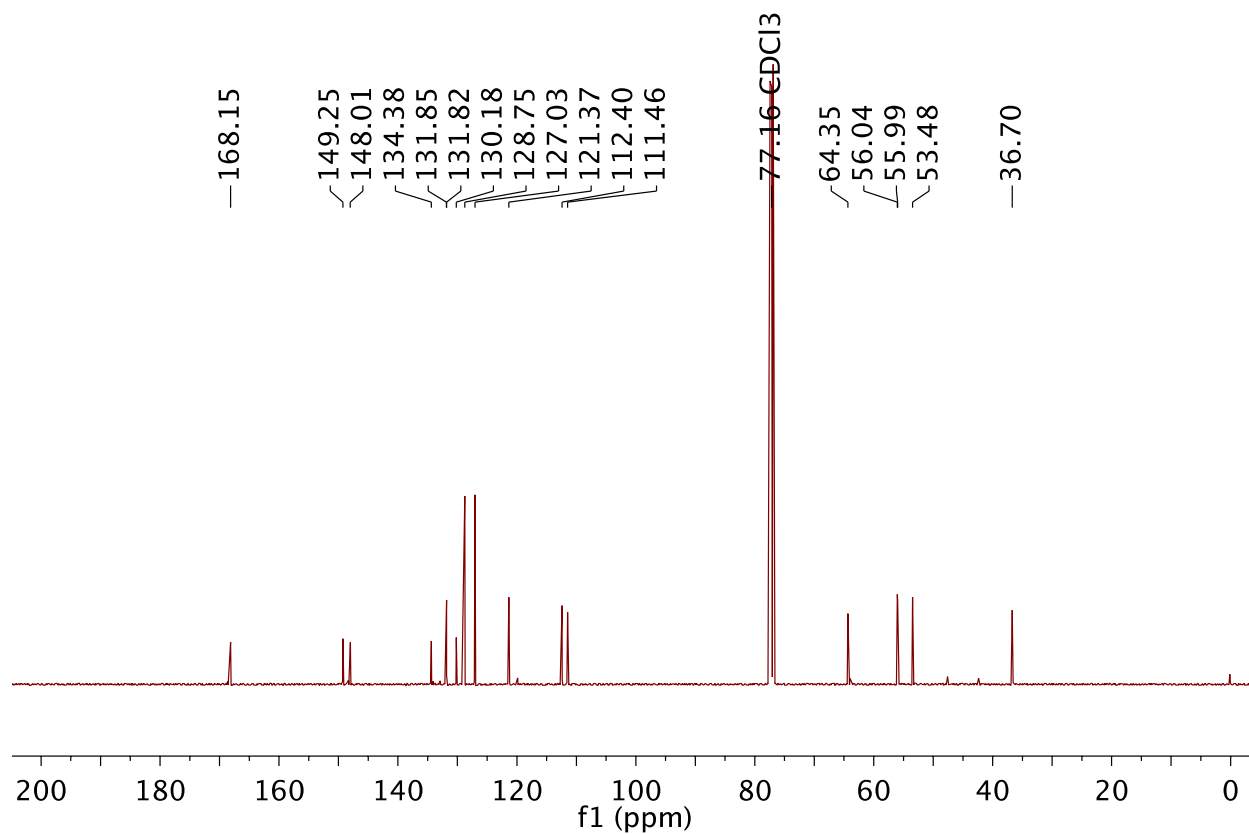
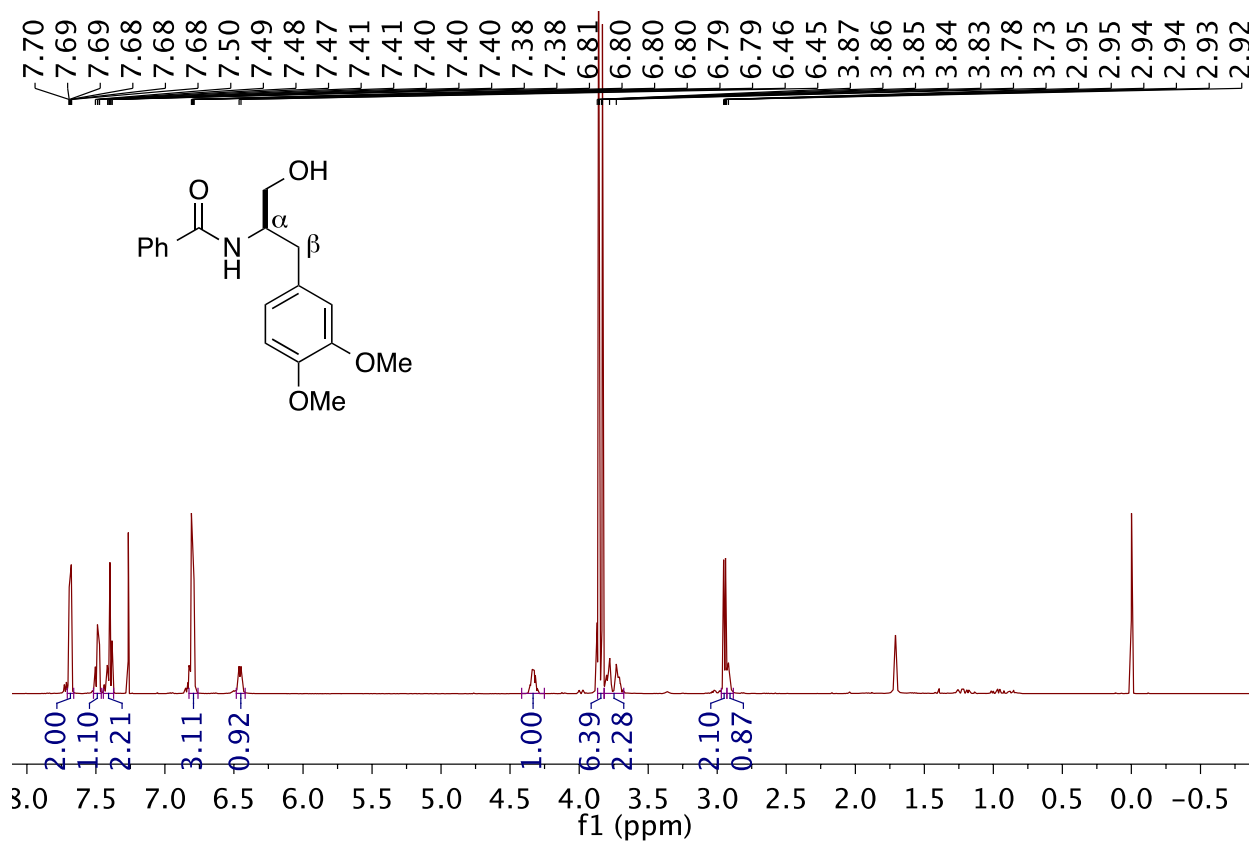




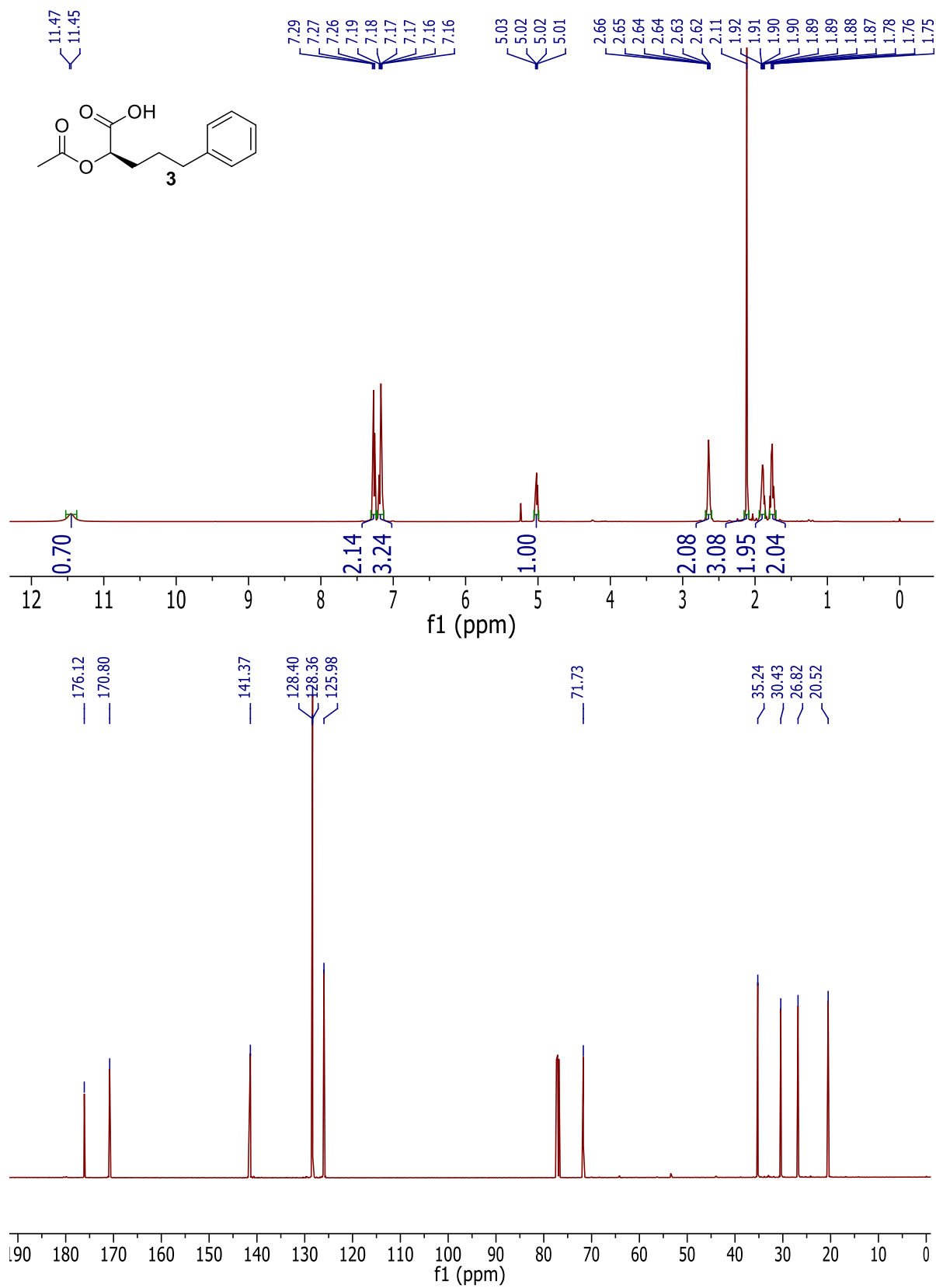


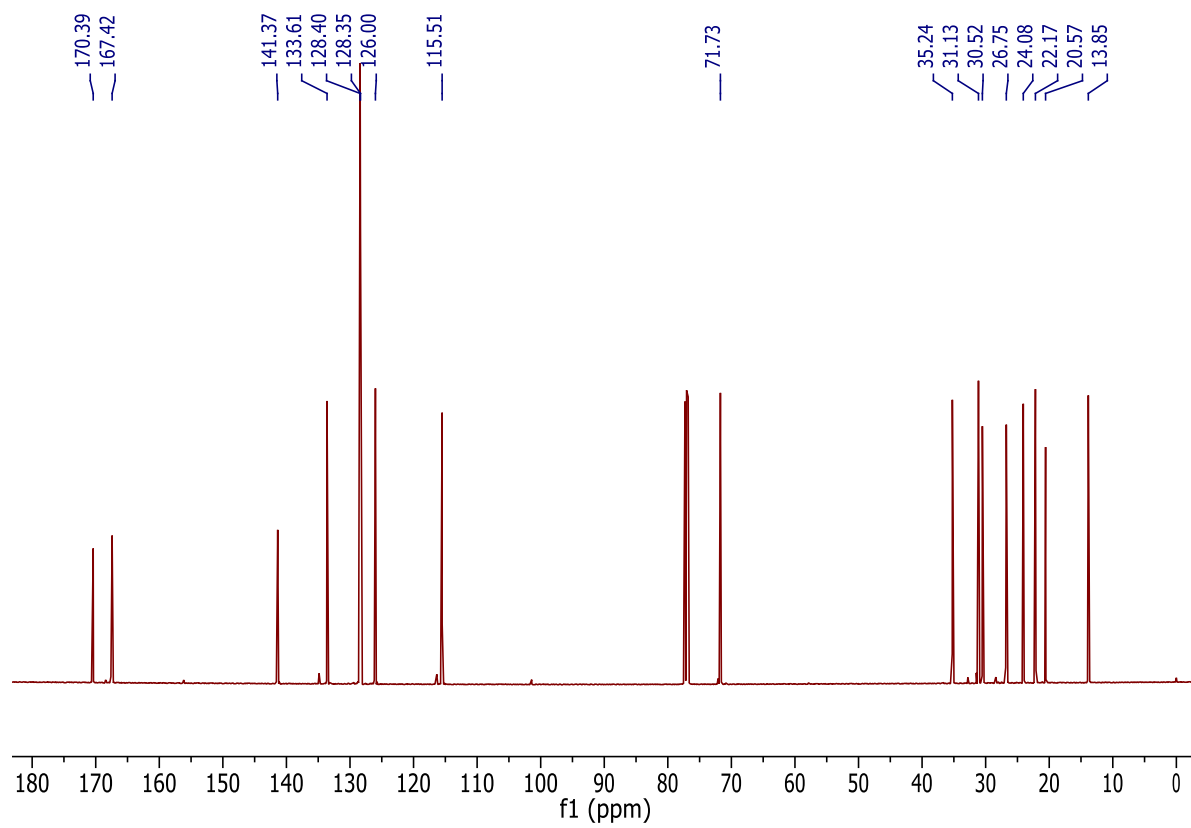
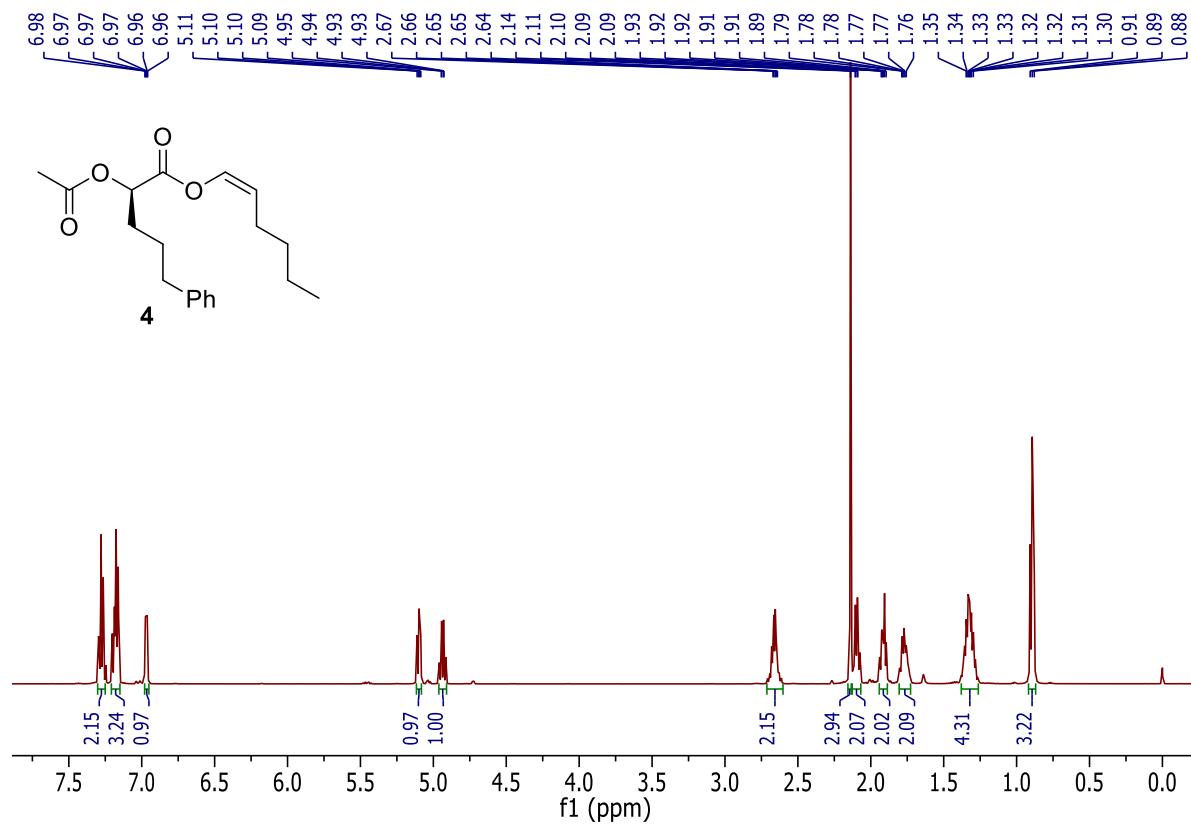
HSQC of the aldehyde to identify isomers

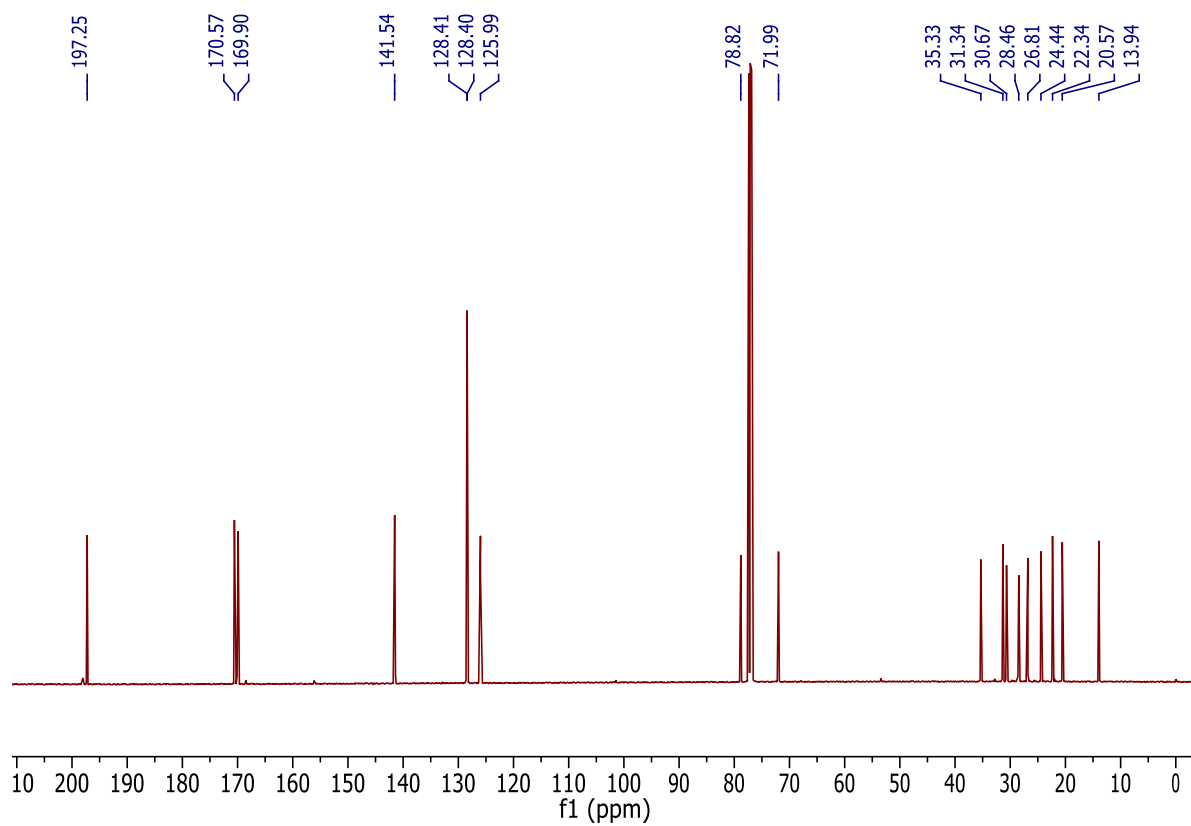
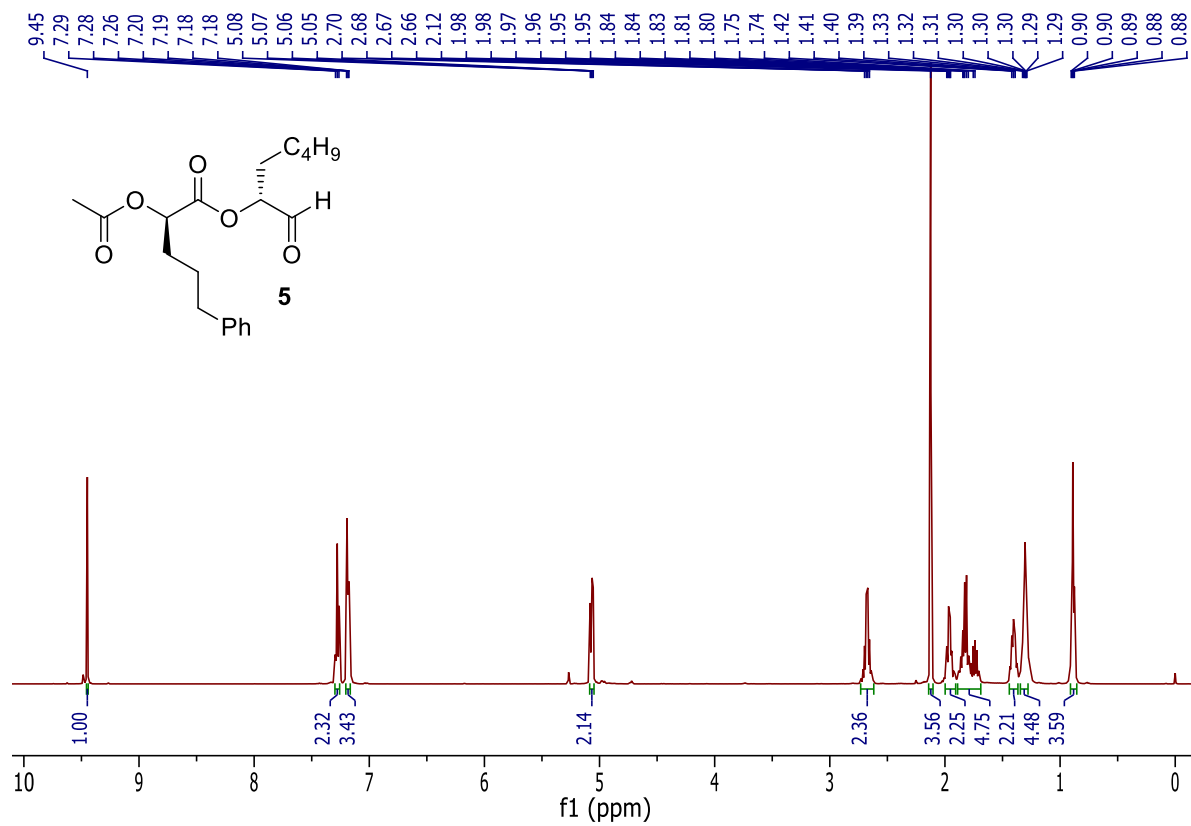


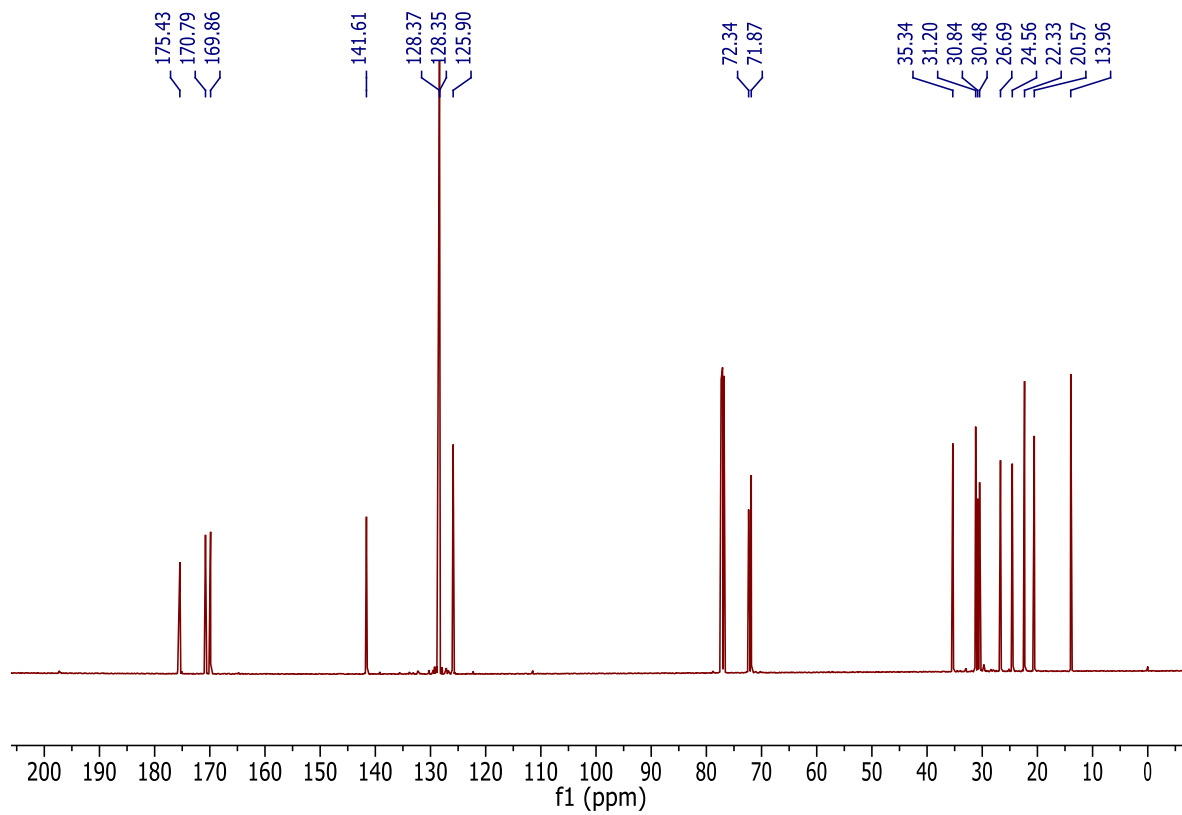
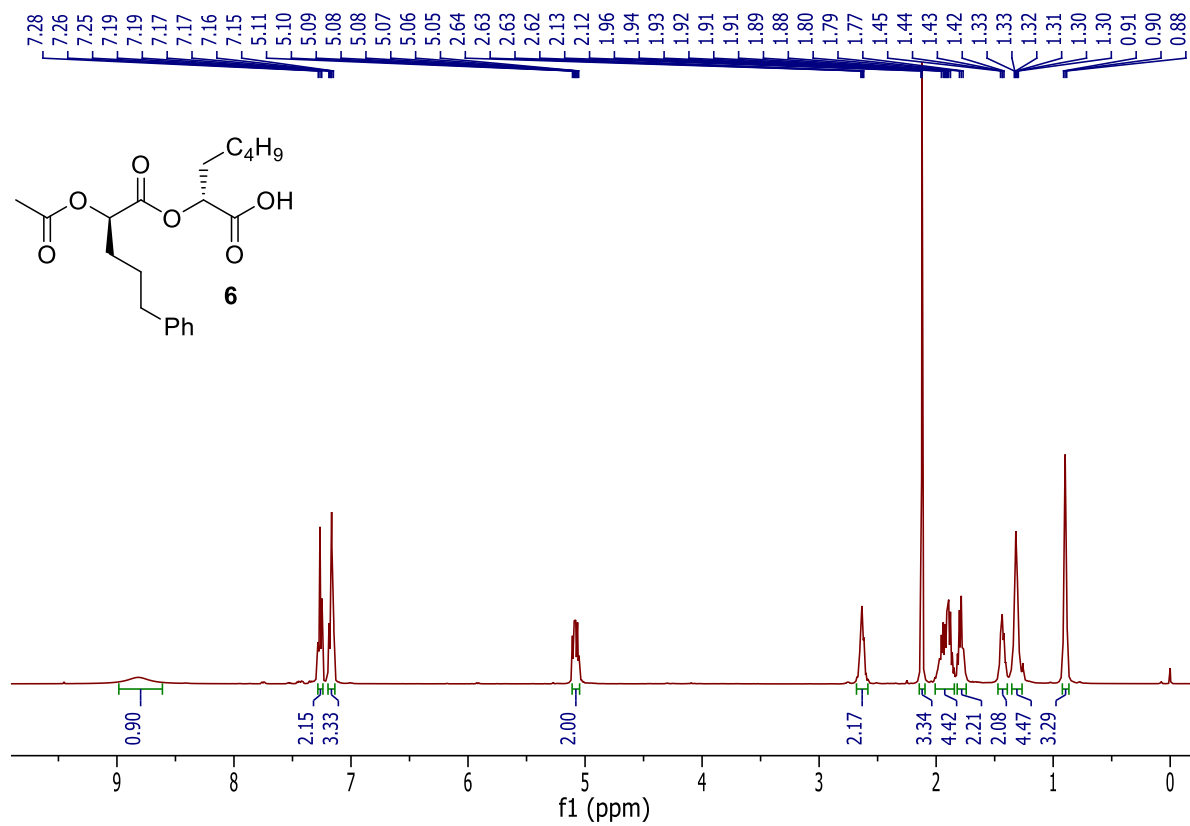


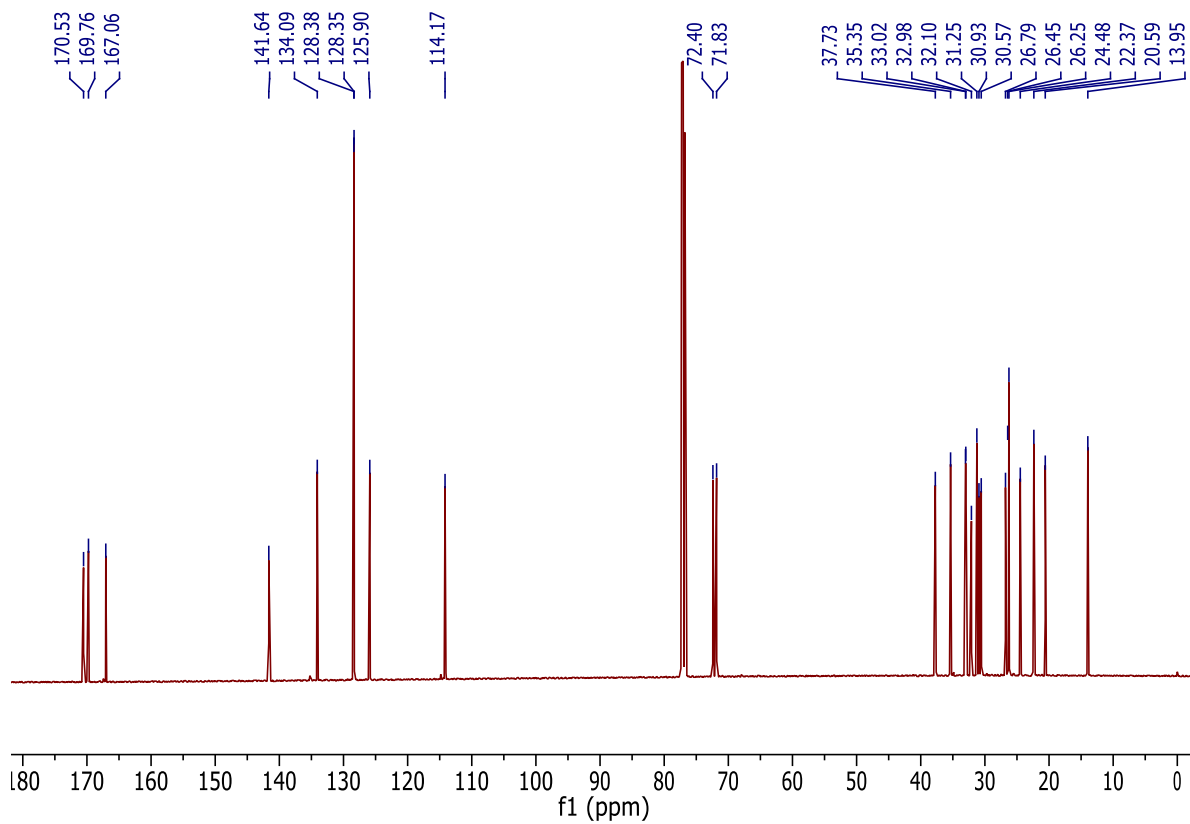
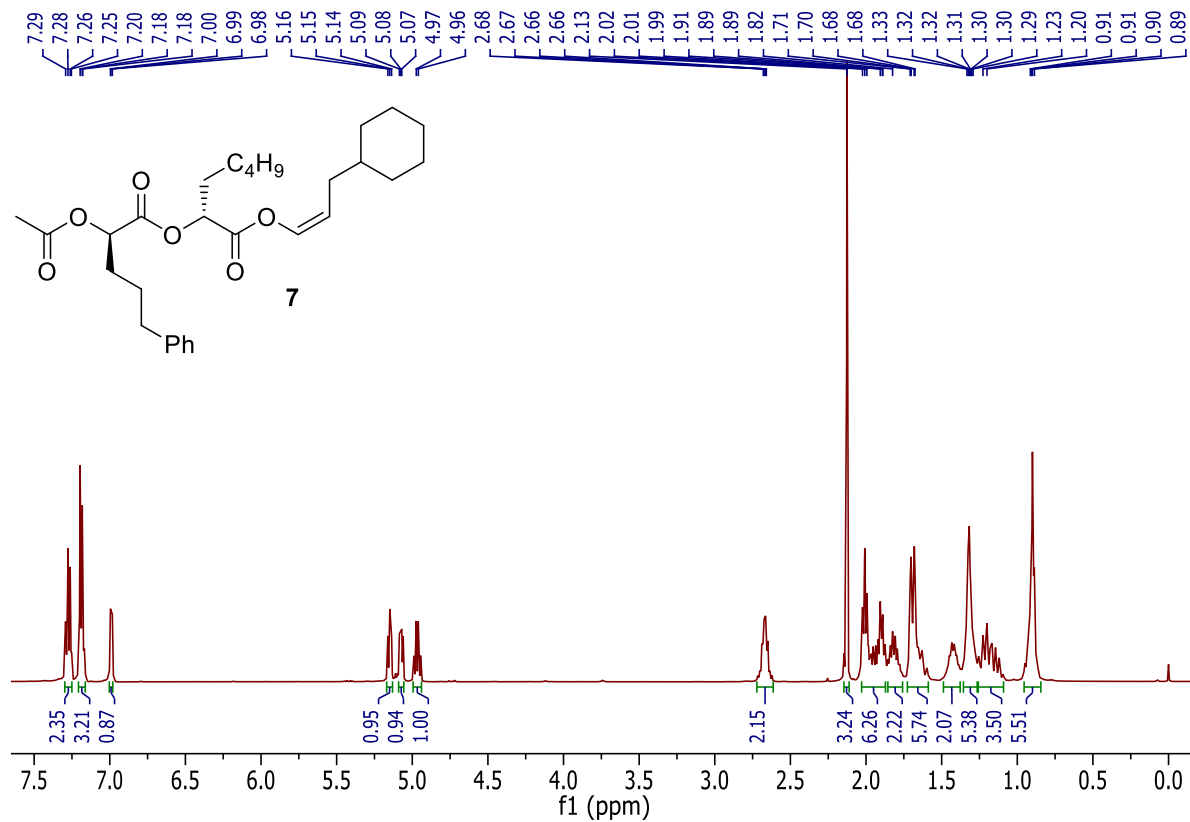
NMR spectra for Chapter 3

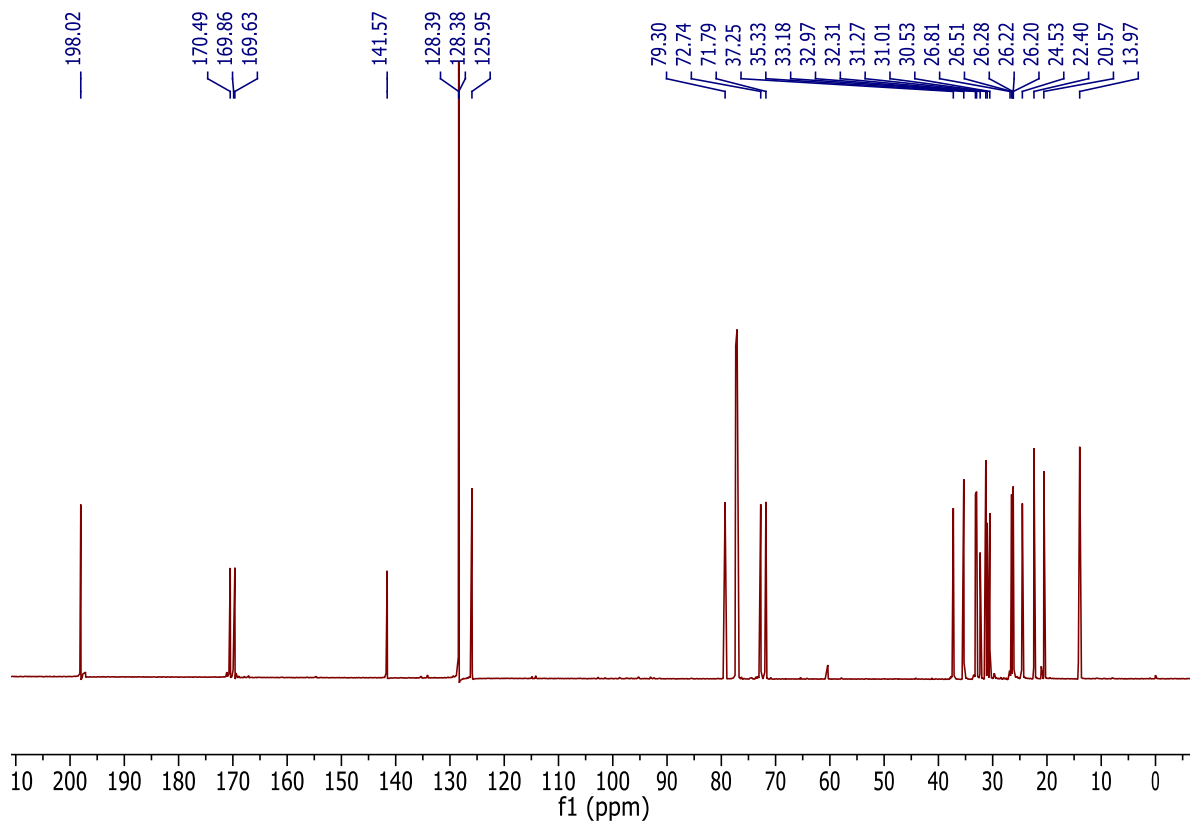
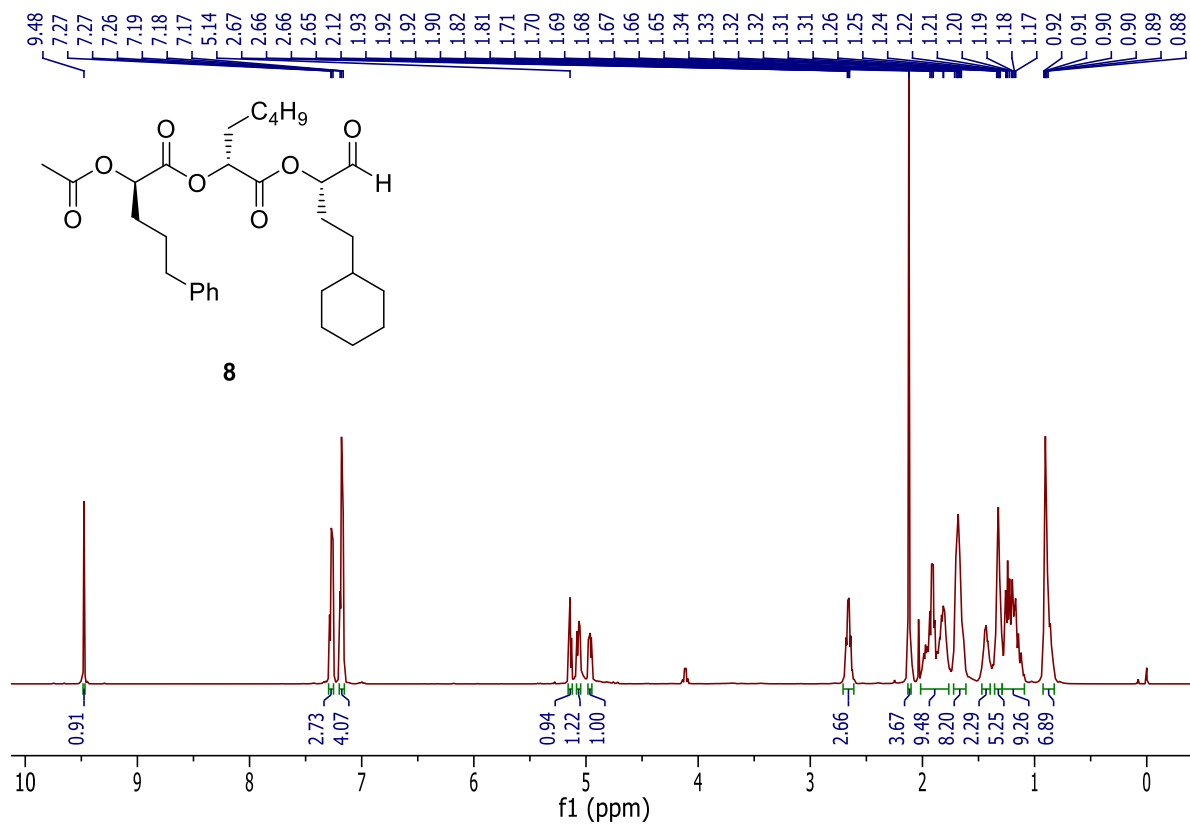


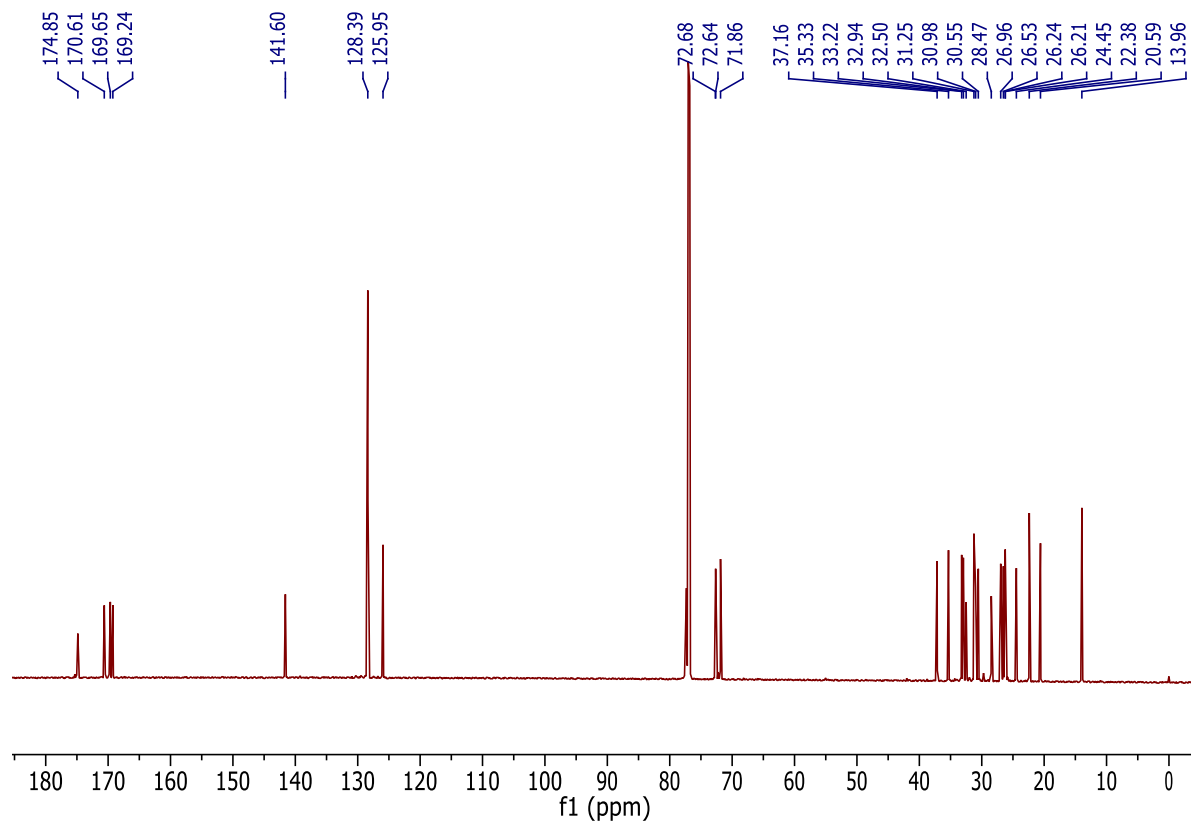
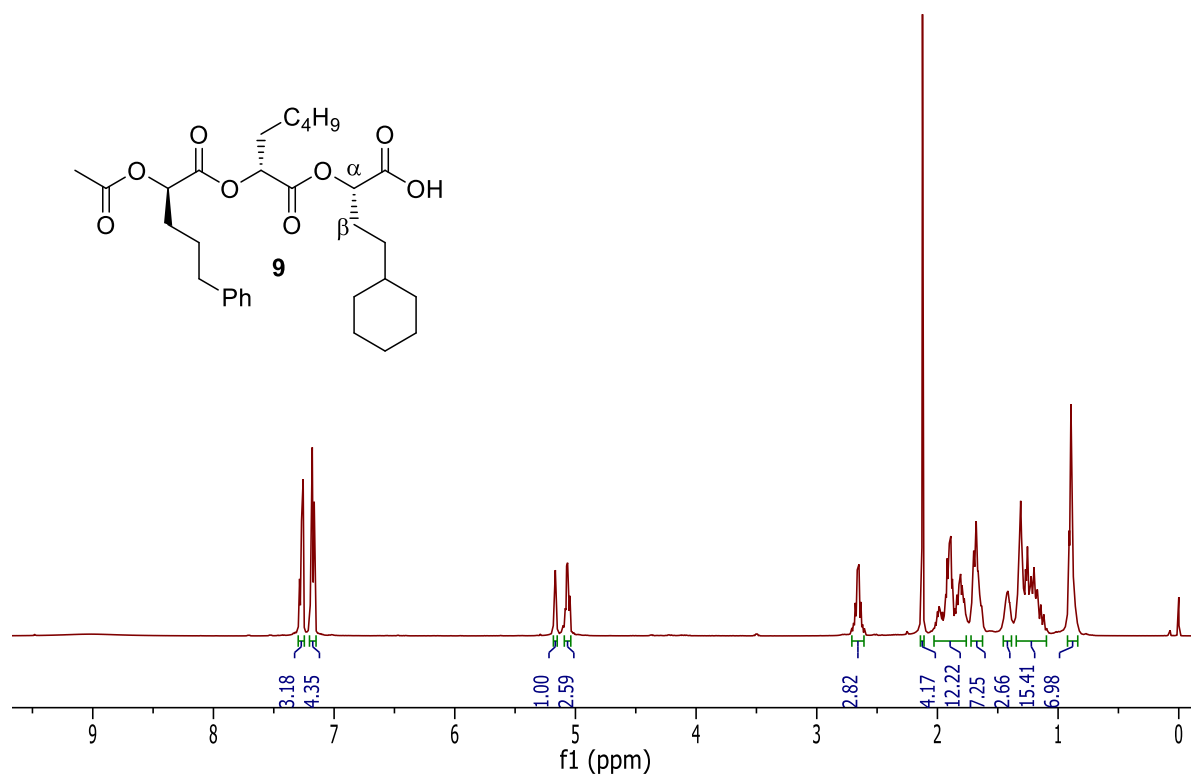


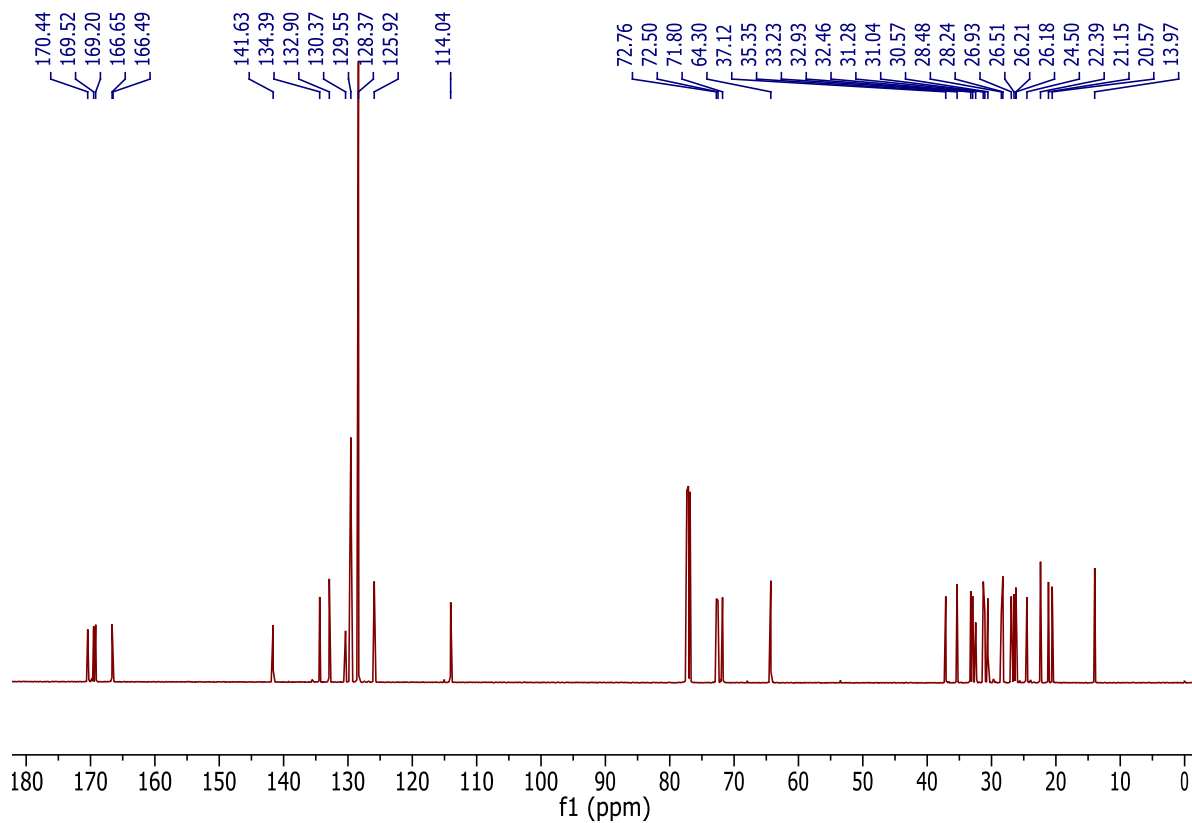
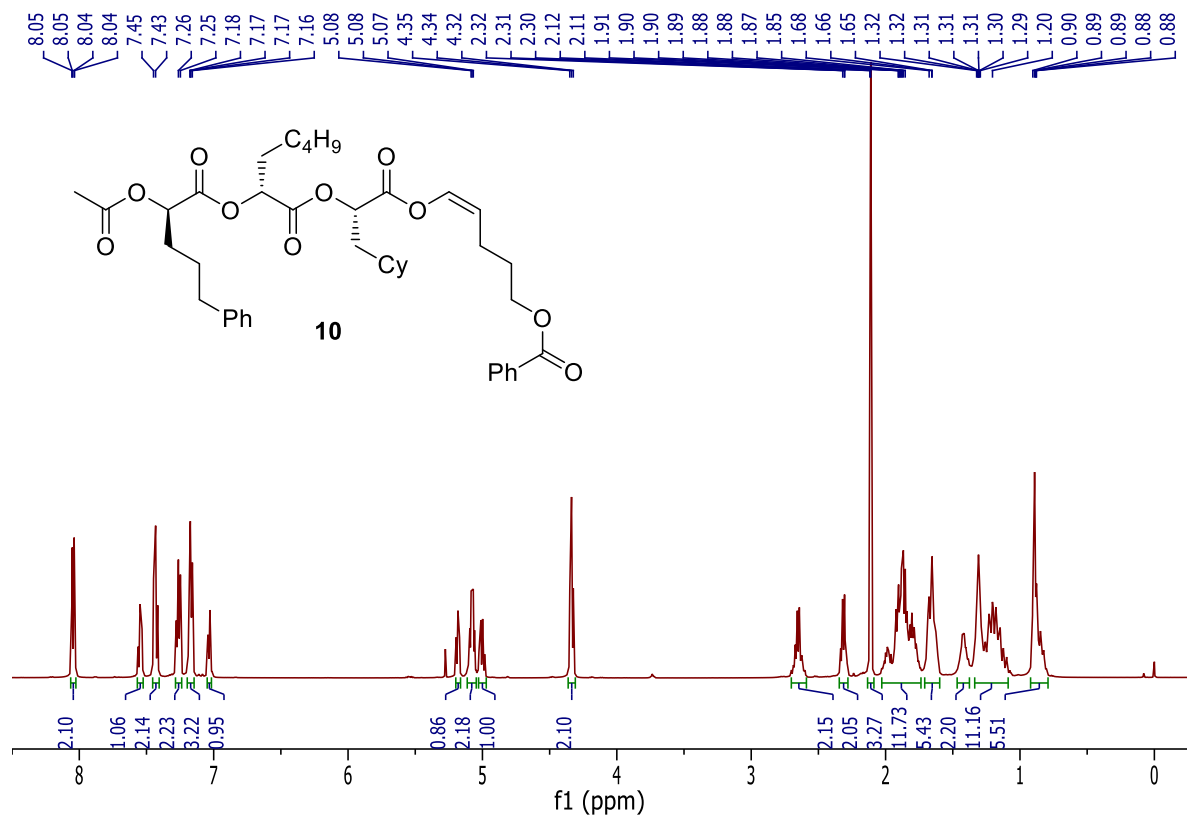


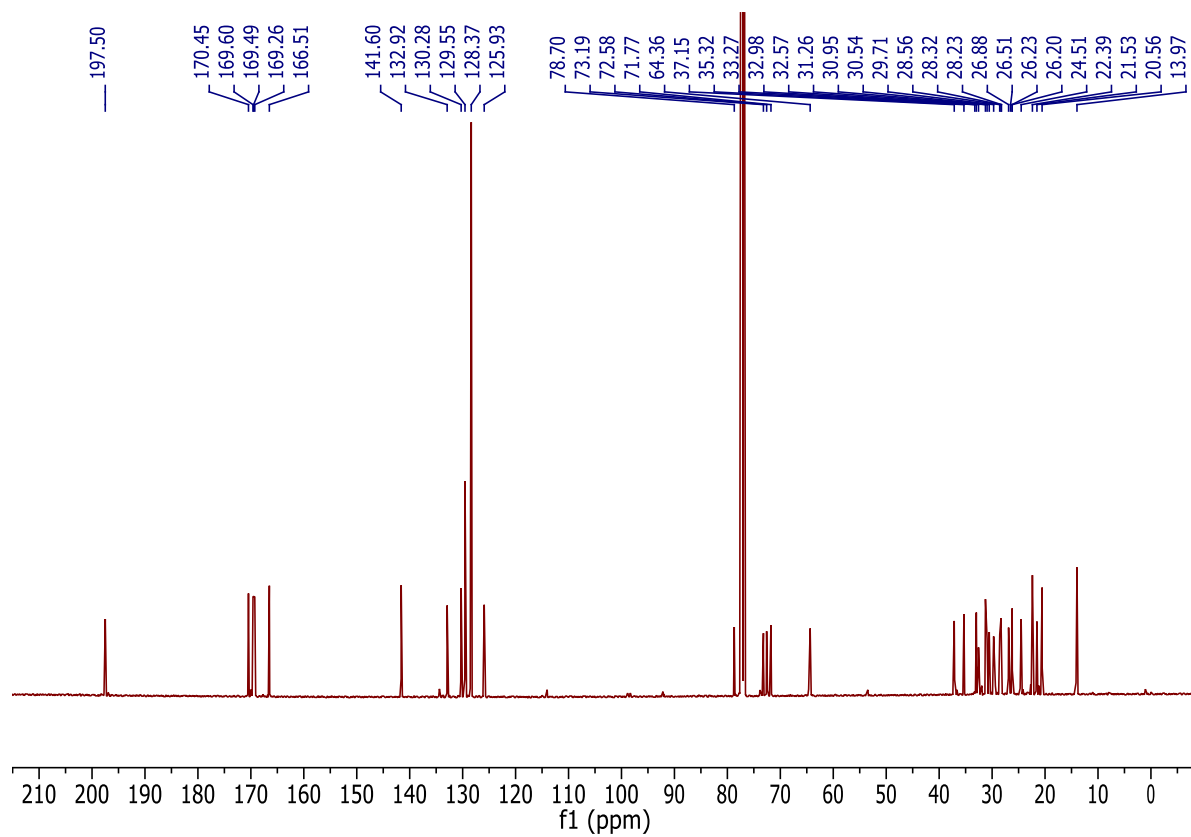
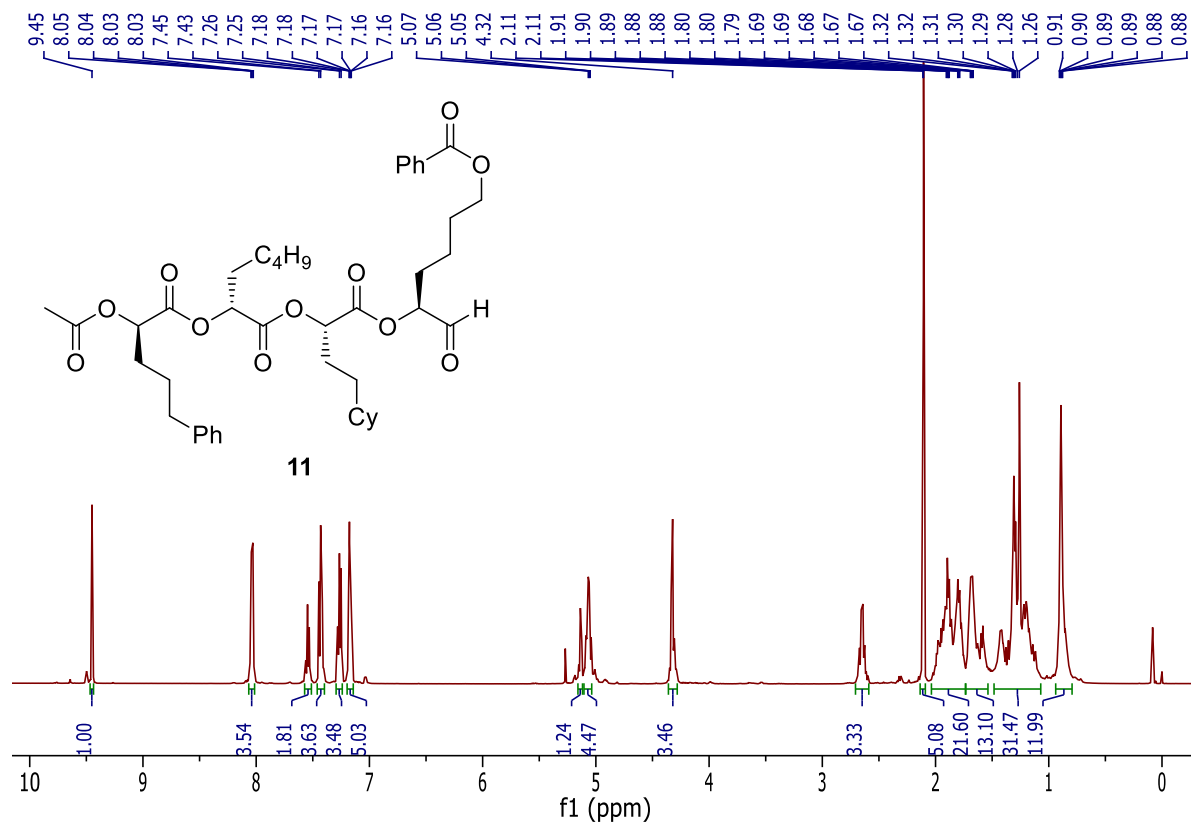


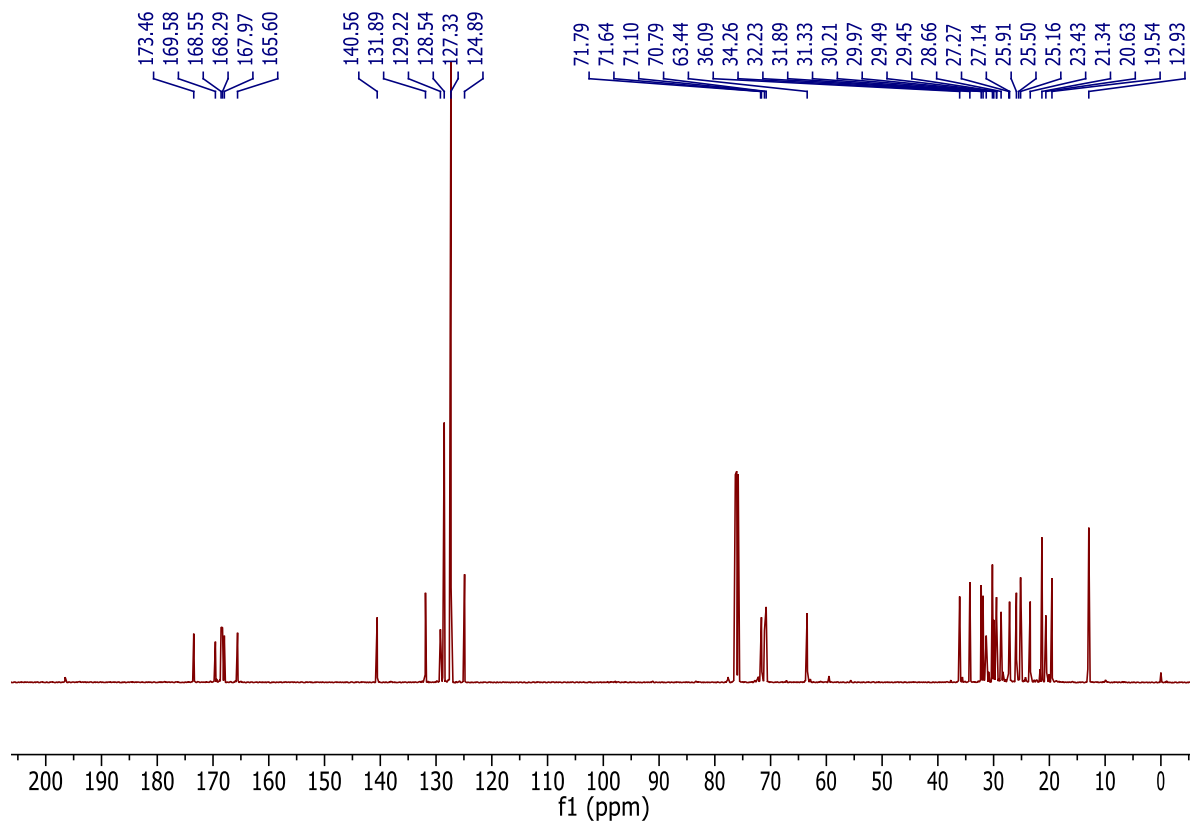
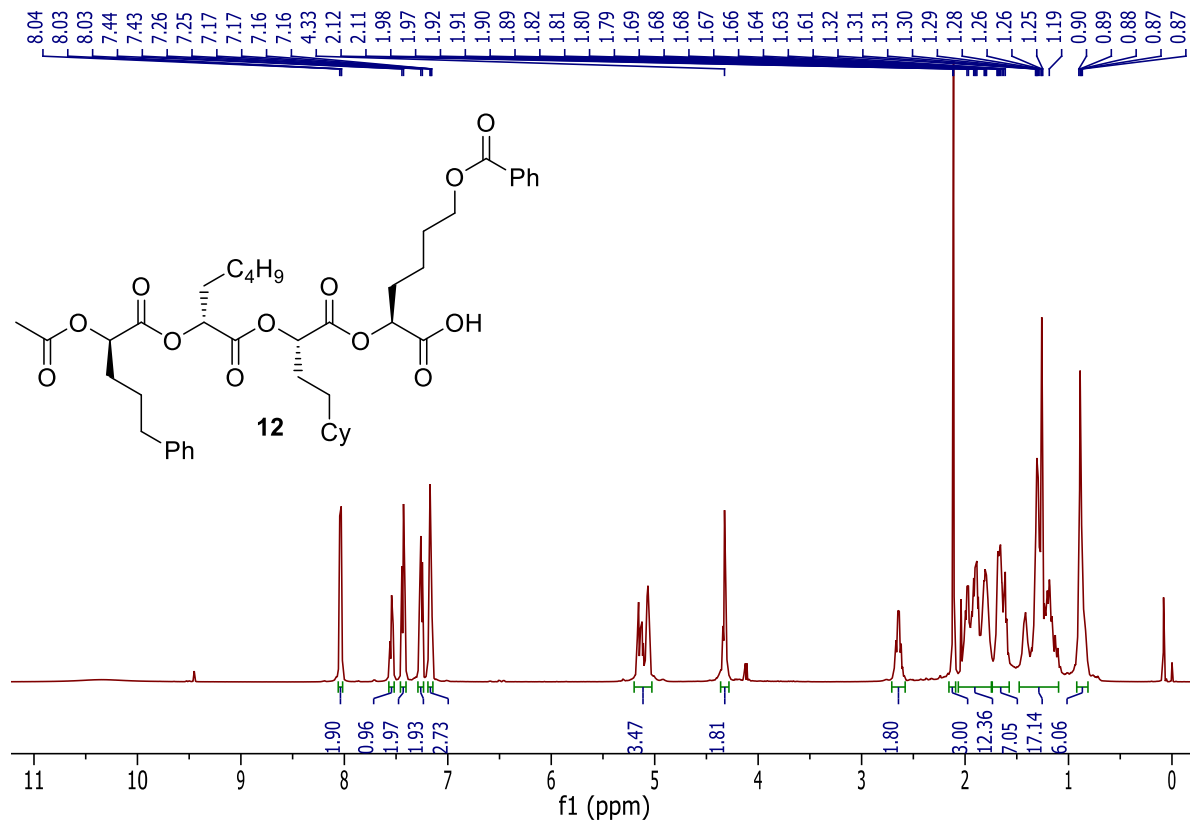


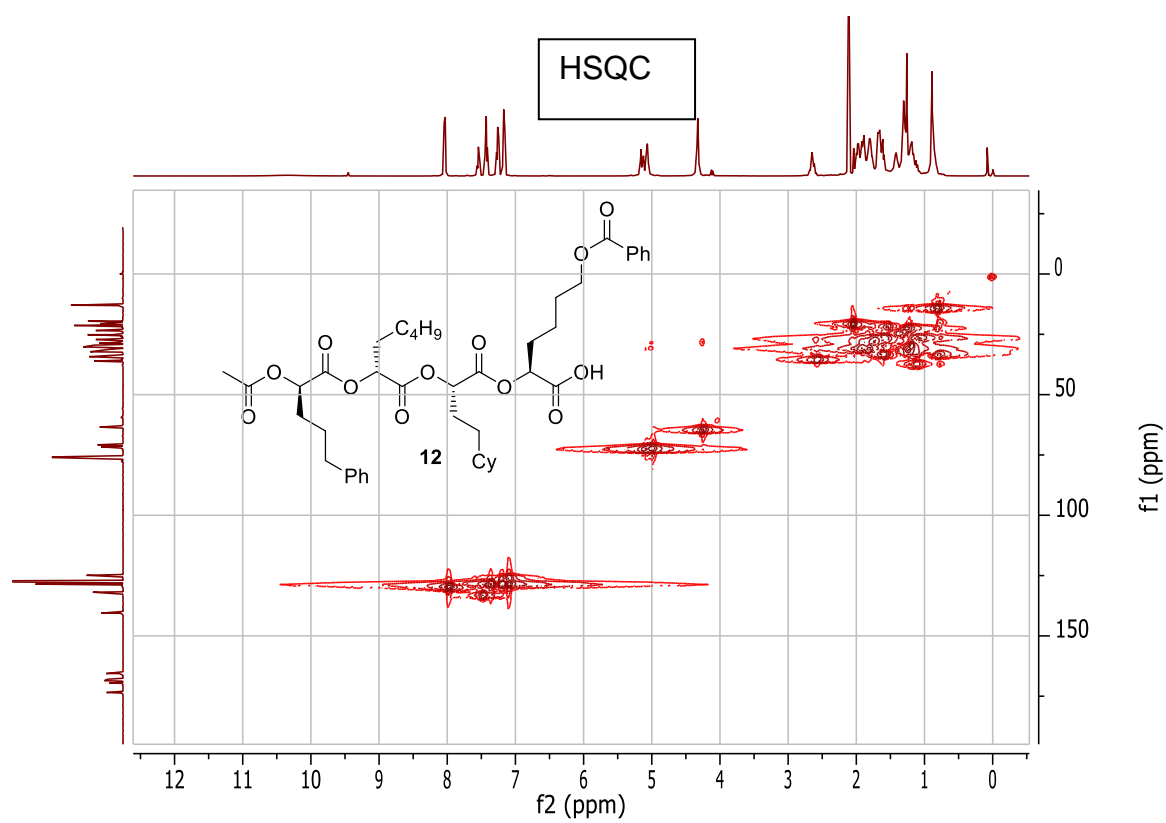


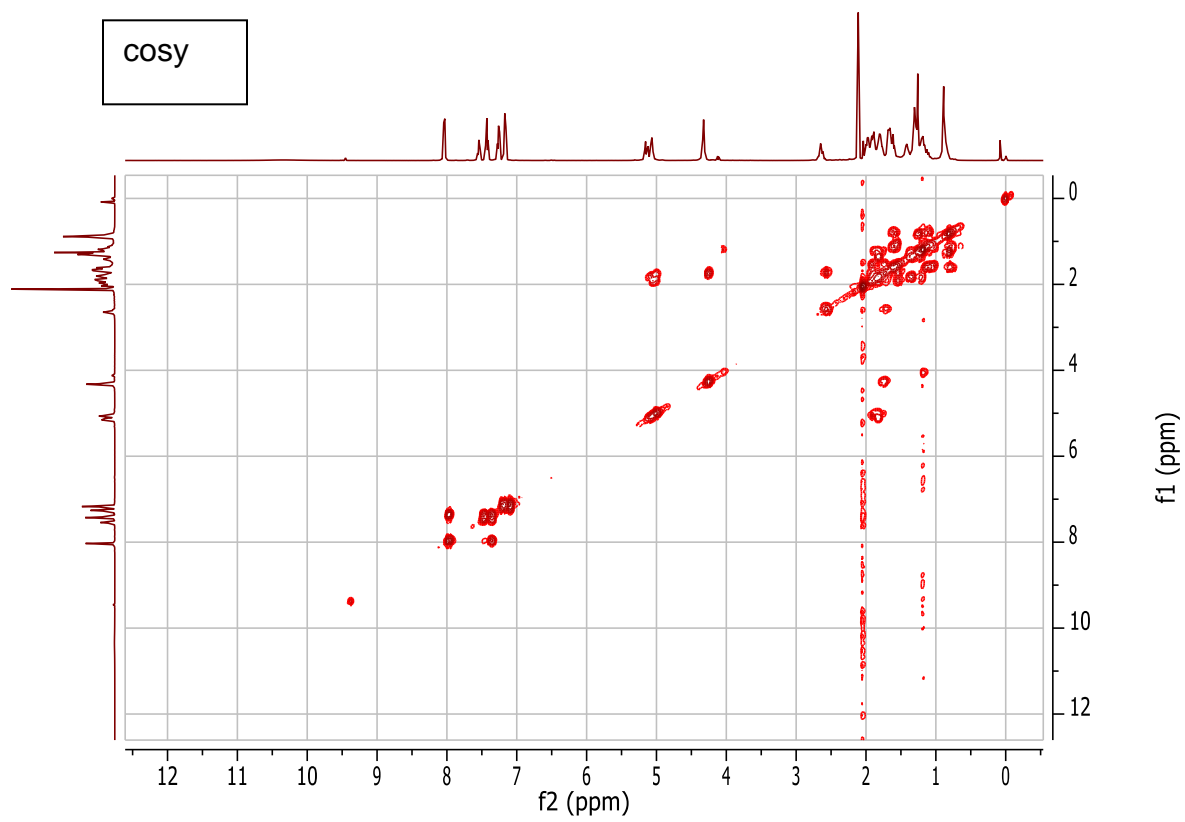
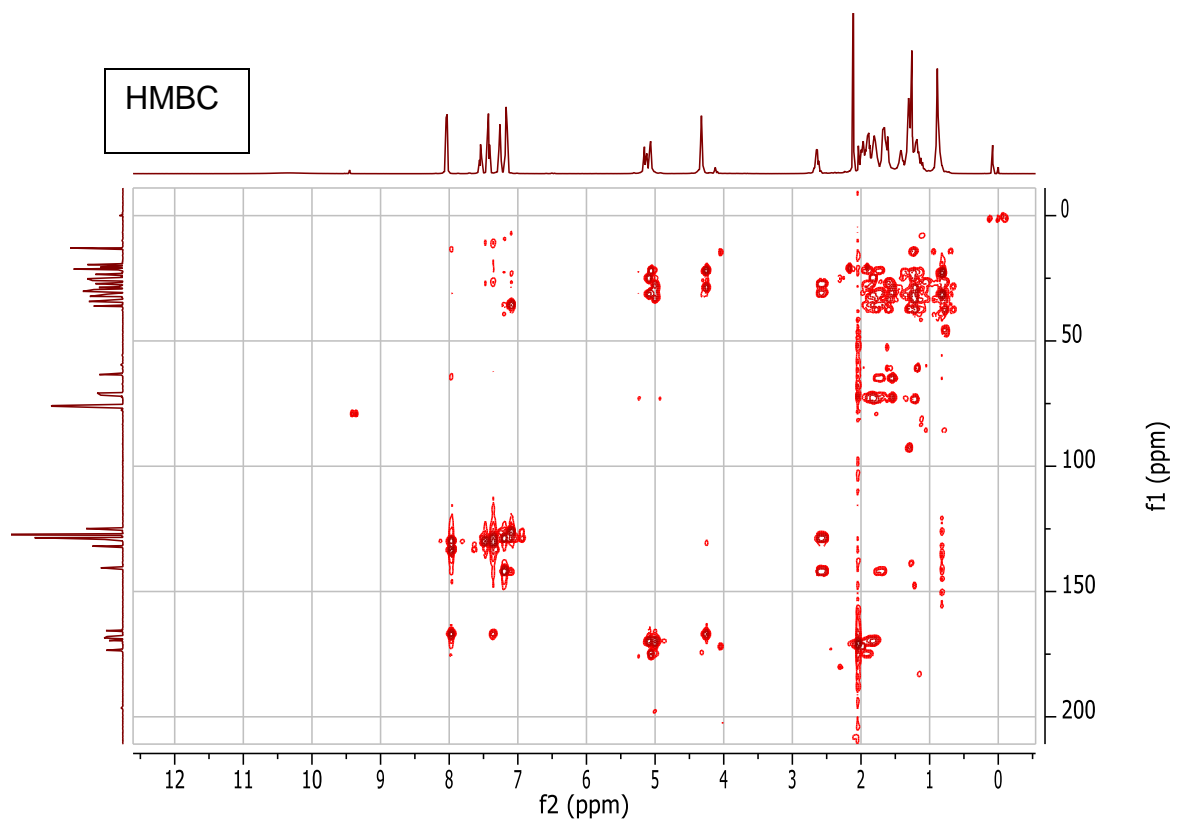


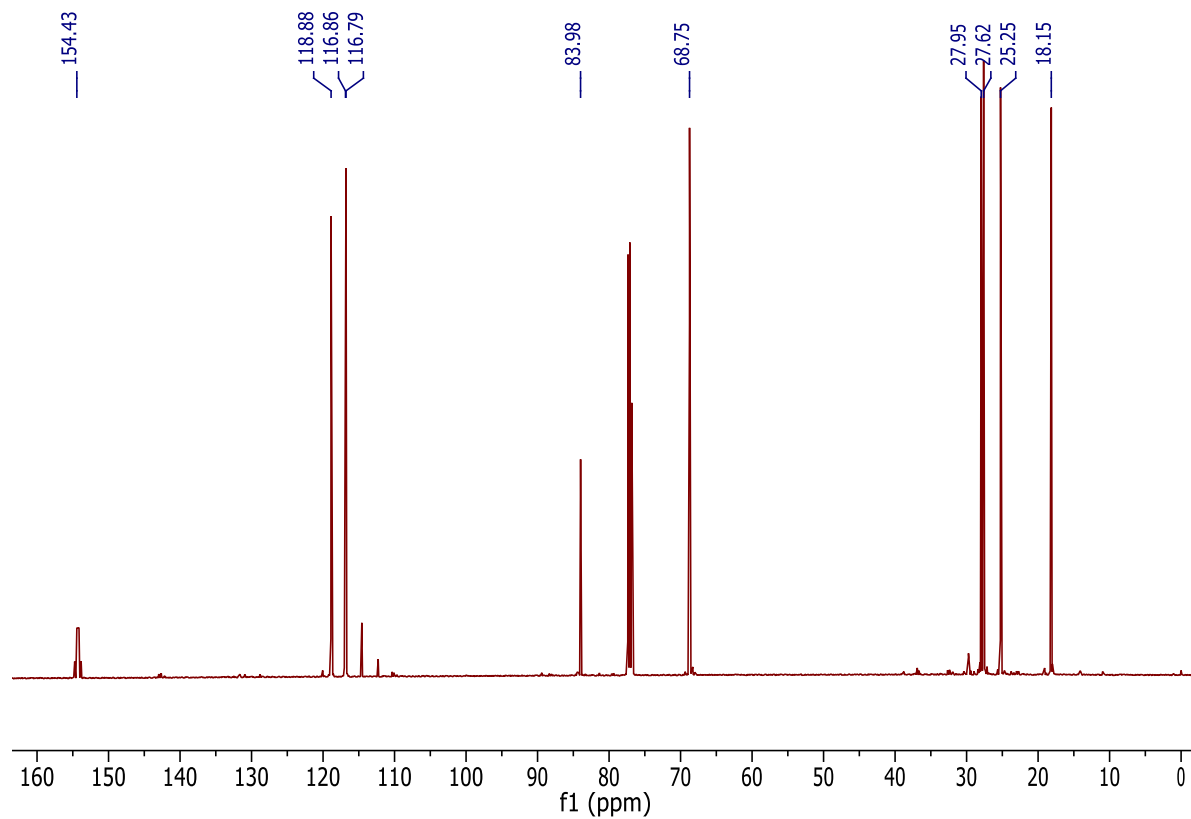
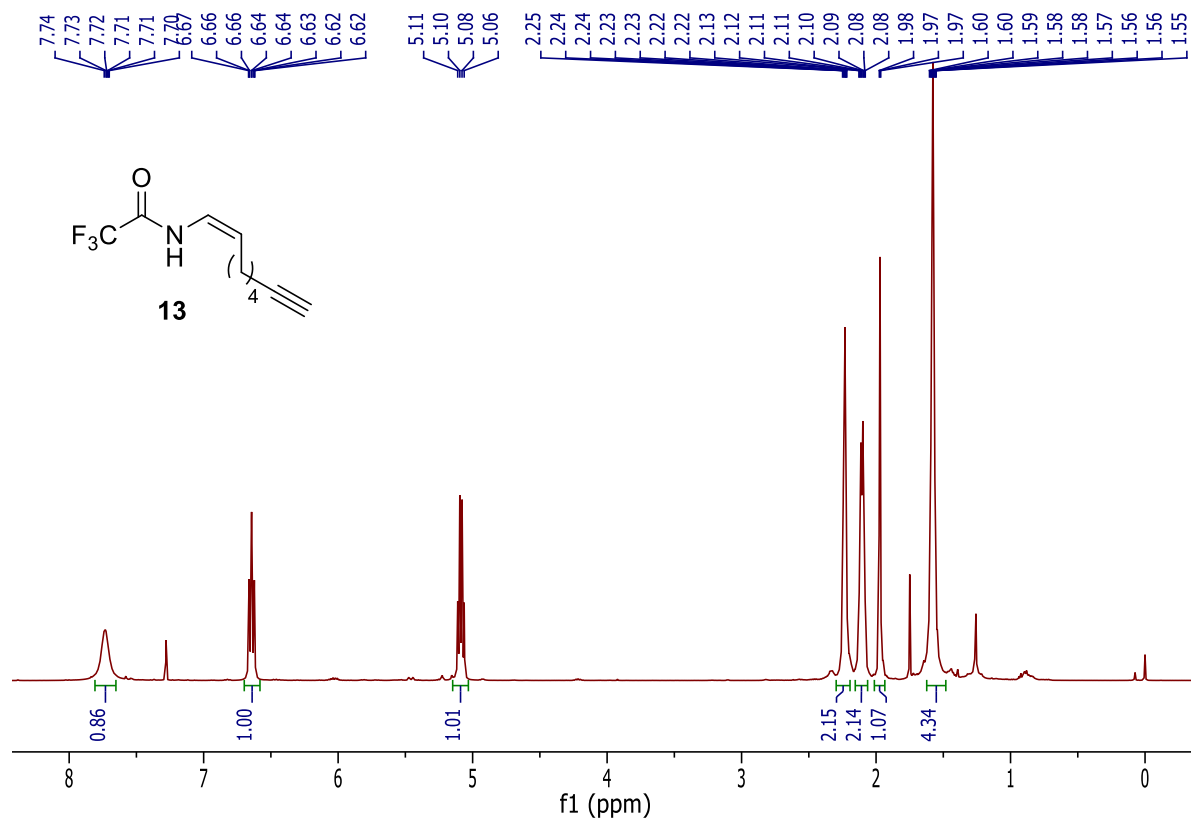


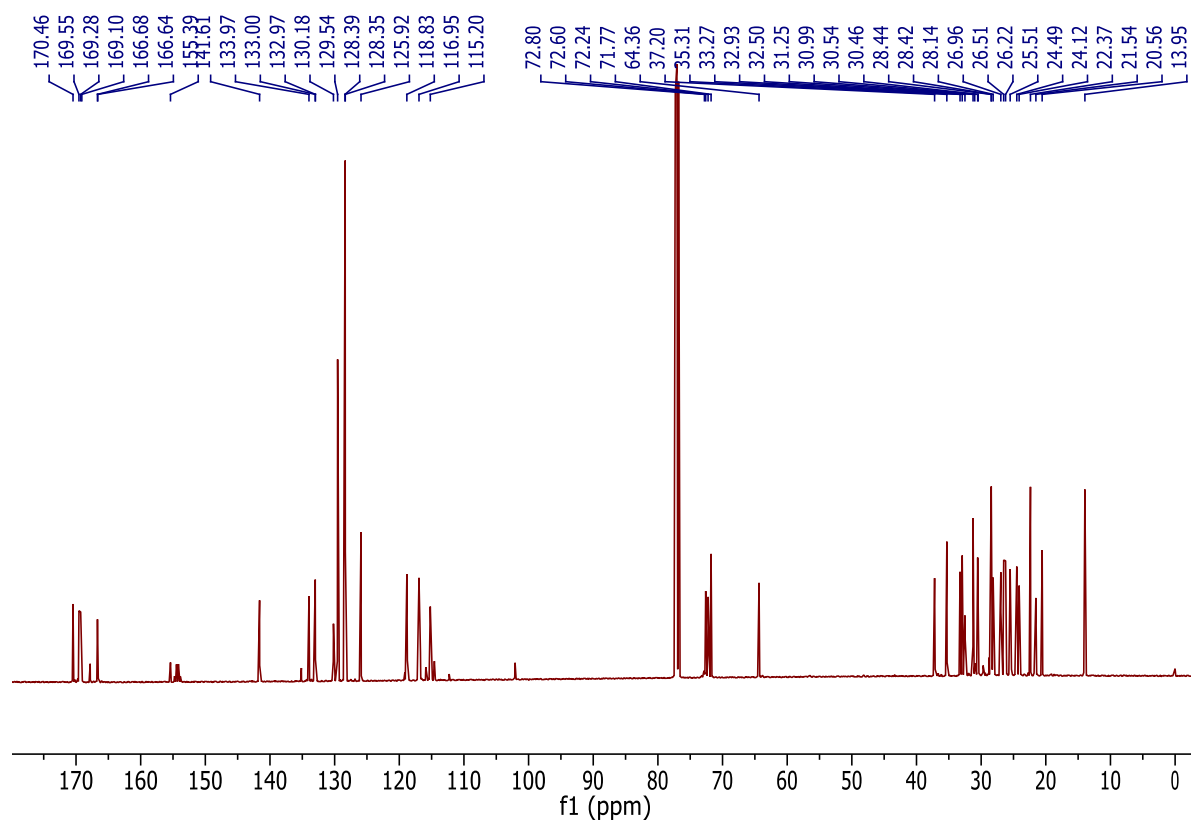
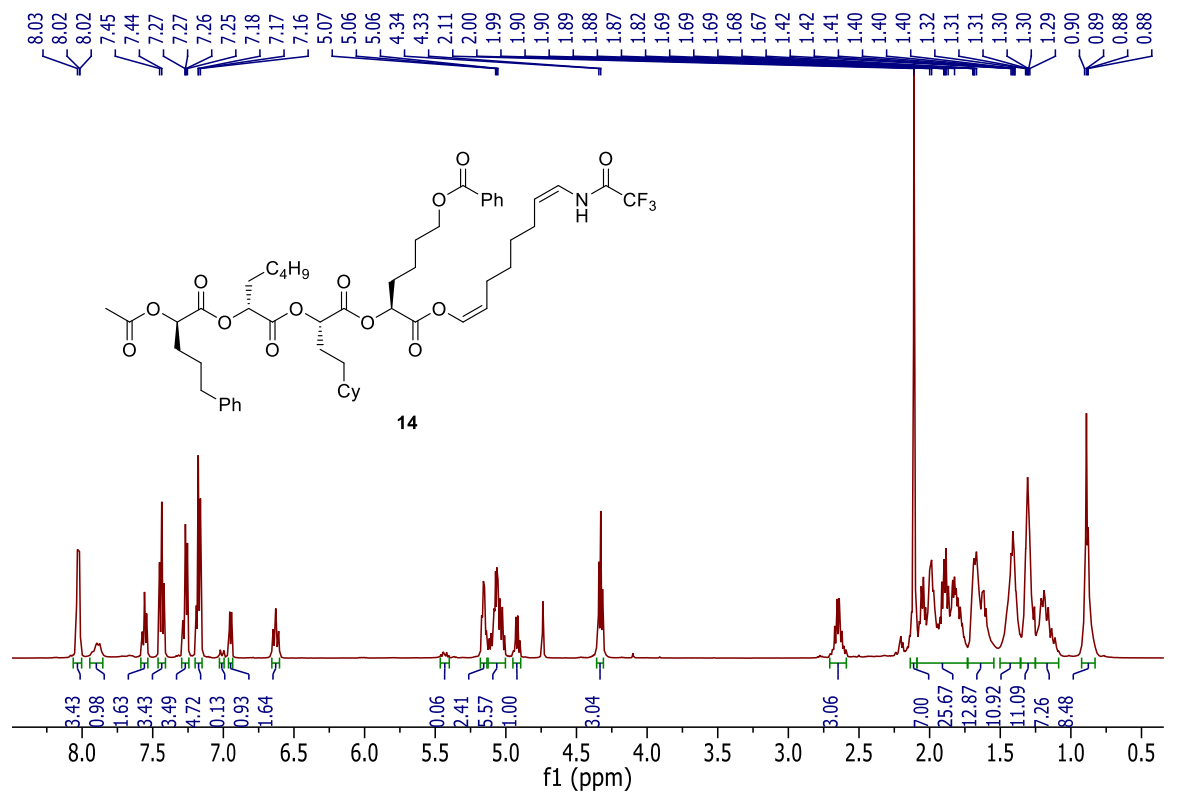




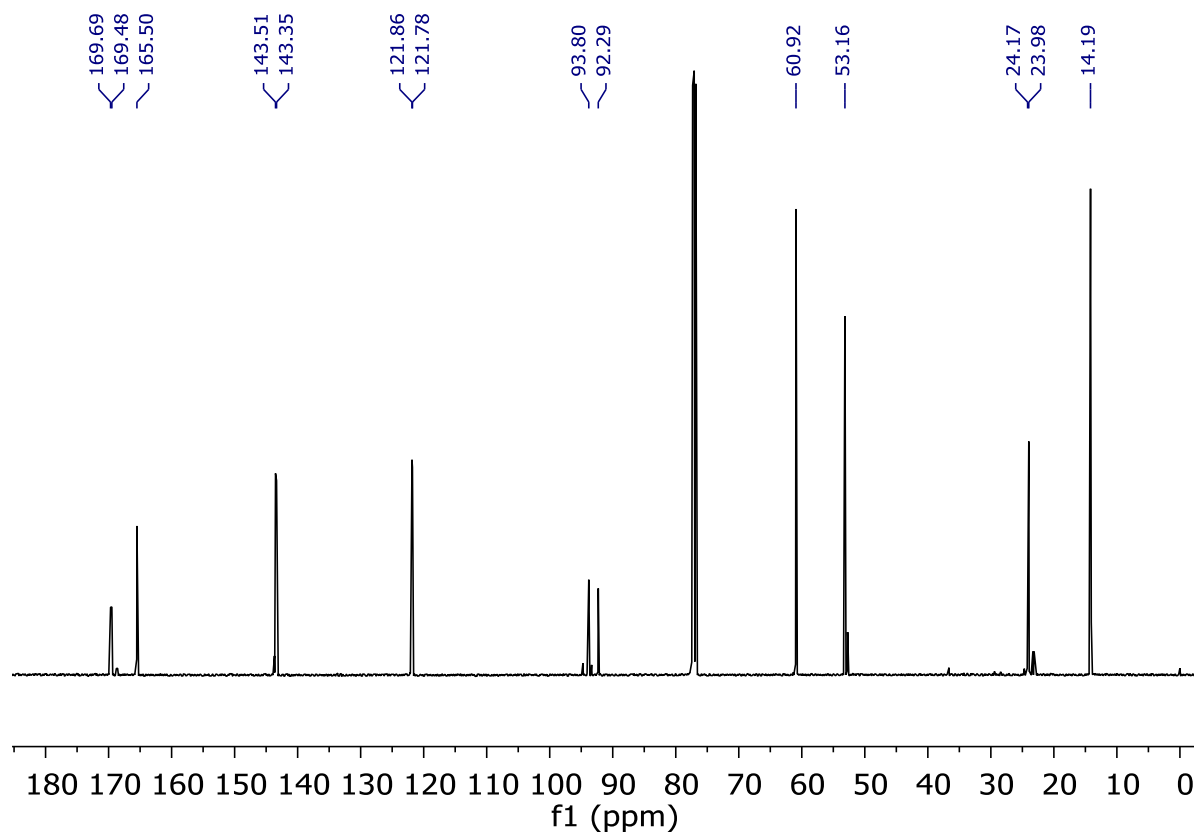
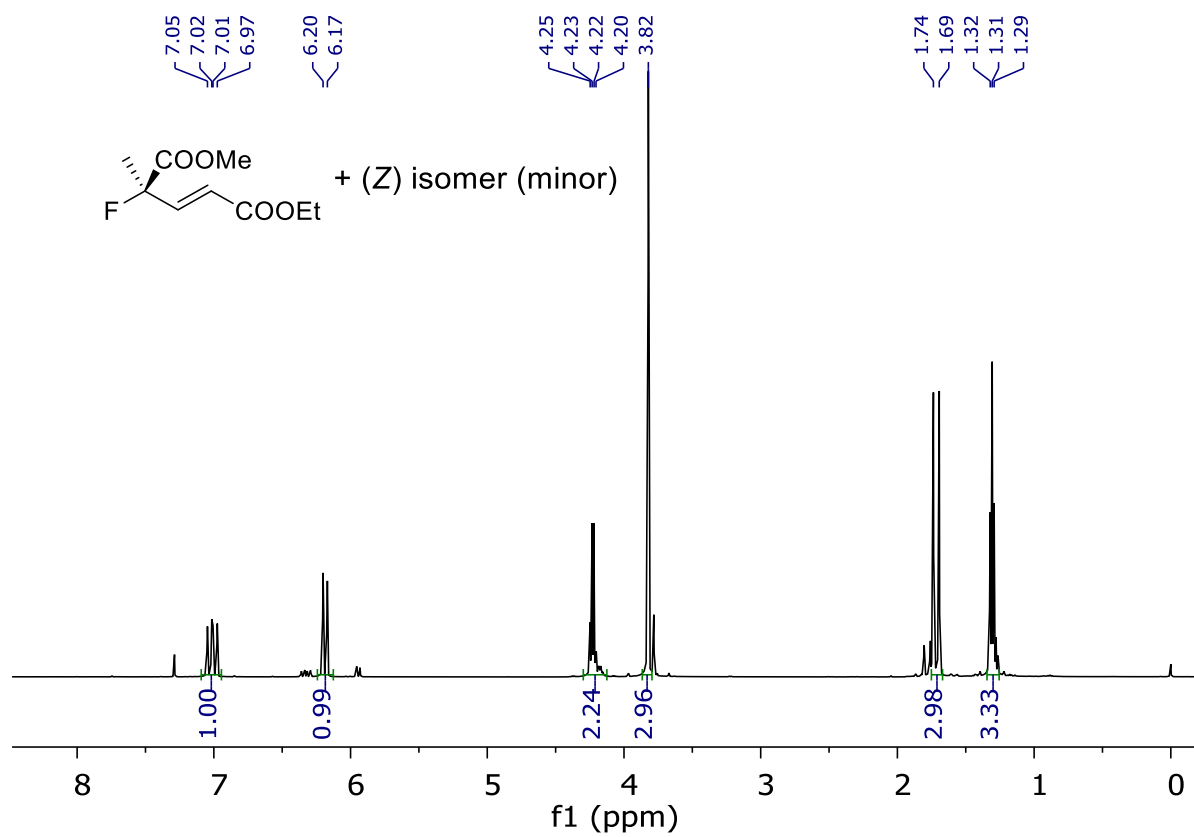


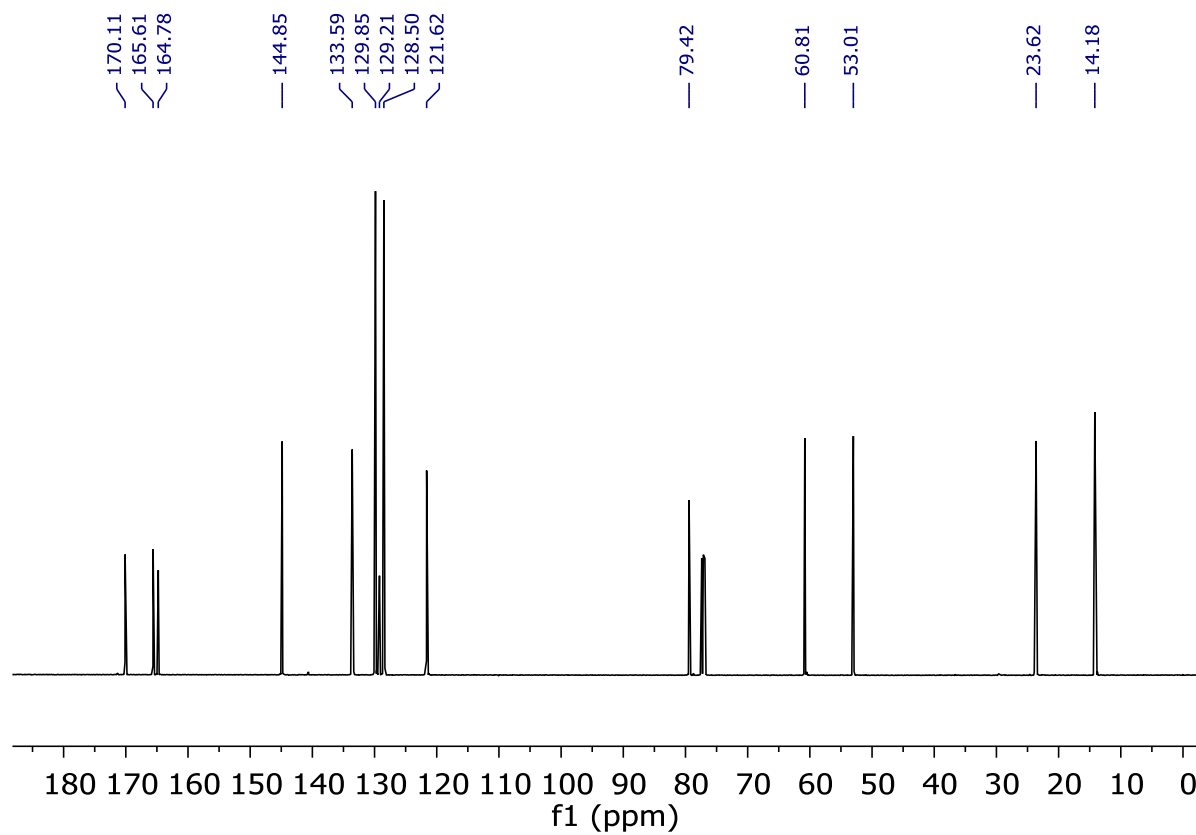
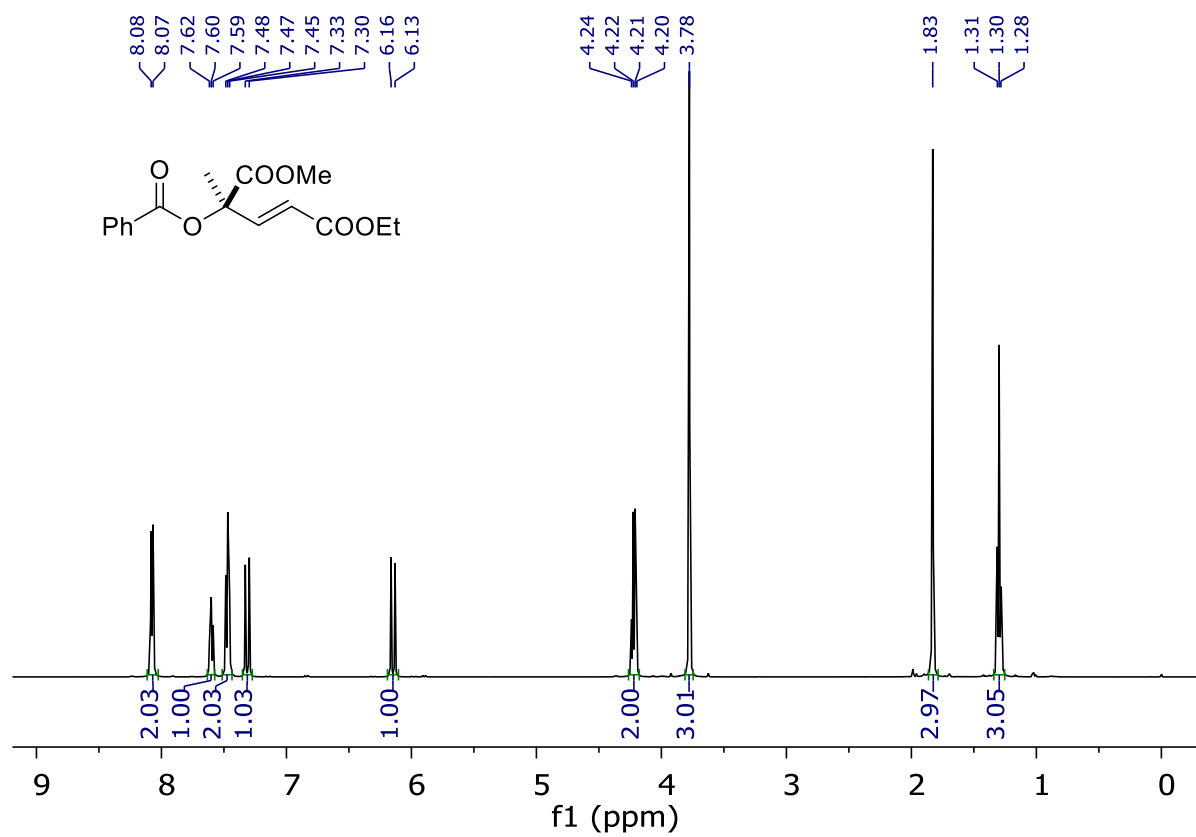


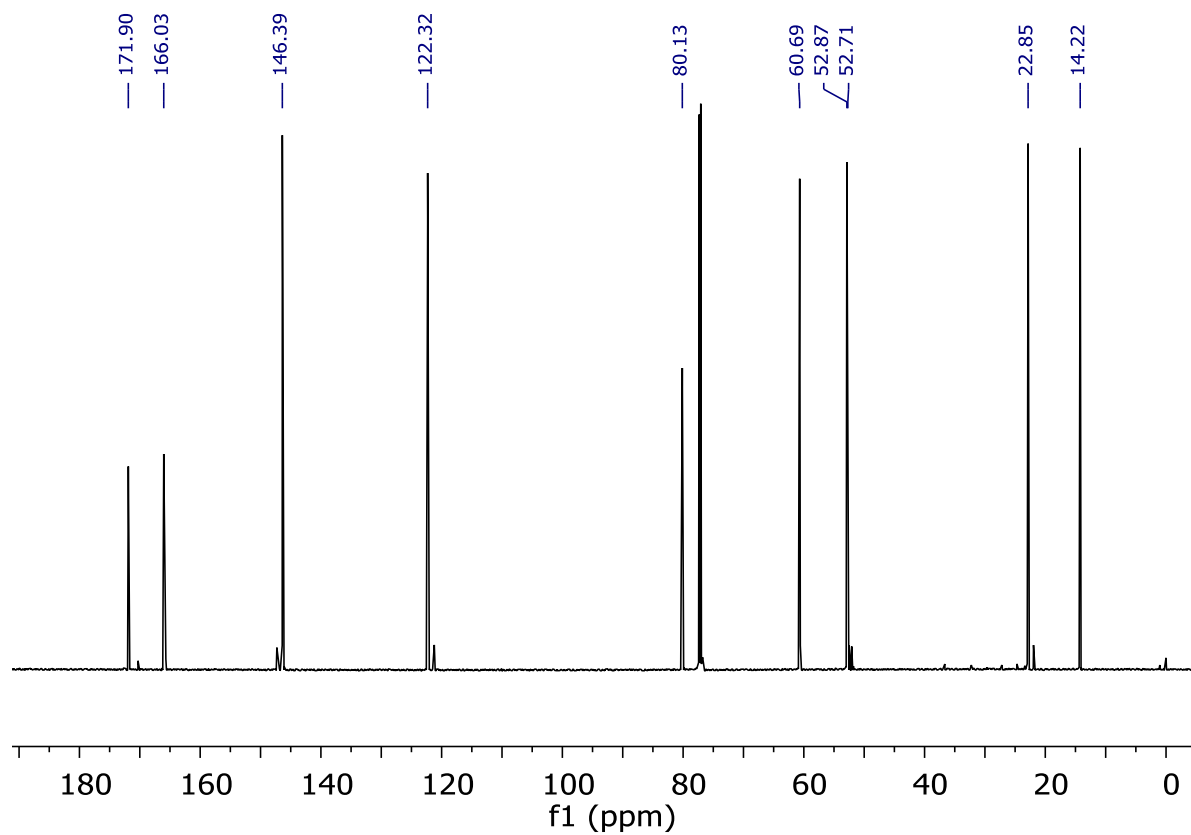
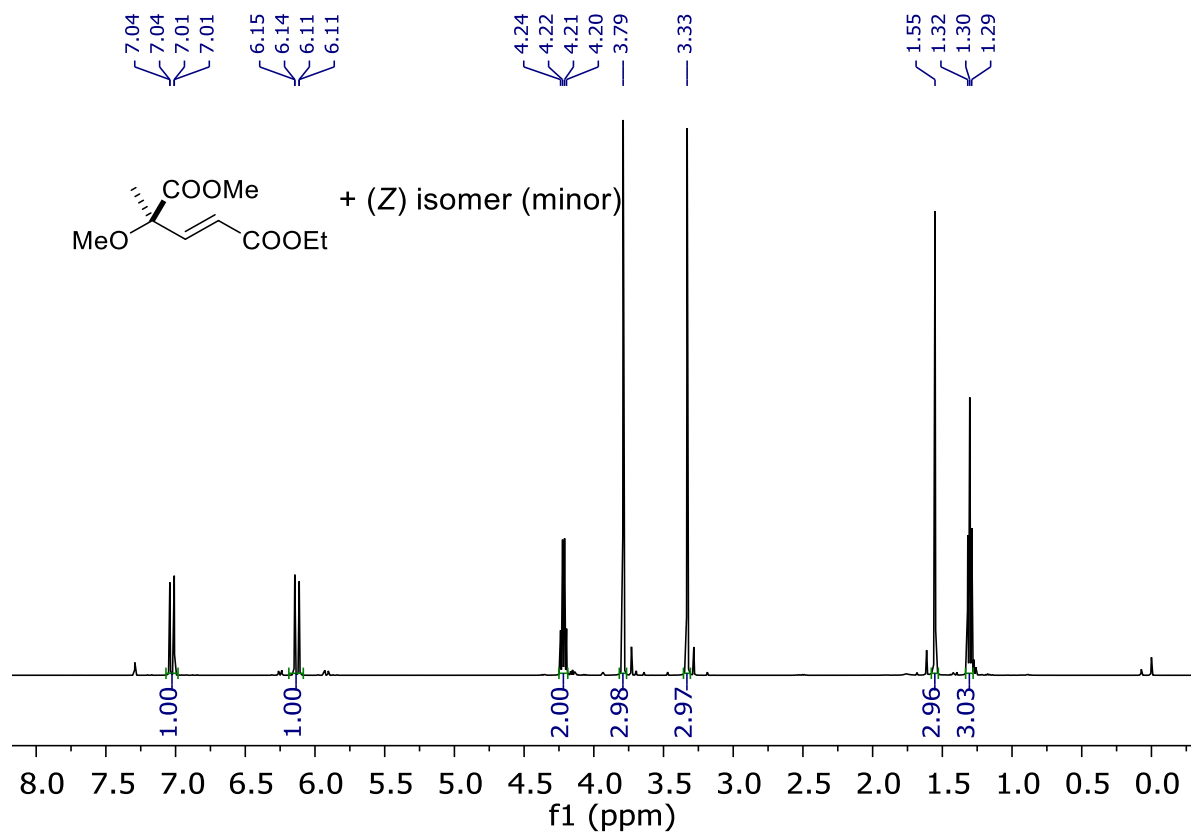


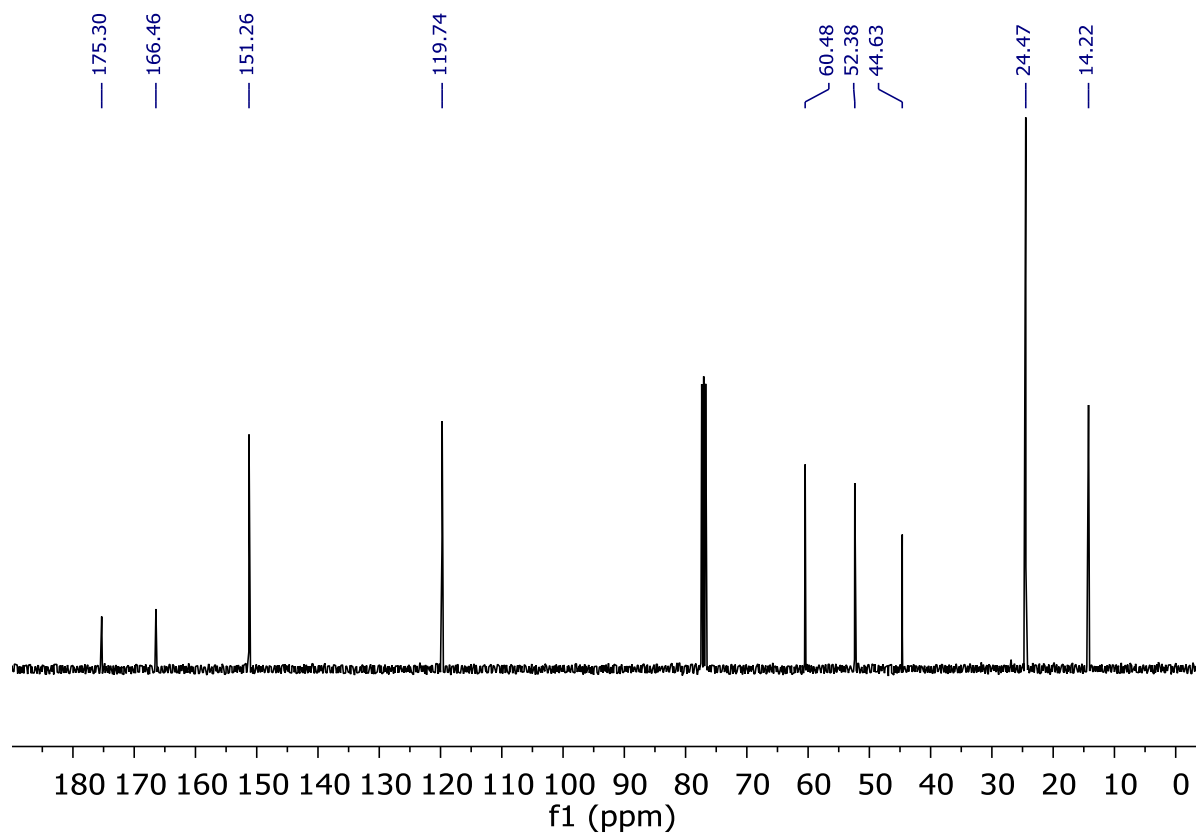
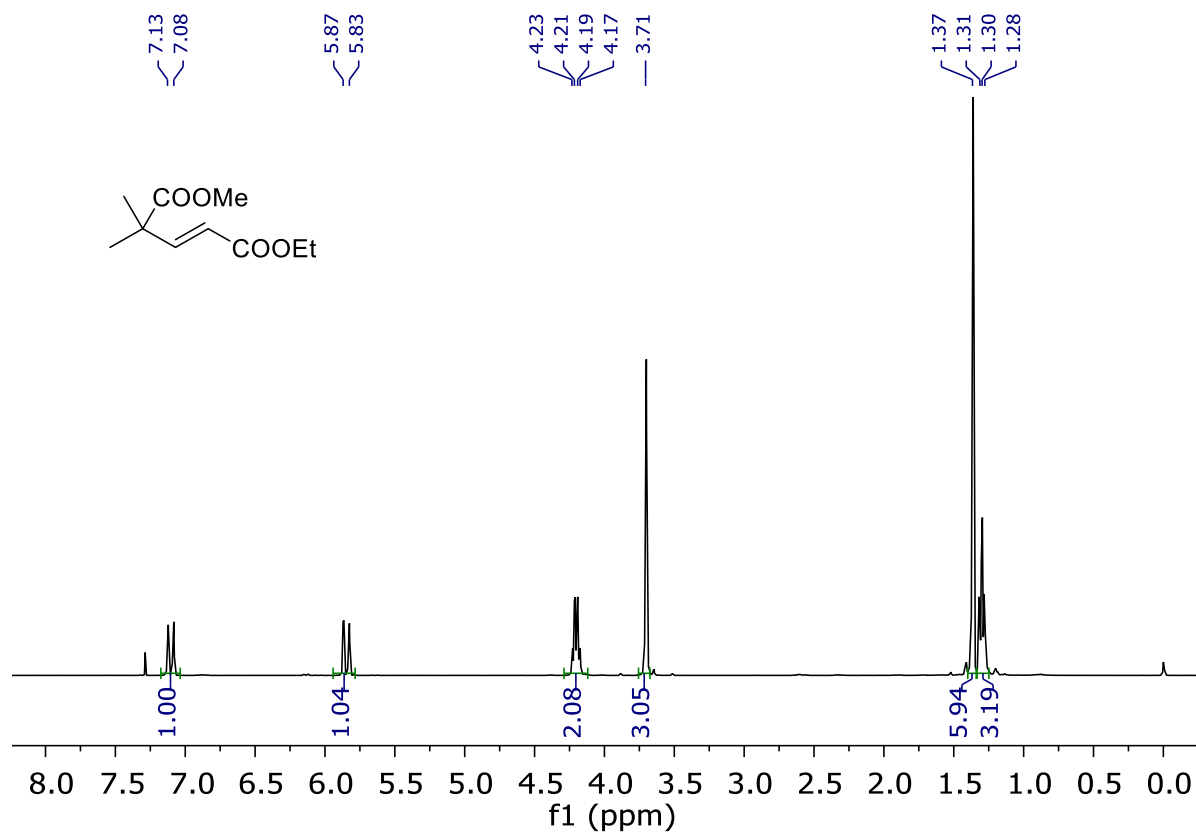


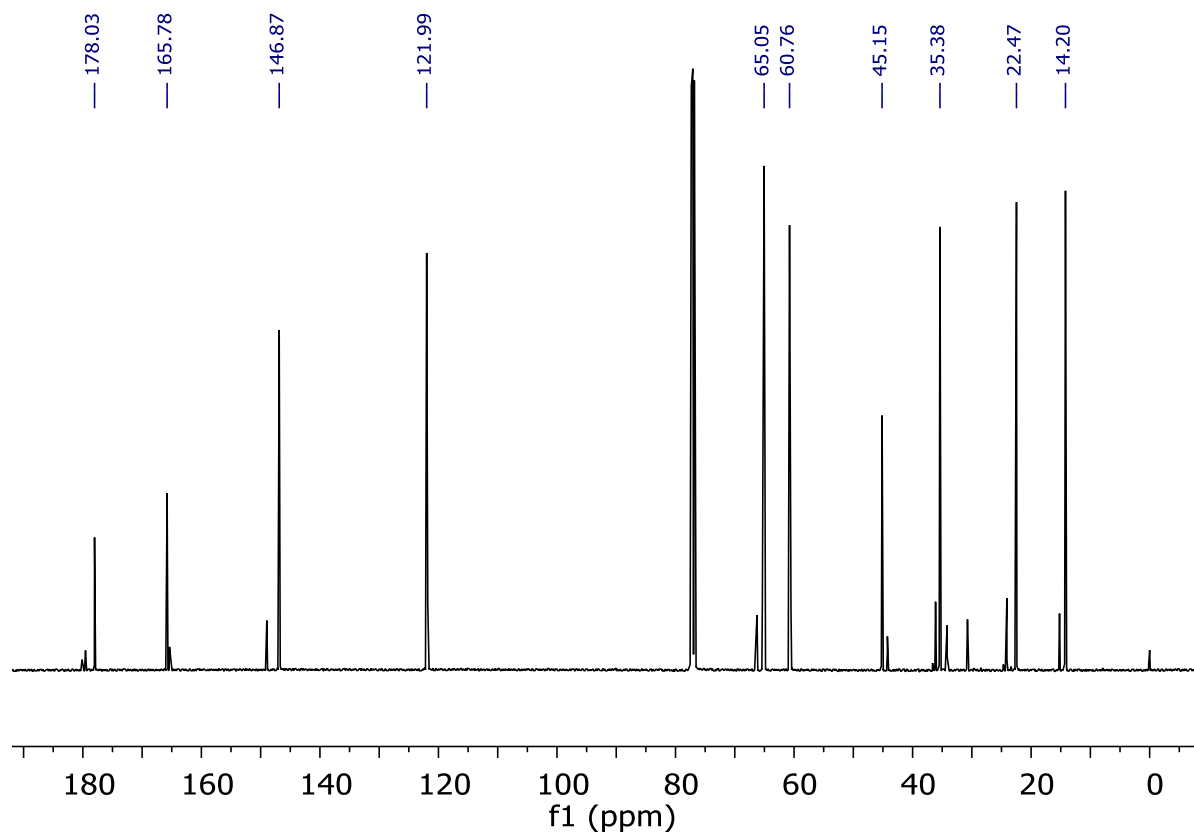
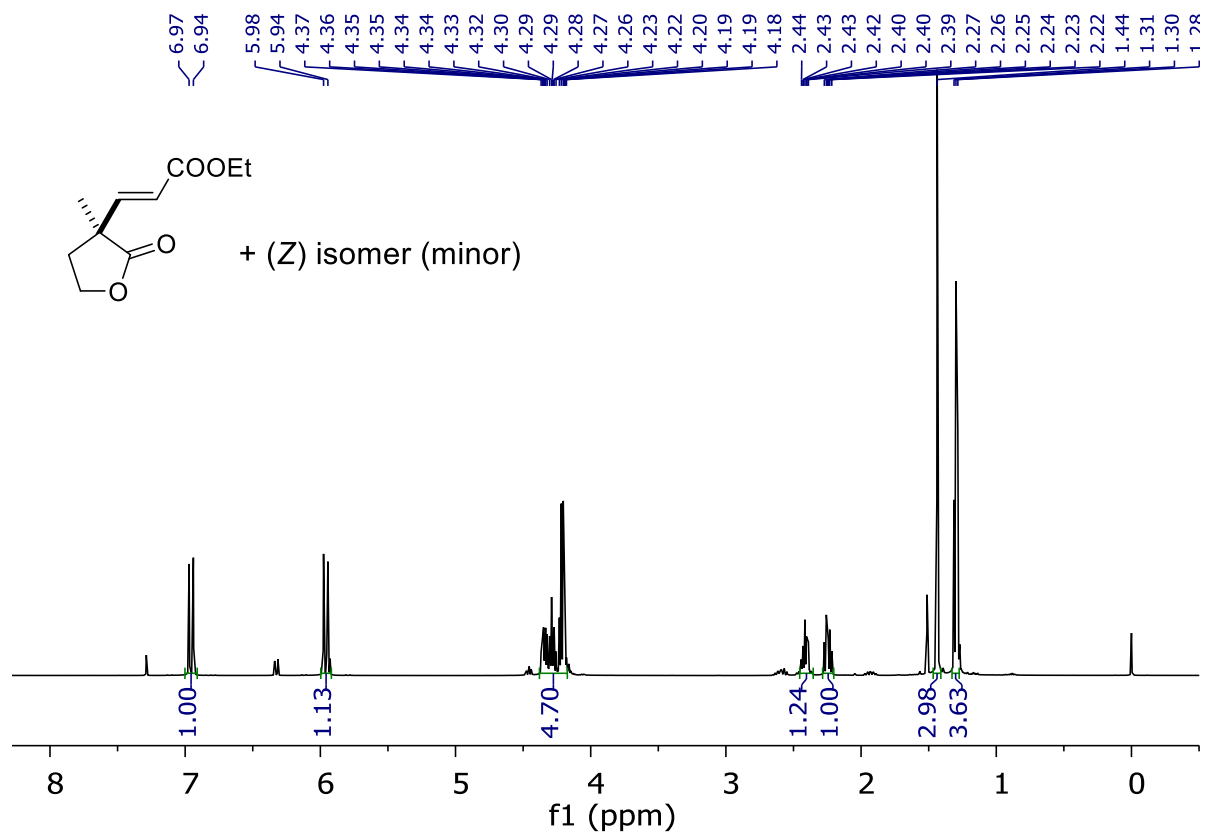
NMR Spectra for Chapter 4

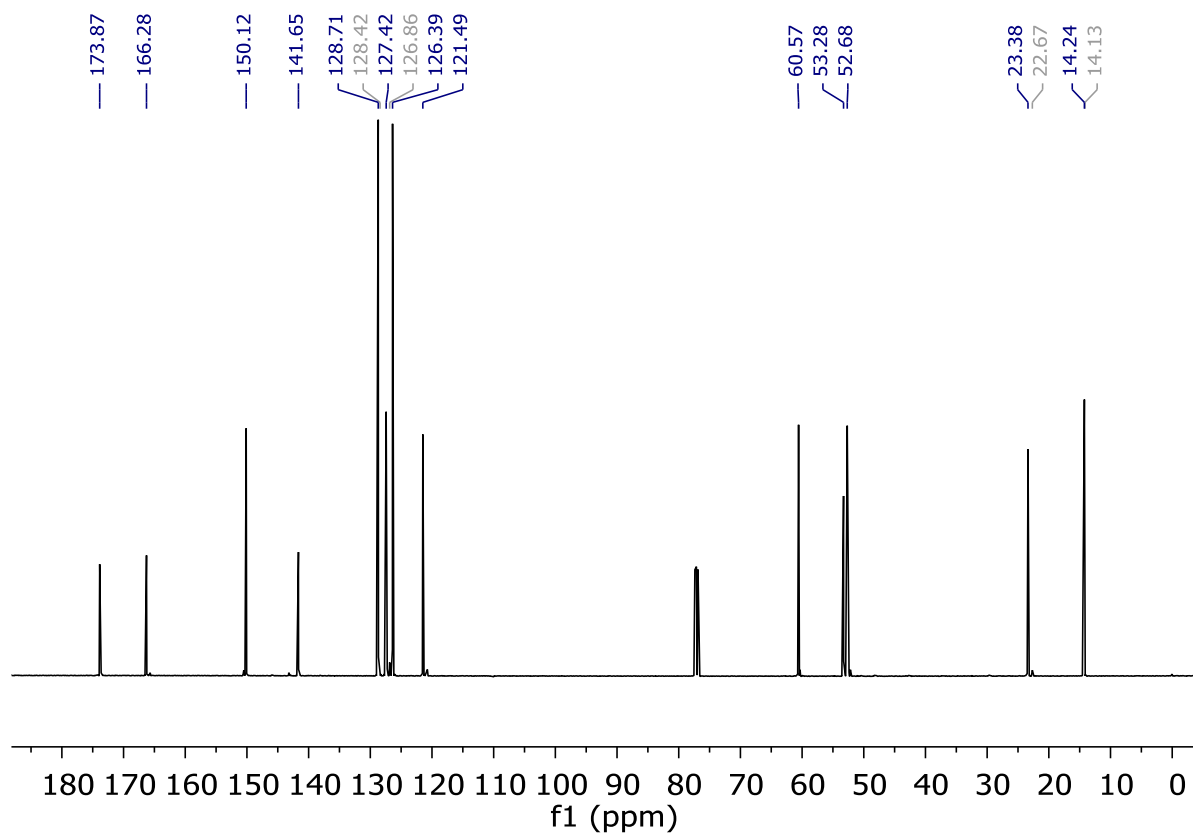
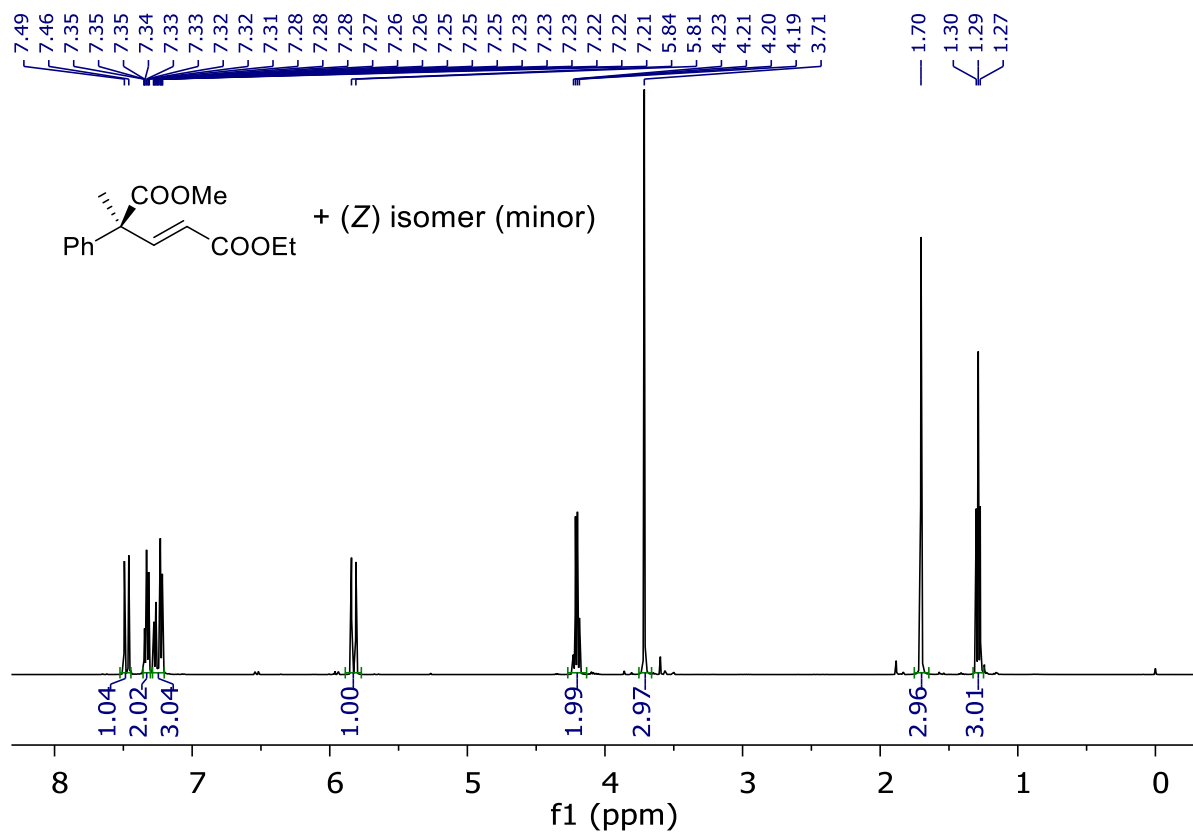


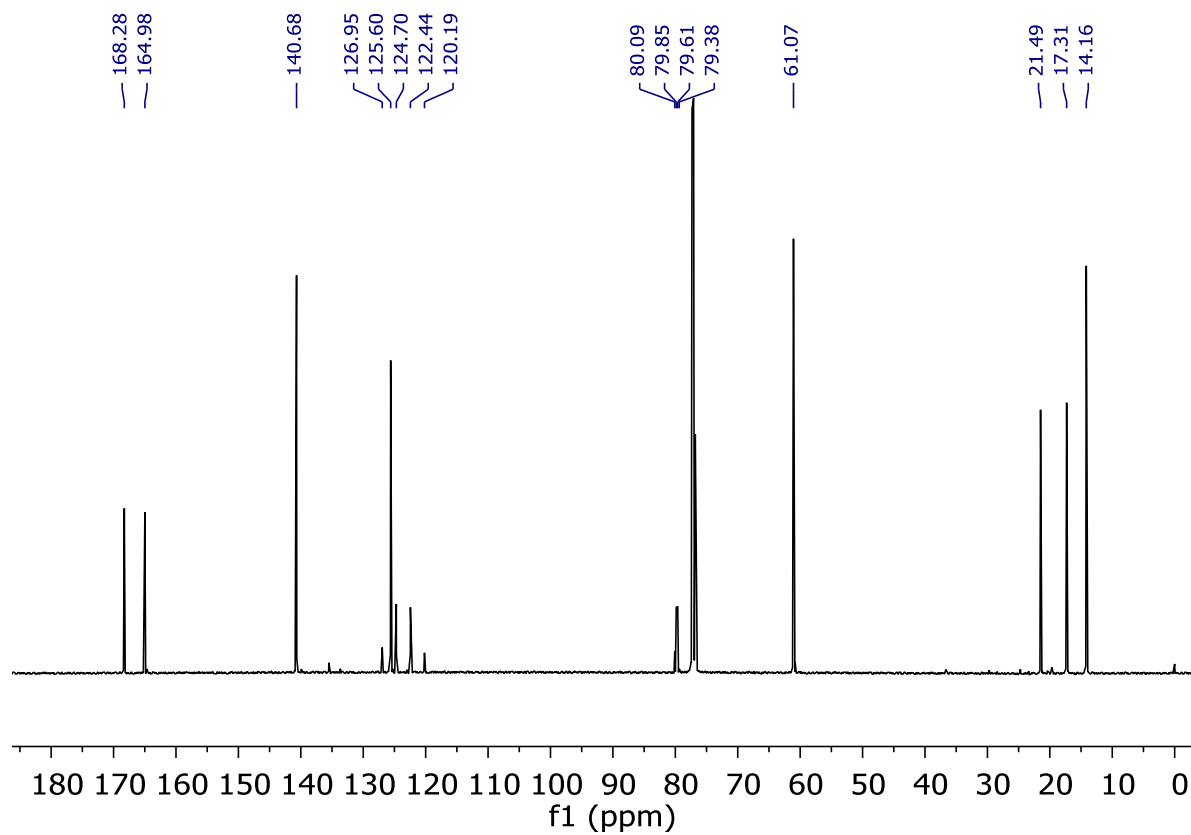
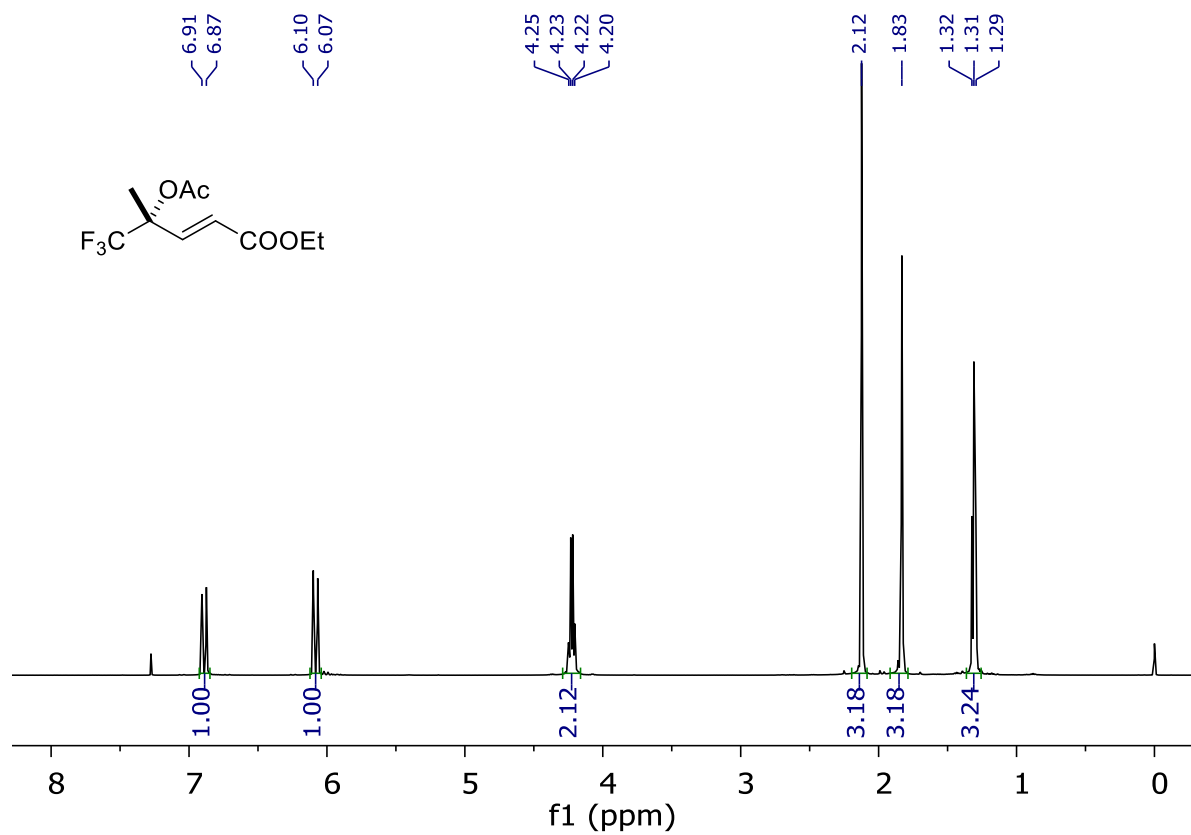


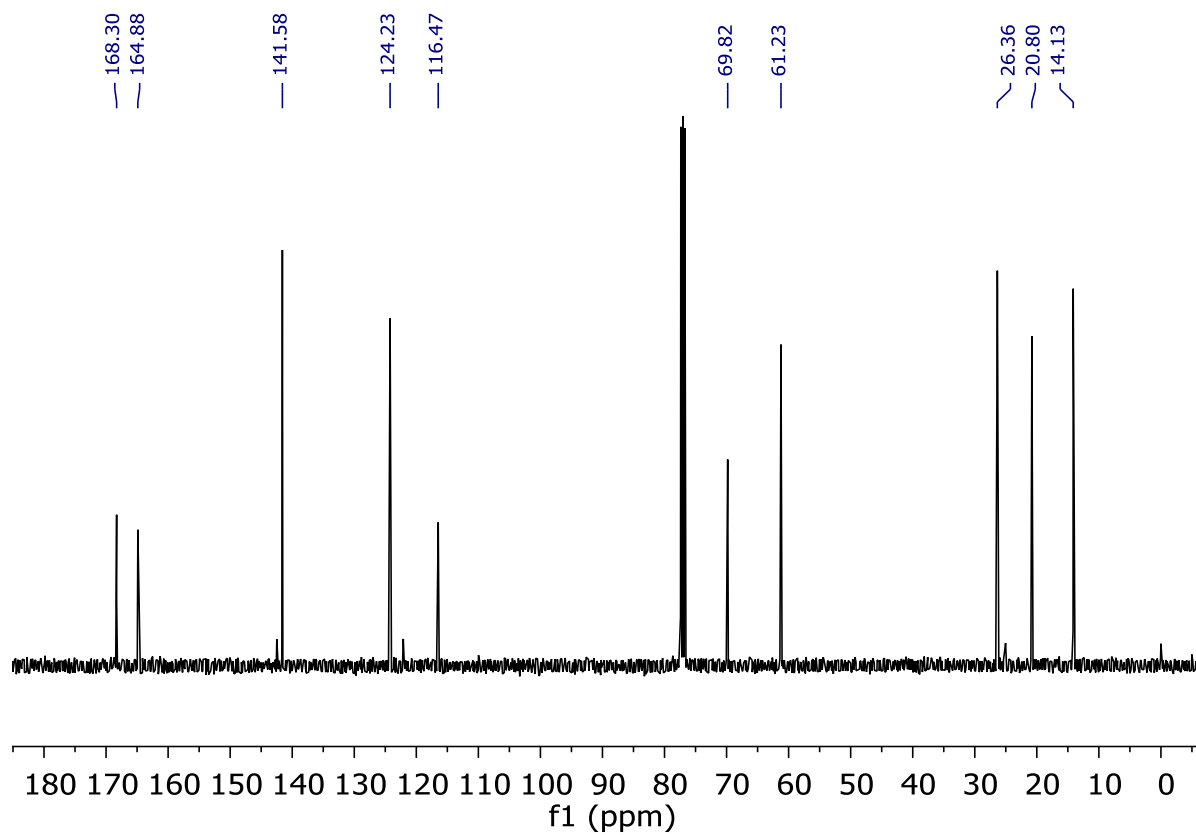
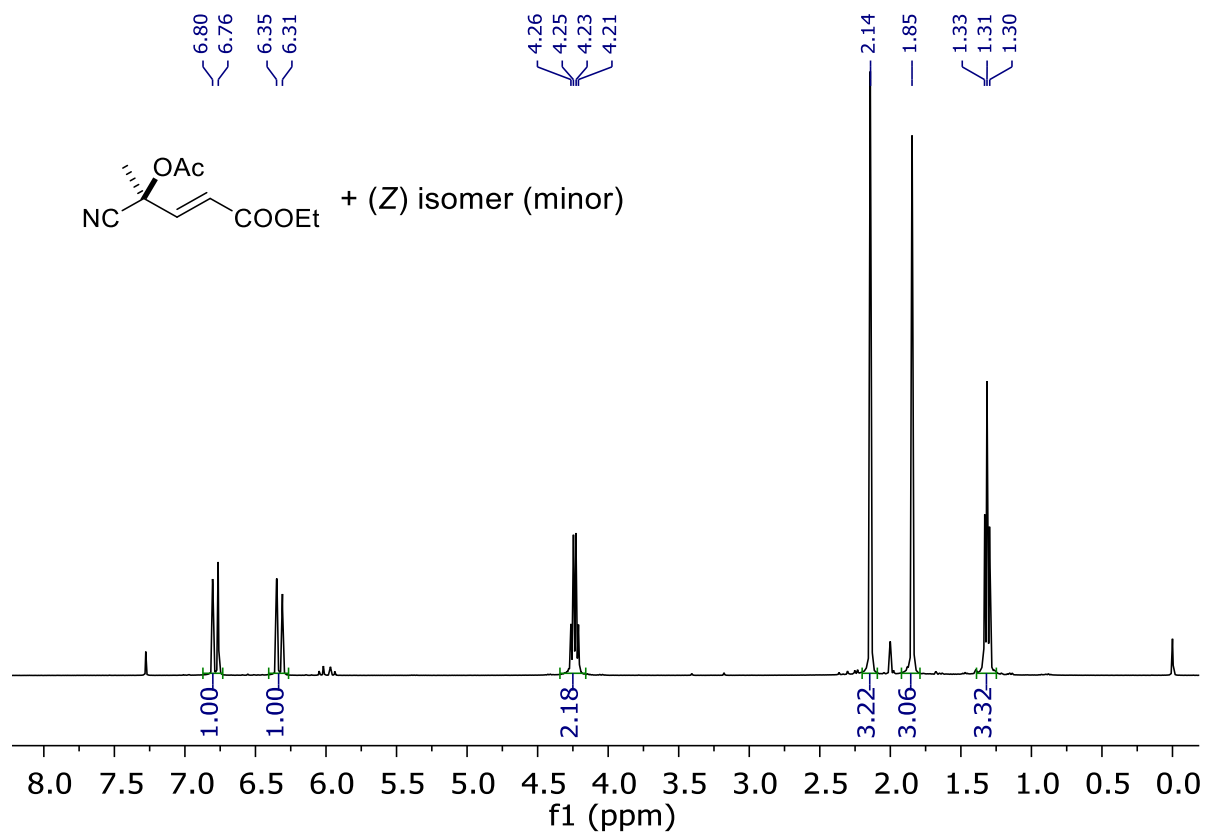


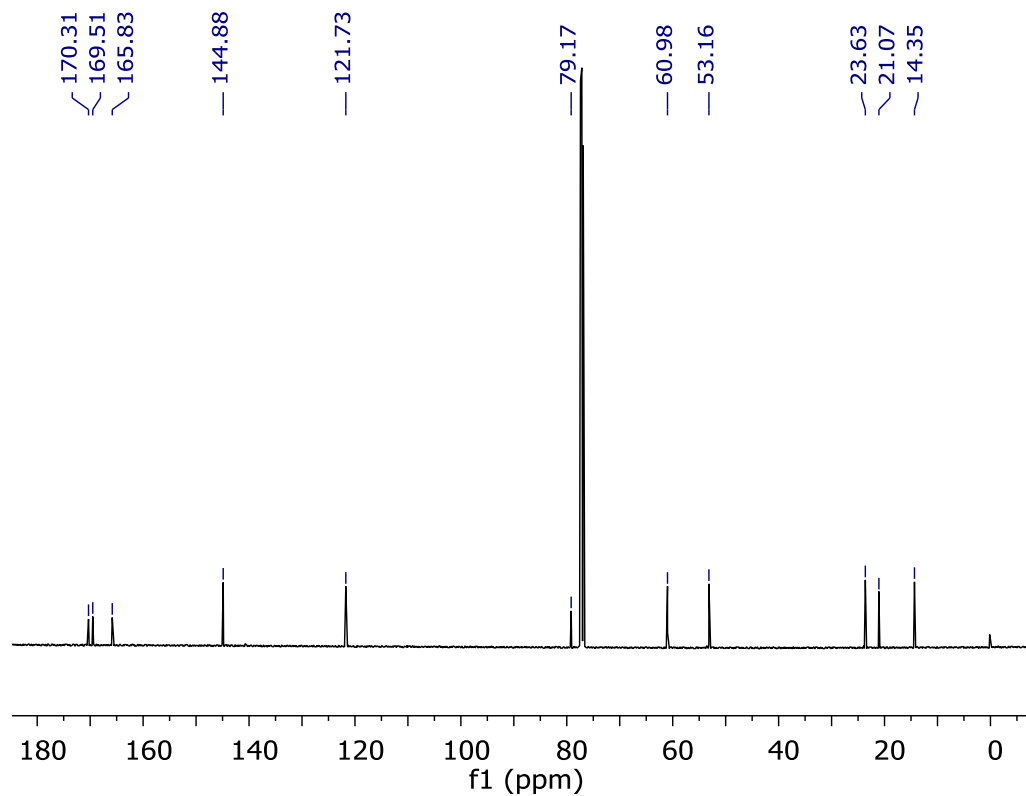
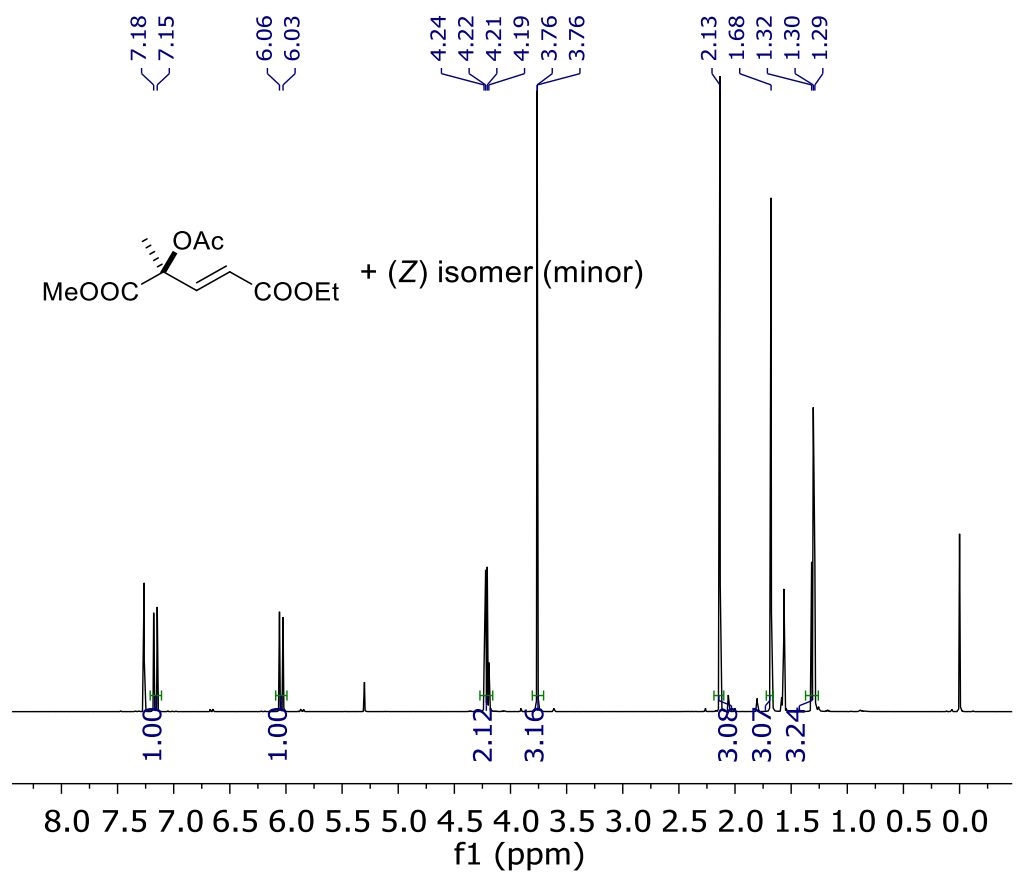


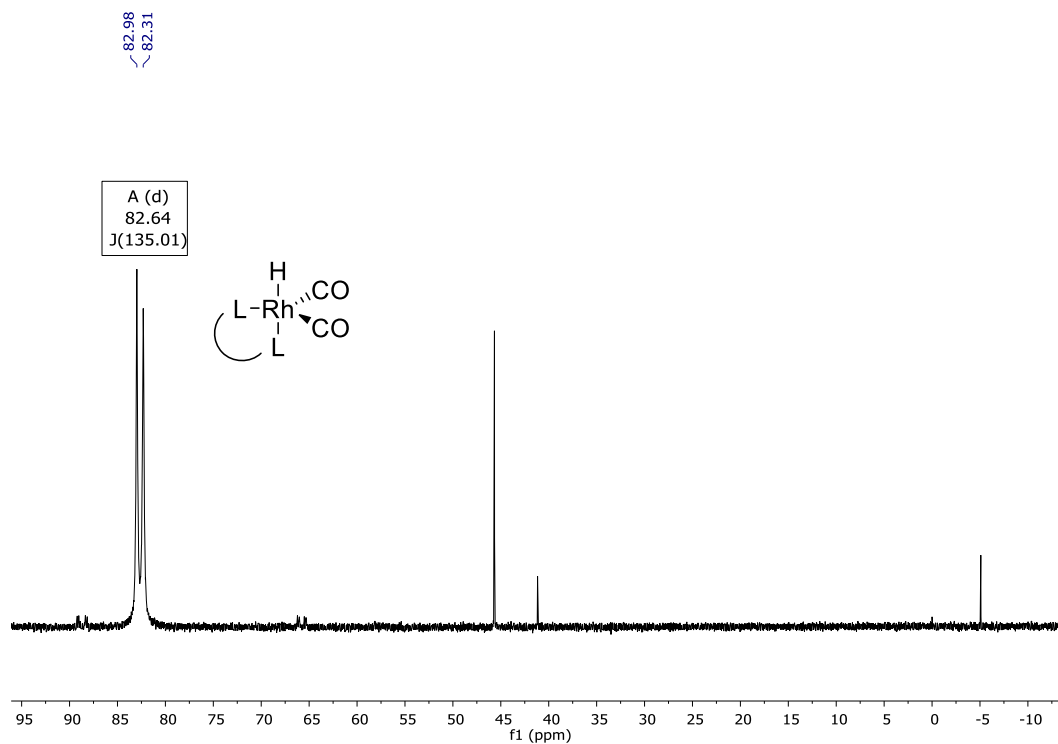




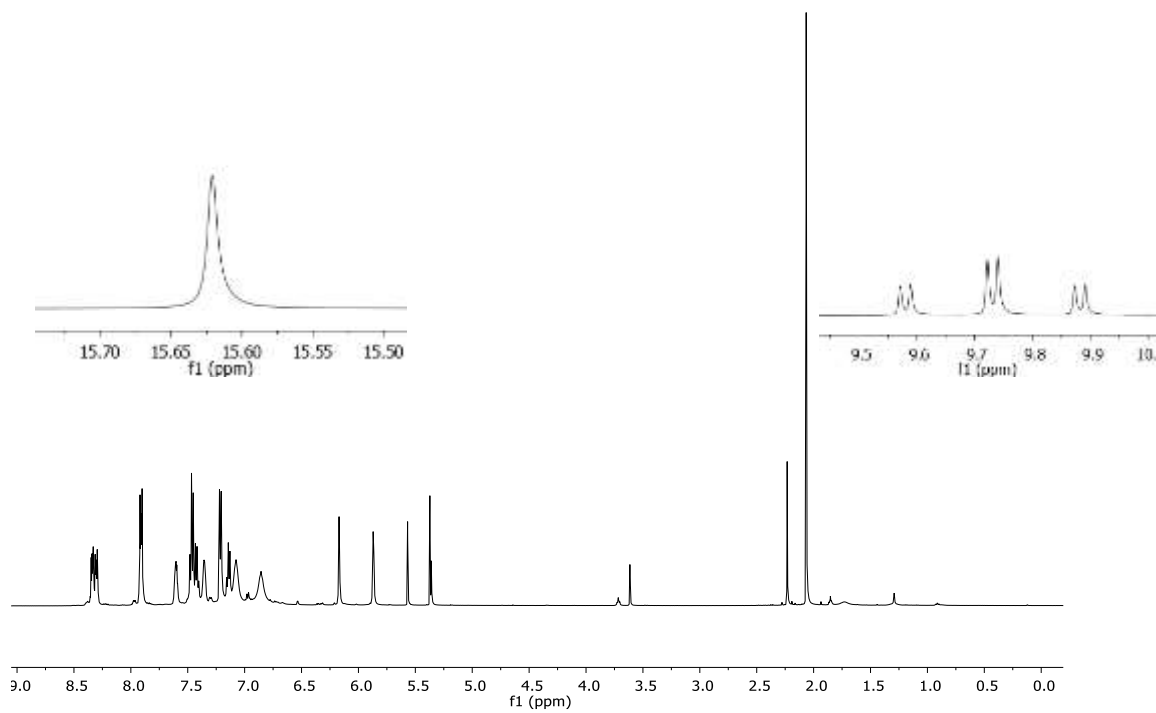




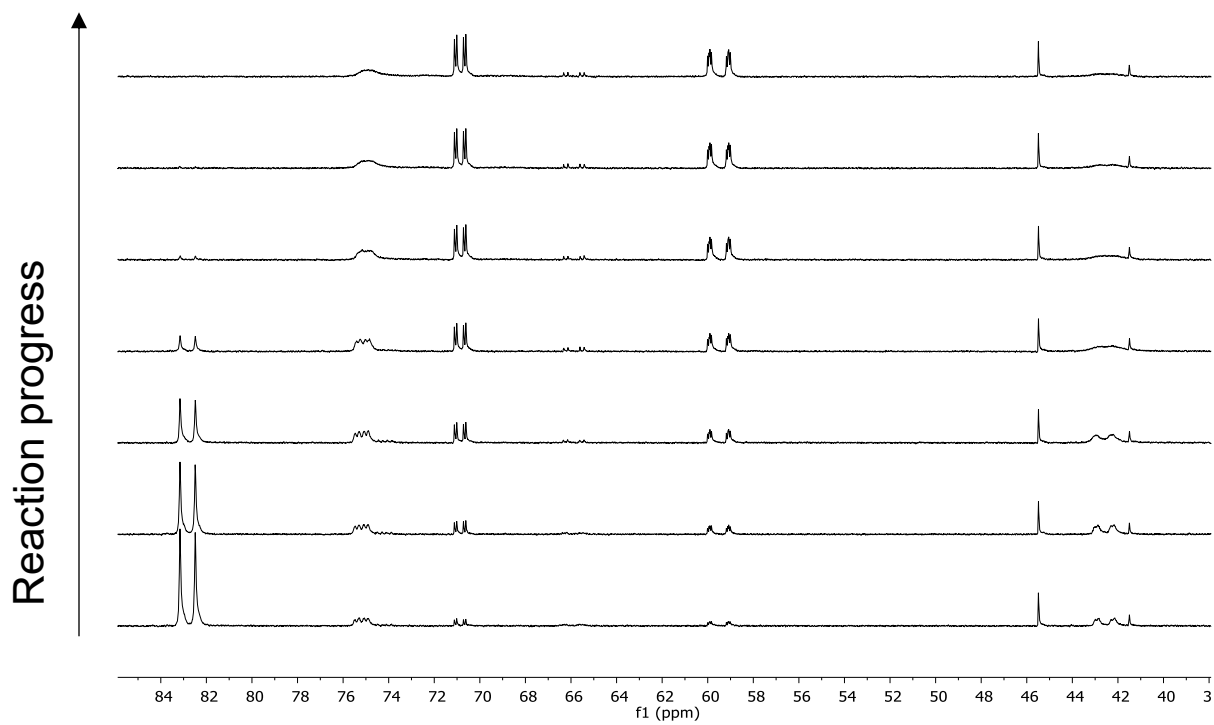




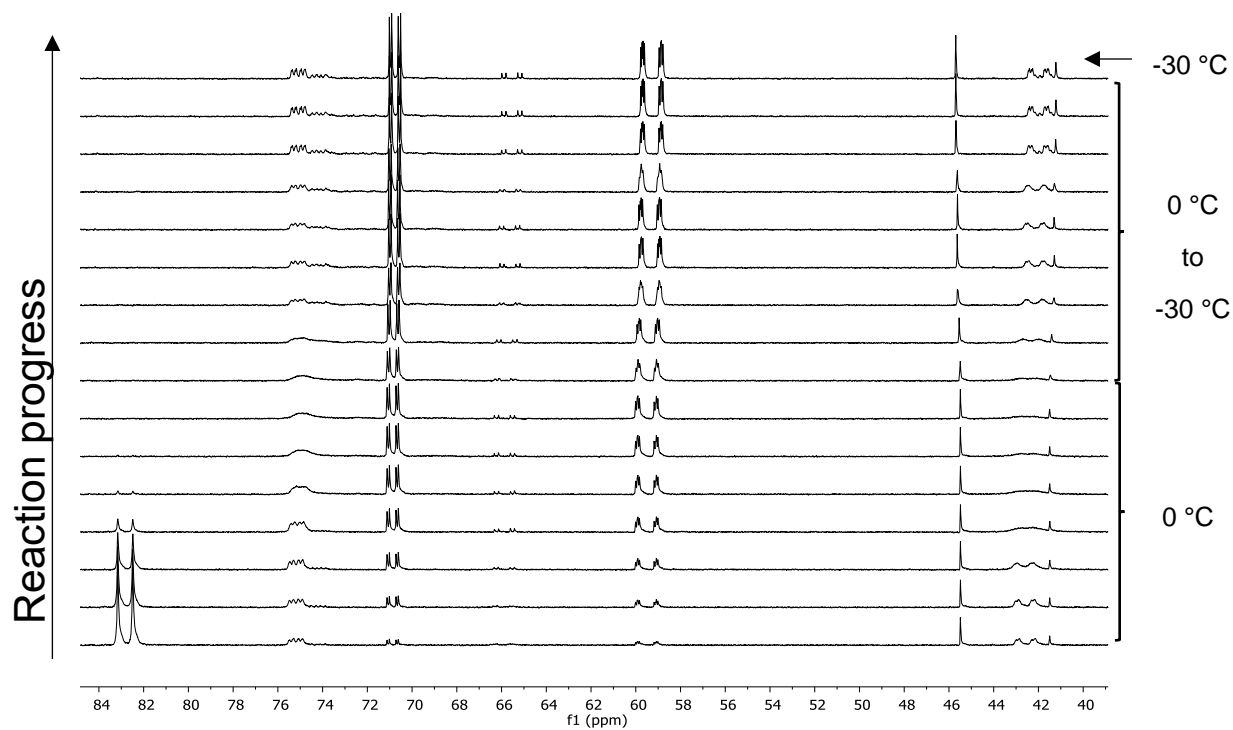
$^{31}\text{P}\{^1\text{H}\}$ of $[\text{Rh}(\text{H})(\text{CO})_2(\text{rac-L7})]$ (83 ppm), 1 atm CO, at 0 °C, before alkene injection



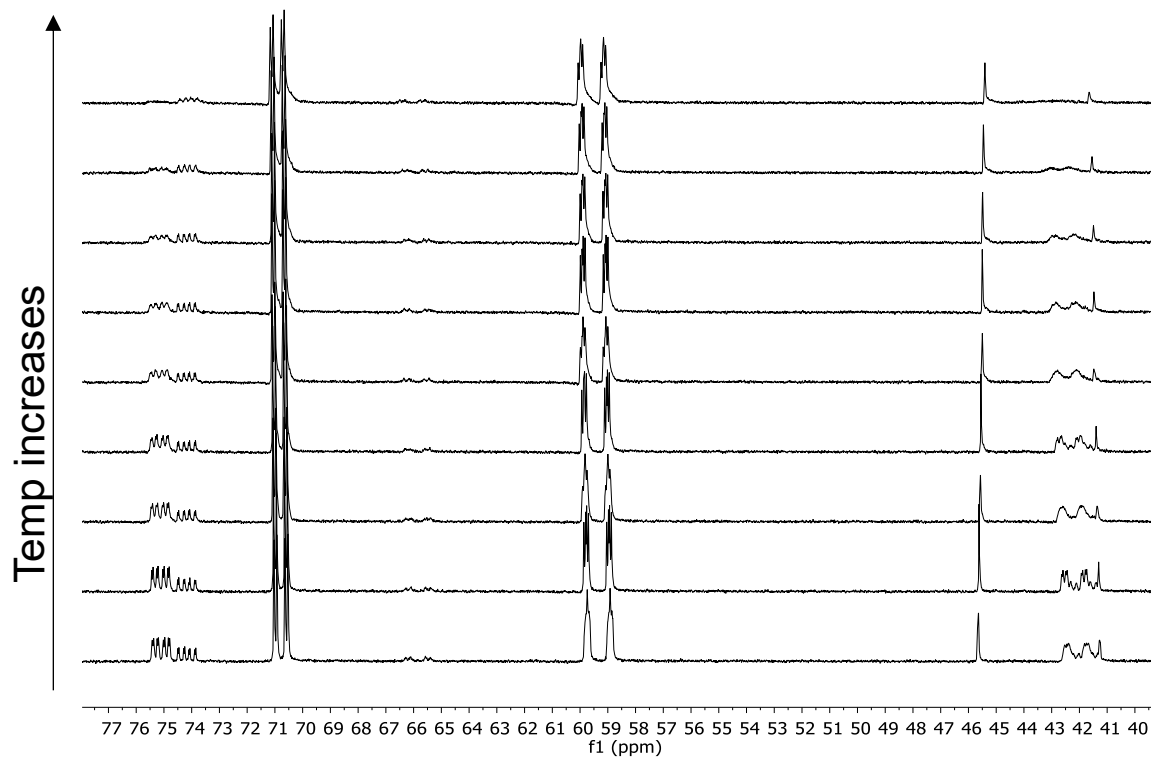
^1H of $[\text{Rh}(\text{H})(\text{CO})_2(\text{rac-L7})]$, 1 atm CO, at 0 °C, before alkene injection



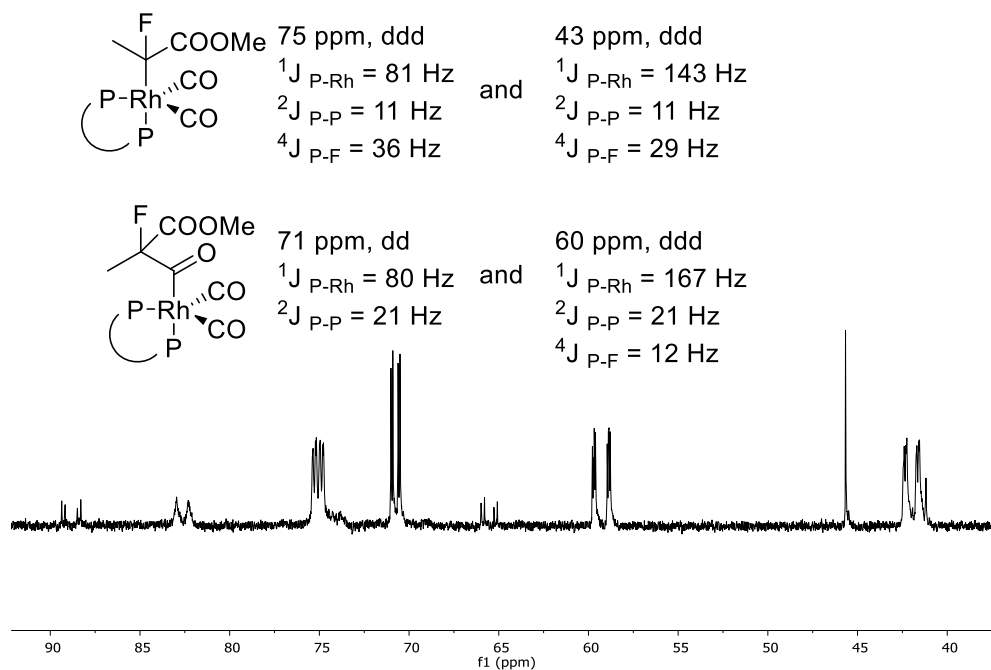
$^{31}\text{P}\{^1\text{H}\}$ monitoring the reaction between $[\text{Rh}(\text{H})(\text{CO})_2(\textit{rac}\text{-L7})]$ with methyl 2-fluoroacrylate (10 equiv.) at 0 °C, under 1 atm CO. Spectra every 3.5 min



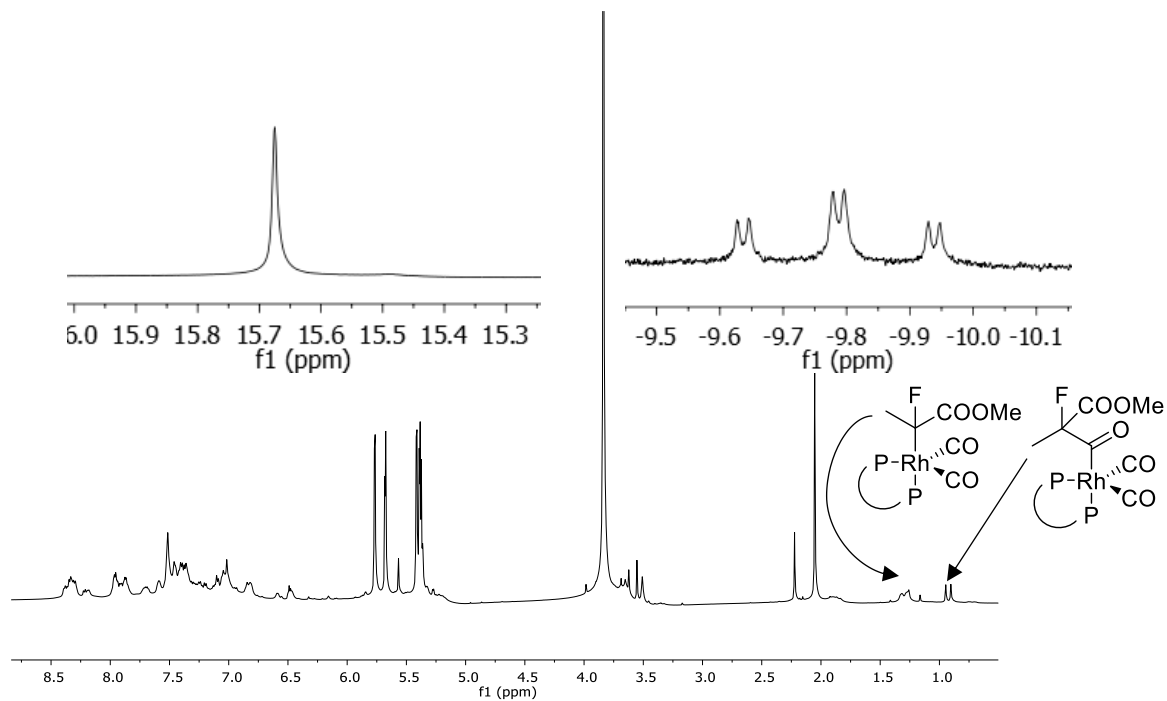
$^{31}\text{P}\{^1\text{H}\}$ monitoring the reaction between $[\text{Rh}(\text{H})(\text{CO})_2(\textit{rac}\text{-L7})]$ (83 ppm, 20 mM) with methyl 2-fluoroacrylate (10 equiv.), 1 atm CO, at 0 °C for 25 min (bottom seven spectra), then while temperature decreases from 0 °C to -30°C. Top spectrum is at -30°C. Spectra every 3.5 min.



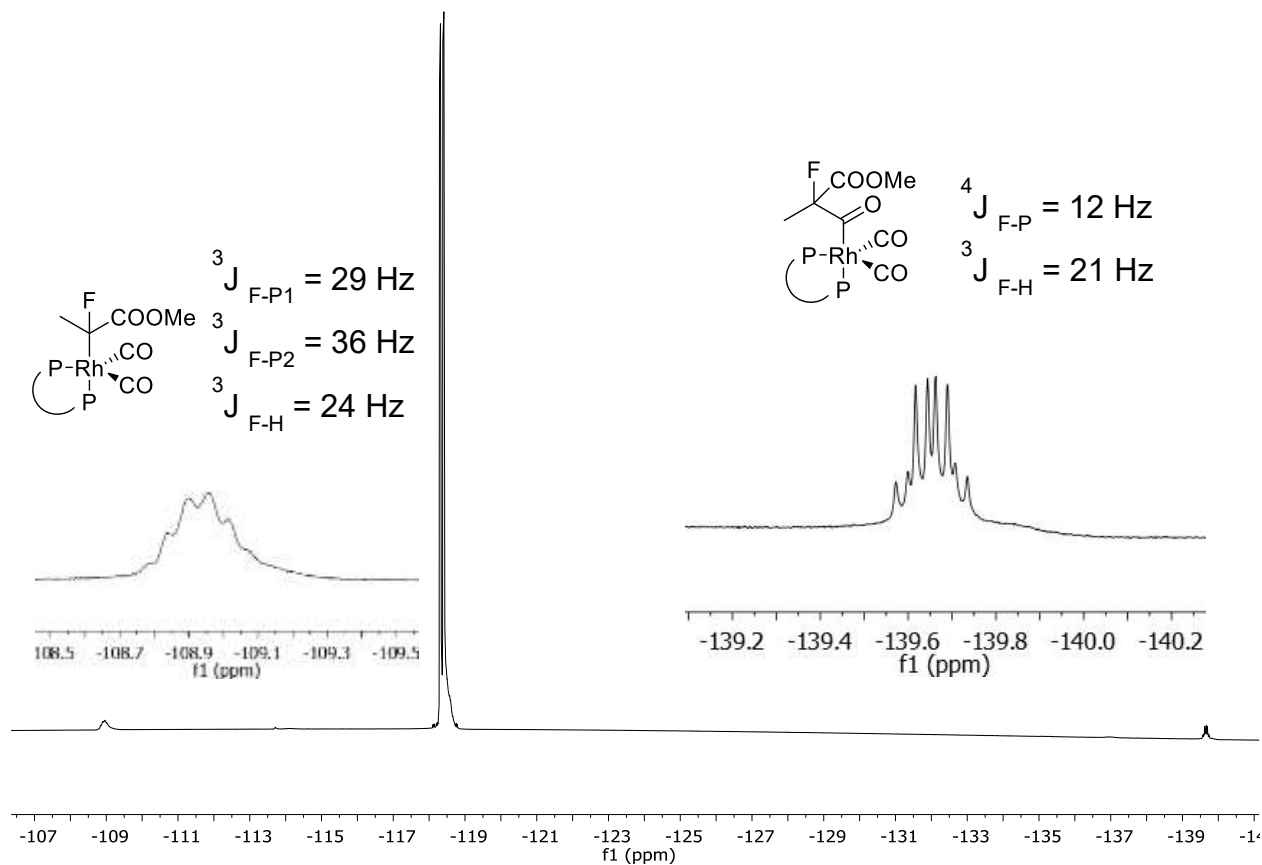
$^{31}\text{P}\{^1\text{H}\}$ monitoring the reaction between $[\text{Rh}(\text{H})(\text{CO})_2(\text{rac-L7})]$ with methyl 2-fluoroacrylate (10 equiv.), under 1 atm CO, while temperature increases from -30°C to room temperature. Spectra every 3.5 min



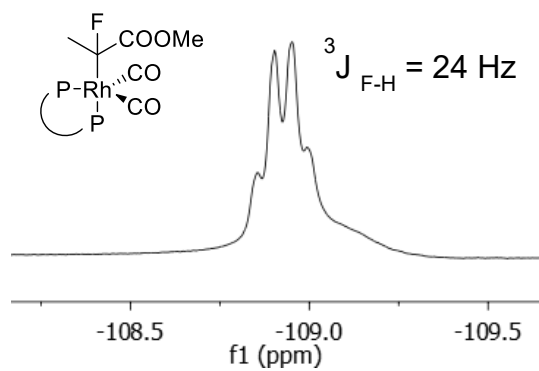
$^{31}\text{P}\{^1\text{H}\}$ NMR at $-30 \text{ }^\circ\text{C}$ during reaction between $[\text{Rh}(\text{H})(\text{CO})_2(\text{rac-L7})]$ (83 ppm) with methyl 2-fluoroacrylate.



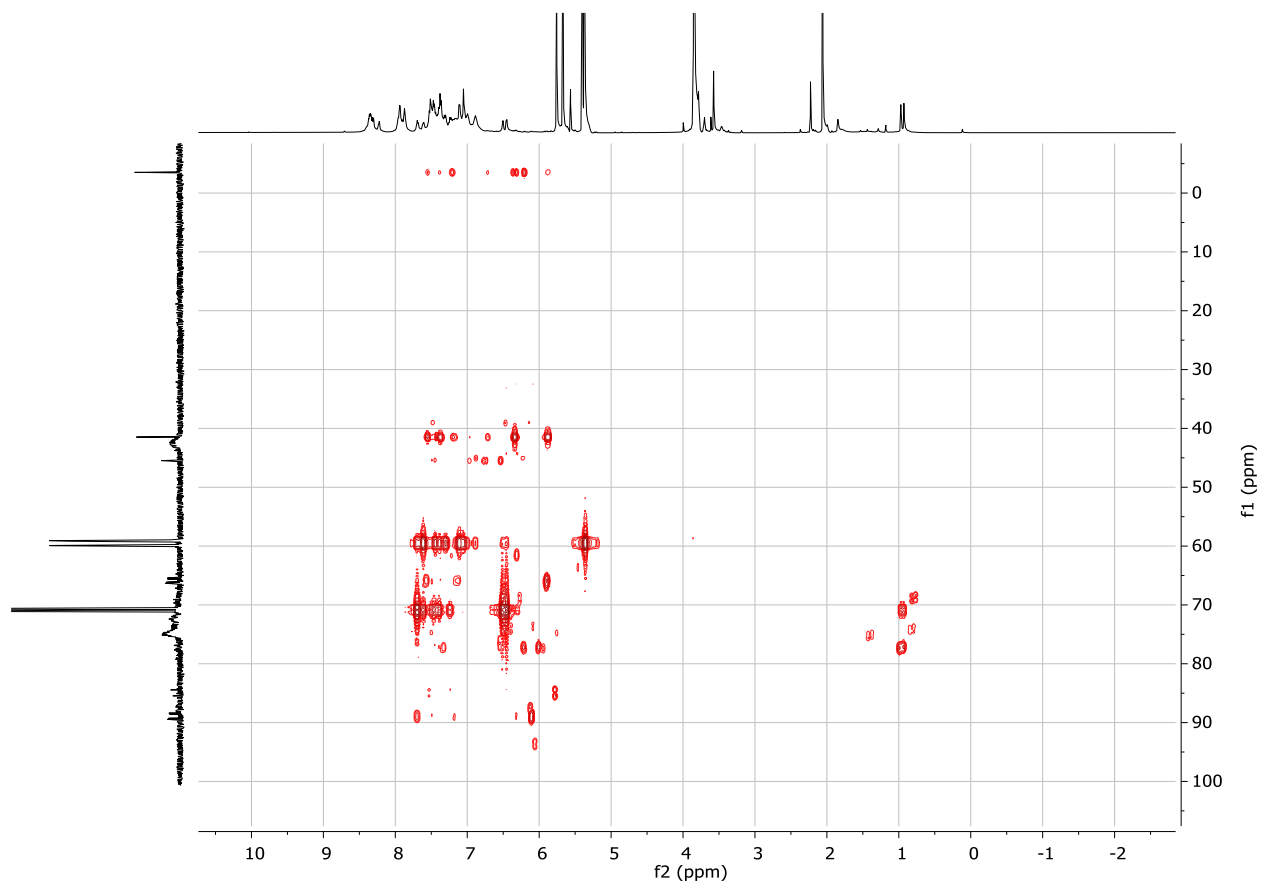
^1H NMR at $-30 \text{ }^\circ\text{C}$ during reaction between $[\text{Rh}(\text{H})(\text{CO})_2(\text{rac-L7})]$ with methyl 2-fluoroacrylate (10 equiv.)



^{19}F NMR at -30°C during reaction between $[\text{Rh}(\text{H})(\text{CO})_2(\text{rac-L7})]$ with methyl 2-fluoroacrylate (-118 ppm)

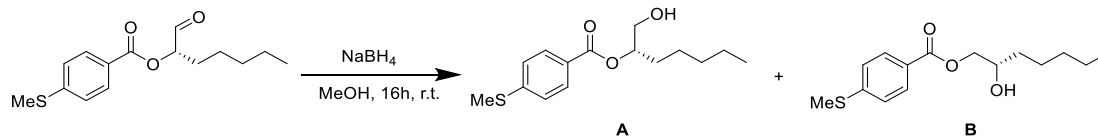


$^{19}\text{F}\{^{31}\text{P}\}$ NMR at -30°C showing loss of F-P coupling for the alkyl intermediate

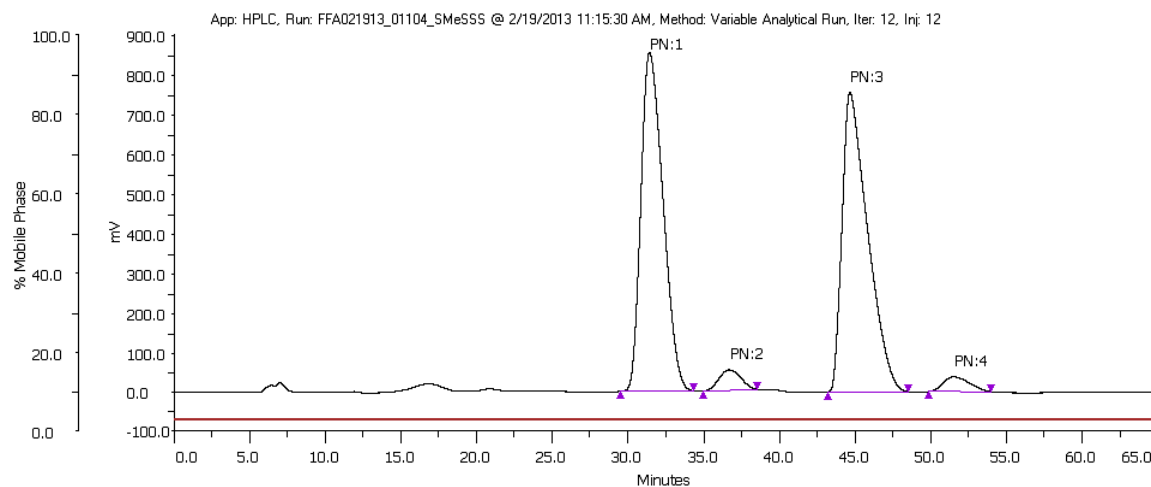
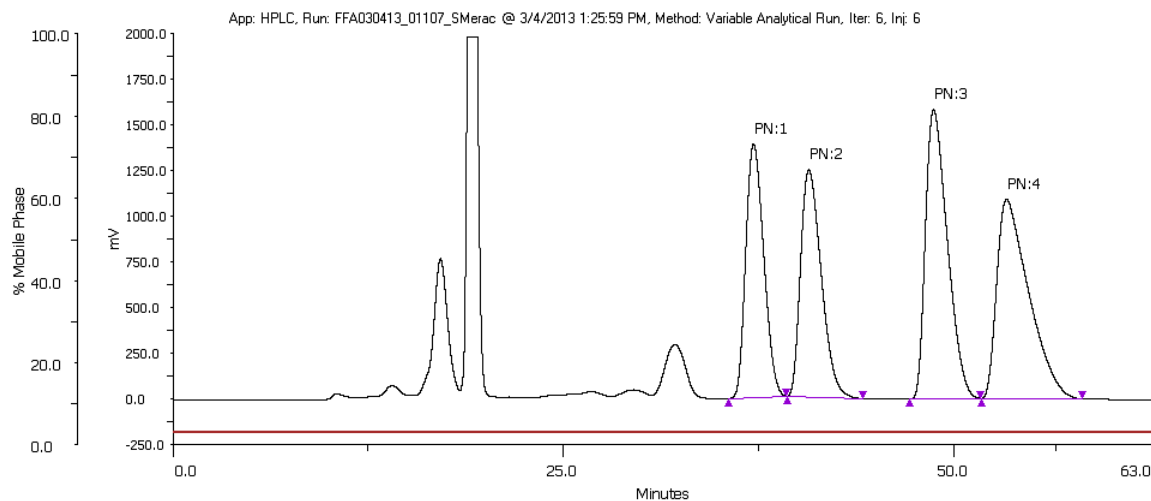


^{31}P - ^1H HMBC at 0 °C during reaction between $[\text{Rh}(\text{H})(\text{CO})_2(\text{rac-L7})]$ with methyl 2-fluoroacrylate

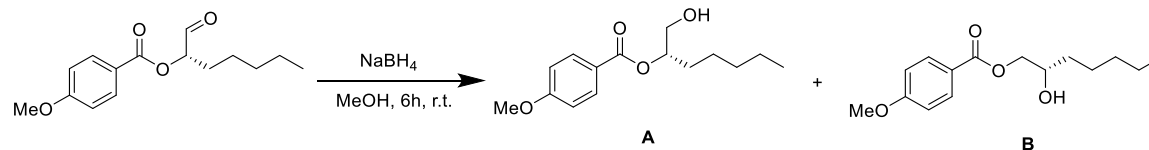
HPLC and SFC traces for Chapter 2



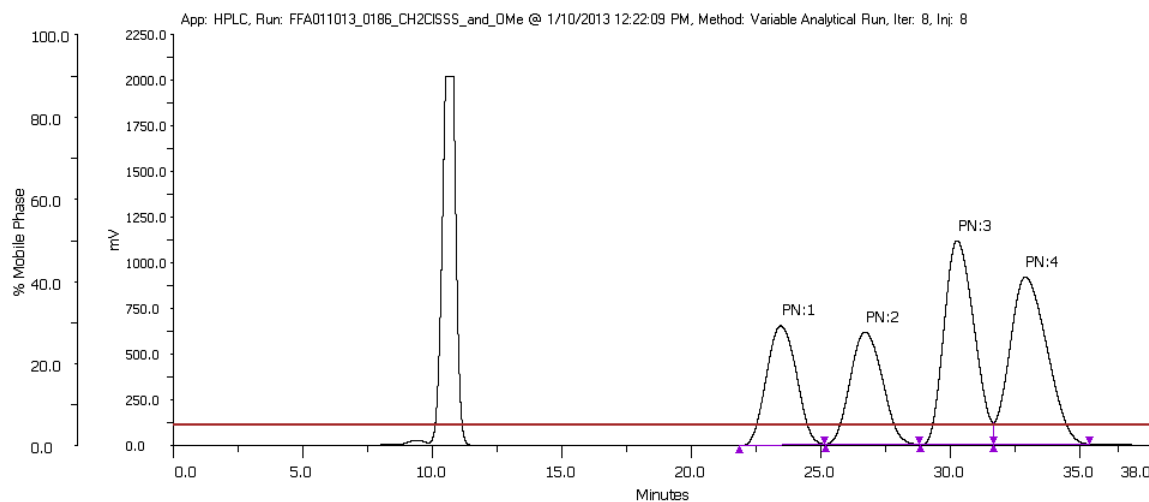
Resolution by HPLC:



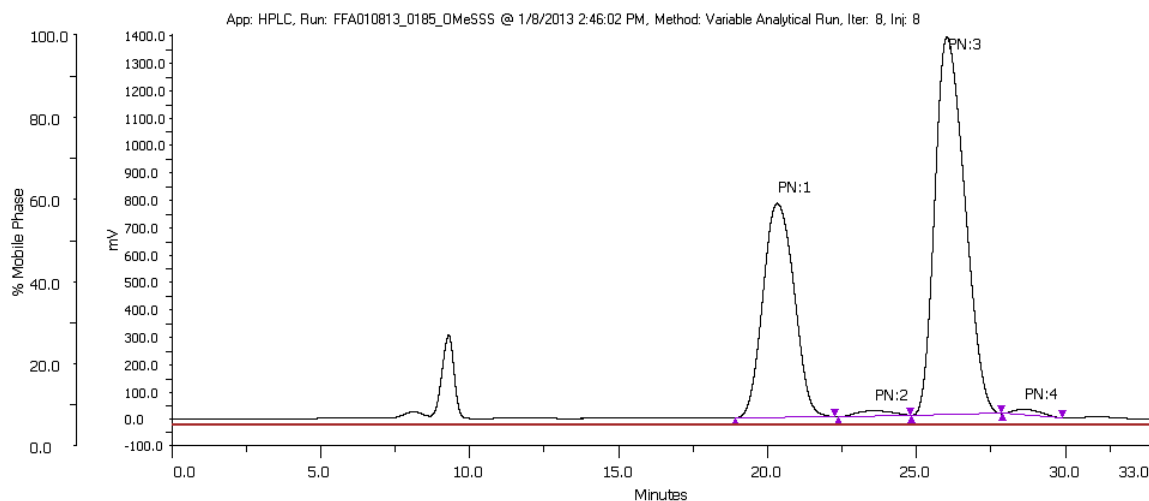
Peak Number (PN)	isomer	r_T (min)	Area ($\mu\text{Vmin} \times 100$)	% Area
1	A	31.5	144958230.8322	46.905
2	A	36.7	8599526.6365	2.783
3	B	44.7	148067052.4987	47.911
4	B	51.6	7419669.9993	2.401



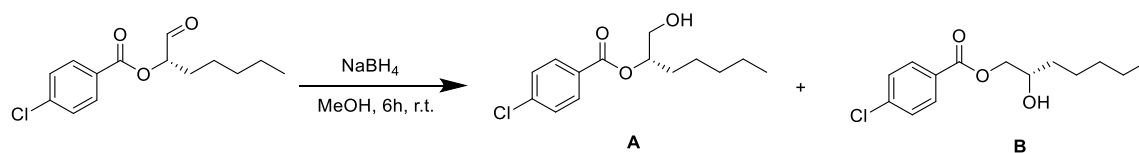
Resolution by HPLC:



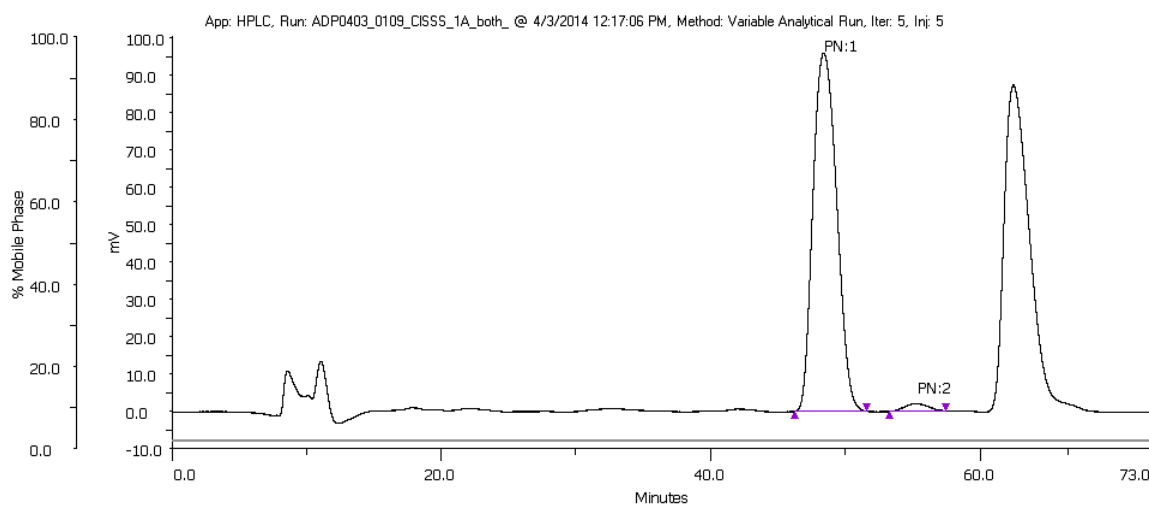
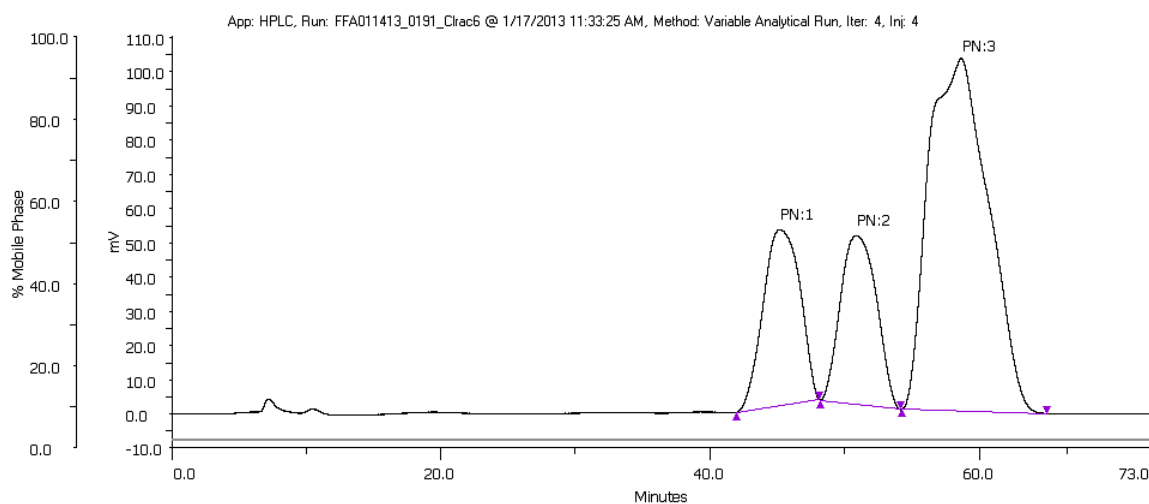
Chiral run: peaks show up at earlier retention times compared to racemic due to different flow rates used (0.8 ml/min for chiral run and 0.7 mL/min for racemic)



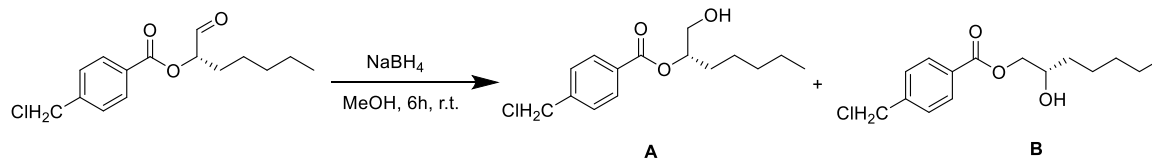
Peak Number (PN)	isomer	t_R (min)	Area ($\mu\text{Vmin} \times 100$)	% Area
1	A	20.3	94911962.1362	36.417
2	A	23.6	2720385.831	1.044
3	B	26.1	160681660.8333	61.653
4	B	28.7	2308812.7922	0.886



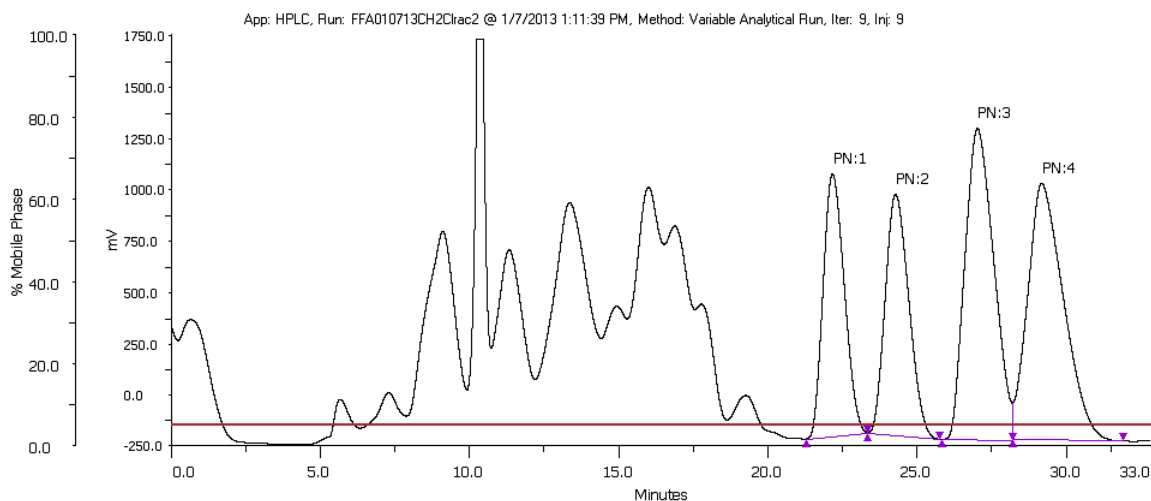
Resolution by HPLC:



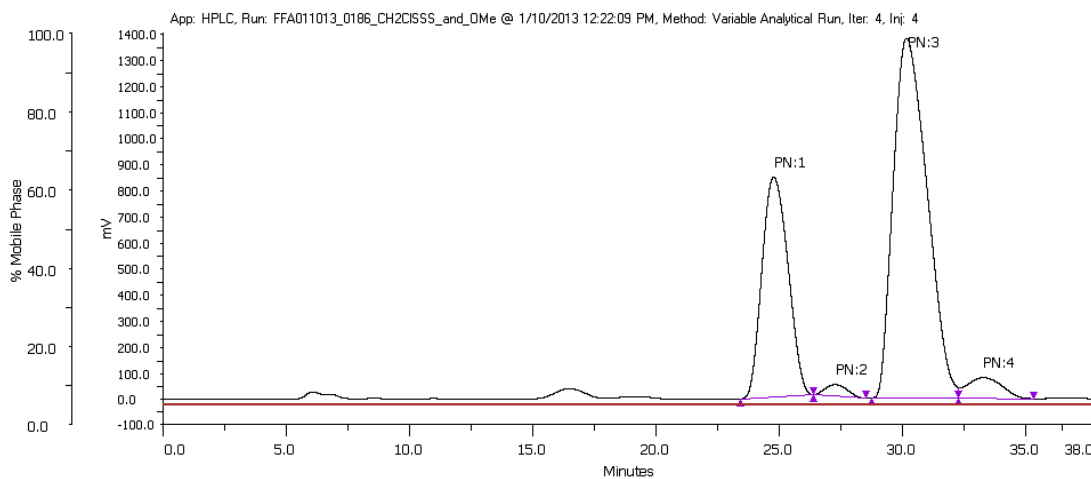
Peak Number (PN)	isomer	r_T (min)	Area ($\mu\text{Vmin} \times 100$)	% Area
1	A	48.4	1955407.9174	98.008
2	A	55.3	397457.6244	1.992



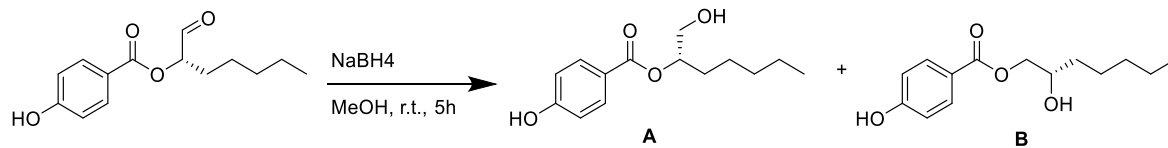
Resolution by HPLC:



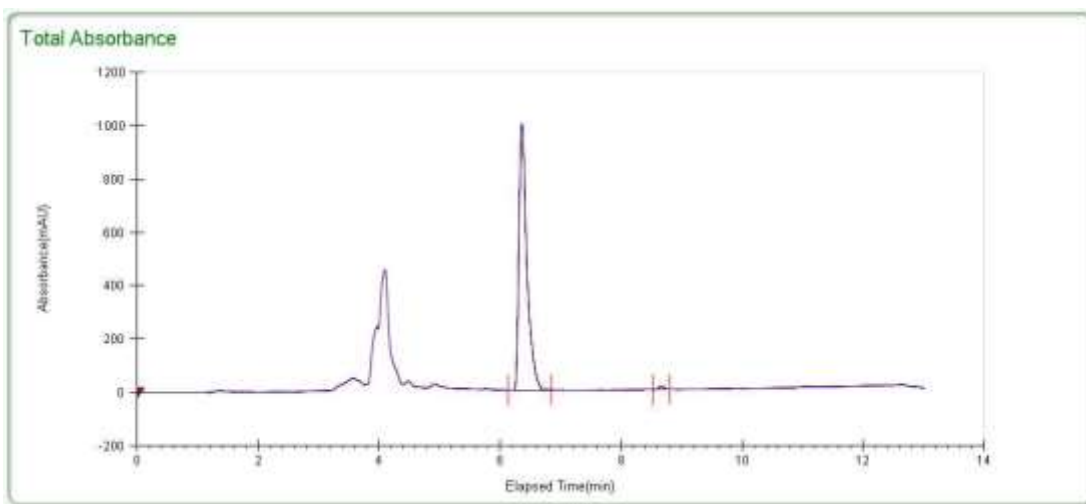
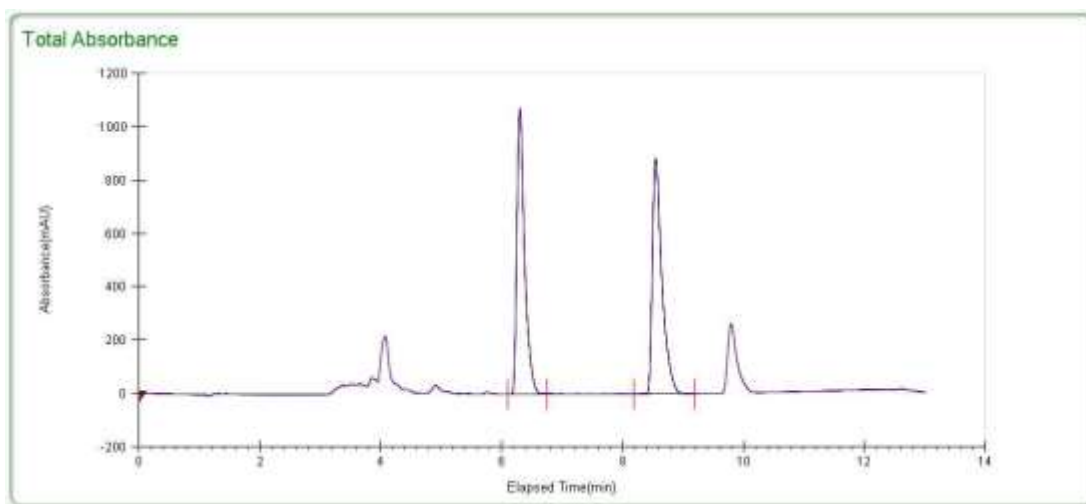
Chiral run: peaks show up at longer retention times compared to racemic due to different flow rates used (0.7 ml/min for chiral run and 0.8 mL/min for racemic)



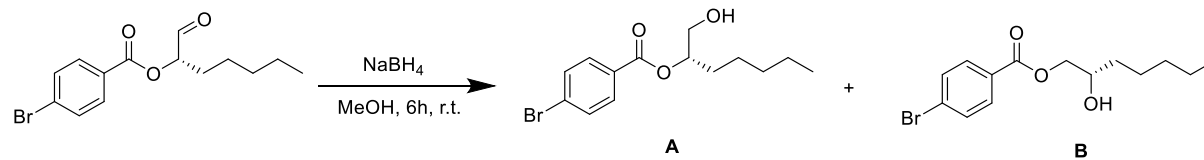
Peak Number (PN)	isomer	t_R (min)	Area ($\mu\text{Vmin} \times 100$)	% Area
1	A	24.8	103527229.1501	30.298
2	A	27.3	4598088.8746	1.346



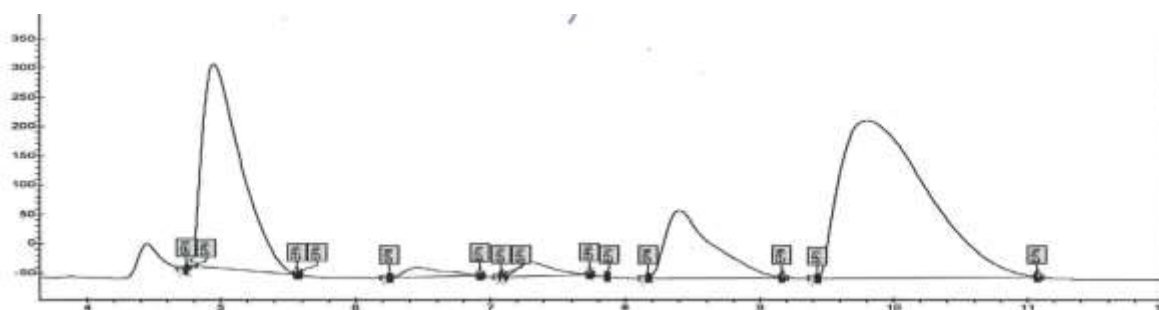
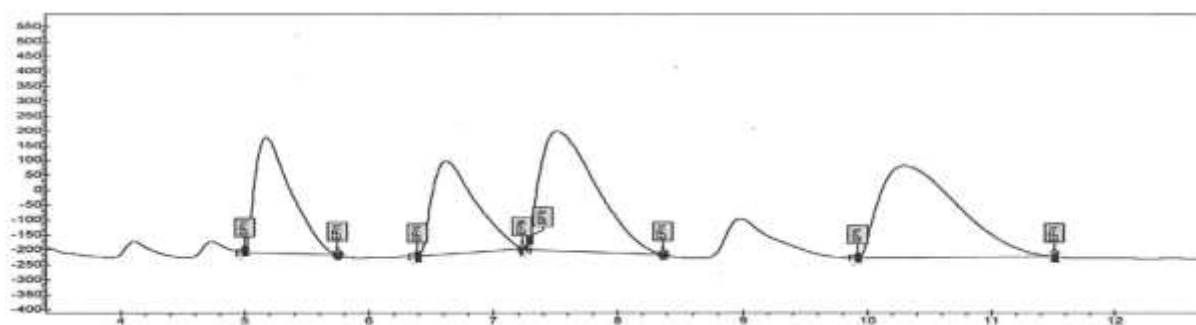
Resolution by SFC:



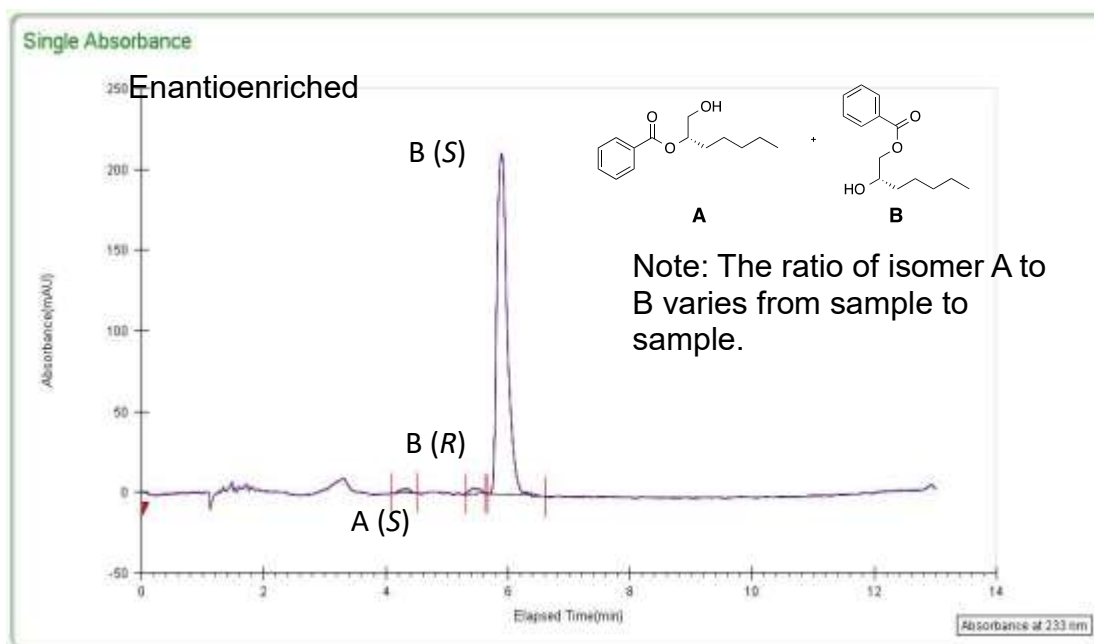
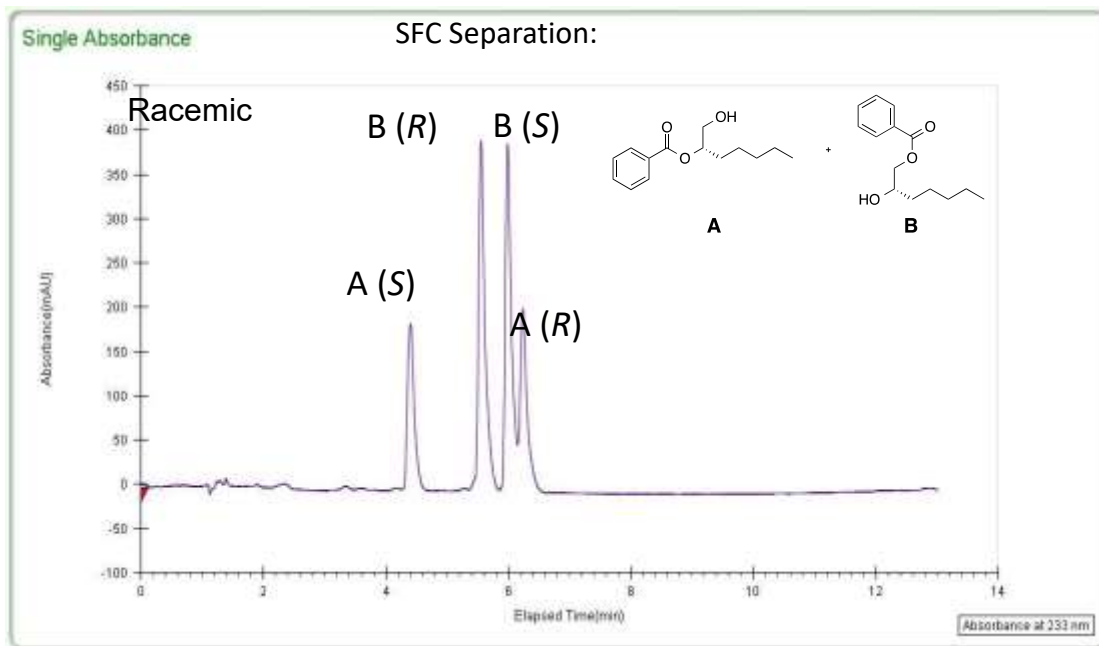
t_r (min)	isomer	Area (uVmin)	% Area
6.36	A	9090.0904	99.3047
8.66	A	63.6455	0.6953



Resolution by SFC:

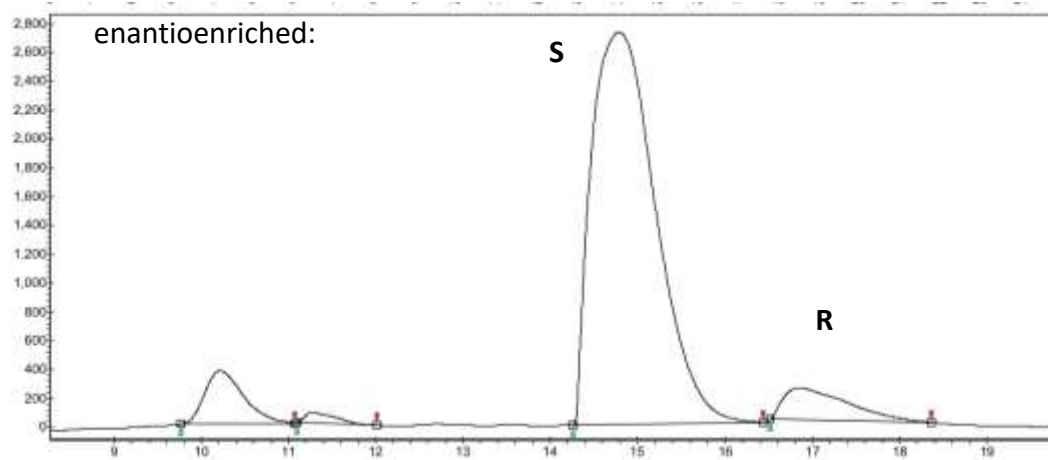
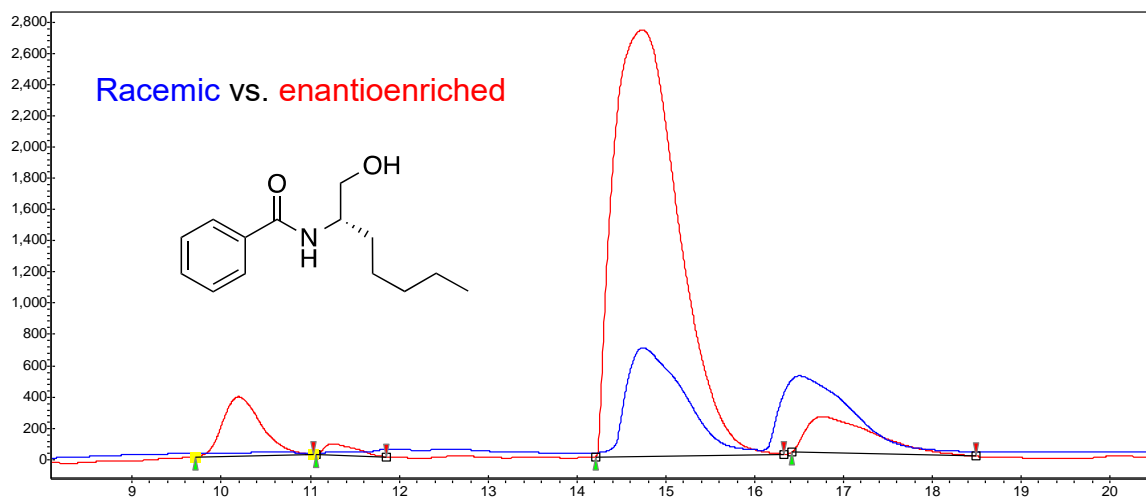


t_r (min)	isomer	Area (uVmin)	% Area
5.0	A	115.7	23.651
6.5	A	5.6	1.143
7.3	B	6.9	1.414
9.81	B	203.1	41.535



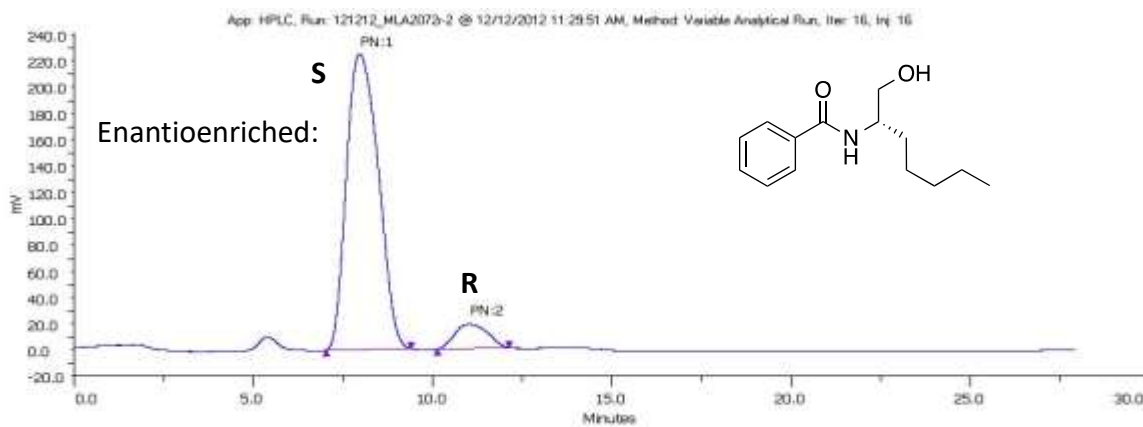
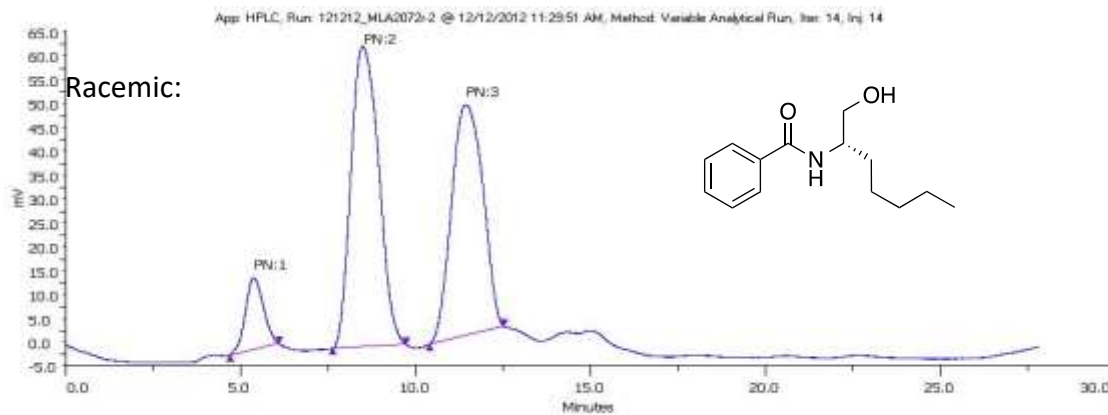
t_R (min)	isomer	Area (uVmin)	% Area
4.36	A	26.525	1.0416
5.45	B	41.4194	1.6264
5.9	B	2478.6963	97.332

SFC separation:



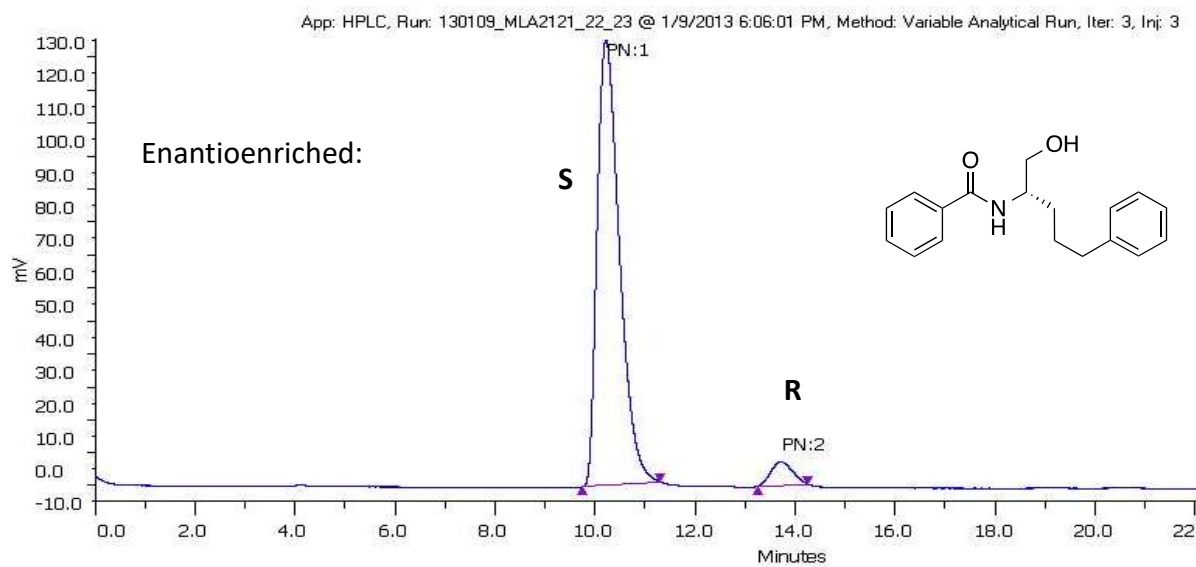
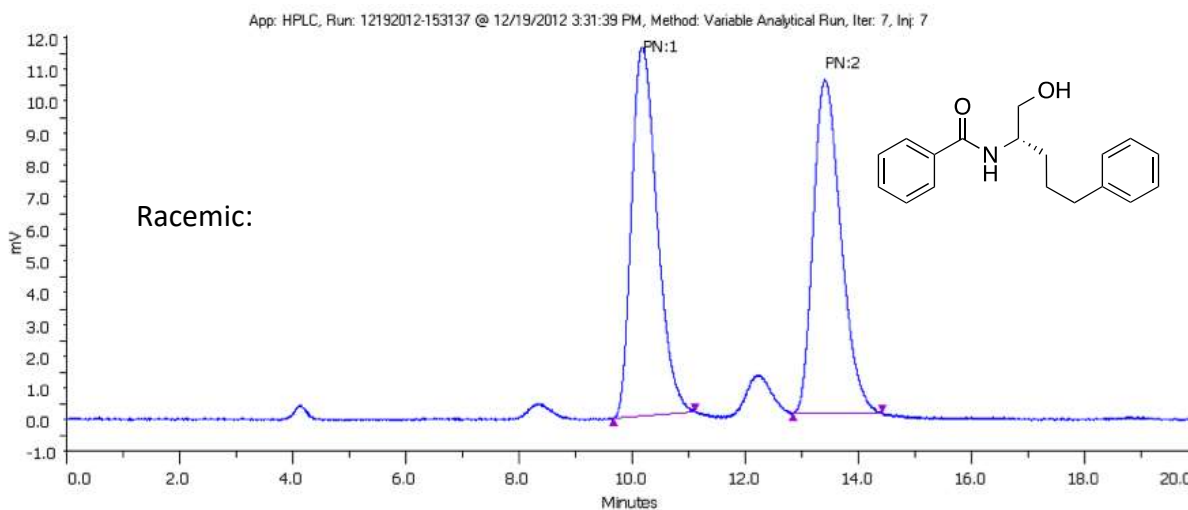
Peak Name	Retention Time (min)	Area (uVmin)	Area %
S	14.78	2313.1	84.937
R	16.86	192.1	7.055

HPLC separation:



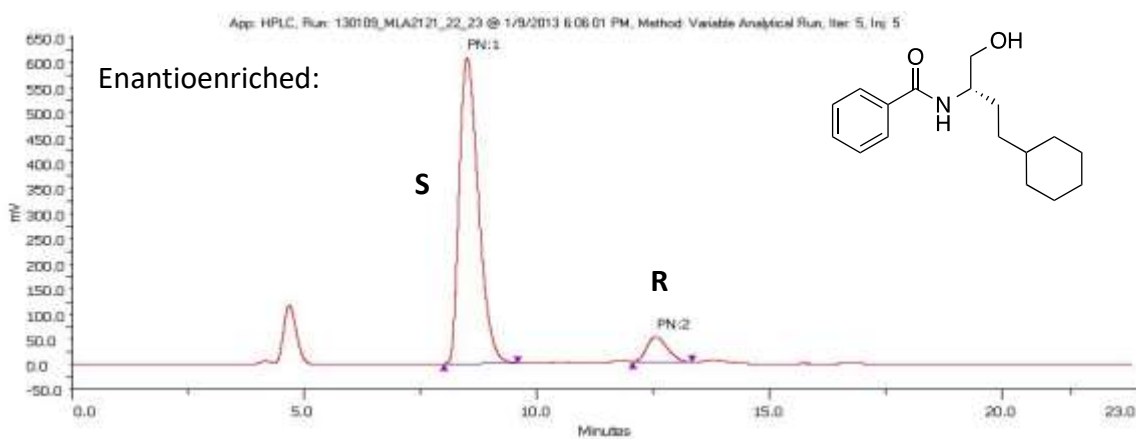
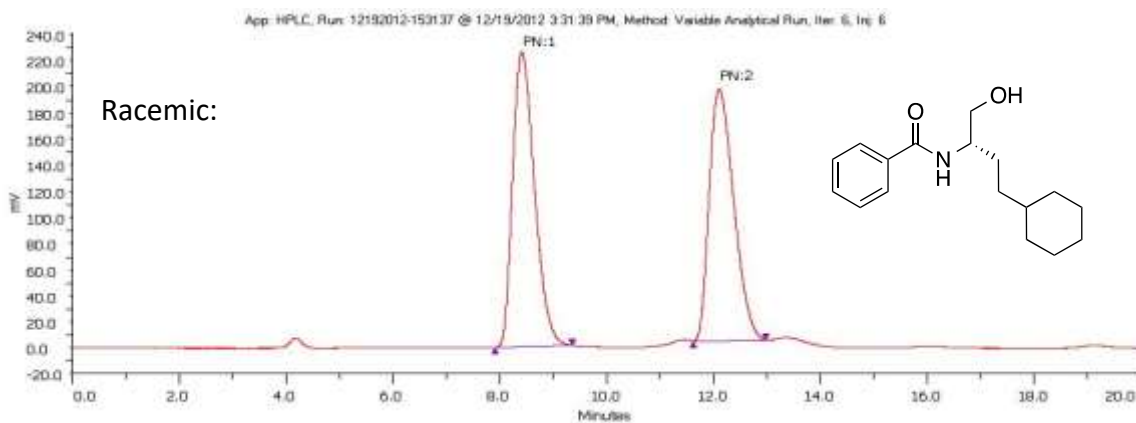
Peak Name	Retention Time (min)	Area (uVmin x100)	Area %
1	7.98	23098779.1658	92.214
2	11.026	1950412.4969	7.786

HPLC separation:



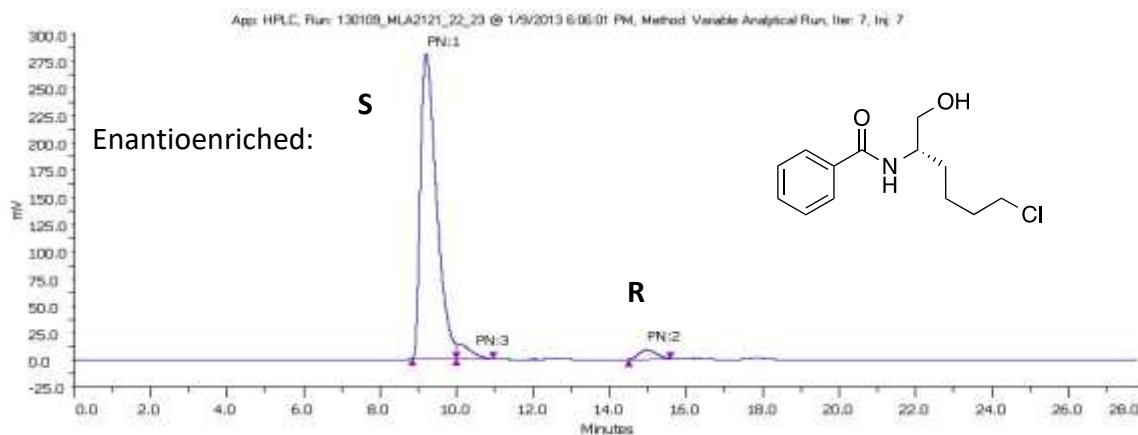
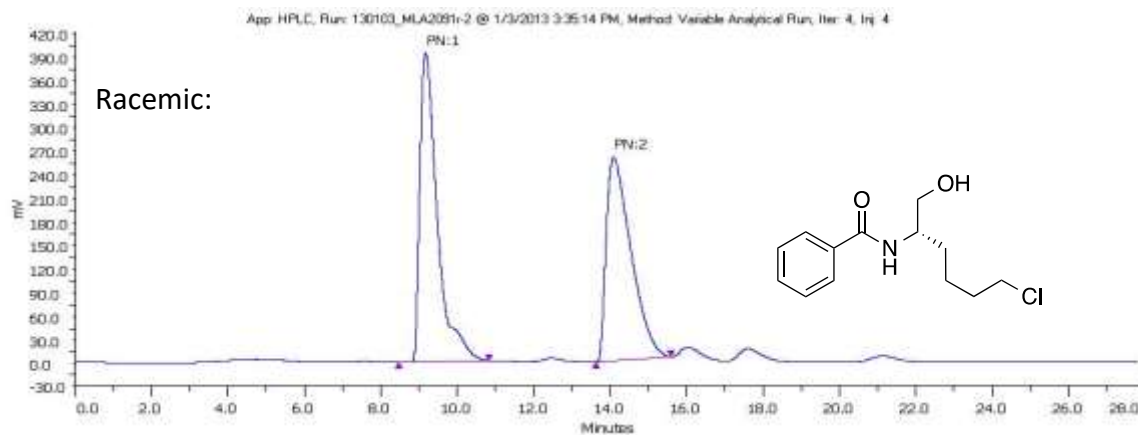
Peak Name	Retention Time (min)	Area (uVmin x100)	Area %
1	10.229	6971986.2537	95.077
2	13.728	361028.7597	4.923

HPLC separation:



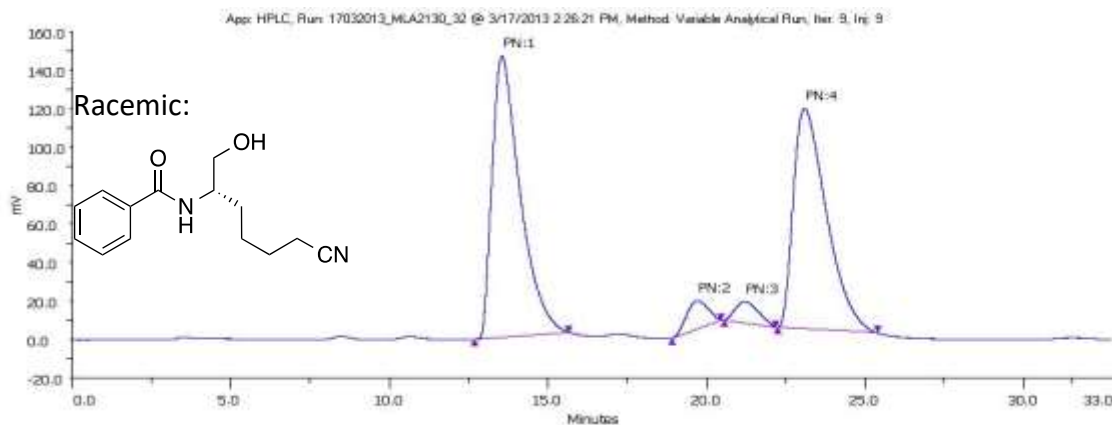
Peak Name	Retention Time (min)	Area (uVmin x100)	Area %
1	8.509	28931946.6674	91.896
2	12.571	2551569.1691	8.104

HPLC separation:

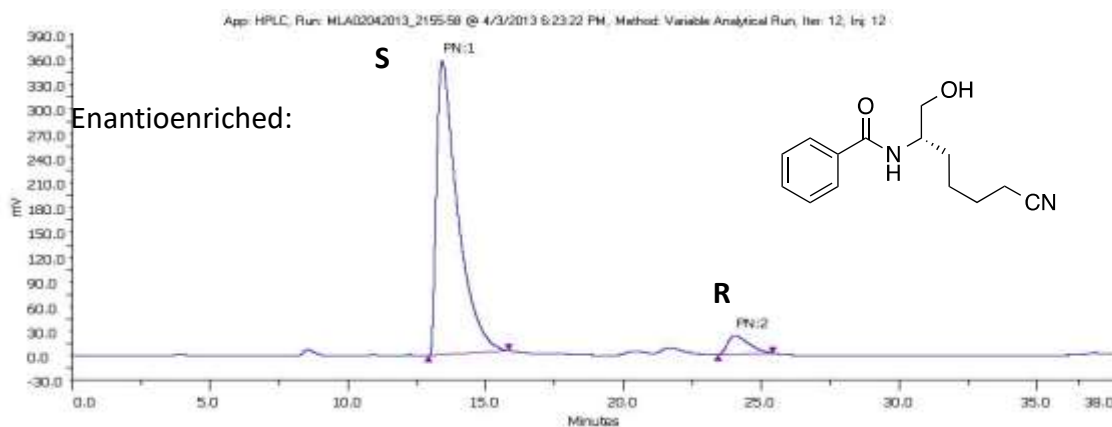


Peak Name	Retention Time (min)	Area (uVmin x100)	Area %
1	9.216	13707290.7953	93.202
2	14.983	441835.835	3.004
3 (impurity)	10.014	557908.081	3.793

HPLC separation:

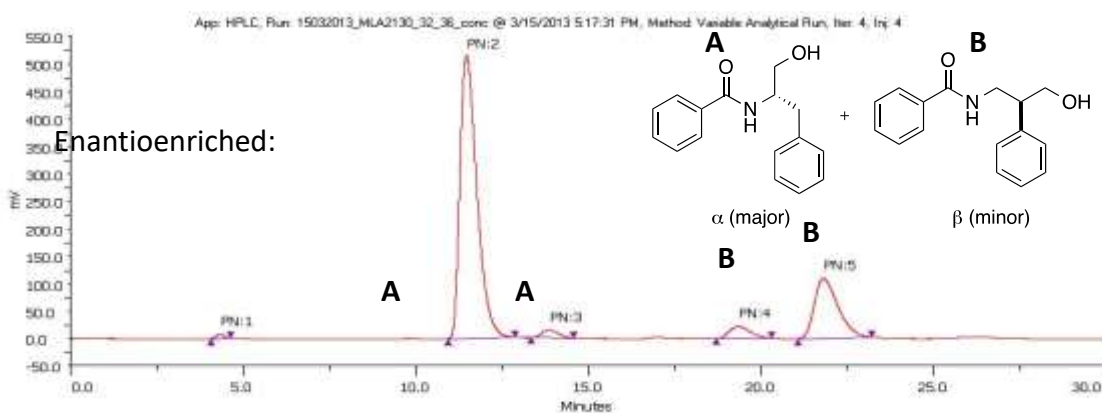
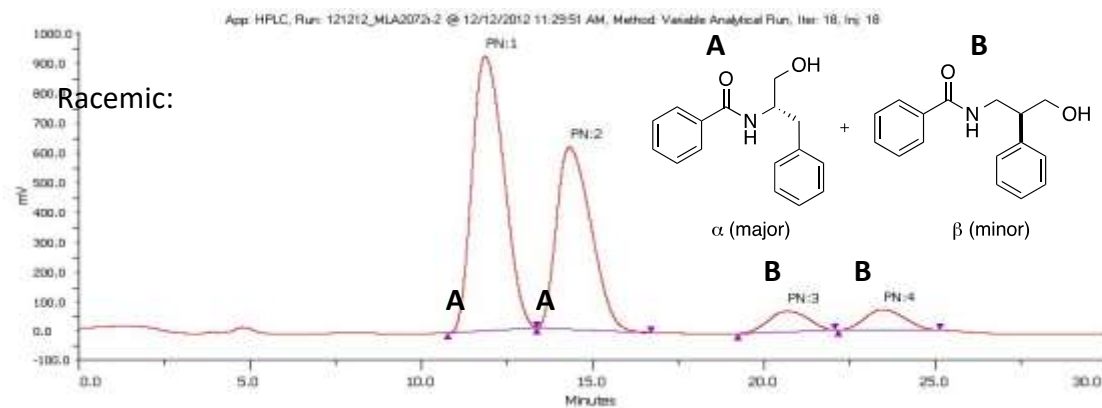


*Note that scales are different on the enantioenriched vs racemic traces.



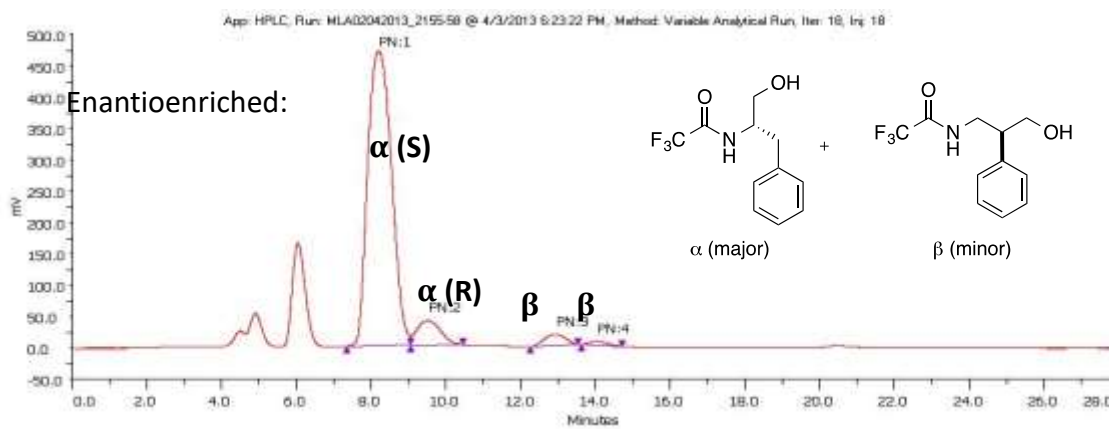
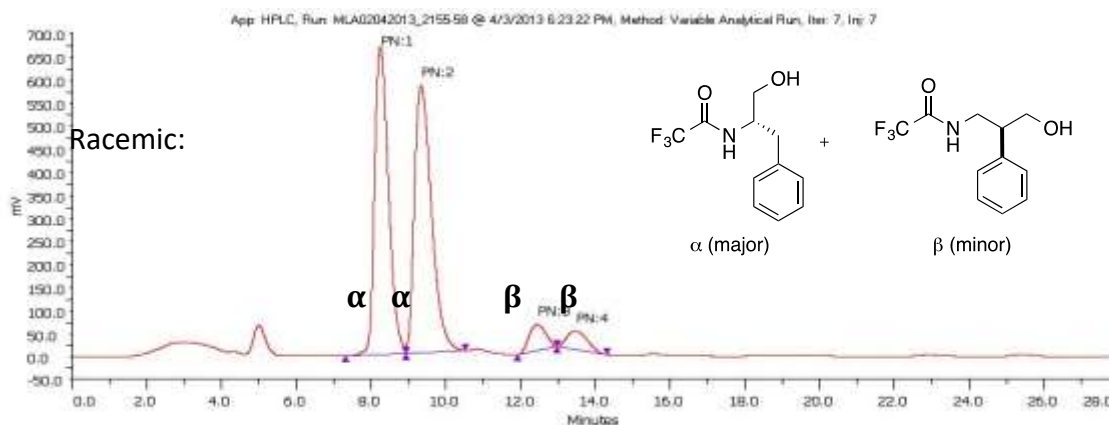
Peak Name	Retention Time (min)	Area (uVmin x100)	Area %
1	13.446	31690445.414	93.997
2	24.071	2024017.91	6.003

HPLC separation:



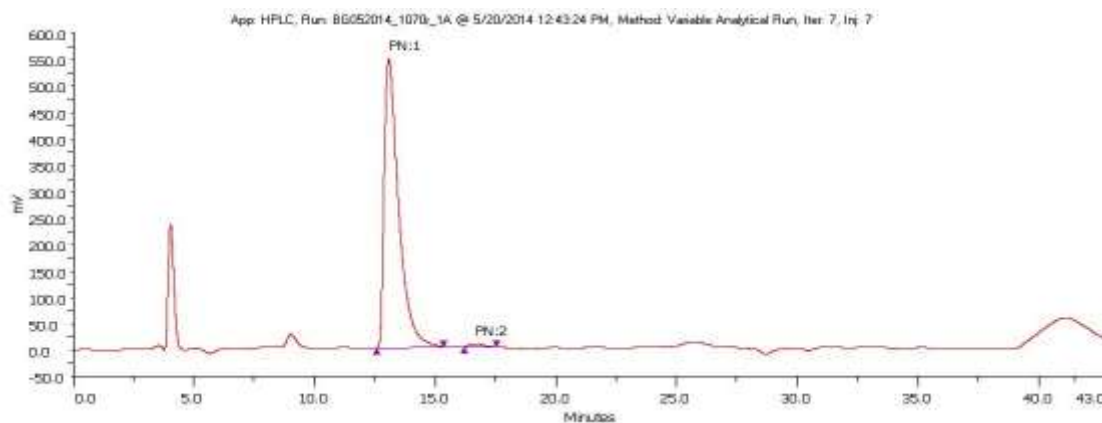
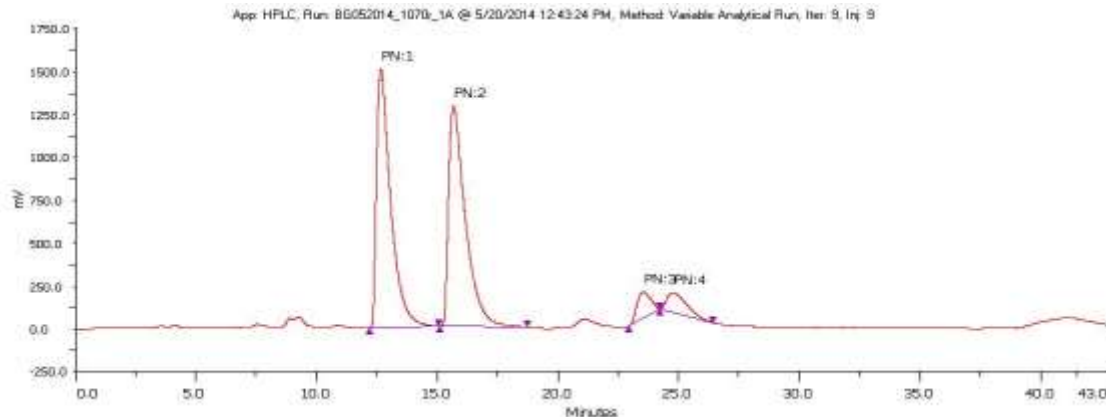
Peak Name	Retention Time (min)	Area (uVmin x100)	Area %
2	11.483	29252597.4926	72.508
3	13.885	768988.3313	1.906
4	19.352	1472231.6663	3.649
5	21.825	8638956.6561	21.413

HPLC separation:



Peak Name	Retention Time (min)	Area (uVmin x100)	Area %
1	8.211	34620060.4828	88.619
2	9.528	2875018.0774	7.359
3	12.898	1206989.9988	3.09
4	14.11	364094.1667	0.932

Racemic:

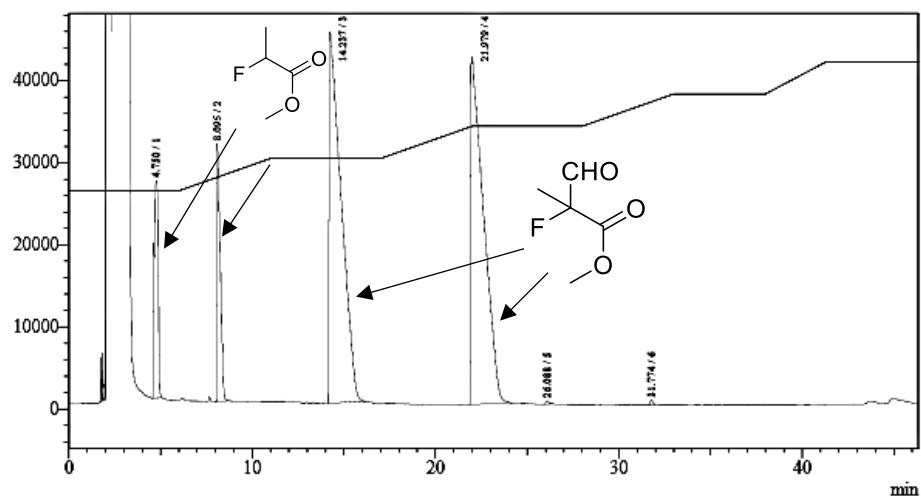


Enantioenriched run shows no β isomer because sample was purified before HPLC and only α isomer was collected.

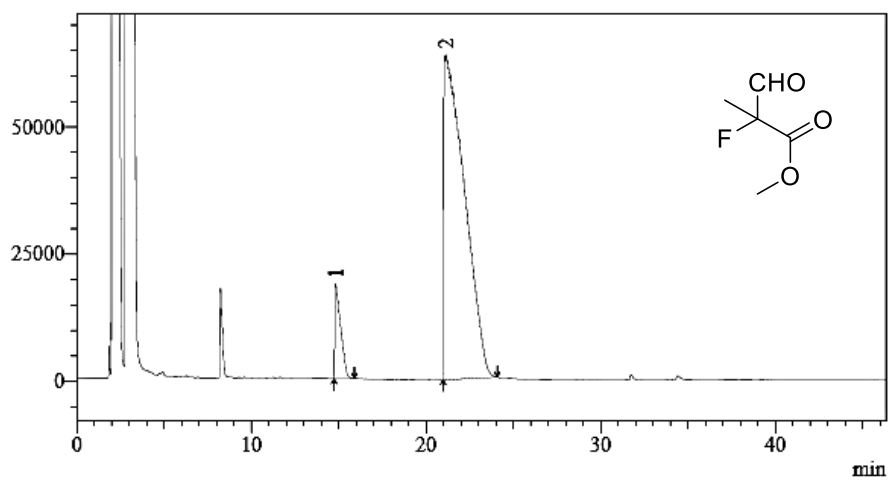
Peak Name	Retention Time (min)	Area (uVmin x100)	Area %
1	13.092	37901592.4973	98.899
2	16.678	422008.3301	1.101

GC traces for Chapter 4

Chiral GC separation

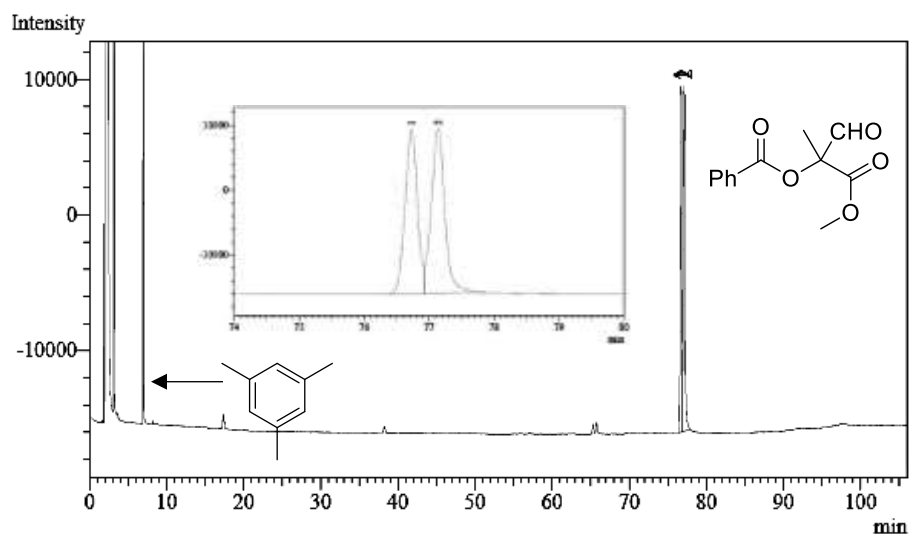
Racemic with *rac*-BDP:

Enantioenriched with (S,S,S)-BDP (L1)

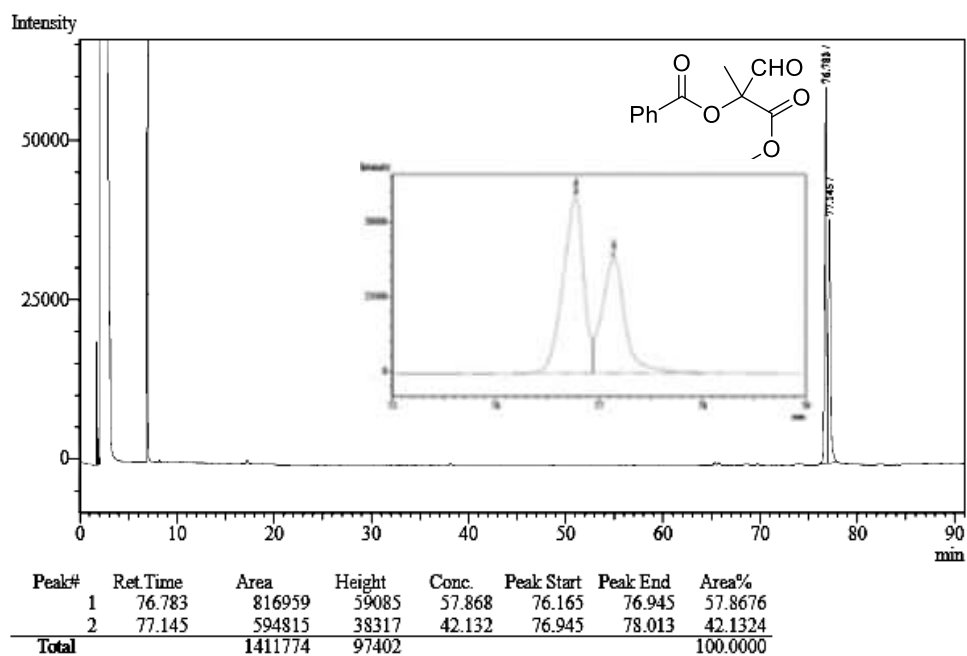


Peak#	Ret.Time	Area	Height	Area%	Peak Start	Peak End
1	14.820	432124	18632	7.6495	14.724	15.895
2	21.124	5216955	63897	92.3505	20.968	24.081
Total		5649079	82529	100.0000		

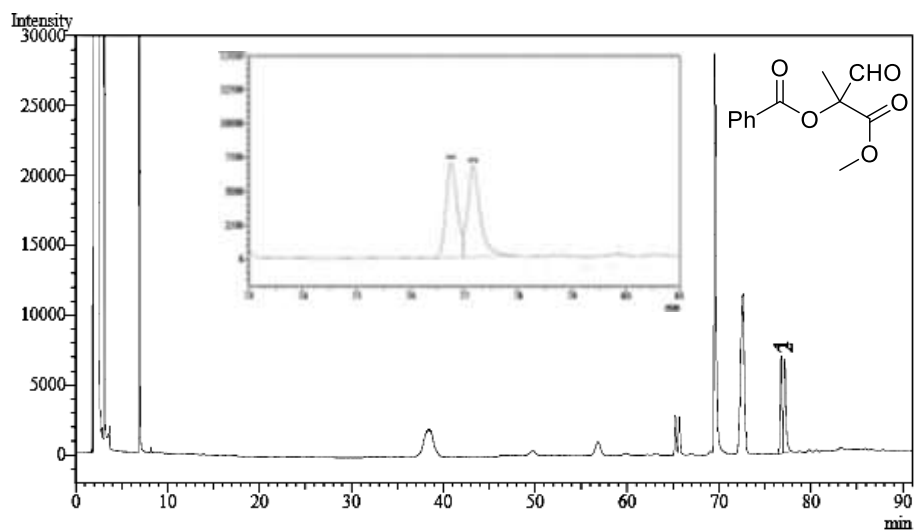
Chiral GC separation

Racemic with *rac*-BDP:

Enantioenriched with (S,S,S)-BDP (L1)

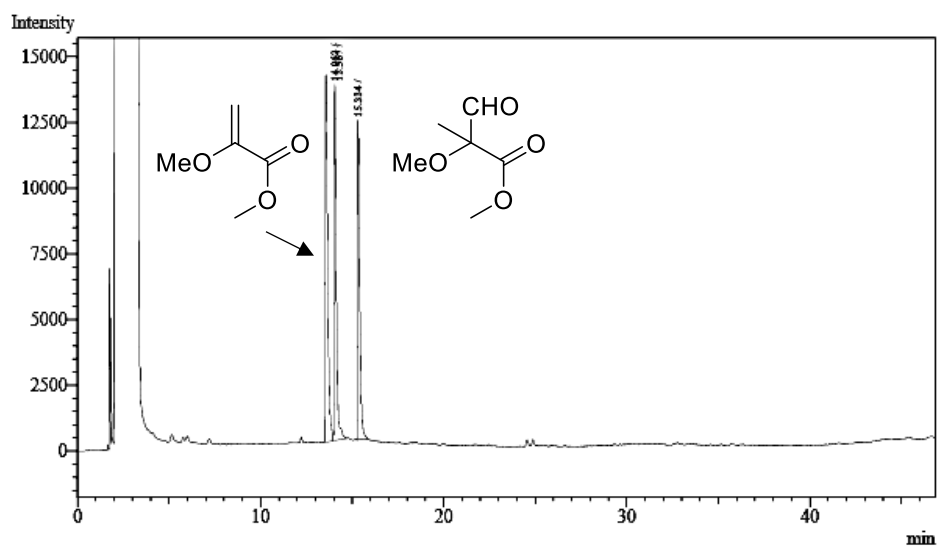


Enantioenriched with (S,S)-Ph-BPE (L2)

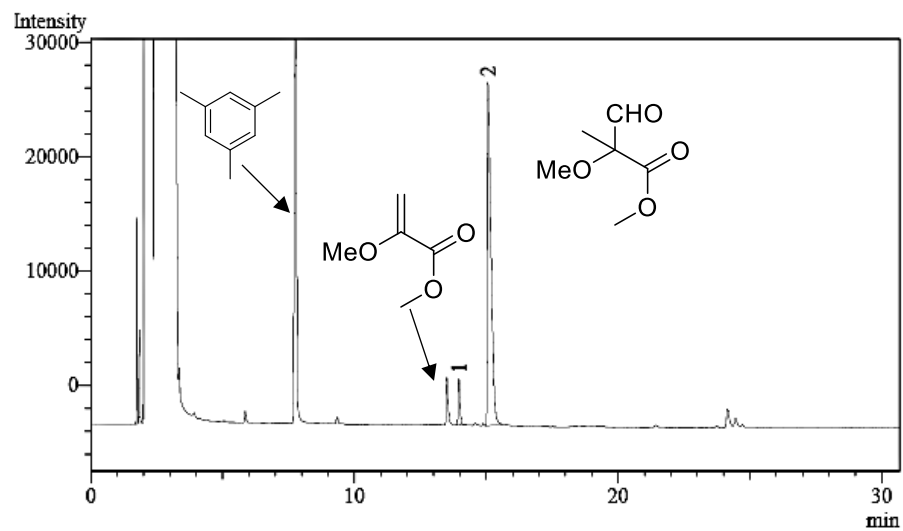


Peak#	Ret. Time	Area	Height	Peak Start	Peak End	Area%
1	76.754	100302	6994	76.445	76.977	47.9047
2	77.161	109076	6701	76.977	77.878	52.0953
Total		209378	13695			100.0000

Chiral GC separation

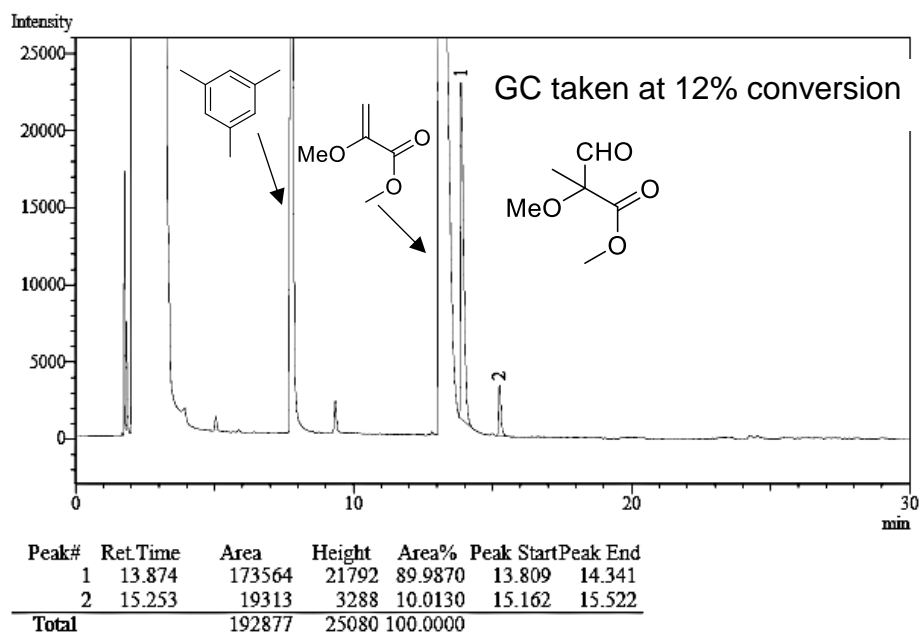
Racemic with *rac*-BDP:

Enantioenriched with (S,S,S)-BDP (L1)

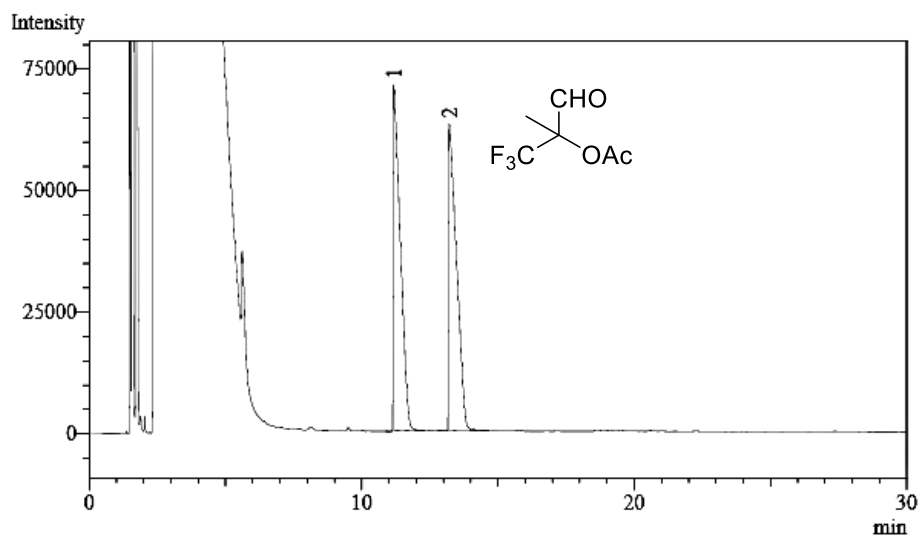


Peak#	Ret.Time	Area	Height	Peak Start	Peak End	Area%
1	13.966	19208	4064	13.875	14.229	6.0976
2	15.062	295805	29956	14.985	15.615	93.9024
Total		315013	34020			100.0000

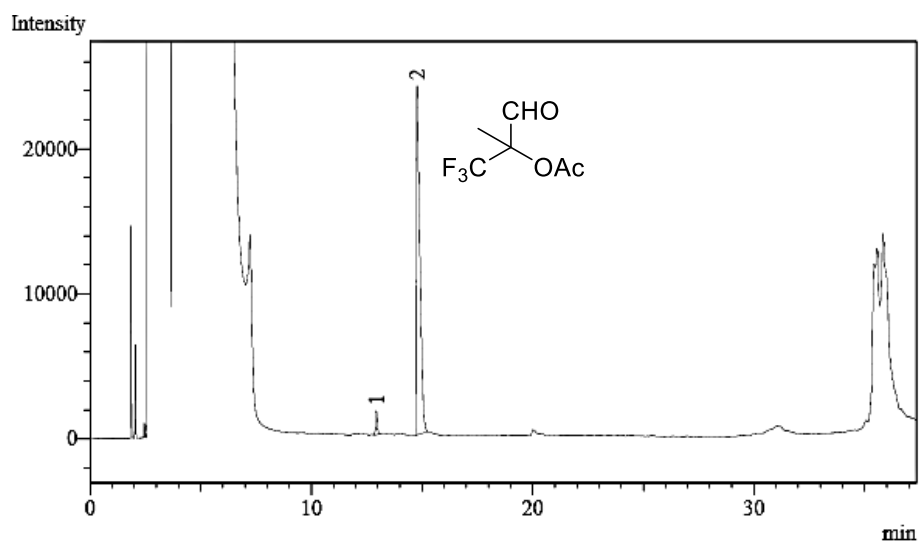
Enantioenriched with (S,S)-Ph-BPE (L2)



Chiral GC separation

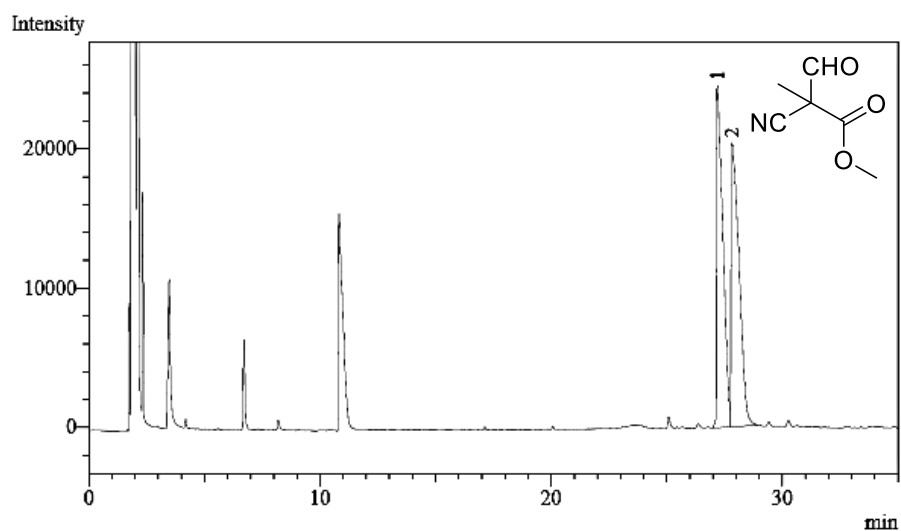
Racemic with *rac*-BDP:

Enantioenriched with (S,S,S)-BDP (L1)

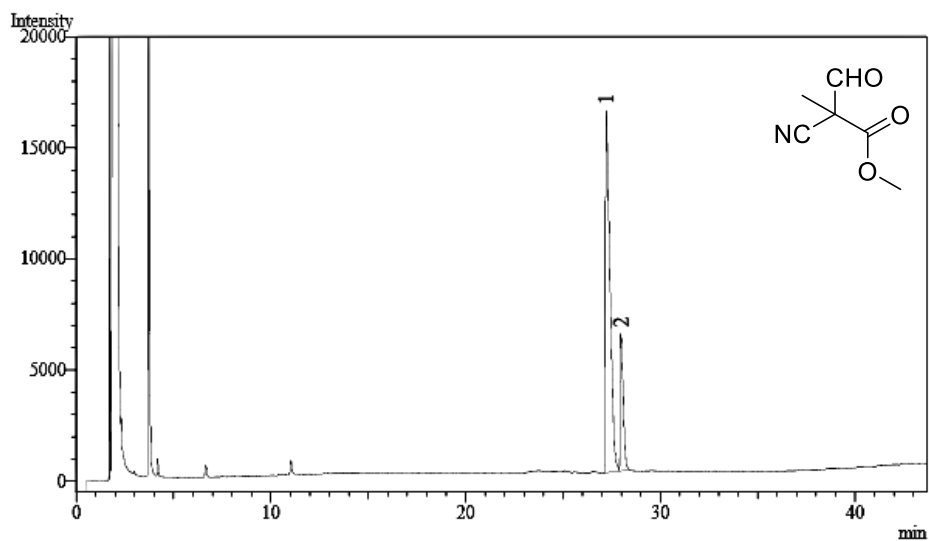


Peak#	Ret.Time	Area	Height	Peak Start	Peak End	Area%
1	12.938	8737	1628	12.829	13.128	3.2871
2	14.775	257067	24035	14.686	15.256	96.7129
Total		265804	25663			100.0000

Chiral GC separation

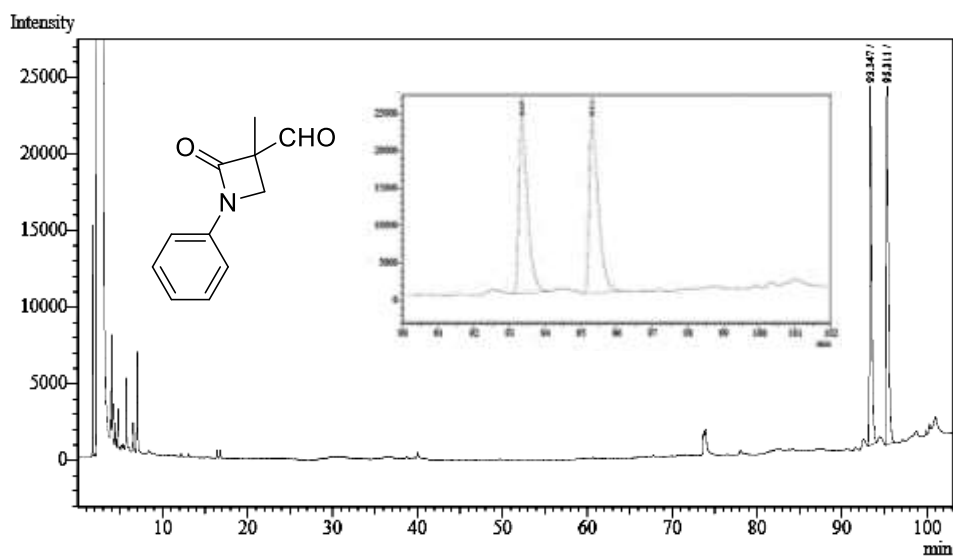
Racemic with *rac*-BDP:

Enantioenriched with (S,S,S)-BDP (L1)

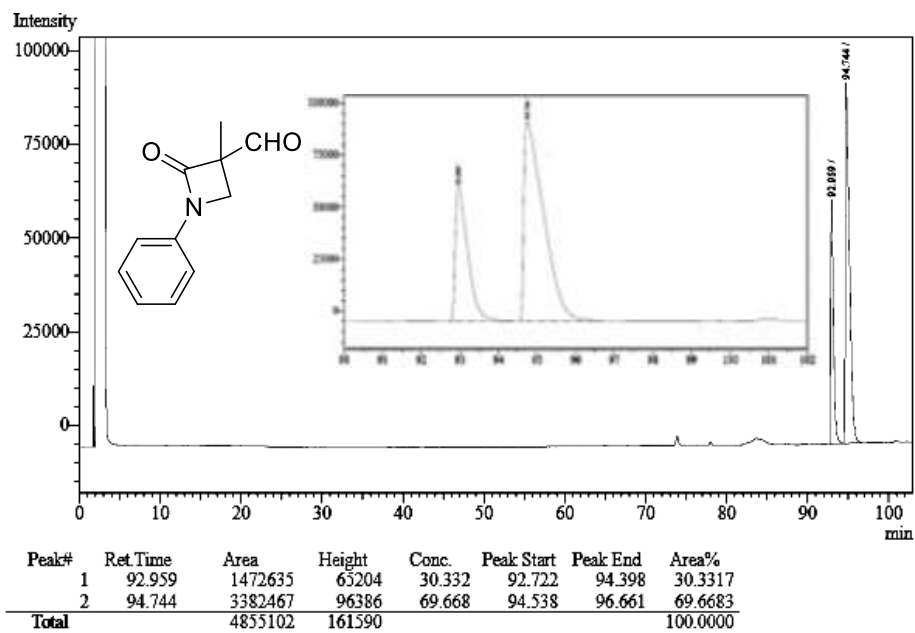


Peak#	Ret.Time	Area	Height	Peak Start	Peak End	Area%
1	27.216	252857	16297	27.133	27.884	79.2851
2	27.977	66064	6191	27.884	28.458	20.7149
Total		318921	22488			100.0000

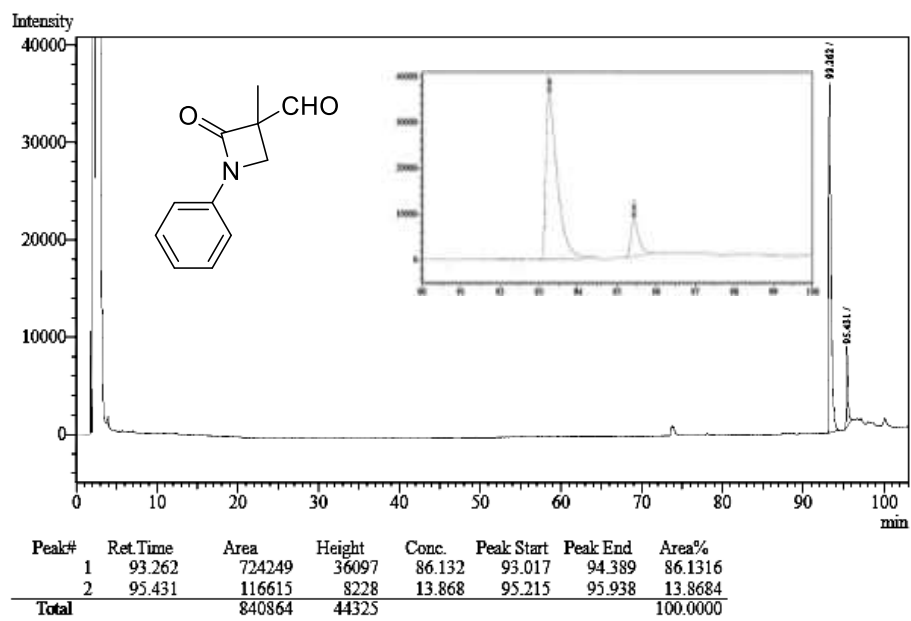
Chiral GC separation

Racemic with *rac*-BDP:

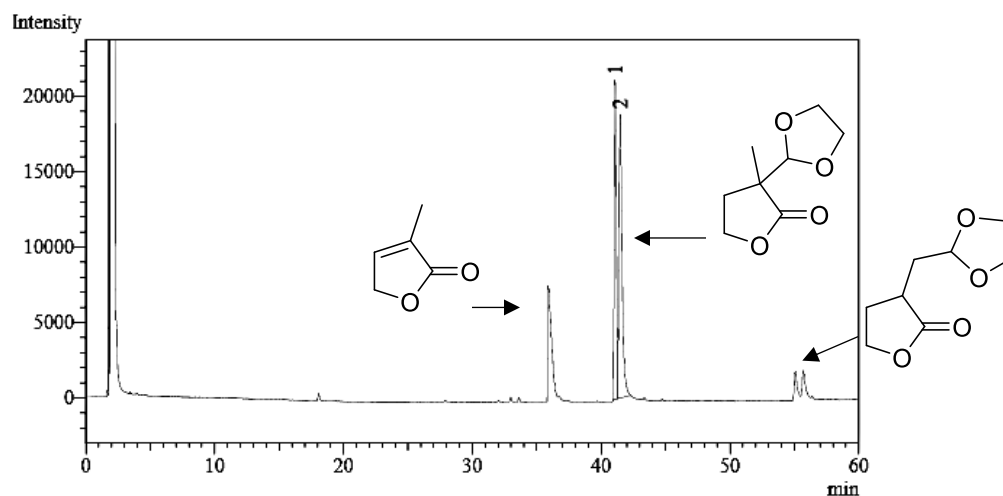
Enantioenriched with (S,S,S)-BDP (L1)



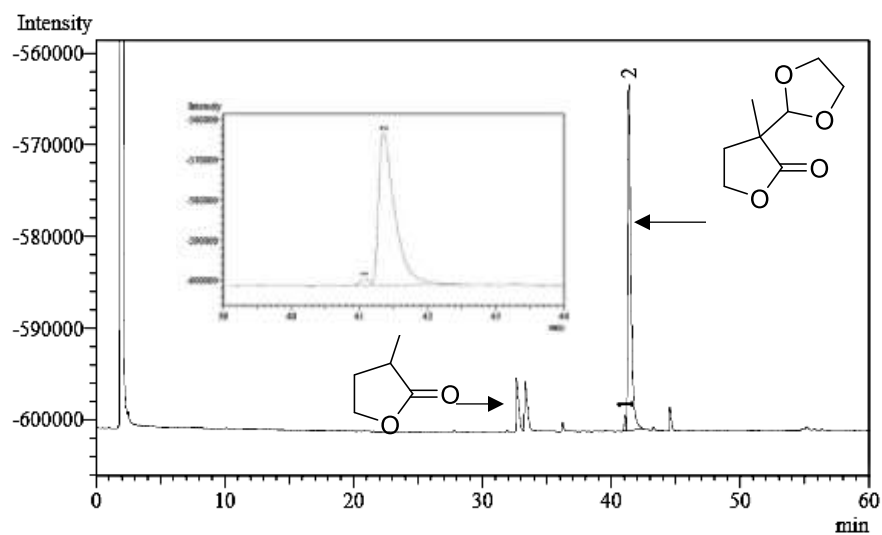
Enantioenriched with (S,S)-Ph-BPE (L2)



Chiral GC separation

Racemic with *rac*-BDP:

Enantioenriched with (S,S)-Ph-BPE (L2)



Peak#	Ret.Time	Area	Height	Area%	Peak Start	Peak End
1	41.069	15270	1705	2.3659	40.885	41.174
2	41.355	630182	37714	97.6341	41.174	42.514
Total		645452	39419	100.0000		